

UNIVERSITA' VITA-SALUTE SAN RAFFAELE

**CORSO DI DOTTORATO DI RICERCA
IN NEUROSCIENZE COGNITIVE**

Individual neuroanatomical constraints on
cognition and language

DoS: prof. Jubin Abutalebi



Tesi di DOTTORATO di RICERCA di Davide Fedeli

matr. 013862

Ciclo di dottorato XXXIV

SSD M-PSI/02

Anno Accademico 2018/2019

CONSULTAZIONE TESI DI DOTTORATO DI RICERCA

Il/la sottoscritto/I Davide Fedeli

Matricola / registration number 013862

nat_ a/ born at GALLARATE (VA)

il/on 10/03/1992

autore della tesi di Dottorato di ricerca dal titolo / author of the PhD Thesis titled
Individual neuroanatomical constraints on cognition and language

AUTORIZZA la Consultazione della tesi / AUTHORIZES the public release of the thesis

NON AUTORIZZA la Consultazione della tesi per 6 mesi /DOES NOT AUTHORIZE the public release of the thesis for months

a partire dalla data di conseguimento del titolo e precisamente / from the PhD thesis date, specifically

Dal / from 30/09/2021 Al / to 30/03/2022

Poiché /because:

l'intera ricerca o parti di essa sono potenzialmente soggette a brevettabilità/ The whole project or part of it might be subject to patentability;

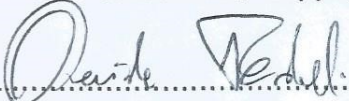
ci sono parti di tesi che sono già state sottoposte a un editore o sono in attesa di pubblicazione/ Parts of the thesis have been or are being submitted to a publisher or are in press;

la tesi è finanziata da enti esterni che vantano dei diritti su di esse e sulla loro pubblicazione/ the thesis project is financed by external bodies that have rights over it and on its publication.

E' fatto divieto di riprodurre, in tutto o in parte, quanto in essa contenuto / Copyright the contents of the thesis in whole or in part is forbidden

Data /Date 22/10/2021.....

Firma /Signature



DECLARATION

This thesis has been composed by myself and has not been used in any previous application for a degree. Throughout the text I use both 'I' and 'We' interchangeably.

All the results presented here were obtained by myself, except for:

- 1) Imaging data used in Experiment 3 were collected before the start of my PhD and were available as part of the CNPL lab database. Data were collected by prof. J. Abutalebi (Faculty of Psychology, Università Vita-Salute San Raffaele, Milan, Italy; Division of Speech and Hearing Sciences, University of Hong Kong, Hong Kong); and by dr. K. Ramanujan under the joint supervision of prof. J. Abutalebi and prof. B. Weekes (Division of Speech and Hearing Sciences, University of Hong Kong, Hong Kong).
- 2) Behavioural analyses in Experiment 3 (Flanker Effects) were performed by dr. S. Sulpizio (Faculty of Psychology, Università Vita-Salute San Raffaele; Department of Psychology, Università degli Studi di Milano-Bicocca).
- 3) Delta plot analyses in Experiment 2 were performed in collaboration and with the technical support of dr. S. Sulpizio (Faculty of Psychology, Università Vita-Salute San Raffaele; Department of Psychology, Università degli Studi di Milano-Bicocca).

Experiments 1,3, and 4 have been previously published in peer-reviewed scientific journals, although with a marginally different wording and structure (Fedeli et al., 2020; Del Maschio et al., 2019a; Fedeli et al., 2021). As of September 2021, Experiment 2 is currently submitted for publication to an international peer-reviewed scientific journal (Fedeli et al., submitted).

ACKNOWLEDGEMENTS

The present dissertation is the final product of the joint efforts and collaboration with my supervisor, prof. J. Abutalebi, my colleagues dr. S. Sulpizio, dr. N. Del Maschio, G. Del Mauro, and the other students of the Centre for Neurolinguistics and Psycholinguistics. I am extremely thankful to all of you.

Full list of peer-reviewed scientific publications in chronological order:

- **Fedeli, D.**, Del Maschio, N., Del Mauro, G., Defendenti, F., Sulpizio, S., Abutalebi., J, (submitted). ACC morphology modulates Inhibitory Control: Evidence from neurofunctional activity and behavioral performance. *Cortex*.

The present work was performed by Davide Fedeli in partial fulfilment of the requirements for obtaining the PhD degree at Vita-Salute San Raffaele University, Milano, Italy.

- Del Mauro, G., Del Maschio, N., Sulpizio, S., **Fedeli, D.**, Perani, D., Abutalebi., J, (2021). Investigating sex differences in human brain structure using source, voxel, and surface-based morphometry. *Brain Structure and Function*, 1-11.

Work performed by Gianpaolo Del Mauro and colleagues was in partial fulfilment of the requirements for obtaining the PhD degree at Vita-Salute San Raffaele University, Milano, Italy.

- **Fedeli, D.**, Del Maschio, N., Sulpizio, S., Rothman J., Abutalebi., J, (2021). The Bilingual Structural Connectome: Dual-language experiential factors modulate distinct cerebral networks. *Brain and Language*, 220, 104978.

The present work was performed by Davide Fedeli in partial fulfilment of the requirements for obtaining the PhD degree at Vita-Salute San Raffaele University, Milano, Italy.

- **Fedeli, D.**, Del Maschio, N., Caprioglio, C., Sulpizio, S., Abutalebi., J, (2020). Sulcal Pattern Variability and Dorsal Anterior Cingulate Cortex Functional Connectivity Across Adult Age. *Brain Connectivity*, 10 (6), 267-278

The present work was performed by Davide Fedeli in partial fulfilment of the requirements for obtaining the PhD degree at Vita-Salute San Raffaele University, Milano, Italy.

- Sulpizio, S., Del Maschio, N., Del Mauro, G., **Fedeli, D.**, Abutalebi., J, (2019). Bilingualism as a gradient measure modulates functional connectivity of language and control networks. *NeuroImage*, 205, 116306

Work performed by dr. Simone Sulpizio and colleagues was in partial fulfilment of the requirements for obtaining the PhD degree at Vita-Salute San Raffaele University, Milano, Italy.

- Sulpizio, S., Del Maschio, N., **Fedeli, D.**, Abutalebi., J, (2019). Bilingual language processing: A meta-analysis of functional neuroimaging studies. *Neuroscience and Biobehavioral Reviews*, 108, 834-853.

Work performed by dr. Simone Sulpizio and colleagues was in partial fulfilment of the requirements for obtaining the PhD degree at Vita-Salute San Raffaele University, Milano, Italy.

- Del Maschio, N., **Fedeli, D.**, Sulpizio, S., Abutalebi., J, (2019). The relationship between bilingual experience and gyrification in adulthood: A cross-sectional surface-based morphometry study. *Brain and language*, 198, 104680.

Work performed by dr. Nicola Del Maschio and colleagues was in partial fulfilment of the requirements for obtaining the PhD degree at Vita-Salute San Raffaele University, Milano, Italy.

- Del Maschio, N., Sulpizio, S., Toti, M., Caprioglio, C., Del Mauro, G., **Fedeli, D.**, Abutalebi., J, (2019). Second language use rather than second language knowledge relates to changes in white matter microstructure. *Journal of Cultural Cognitive Science*, 1-11.

Work performed by dr. Nicola Del Maschio and colleagues was in partial fulfilment of the requirements for obtaining the PhD degree at Vita-Salute San Raffaele University, Milano, Italy.

- Sulpizio, S., Toti, M., Del Maschio, N., Costa, A., **Fedeli, D.**, Job, R., Abutalebi., J, (2019). Are you really cursing? Neural processing of taboo words in native and foreign language. *Brain and Language*, 194, 84-92.

Work performed by dr. Simone Sulpizio and colleagues was in partial fulfilment of the requirements for obtaining the PhD degree at Vita-Salute San Raffaele University, Milano, Italy.

(Before PhD start)

- Del Maschio, N., Sulpizio, S., **Fedeli, D.**, Ramanujan, K., Ding, G., Weekes., B., Cachia, A., Abutalebi., J, (2018). ACC Sulcal Patterns and their Modulation on Cognitive Control Efficiency across Lifespan. *Cerebral Cortex*, 1, 11.
- Del Maschio, N., **Fedeli, D.**, Abutalebi., J, (2018). Bilingualism and aging: why research should continue. *Linguistic approaches to bilingualism*. 11(4), 505-519.
- Del Maschio, N., Sulpizio, S., Gallo, F., **Fedeli, D.**, Weekes., B., Abutalebi., J, (2018). Neuroplasticity across the lifespan and aging effects in bilinguals and monolinguals. *Brain and cognition*, 125, 118-126.
- Lo Gerfo, E., Pisoni, A., Ottone, S., Ponzano, F., Zarri, L., Vergallito, A., Varioli, E., **Fedeli, D.**, Romero Lauro, L. J., (2018). Goal achievement failure drives corticospinal modulation in promotion and prevention contexts. *Frontiers in behavioral neuroscience*, 12.

(Book Chapters)

- **Fedeli, D.**, Abutalebi., J, (2019) Neuroimaging e Afasia in Gilardone, M., Monti, A. (Eds.). (2019) Afasiologia: Clinica, valutazione, trattamento. FrancoAngeli.

The present work was performed by Davide Fedeli in partial fulfilment of the requirements for obtaining the PhD degree at Vita-Salute San Raffaele University, Milano, Italy.

DEDICATION

To my brother Luca,

When I first met prof. Abutalebi, in March 2017, he took me for a tour of the fifth floor of the DIBIT 1 building at UniSR. He had just finished rearranging some cardboard boxes (probably some books?) in his new office at the CNPL. I asked him if he had just moved in, and he answered that indeed the CNPL had been founded just recently. He also told me that it was a matter of Destiny that I came at that exact time when everything was starting.

As it happened on many other occasions, he was definitely right.

I am writing these lines four and a half years later (internship + PhD), and I have had a truly wonderful experience as a PhD student. I'm extremely thankful to a number of people that have been with me and supported me throughout these years.

Prof. Jubin Abutalebi: You are, hands down, the coolest boss someone could ask for. Who else makes their doctoral student drive their Lotus car after they have been admitted to the PhD program? I have to really thank you for the extraordinary possibilities and opportunities you gave me as a CNPLer, and for the enormous freedom you allowed me to enjoy in suggesting and conducting my own research.

From now on, drinks will always be on me!

Nicola and Simone, you know that nothing of this could have been possible without your help.

Nicola: During these years, you have been so supportive, so present, and so encouraging. I learned so much from you, from scientific paper writing to an unexpected number of detailed notions about Scandinavian design and Bauhaus furniture. Someone should give you a medal for your managerial skills with master's and PhD students. I'm proud of having been one of your "Dogs" or, even better, "Maledetti cagnacci!" (Which should be yelled at a moderate-to-loud tone of voice with a coffee in the hands and a hidden smile on the face).

Simone: When I think of an exemplar researcher in our field of study, I think of you. You always brought so much enthusiasm for good research at the CNPL, and I really appreciated discussing with you about professional and personal matters. I will always remember some

catchphrases such as the legendary “smell of paperino” (paperino = scientific paper) and the earworm/summer hit: “Switch dreams” (in the context of L1-to-L2 language switching). Always stay “Fedeli alla linea!” (got the pun and the reference?).

Gianpaolo: We’ve been looking together at rotating brains and Matlab scripts from the beginning of your master’s to the end of my PhD. In the meanwhile, you’ve become a great researcher and a great friend. We have shared countless unhealthy sandwiches, gallons of burnt coffee, several good beers, some tears, and so many laughs. We enjoyed together the crazy summer of 2019, with the “old gen” of internship students: Camilla, Michelle, and Raina, with the honorable mention of “Rocco il frisellaro”. I will treasure the memories we all made together, as well as the beautiful pirate hat you gave me for my birthday.

Gianpa, please keep an eye on the “new gen” of students: Camilla, Gioia, Fede, Marco, and Luca. And, of course, Fede Gallo, the king in the North!

Silvione: More an older brother than an MRI technician. I’ve done the math, and we collected more than 200 MRIs together! Being that close to you, I’ve developed a respectful theoretical knowledge of bikers’ gear, and I discovered that I like cafe racer motorcycles despite never having even tried a scooter. But, most important, I’ve also had the chance to spend that much time with an empathetic, deep, curious, and hilarious person. Thanks for everything, Silvio. I’ll always be there when you need someone for a beer and burger!

Keerthi: You have been my first friend at the CNPL, and I will always remember our funniest conversations about Skippy the bush kangaroo, Monty Python’s filmography, and the general YouTube binge-watching. When you came back to HK, I was literally crying like a baby, you know that. Please, the next time you pass by Milan, stop to have some more homemade pesto by Mamma Fedeli!

Cri: You are an amazing person, with a kind heart and an extraordinary brain (I know that because I’ve scanned it twice!). Thanks for everything we have shared, including the lockdown life during the pandemic. You taught me some of the most important lessons I’ve learned during my PhD. I wish you all the best for your future, and please remember to cite me sometimes when you become a full professor (you know you will). I will always treasure the lyrics of your infamous camel song.

I consider myself a very lucky person because I have more than just one Family. One Family is entirely made by my best friends (in alphabetical order): Guenza, Marco, Mitch,

Paolo, and Tommy. We have a bond that extends over literally decades, and you don't even understand how much your existence means to me. Our crew, which includes Ale, Chiara, Chiara, Deborah, Eli & Gigi, Forgia, Giulia, and Lorena, is the greatest blessing I could have ever asked for. THANKS.

Another Family is made by my Improv theatre friends from "Plateali", "King Salmone and the Impro Humans", and "Senzatesto". You all are so special and having the privilege to share the stage with you is simply incredible. There would be no "Duzzo", without improv, and there is no improv without you.

Speaking of improv friends and, in general, great friends, thanks to Acca, Pietro, Guenza, Ale, and Luca for our Dungeons & Dragons adventures. We really had tons of fun bringing to life the morally questionable adventures of "Sir. Tengar Flamebeard and the fellowship of at-all-costs peace" in pandemic times!

This dissertation is dedicated to my brother Luca. This was a very easy choice: I can remember, as if it were yesterday, the big, excited smile on your face when I told you I had been accepted to the PhD program! You had been a PhD student too, and you knew very well what an incredible journey I was venturing in.

You are my favorite human being. You have shaped so much of what I am, and I will always be thankful to you for your fraternal and always unconditional love. Also, you were the one who insisted on installing Linux on my PC so many years ago, so I basically owe you much of this doctorate!

You are very lucky that a great 100%-Tuscan girl keeps an eye on you and all your shenanigans! Thank you, Lucia, for anchoring my brother to planet Earth! You really are the best.

Mamma and Papà, you are my positive role models.

Mamma: You are probably the most empathetic person I know. You can instantly tell how I feel, and you put your whole heart into helping the people you love. Thank you for being so caring and for having always been there when I needed a shoulder. You are a great mom, and you deserve a thousand hugs.

Papà: You are always positive. You are a rock for our Family, but with a heart made of pure chocolate. Thank you for never losing hope and always lighting up the world around you. I wish one day I could be even a fraction of the father you are.

You are two beautiful souls... Even if you don't want to adopt a dog!

Whenever I was facing any challenge, my grandparents were there, supporting me. They are not here physically anymore. But the pair of shoes they gave me (nonni, you know what I'm referring to) have taken me much further than I could ever imagine. You are my sweetest memory.

I'm sure I've missed somebody in this dedication since I owe so much to so many.

Please, feel free to ask me to buy you a beer: I'll buy two!

Gallarate, 22-October-2021

Davide "Duzzo" Fedeli

ABSTRACT

Converging evidence shows that individual differences in cognitive abilities are partly driven by neuroanatomical constraints determined during fetal life and largely unaffected by postnatal events. For instance, the large degree of intersubject variability in sulcal anatomy of the Anterior Cingulate Cortex has been associated with long-term differences in executive performance and functional activity. The consequences of these observations are far-reaching and represent a new perspective on the neural architecture of behavioral differences. On the other hand, neuroplastic processes continuously modify the brain organization in response to internal and external demands. This dissertation provides a systematic investigation on the dynamic interplay between early neuroanatomical constraints, environmental neuroplastic factors, brain activity, and cognitive performance across age. This work adopts a combination of complementary multimodal neuroimaging techniques (i.e., surface-based morphometry, structural and functional connectivity, and task-based fMRI), neuropsychological testing, and psycholinguistic assessment to better understand this complex relationship.

TABLE OF CONTENTS

TABLE OF CONTENTS	1
ACRONYMS AND ABBREVIATIONS	3
LIST OF FIGURES AND TABLES	7
Chapter 1 - INTRODUCTION	9
1.1 – <i>Outline of the manuscript</i>	10
1.2 – <i>Models of cortical development and cortical folding</i>	13
1.3 – <i>Individual morphological variability of Anterior Cingulate Cortex sulcation patterns</i>	22
Parcellation models of the Cingulate Cortex	22
ACC	24
MCC	25
ACC-MCC complex labeling	28
Paracingulate Sulcus	29
1.4 <i>Neural plasticity: the case of bilingualism</i>	44
1.5 – <i>Experiment 1 (introduction): “Sulcal Pattern Variability and Dorsal Anterior Cingulate Cortex Functional Connectivity Across Adult Age”</i>	58
1.6 – <i>Experiment 2 (introduction): “ACC folding patterns variability modulates neurofunctional activity and behavioral performance during inhibitory control”</i>	60
1.7 – <i>Experiment 3 (introduction): “The relationship between bilingual experience and gyrification in adulthood: A cross-sectional surface-based morphometry study”</i>	64
1.8 – <i>Experiment 4 (introduction): The bilingual structural connectome: Dual-language experiential factors modulate distinct cerebral networks</i>	68
Chapter 2 - AIM OF THE WORK	72
Chapter 3 – RESULTS	73
3.1 – <i>Experiment 1 (results):</i>	73
3.1.1 – Discussion.....	78
3.2 – <i>Experiment 2 (results):</i>	82
3.2.1 – Discussion.....	94
3.3 – <i>Experiment 3 (Results):</i>	101
3.3.1 – Discussion.....	104
3.4 – <i>Experiment 4 (Results):</i>	110
3.4.1 – Discussion.....	119
Chapter 4 – DISCUSSION	127
4.1 Resume of background and experimental findings.....	127
4.2 General Discussion.....	130
4.3 Limitations.....	138
4.4 Future directions	140
4.5 Concluding remarks	141
Chapter 5 – MATERIALS AND METHODS	143

<i>5.1 – Experiment 1 (Materials and Methods):</i>	<i>143</i>
<i>5.2 – Experiment 2 (Materials and Methods):</i>	<i>152</i>
<i>5.3 – Experiment 3 (Materials and Methods):</i>	<i>161</i>
<i>5.4 – Experiment 4 (Materials and Methods):</i>	<i>166</i>
Chapter 6 - REFERENCES	176
Chapter 7 – APPENDICES	240

ACRONYMS AND ABBREVIATIONS

A/P	Anterior/Posterior
ABBA	Arousal, Balance, and Breadth of Attention model
ACC	Anterior Cingulate Cortex
aCompCor	anatomical Component-based noise Correction method
AC-PC	Anterior Commissure – Posterior Commissure bicommissural line
ACT	Anatomically Constrained Tractography
AD	Alzheimer’s Disease
AF	Arcuate Fasciculus
ALE	Activation Likelihood Estimation
ANT	Attention Network Task
AoA	Age of (second language) Acquisition
ART	Artifact Rejection Toolbox
BCT	Brain Connectivity Toolbox
BOLD	Blood-Oxygen-Level Dependent
BSWQ	Bilingual Switching Questionnaire
C.E.R.M.A.C.	Centro di Eccellenza Risonanza Magnetica ad Alto Campo
CAT	Computational Anatomy Toolbox
CC	Corpus Callosum
CCZ	Caudal Cingulate Motor Zone
CS, cgs	Cingulate Culcus
CSD	Constrained Spherical Deconvolution
CSF	Cerebrospinal Fluid
CT	Cortical Thickness
CVLT	California Verbal Learning Task
D1, D2, D3	Dorsal seeds in Experiment 1
DA, SS	Double Absence (Single/Single) pattern
dACC	dorsal Anterior Cingulate Cortex
DAN	Dorsal Attention Network
DP, DD	Double Presence (Double parallel/Double parallel) pattern
DMN	Default Mode Network

DTI	Diffusion Tensor Imaging
DWI	Diffusion-weighted imaging
Eglob	Global Efficiency
Eloc	Local Efficiency
EPI	Echo Planar Imaging
F	Female
FA	Fractional Anisotropy
FOD	Fiber Orientation Distribution
FLAIR	Fluid-Attenuated Inversion Recovery
fMRI	functional Magnetic Resonance Imaging
FOV	Field of view
FSL	FMRIB Software Library
FWE	Family Wise Error (Rate)
FWHM	Full-Width at Half Maximum
GI	Gyrification Index
GLM	General Linear Model
GM	Gray Matter
GMV	Gray Matter Volume
GRAPPA	GeneRALized Autocalibrating Partial Parallel Acquisition
HCP	Human Connectome Project
HRF	Hemodynamic Response Function
IFOF	Inferior Frontal Occipital Fasciculus
ILF	Inferior Longitudinal Fasciculus
L1	First (dominant) Language
L2	Second (non-dominant) Language
LA	Leftward Asymmetry pattern
LAS	Local Adaptive Segmentation
LEMON	Leipzig Study for Mind-Body-Emotion Interactions
LPS 2	Leistungsprüfsystem 2
M	Male
M1, M2, M3	Middle seeds in Experiment 1
MANGO	Multi-image Analysis GUI

MCC	Middle Cingulate Cortex
MD	Mean Diffusivity
MesLS	Mesial Longitudinal System
MMSE	Mini Mental State Examination
MNI	Montreal Neurological Institute
MP2RAGE	Magnetization-Prepared 2 Rapid Acquisition Gradient Echoes
MPRAGE	Magnetization-Prepared Rapid Acquisition Gradient Echoes
MRI	Magnetic Resonance Imaging
MSMT	Multi-Shell Multi-Tissue
NART	National Adult Reading Test
NBS	Network-based Statistics
NMDA	N-methyl-D-aspartate
PBT	Projection-Based Thickness
PCA	Principal Component Analysis
PCC	Posterior Cingulate Cortex
PCG	Paracingulate Gyrus
PCS, pcgs	Paracingulate Sulcus
PE	Phase Encoding
PET	Positron Emission Tomography
pre-SMA	pre-Supplementary Motor Aarea
PVE	Partial Volume Estimation
RA	Rightward Asymmetry pattern
RCZa	Anterior Rostral Cingulate Motor Zone
RCZb	Posterior Rostral Cingulate Motor Zone
RWT	Regensburger Word Fluency Test
RI	Response Inhibition
ROI	Region Of Interest
RSC	Retrosplenial Cingulate Cortex
rsFC	resting-state Functional Connectivity
RT	Response Time
SAF	Superoanterior Fasciculus
SANLM	Spatial Adaptive Non-Local Mean

SBM	Surface-Based Morphometry
SENSE	SENSitivity Encoding
SES	Socio-Economic Status
SIFT2	Spherical-deconvolution Informing Filtering of Tractograms 2
SNR	Signal-to-Noise Ratio
SLF	Superior Longitudinal Fasciculus
SN	Salience Network
SPM	Statistical Parametric Mapping
SWI	Susceptibility-weighted imaging
TAP	Test of Attentional Performance
TBSS	Tract-Based Spatial Statistics
TE	Echo Time
TIB	Test di Intelligenza Breve
TIV	Total Intracranial Volume
TMT	Trail Making Test
TR	Repetition Time
US	Unintended Switching (BSWQ)
V1, V2, V3	Ventral seeds in Experiment 1
VBM	Voxel-Based Morphology
WM	White Matter
WST	Wortschatztest

LIST OF FIGURES AND TABLES

Figure 1	p. 24
Figure 2	p. 34
Figure 3	p. 35
Figure 4	p. 54
Figure 5	p. 135
Figure 6	p. 136
Experiment 1; Table 1	p. 73
Experiment 1; Table 2	p. 75
Experiment 1; Table 3	p. 77
Experiment 1; Table 4	p. 144
Experiment 1; Figure 1	p. 76
Experiment 1; Figure 2	p. 78
Experiment 1; Figure 3	p. 146
Experiment 2; Table 1	p. 83
Experiment 2; Table 2	p. 86
Experiment 2; Figure 1	p. 84
Experiment 2; Figure 2	p. 88
Experiment 2; Figure 3	p. 90
Experiment 2; Figure 4	p. 92
Experiment 3; Table 1	p. 101
Experiment 3; Table 2	p. 102
Experiment 3; Table 3	p. 104
Experiment 3; Table 4	p. 162
Experiment 3; Table 5	p. 162
Experiment 3; Figure 1	p. 103
Experiment 4; Table 1	p. 112
Experiment 4; Table 2	p. 113
Experiment 4; Table 3	p. 116
Experiment 4; Table 4	p. 118
Experiment 4; Table 5	p. 167
Experiment 4; Figure 1	p. 114

Experiment 4; Figure 2	p. 115
Experiment 4; Figure 3	p. 116
Experiment 4; Figure 4	p. 118
Experiment 4; Figure 5	p. 170
Appendix; Table S1	p. 240
Appendix; Experiment 1; Figure S1	p. 243
Appendix; Experiment 1; Table S1	p. 245
Appendix; Experiment 2; Table S1	p. 247
Appendix; Experiment 2; Table S2	p. 249
Appendix; Experiment 4; Table S1	p. 250
Appendix; Experiment 4; Figure S1	p. 251

Chapter 1 - INTRODUCTION

We invite the readers to lift one of their hands from the pages of this dissertation (or the digital device they are using to read it) and look at the point of their fingers. The ridges and fissures on the skin form a series of fingerprints: Unique patterns that are not shared by any other human being. Other evident features can also be observed: some readers may have the hands of a musician with years of finger training, others may have calluses from their manual work or a hobby such as climbing or wood carving. The way we use our hands shapes and defines them.

The human brain is a far more complex structure than the tip of a finger. It has fascinated researchers and academics for centuries, arguably thousands of years. However, only in the last few decades, it became possible and easy to investigate *in vivo* its structural and functional properties with an unprecedented level of accuracy. Interestingly, just like the tip of the finger, the cortical brain ribbon has its unique patterns of sulci and gyri. While all neurologically healthy individuals share the same macroscopic cerebral morphological features, large individual variability is still present. Moreover, not differently from the hands of a pianist or a carpenter, experience and external factors can reshape the brain to some extent. This dissertation aims at providing new insights into the understanding of the dynamic relationship between individual brain morphology, brain functional activity, and cognitive abilities. On one side, we will focus on individual differences in structurally invariant features such as cortical sulcation patterns. On the other, we will describe the impact of environmental factors on brain morphology and structural architecture. Eventually, we will also describe how cognitive abilities may be partially influenced both by lifelong stable and dynamically plastic neural phenomena.

1.1 – OUTLINE OF THE MANUSCRIPT

“Neuroanatomical constraints” are morphological features of the human brain determined during foetal life and largely unaffected by postnatal events. This definition includes gyrification and sulcal patterns of the cerebral cortex, brain morphology asymmetries, as well as other relatively stable structural properties of the brain. By contrast, “neural plasticity” is the capacity of the brain to reorganize itself and reshape its structural and functional features as a response to external events and environmental factors. Neural plasticity occurs when we learn to play an instrument or a second language, but also as a recovery and/or compensation process following neurological damage. These two aspects, lifelong stable properties of the brain and processes of neural adaptation, seem counterposed. However, they both contribute to the neural development and functioning of individuals. The present work provides a description of the relationship between brain structure, brain functional activity, and cognitive abilities by considering both the deterministic impact of invariable individual neuroanatomical differences and neural plasticity as a mediator of the environmental impact variability. In particular, the present work comprises four studies. Three of these studies (Experiment 1, 3, and 4) have been previously published in peer-reviewed scientific journals, although with a marginally different wording and structure (Fedeli et al., 2020; Del Maschio et al., 2019a; Fedeli et al., 2021). As of September 2021, Experiment 2 (Fedeli et al., submitted) is currently submitted for publication to an international peer-reviewed scientific journal. Experiments 1 and 2 inspect the impact of the individual morphological variability of sulcation patterns of the Anterior Cingulate Cortex (ACC) respectively on brain functional activity at rest and during executive tasks. Experiment 3 investigates the role of second language usage (here intended as a proxy measure of cognitive experience and training) in modulating relatively stable features of the brain cortex (i.e., cortical gyrification). Experiment 4 investigates the impact of individual differences in second language experience on white matter structural plasticity. The four studies represent a continuum with a first half of the dissertation starting from the depiction of elements of neural stability (Experiment 1 and 2) and a second half ending

with the investigation of the dynamics of neural plasticity (Experiment 3 and 4). We opted to present the experiments in this specific order to first describe the neurocognitive impact of prenatally-determined individual differences in cortical morphology and to continue by portraying the role of individual differences in postnatal and lifelong environmental experience.

The present manuscript is organized into 7 chapters.

Chapter 1 - Introduction is divided as follows:

- *Section 1.1* provides a brief presentation of the work and outlines the structure of the current manuscript.
- *Section 1.2* focuses on the theories behind the neural development of cortical gyrification and fissurization patterns.
- *Section 1.3* describes individual morphological variability of the anterior cingulate fissurization patterns, which represents a topic of interest of the present manuscript.
- *Section 1.4* describes second language experience as a proxy measure of neural plasticity
- *Section 5, 6, 7, and 8* introduce the four studies included in the thesis. For each of these introductory chapters, a literature background and the scientific rationale of the study is presented, as well as the scientific hypotheses and the potential implications of the results.

Chapter 2 – Aim of the work follows the introduction and shortly resumes the goals of the studies presented in this manuscript.

Chapter 3 – Results reports the empirical findings of the four performed experiments. This chapter is divided into four sections, one for each study. For sake of practicality, a brief discussion of the results of every experiment is reported in each of these sections, while a general discussion of our findings and their implications is reported in a dedicated chapter.

Chapter 4 - Discussion includes a broad commentary of the experimental results and ends with a concluding section that resumes the contribution and the novelty of the performed research.

Chapter 5 – Materials and Methods provides a complete description of the experimental materials and methodological techniques adopted in the studies. The chapter is divided

in four sections corresponding to the four experiments. Note that a specific neuroimaging data analysis technique was applied in each of the studies (i.e., seed-based resting-state functional connectivity in experiment 1; task-based fMRI in surface space in experiment 2; surface-based structural MRI in experiment 3; probabilistic tractography of diffusion-weighted data and structural connectivity estimation in experiment 4). For the sake of practicality and overall readability, these techniques are introduced in the chapter that describes the materials and methods of each experiment, rather than being presented into a single dedicated section.

Chapter 6 – References includes the complete bibliography in alphabetical order. Note that references are not divided by experiment.

Chapter 7 – Appendices comprises supplementary materials and results of the studies presented throughout the manuscript. Appendices also include the full list of scientific publications I authored or co-authored from the beginning of the PhD until September 2021. Some of these publications are relevant to the topics treated in the manuscript (e.g., neurobiology of second language representation and processing), but they lack the anatomical focus that is central to the present dissertation. Hence, while mentioned frequently, these studies are not treated in full length in the manuscript.

1.2 – MODELS OF CORTICAL DEVELOPMENT AND CORTICAL FOLDING

Introduction to the Cerebral Cortex

The human brain is the nervous structure on which all mental processes depend. It appears as a walnut-shaped complex organ, divided into two connected hemispheres. One of its most evident features is the intricate series of folds and fissures that compose the brain's outer surface, the cerebral cortex. These convolutions and depressions are respectively known as gyri (smooth rounded convexities bending outwards) and sulci (sharp concave furrows bending inwards). The longest and deepest sulci, such as the Sylvian and the Rolandic fissures, constitute evident landmarks that allow parcellating the cerebral cortex into large divisions known as “lobes” (frontal, parietal, occipital, temporal, limbic, and insular). Other superficial buckles and folds, as well as branches spurring from the major sulci, contribute to generating the overall complexity of the brain's surface, and determine “sulcation patterns”.

In the present dissertation, we will discuss stable and invariant aspects of the cerebral cortex morphology as well as other more ductile features that are susceptible to changes due to environmental factors.

The cerebral cortex corresponds to a ribbon of gray matter (GM) that surrounds and encapsulates the underlying white matter (WM). It extends for approximately 2500 cm² and has a regional thickness varying from 2.5 to 4 mm (Matelli and Umiltà, 2007). The GM cortex contains ~20% of all brain neurons (Lent et al., 2012). These neurons are supported by glial cells and blood vessels, with a glia/neurons ratio of ~1.48 (Herculano-Houzel, 2012a,b; von Bartheld et al., 2016). Up to 90-95% of the cerebral cortex of both adults and fetuses is constituted by the isocortex (or neocortex), while the remaining parts are defined allocortex (Matelli and Umiltà, 2007; Zilles and Amunts, 2012). The neocortex is arranged into six horizontal layers visible in cell body-stained sections (the only exception being the primary visual cortex and the agranular motor cortex, that show a different layering). This organization develops in utero and remains preserved in adulthood, with the six layers being classified as: i) molecular layer; ii) external granular layer; iii) external pyramidal layer; iv) internal granular layer; v)

internal pyramidal layer; vi) multiform layer. Each layer differs in the distribution of specific neurons, and in the efferent and afferent connections with cortical and subcortical structures. The cerebral cortex is also organized into vertical modules of synaptically interconnected cells, known as columns (Mountcastle, 1997). Columns tend to respond as functional units and the cells within one column share functional properties that are distinct from the ones of neighboring columns. Such columnar-specific functional correspondence is clearly noticeable in the visual and motor cortices. The six-layer organization of GM can also exhibit regional differences (e.g., in the cell density of one or more layers; neuron size; additional laminar subdivisions). These local differences have been used to divide the cerebral cortex into fields sharing the same organization and morphological features, forming cytoarchitectural maps (Brodmann, 1909). There are more than 50 cytological areas across the human brain, with both aspects of large similarity and difference with the cytoarchitecture of other primates such as macaque monkeys.

Interestingly, there is a certain degree of correspondence between sulcal patterns of the cerebral cortex, local cytology, and local functional activity. Post-mortem measurements have revealed a link between cortical sulcation and the microstructural organization of the cerebral cortex, suggesting that the fundus of a sulcus can sometimes act as a transition area between cytoarchitectonic fields (Fischl et al., 2008). This correspondence is particularly striking for primary motor and sensory areas, where the folds resulted more efficient predictors of sharp transitions between the Brodmann areas than previously thought (Zilles et al., 1997). Cytoarchitectural differences have been also observed between gyri, sulcal walls, and sulcal fundi (Welker et al., 1990). However, it should be noted that the relationship between macroscopic cortical landmarks and architecture is not established for all brain regions, and transitions are more frequently gradual than abrupt (Von Bonin and Bailey, 1961). As for the cytological-functional correspondence, electrophysiological mapping in humans and non-human primates has been used to reveal often precise overlap of cytoarchitectonic fields and local functional activity (see e.g., Penfield and Rasmussen, 1950; Vogt and Vogt, 1926). With technology and neuroimaging methods improvements, more studies have started investigating this association, allowing to gradually expand our knowledge

of this relationship (Bludau et al., 2014; Ruan et al., 2018; Weiner et al., 2017; Yeo et al., 2010).

Cortical gyrfication developmental trajectories

The degree of convolution and cortical complexity of the cerebral cortex is typically referred to as “Gyrification”. Gyrification varies from species to species. In mammals, the occurrence and the number of cerebral sulci range from the relatively lissencephalic brain of the muskrat and other rodents (absence of sulci) to the highly gyrified brain of primates and cetaceans (Welker, 1990). Comparative neuroanatomy suggests that larger animals have bigger brains, and that bigger brains tend to be more convoluted. It has been proposed that increased gyral folding permits the cortical surface area to expand scaling linearly with volume (instead of the expected two-thirds). This mechanism would allow the large cerebral cortex to fit inside of the small cranium. It seems plausible that animals with bigger and more gyrified brains should also show greater cognitive abilities. While the “bodyweight/brain size/brain gyrification” relationship is confirmed¹, the association between cortical folding and cognitive abilities is a much more complex point to demonstrate. Mammals with less gyrified brains have the same basic cortical circuits as mammals with highly gyrified brains. However, the former group has fewer, simpler, and less interconnected cortical areas than the latter, therefore linking gyrification with greater neural complexity and possibly cognitive abilities (Welker et al., 1990). In this context, the case of the human brain is particularly interesting. The human brain has often been depicted as “superior” to those of all other animals. On one side this affirmation may seem reasonable, given our experience as the most cognitively developed living species. On the other hand, the human brain weighs just 1.5 kgs, it is smaller than those of pachyderms and cetaceans, and compared with other primates it is not exceptionally different under many aspects. For all these reasons, the human brain has been redefined as “remarkable yet not

¹ *This relationship is generally true, however there are some exceptions such as the smooth brain of the big Florida manatee or the convoluted brain of the small least weasel*

extraordinary” (Herculano-Houzel, 2012a,b). Nonetheless, *homo sapiens* still represents the apex of the linear scaling of primate brains, which have proportionally more neuronal and non-neuronal cells than all the other species. In fact, primates have the most efficient neural scaling in the number of neurons/brain mass relationship. For comparison, a rodent brain of the same size would have sevenfold fewer neurons, and similar scenarios would happen also for larger brains like those of elephants or whales (Herculano-Houzel, 2012a,b). For this reason, the human brain stands out from all other mammals. Such achievement is obtained, among many other factors, through efficient cortical gyrification that allows packing a large surface area containing billions of neurons within the anatomical constraints of the human brain volume.

The mechanisms that determine the ontogeny of the folding patterns of the human cerebral cortex are partially known. A series of fundamental neural events anticipate the genesis of gyri and sulci in the foetal brain. The first stage, neurogenesis, corresponds to the formation and development of neurons from neural progenitor cells (neuroepithelial cells and radial glia) in the neuroepithelium of the neural tube. Once neuronal cells are mature, they migrate into their final cortical position in a stage known as migration, that paves the way for further cortical development (Marín et al., 2010). Neuronal migration occurs as early as the second month of gestation. In this stage populations of mature neurons move radially, ascending perpendicular to the neural tube and guided by astroglial cells, or tangentially, moving parallel to the neural tube. Once in the cortical plate, they stack in appropriate layers generating the cortical lamination. This is an inside-out process that occurs first for lower cortical layers and continues progressively for the more superficial ones (Cooper et al., 2013; Ronan and Fletcher, 2015; Welker et al., 1990; see also Rahimi-Balaei et al., 2018). This movement originates from the dorsal part of the ventricular system in the neural tube and gradually forms the two separated brain hemispheres. Neural migration is followed by neural wiring, which generates circuits of connected populations of neurons. Afferent axons innervate the cortical plate and participate in the formation of the structural connectome underneath the cerebral cortex.

This complex, yet elegant, mechanism determines a smooth lissencephalic cerebral cortex. Throughout foetal life, this minimal structure develops into one that is highly convoluted. According to Welker (1990), four types of macroscopic change can be

detected in the developing cerebral cortex: gyrogenesis, operculation, expansion, and lobation. Gyrogenesis corresponds to the rapid growth of specific portions of the brain that develop faster than neighbouring regions. This imbalance bends the cerebral cortex in a manner that sulci are generated between these newly formed gyri. Many biomechanical forces, as well as other structural features of the brain, are thought to participate in defining gyrogenesis. Further in this chapter, we will discuss different models of cortical development, and alternative causal mechanisms of gyrogenesis. Operculation, such as in the case of the insular cortex, occurs when a cortical region with relatively slow growth is “encapsulated” and hidden by other portions of the cortex spreading over it. Expansion occurs when subcortical regions and WM grow and extends underneath the cortical mantle, pushing the GM outwards. Finally, lobation corresponds to the overall growth and size increase of large brain regions such as the frontal, parietal, temporal, and occipital lobes. The conjoint occurrence of these processes and forces participates in shaping and defining the folding patterns of the cortical ribbon throughout neural development and continues after birth.

Gyrification develops following precise trajectories and can be measured with the Gyrification Index (GI). GI is generally intended as the ratio between the superficial (pial) and the outer contours of the brain cortex (Hogstrom et al., 2013), although other measures of GI exist (e.g. absolute mean curvature, Luders et al., 2006; 2012). GI can be intended as a comprehensive measure of gray matter volume (GMV). Significant, strong positive correlations have been reported between the two metrics, suggesting a noticeable degree of overlapping and interdependence (see Gautam et al., 2012, for a large correlational analysis on the relationship between distinct cortical measures in a sample of ~400 participants; see also Hogstrom et al., 2013; Lemaitre et al., 2012). Therefore, despite the lack of a one-to-one relationship, cortical curvature and complexity information expressed by GI are mostly dependent on the local GMV. As a matter of fact, cortical folding originates from forces generated during early brain development through processes that change brain volume. The folding starts around 10-15 gestational weeks with the development of primary sulci (e.g., central sulcus) and is followed by secondary (from the 32nd week) and tertiary sulci (36th week) (Chi et al., 1977; Dubois et al., 2007; Gholipour et al., 2017; Rajagopalan et al., 2011). GI increases as a function of gestational age and body/brain size. Armstrong et al. (1995)

have observed GI in 97 brains ranging from 11 weeks to 95 years. They reported that GI is very small in the second trimester and increases abruptly in the third trimester of gestation. After birth, gyrification continues to grow and reaches maximal GI at 5-6 postnatal months. After this overshoot, GI plateaus and decreases reaching adult levels at around 23-30 years (Armstrong et al., 1995; Cao et al., 2017). The GI remains largely stable throughout adult life and slightly decreases after midlife as an effect of aging. Aging causes the flattening and opening of the sulci, with regional vulnerabilities identified in the temporal lobes and frontal cortices (Cao et al., 2017; Dahnke and Gaser, 2018; Hogstrom et al., 2013; Jockwitz et al., 2017; Shen et al., 2018; Madan, 2021). Being GI largely correlated with GMV and other metrics, it is not surprising that both GM and WM volume decrease have been suggested to drive these aging-related alterations (Shen et al., 2018; Symonds et al., 1999), although the specific dynamics of cortical atrophy are still partially unknown. Overall, it has been suggested that GI trajectories after birth are relatively stable (with respect to other surface measures such as CT) and change nonlinearly as a negative logarithmic function of age (Cao et al., 2017). Several models have been proposed to describe the biomechanical and environmental factors that could induce and modulate cortical folding. In the next section, we discuss the principal models of brain gyrification.

Mechanisms at the origin of gyrification

Following Striedter et al. (2015), here we review a series of hypotheses that have been suggested to explain cortical folding, including tissue buckling from mechanical forces (Le Gros Clark, 1945), axon binding (Van Essen, 1997; 2020), localized proliferation (Kriegstein et al., 2006), and tangential expansion (Tallinen et al., 2014, 2016). However, it should be noted that numerous models have been put forward to explain the formation of cortical folds, such as genetic expression (Zilles et al., 2013), cerebral cortex growth (Toro and Burnod, 2005), thalamic axons (Rakic, 1988), and disparity of cortical thickness (CT) between cytologically different adjacent cortical areas (Le Gros Clark, 1945) (see Amiez et al., 2019; Welker et al., 1990). Since the full

description of these models is beyond the objectives of this dissertation, here we limit ourselves to presenting only the major theories reported by Streidter et al. (2015).

Skull constraints hypothesis (Le Gros Clark, 1945)

The first model we present is based on the work by Le Gros Clark (1945; see also Raghavan et al., 1997). The author observed that the skull rigidly encapsulates and constrains the brain. Therefore, gyrification would be a consequence of the resistance opposed by the cranium to the tangential growth of the brain during development. Once compressed onto the braincase, folding of the surface area would be the only possible remaining method for cerebral expansion and growth. This model has been disproven by the post-mortem analyses of lamb brains by Barron (1950). The author performed intrauterine surgical removal of portions of foetal brain in ewes. He observed that, despite the reduction of the cerebral volume, the surface area did not expand in the unoccupied cavities of the skull. Moreover, the remaining brain showed normal patterns of cortical folding, suggesting that the compression of the cerebral cortex against the skull is not necessary to determine surface gyrification. It should also be noted that the cranium ossifies only in the late stages of development, further disconfirming this hypothesis. If the skull impacts the brain gyrification, the size of this effect is probably minimal or negligible (Streidter et al., 2015).

Differential proliferation hypothesis (Kriegstein et al., 2006; Reillo et al., 2011)

The differential proliferation hypothesis is based on the positive correlation found between the quantity of progenitor cells in the developing cerebral cortex and cortical gyrification (Kriegstein et al., 2006; Reillo et al., 2011; Borrell, 2018). This hypothesis links the degree of cortical folding to the size of the subventricular (and outer subventricular) zone, a proliferative layer between the ventricular zone and the developing cortical plate, to the formation of sulci and gyri. Therefore, the subventricular zone would be thicker below forming gyri and thinner below forming sulci (Kriegstein et al., 2006). This cellular mechanism of cortical gyrification has been proposed to be a consequence of gene expression (Reillo et al., 2011; Borrell, 2018). A limitation of this model is that it posits that gyri originate because of increased CT,

which is in contrast to the notion that the cortex folds while maintaining relatively the same width (Striedter et al., 2015). While the genetically determined correspondence between progenitor cells and gyrification is a fascinating finding, this model is not exhaustive in explaining cortical folding and requires accounting for other biomechanical forces.

Tangential expansion hypothesis (Tallinen et al., 2014, 2016)

The general concept of the differential tangential expansion model is based on the idea that cortical folding is promoted by the faster tangential expansion of the outer cortical layers with respect to the deeper layers (Richman et al., 1975). Essentially, whenever adjacent cortical layers grow at different rates, mechanical forces and inconsistencies are generated along their points of contact, causing the cerebral cortex to wrinkle (Van Essen, 2020). So-called “buckling shell models” have been adopted to define and simulate cortical folding as a result of tangential expansion (Striedter et al., 2015). The outer layer of the cortex would represent a rapidly expanding “shell” anchored to a slowly expanding “core”. The degree of surface fissurization would then depend on the physical properties of both the shell and the core, such as the shell’s thickness and the rigidity of the deepest core layers (Ronan et al., 2014; Tallinen et al., 2014, 2016). At different stages of neural development, the core and the shell would be represented by distinct aspects of the forming cortex. The shell passes from consisting of the whole telencephalon to just the outer layers of the cortical plate. Similarly, in early development, the core is represented by subcortical proliferative zones and moves to WM and subcortical structures in advanced stages. The core and the shell are tethered by radial glial fibers and axons. Models based on the tangential expansion hypothesis are very popular, even if they generally do not explain the mechanism underlying the preferential directions of expansion of the cerebral cortex (Striedter et al., 2015)

Axonal tension hypothesis (Van Essen 1997)

Possibly the most well-known model of the biological mechanisms underlying cortical folding is the axonal tension hypothesis (also “Tensor-based morphogenesis”) suggested by Van Essen (1997, 2020). In this model, cortical gyrification is thought to

be a byproduct of the mechanical tension (i.e., “pulling together”) exerted along the preferred orientation of axons, dendrites, and glial processes that connect distant cortical regions. As the cerebral cortex expands tangentially and pushes against the brain’s hydrostatic pressure, axons would pull highly connected regions of the cortical sheet, generating gyri. In contrast, sulci would occur between areas that drift apart since the strength of their axonal connectivity is low. According to the author, cortical folding would represent the optimal configuration to reduce WM tension underneath the surface and improve connection time. This model entails a series of predictions regarding contrasting and compensatory forces that would shape the thickness of superficial and deep layers of the gyri and sulci. One of these predictions is that adjacent walls of a gyrus would be more connected together than with other gyri. Given this tension, a gyral cut in the radial direction would cause the tissue to spread. To test axonal strength within gyri, Xu et al. performed brain tissue cuts in mice and ferrets (2009, 2010). They observed that, while cuts in deep WM did, in fact, reveal considerable tension in long-distance axon bundles, gyral cuts did not cause the tissue to split in a way consistent with intra-gyral tension. These findings disconfirm the hypothesis that cortical folding could be driven by axonal tension. However, a recent reformulation of the model (Van Essen, 2020) emphasized that the results by Xu et al. are obtained *ex-vivo*, and therefore are of limited reliability. The axonal tension model has been further expanded and integrated with aspects of other models of cortical folding, such as the differential tangential expansion hypothesis (Tallinen et al., 2014, 2016; Van Essen, 2020). This new model mirrors the recently acknowledged concept that more than one force and biomechanical principle determine cortical folding. Only by integrating all the biological phenomena and mechanical forces that occur underneath and within the cerebral cortex it would be possible to define conclusive models of cortical gyrification (Striedter et al., 2015).

1.3 – INDIVIDUAL MORPHOLOGICAL VARIABILITY OF ANTERIOR CINGULATE CORTEX SULCATION PATTERNS

The present work focuses on the relationship between brain structure, brain functional activity, and cognitive abilities. The dorsal ACC (also dACC) represents an ideal candidate brain region for the investigation of this dynamic interplay. In fact, this structure is characterized by large individual morphological variability and plays a fundamental role in sustaining essential cognitive functions. In this section we provide a description of the neuroanatomical and neurofunctional features of the ACC and we focus on the literature on individual morphological differences of ACC sulcation patterns.

Parcellation models of the Cingulate Cortex

The cingulate cortex is the largest cortical region in the brain's medial wall. It is located above the Corpus Callosum (CC), the biggest WM tract which connects the two hemispheres allowing inter-hemispheric information transfer. The cingulate cortex extends rostro-caudally from the rostrum of the corpus callosum to its splenium. The ventral border of the cingulate cortex is typically identified as the callosal sulcus, while the dorsal border is generally considered the dorsal bank of the Cingulate Sulcus (CS, also "cgs") (Heilbronner and Hayden, 2016). Further in this chapter, we will assess more in detail the role of sulcation pattern variability in shaping the size and the anatomical borders of the cingulate cortex.

Macroscopically, the cingulate cortex appears as a unique continuous structure. However, because of its anatomical and functional heterogeneity, several models have suggested criteria to divide it into distinct subregions. The original dual-model proposed by Brodmann in 1909 was based on the cytological properties of the cingulate cortex and partitioned it into an anterior division (areas 24 and 32) and a posterior division (areas 25 and 31). This model was followed by many others over time. Vogt and colleagues proposed a three-region parcellation and then an updated four-region version of the same model (Vogt, 1993; Vogt et al., 2004; Vogt and Palomero-Gallagher, 2012). Vogt's model rapidly became widely adopted by the neuroscientific community and outshined other partitioning systems. According to the model, the cingulate cortex can

be divided rostro-caudally into the Anterior Cingulate Cortex (ACC), the Middle Cingulate Cortex (also referred to as Midcingulate Cortex, MCC), the Posterior Cingulate Cortex (PCC), and the Retrosplenial Cingulate Cortex (RSC), see Figure 1. This parcellation was obtained by combining information from histological results, cytoarchitectural features, anatomical connectivity, and functional mapping (Vogt and Palomero-Gallagher, 2012). While more complex and detailed partitions have been developed (see e.g., Beckmann et al., 2009; Glasser et al., 2016), the model by Vogt and colleagues remains a well-known reference for an easy-to-understand macroscopic division of the cingulate cortex.

In the present manuscript, we will focus on Vogt's ACC and MCC subregions of the cingulate cortex, the ones that are most affected by individual morphological differences in cortical sulcation.

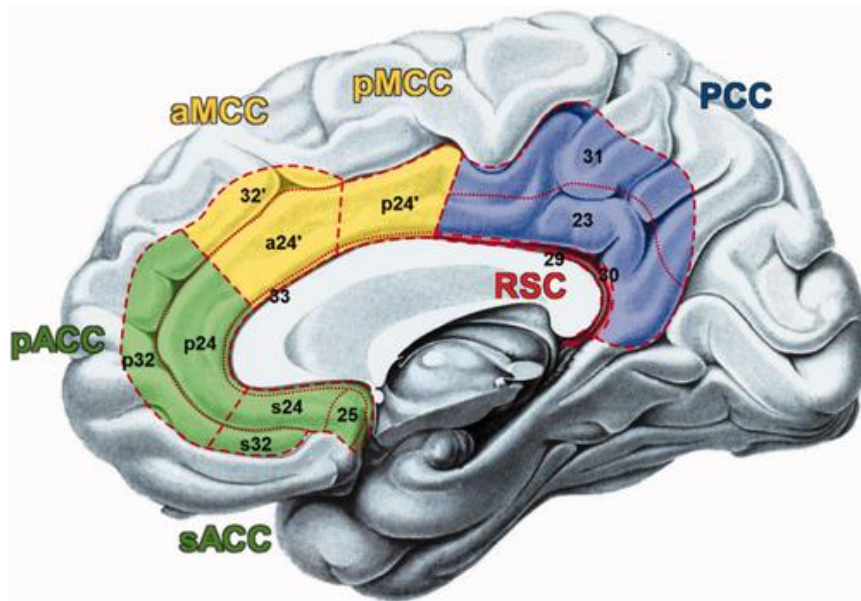


Figure 1. Vogt's Cingulate Cortex Parcellation. ACC (green) = Anterior Cingulate Cortex. pACC = perigenual ACC; sACC = subgenual ACC. MCC (yellow) = Middle Cingulate Cortex. aMCC = anterior Middle Cingulate Cortex; pMCC = posterior Middle Cingulate Cortex. PCC (blue) = Posterior Cingulate Cortex. RSC (red) = Retrosplenial Cingulate Cortex. Dashed lines = regional borders. Dotted lines = areal border. (The figure is adapted with permission from Hoffstaedter et al., 2014).

ACC

The ACC is the most rostral region of the cingulate cortex. It is ventrally delimited by the rostral sulcus and comprises Brodmann areas 33, 25, 24a, 24b, 24cv, 24cd, and 32. Because of its convex shape, the ACC extends both below (subgenual ACC) and above (pregenual ACC) the genu of the corpus callosum (Palomero-Gallagher et al., 2009). Diffusion-based tractography and anatomical dissection studies have assessed the structural properties of the cingulate bundle, a long WM tract that encompasses the cingulate cortex for all its length. Results revealed that the ACC is structurally connected with several subcortical regions such as the amygdala, the hippocampus, the hypothalamus, and the ventral striatum (nucleus accumbens). The ACC is also connected with cortical regions such as the orbitofrontal cortex and other portions of the cingulate cortex (Beckmann et al., 2009; Bubb et al., 2018; Stevens et al., 2011). These subcortical and cortical areas are known for their importance in

emotion regulation, autonomic functions, long-term memory, and reward processing. Therefore, it is not surprising that the ventral portion of the cingulate cortex has been frequently (and also quite simplistically) referred to as the “Emotional ACC”. This label can be debatable, as emotional processing involves numerous subregions within the cingulate cortex (including dorsal aspects), but functional evidence still largely concurs in highlighting the pivotal role of the ACC in the regulation and processing of autonomic arousal and emotional states (Vogt and Palomero-Gallagher, 2012; Stevens et al., 2011).

From a functional perspective, the ACC is of extraordinary interest. The most rostral and ventral part of the ACC, the ventromedial prefrontal cortex, is a core region of the Default Mode Network (DMN) along with insular, opercular, and temporo-occipital cortices. The DMN is a group of interconnected brain areas whose activity increases at rest and during “non-task” states (e.g., as self-referential processing and mind wandering) and decreases in attention-demanding goal-directed tasks (Raichle, 2015). Efficient cognitive functioning correlates with the strength of the connectivity within the DMN (Mak et al., 2017). Conversely, altered DMN connectivity has been reported for several pathological conditions including psychiatric disorders such as depression (Sheline et al., 2009) and anxiety (Zhao et al., 2017), neurodevelopmental disorders such as autism (Padmanabhan et al., 2017; Washington et al., 2014), and neurodegenerative disorders such as Alzheimer’s Disease (AD) (Greicius et al., 2004; Jones et al., 2011). These results highlight the role of the ACC as a central connectivity hub and its relevance in the overall functional organization of the brain. Experiment 1 investigates in detail the role of individual morphological variability of ACC sulcation patterns in modulating the functional connectivity of this structure.

MCC

Moving caudally from the ACC, the MCC corresponds to a large portion of the cingulate cortex that extends until the marginal sulcus and includes Brodmann areas 33’, 32’, and 24’. The apostrophe denotes that the cytoarchitectural properties of these areas in the MCC vary from those in the ACC, thus implying a discontinuity between the two subregions (Vogt et al., 1995). The MCC is structurally connected with the ventral and dorsal striatum (caudate nucleus and putamen), the parietal cortex, the

premotor cortex, the precentral gyrus, and the dorsal prefrontal cortex (Beckmann et al., 2009). The nature of these connections, including both motor and prefrontal areas, reveals the two major functional features of the MCC: motor functions and high-order cognitive functions. While not treated here in detail, meta-analyses of functional neuroimaging studies have also assessed that the MCC plays a relevant role in the processing of painful stimuli (Beckmann et al., 2009; Jahn et al., 2016).

Motor Functions

The interconnection of the MCC with motor regions is well-known from post-mortem and stimulation studies on non-human primates (Dum and Strick, 1993; Hutchins et al., 1988; Luppino et al., 1991; Morecraft and van Hoesen, 1992). More recently, functional neuroimaging has allowed identifying three specialized clusters of motor-related brain activity in the ACC and MCC in humans (Amiez and Petrides, 2014; Beckmann et al., 2009; Picard and Strick, 2001). Picard and Strick originally named these areas “anterior rostral cingulate motor zone” (RCZa), “posterior rostral cingulate motor zone” (RCZb), and “caudal cingulate motor zone” (CCZ). Interestingly, these functional cingulate motor areas seem to reflect a certain level of somatotopic organization that overlaps with the data on non-human primates. By adopting a motor paradigm, Amiez and Petrides (2014) revealed that RCZa and RCZb were involved in the hand, foot, saccadic, and tongue movements, CCZ was involved in hand and foot movements, while the supplementary motor area (SMA), located more dorsally, was active for all movements. The authors also observed a morphology-based modulation of the topological properties of these clusters of functional activity. This interesting finding and other similar results will be discussed in detail further in this chapter.

High-order Cognitive Functions

According to the widely recognized formulation by Botvinick et al. (2001, 2004), the MCC performs a continuous form of general conflict monitoring and evaluation of action outcomes. This region would become active in circumstances of conflicting information processing such as the presence of interfering information or

when two competing responses are concurrently activated. The MCC, along with other brain regions, would then participate in the resolution of the conflict and in the promotion of compensatory behavior. This model is in line with the findings of two recent meta-analyses of hundreds of neuroimaging studies that have observed an MCC involvement in inhibitory control (i.e., the ability to withhold and suppress prepotent but inappropriate responses) (Hung et al., 2018; Zhang et al., 2017). This executive function is fundamental for regulating a broad spectrum of cognitive processes that sustain efficient environmental adaptation such as perception, attention, and learning (Hung et al., 2018). With these premises, it is no wonder that the MCC has been so frequently referred to as the “Cognitive ACC” (as opposed to the “Emotional ACC” described above). Experiment 2 investigates in detail the role of individual morphological variability of MCC sulcation patterns in modulating the functional activity during inhibitory control.

An interesting example of conflict monitoring and resolution is represented by the simultaneous handling of two or more languages in bilingual individuals. Correctly switching from one to another while preventing other language intrusions requires the engagement of a network of brain areas highly involved in cognitive control (Abutalebi and Green 2016; Calabria et al., 2018; Green and Abutalebi, 2013; Kroll et al., 2005; Sulpizio et al., 2020). fMRI studies have shown that, among these regions, the MCC becomes particularly engaged during language switching and provides a central contribution to the monitoring and regulation of both linguistic and cognitive conflicts (Abutalebi et al., 2012; Branzi et al., 2016; Calabria et al., 2018; Luk et al., 2012; Worringer et al., 2019). The role of the cingulate cortex in sustaining language switching has been recently synthesized in our meta-analysis of 52 neuroimaging studies, confirming that activity in this region reflects increased monitoring demands (Sulpizio et al., 2020a).

However, the functional role of the MCC is not limited to conflict monitoring and resolution. A large corpus of neuroimaging studies has suggested that this region is involved in reward processing. It has been proposed that functional activity in the MCC precedes behavioural choices oriented towards a potential reward (e.g., a physical object or a goal). Therefore, the MCC would support the evaluation of the gains and costs of an action, and then participate in decision-making processes (Beckmann et al. 2009;

Arias-Carrión et al., 2010). This hypothesis is supported by experimental evidence from resting-state functional connectivity (rsFC). The MCC is included in a large-scale intrinsic connectivity network named “Salience Network” (SN, Menon, 2015). Along with the MCC, this network comprises the bilateral anterior insula, amygdala, ventral striatum, and ventral tegmental area, which are part of the dopaminergic system. This system guides behavioral choices towards available rewards, and it is of fundamental importance for motivation and learning (Arias-Carrión et al., 2010). These considerations are supported by the vast literature on the involvement of dopaminergic circuits in addiction disorders, and by the fact that dysregulation of this system is associated with risk-taking, sensation-seeking, and pathological gambling (Norbury et al., 2013; Volkow et al., 2004; Wise and Robble, 2020). The structural connections of the dopaminergic system constitute an anatomical foundation for the SN (McCutcheon et al., 2019). Within this network, the MCC plays a central role in modulating complex social behaviour and contributes to identifying and processing relevant stimuli by integrating emotional, cognitive, and sensory information (Seeley et al., 2007; Menon, 2015).

ACC-MCC complex labeling

The border between the ACC and the MCC is not clearly defined anatomically since no cortical sulcus can act as a landmark in setting the boundary between the two regions (but see Amiez et al., 2019 for insights on a possible sulcation-based model). Nonetheless, the ACC and the MCC are easily distinguishable from their functional and cytological features. This apparent ambiguity reflects the extensive haziness that revolves around the neuroanatomical labelling of the ACC-MCC complex. The term MCC has been introduced by Vogt in 1993 to identify a portion of the cingulate cortex often referred to as “Caudal” or “Dorsal” ACC, in contrast with the “Rostral” or “Ventral” ACC. While formally imprecise, this nomenclature still holds enormous popularity among the neuroimaging community and is probably more widely adopted than the term “MCC”. Note that the gyrosulcal variability of the cingulate cortex impacts both the ACC and the MCC (i.e., a paracingulate sulcus can be present in the ACC and not in the MCC; in the MCC and not in the ACC; or in both the ACC and

MCC). Therefore, throughout the present dissertation we will often refer to the ACC-MCC complex as “ACC”, and we will use the labels “dACC”, “caudal ACC”, and “MCC”, interchangeably. This practical choice is in line with the current literature on the ACC sulcal pattern variability. As a matter of fact, with few exceptions, most of the studies that have investigated this phenomenon refer to the whole ACC-MCC complex with the term “ACC”. Moreover, the labeling of the MCC is also subordinate to the adoption of a specific atlas in neuroimaging analyses which, in turn, frequently depends on the software used to perform such analyses. In the four experiments we present, we used the Desikan/Killiany Atlas (Desikan et al., 2006) for surface-based analyses and the Harvard–Oxford Atlas (Smith et al., 2004) for volume-based analyses. The first atlas divides the anterior part of the cingulate cortex into the “Rostral Anterior Cingulate” and “Caudal Anterior Cingulate” portions, corresponding, respectively to the ACC and MCC in Vogt’s nomenclature system. The second atlas synthesizes the ACC-MCC complex into a single area named “Cingulate Gyrus, anterior division”. This atlas is of particular relevance because, to our knowledge, it is the only popular parcellation explicitly accounting for the Paracingulate Gyrus (PCG), which will be discussed later in this chapter. We invite the readers to check for the adopted anatomical atlases in the material and methods section of each study whenever they might be uncertain relative to the labelling of specific cingulate region. When no further specified throughout the manuscript, it still holds the general rule that by using the term “ACC” we are referring to the whole ACC-MCC complex.

Paracingulate Sulcus

Definition of the Paracingulate Sulcus

In the preface of this dissertation, we have compared the medial wall of the brain to a fingerprint. This comparison conveys the idea that the cingulate cortex is characterized by large inter-individual morphological variability. The work of Ono et al. (1990) on 25 post-mortem brains is especially well known for having explored in detail the gyro-sulcal patterns of this region and for having brought community interest on this topic. The most easily recognizable landmark on the medial wall’s cortical surface is the

CS (Ono et al., 1990). The CS is a primary sulcus that develops in utero from the 14th gestation week and becomes easily recognizable from the 18th week (Chi et al., 1977; Dubois et al., 2008; Rajagopalan et al., 2011). Morphologically, the CS generally appears as a unique, long, and uninterrupted sulcus. However, it can occasionally be fragmented into smaller parts in ~42% of the population (data from Ono et al., 1990), and can also present several vertical branches (Paus et al., 1996a). A set of other smaller sulci, with their own branches and ramifications, typically occurs on the medial wall, including the rostral, marginal, and splenial sulci. Occasionally, a minor tertiary sulcus known as intralimbic sulcus can be present within the cingulate gyrus (Paus et al., 1996a; see also Amiez et al., 2019 for the occurrence of other smaller sulci). Although representing an interesting example of individual variability in cortical folding of the cingulate cortex, to our knowledge the literature on the intralimbic sulcus is extremely limited and it will not be further discussed in this dissertation.

Most relevant to the present work, a tertiary sulcus, the Paracingulate Sulcus (PCS, also “pcgs”), can be present in at least one hemisphere in 30 to 60 % of the general population (Paus et al. 1996a; Yücel et al. 2001, but note that this percentage may vary considerably between studies). The PCS is not usually found in neuroanatomy handbooks, and its first reference is allegedly the “paracingular sulcus” as mentioned by Smith in 1907. The etymology of this name comes from the shape of the PCS, which runs for most of its length dorsally and parallel to the CS. For the same reason, Ono defined the occurrence of a PCS as a “double parallel pattern”, in contrast with the “single” pattern when only the CS is present (1990). Being a tertiary sulcus, the PCS develops in utero during the third trimester of gestation (30th – 36th gestational weeks), hence much later than the CS (Dubois et al., 2008). Recently, a large study on monozygotic twins, dizygotic twins, non-twin siblings, and single children has established that the occurrence and hemispheric distribution of a PCS is associated with strong intra-uterine environmental factors and weak genetic factors (Amiez et al., 2018; see also Pizzagalli et al., 2020 for PCS - labeled “internal frontal sulcus” - heritability). The presence of a PCS is a recent evolutionary acquisition in primates. Amiez and colleagues (2019) have investigated individual variability in the cingulate cortex morphology in Old-world monkeys (rhesus monkey and baboon), and in Hominoidea (chimpanzee and human). Their findings revealed that: i) the PCS is not unique to

humans (as it was previously thought) but it can be found also in the brain of chimpanzees; ii) the occurrence of the PCS is more left-lateralized in humans than in chimpanzees (we will return to the PCS hemispheric distribution and asymmetry later); iii) the occurrence of the PCS is part of the evolutionary trajectory of the medial cortex expansion and organization, as it can be found in Hominoidea but not Old-world monkeys.

Morphological features of the PCS

While some quantitative aspects of the PCS may change over time (e.g., sulcal length and depth), the occurrence of the PCS remains stable throughout the life span and is unaffected by postnatal events (Cachia et al., 2016; Tissier et al., 2018). With respect to the CS, the PCS tends to be shallower and shorter (Paus et al., 1996b). Indeed, primary sulci tend to be deeper than tertiary fissures, which can occasionally manifest only as superficial dimples (Dubois et al., 2008). Interestingly, the occurrence of a PCS seems to impact the intrasulcal GM of the CS and the volume and surface area of the ACC, as revealed by an extensive analysis including hundreds of brains (Fornito et al., 2008; Paus et al., 1996a,b). When a PCS is present, the ACC volume is reduced by 39%, while the volume of the Paracingulate Gyrus is increased by 88% (Fornito et al., 2006). The Paracingulate Gyrus (“PCG”, also called Paracingulate Cortex) corresponds to the GM constrained between the fundus of the CS and the PCS in case of double parallel patterns (CS and PCS present), or to the GM on the dorsal bank of the CS in case of single patterns (only the CS present) (Fornito et al., 2008; Ono et al., 1990; Paus et al., 1996b; Vogt et al., 1995). This landmark definition has been adopted to solve the severe anatomical ambiguity in defining the dorsal constraints of the ACC-MCC cortex. This issue is of particular relevance for neuroimaging analyses, as the double parallel pattern has dramatic effects on brain parcellation algorithms in largely used neuroimaging software, and manual correction is often required (Mikhael et al., 2018). The length of the PCS may vary considerably from individual to individual, and Ono et al. (1990) suggested a widely used nomenclature based on its extension. According to the authors, a PCS is considered “absent” when is shorter than 20 mm, “present” when is comprised between 20 and 40 mm, and “prominent” when is longer than 40 mm. Segments divided by interruptions are considered part of the PCS only when the gap is

smaller than 20 mm; the gap length is not considered in the measurement. The most frequently adopted techniques for measuring a PCS are based on Garrison's manual measurement protocol (2015), and the automatic sulcal reconstruction via BrainVISA software (<https://brainvisa.info/web/>). The measurement of the PCS is complicated by its morphological variability. When the PCS is long and continuous, it is quite easy to detect and measure. However, the PCS can be fragmented into smaller parts scattered over the ACC-MCC complex. Moreover, some branches can occasionally join the CS, forming confusing anastomoses and adding a layer of ambiguity to the classification. To solve the neuroanatomical complexity of the PCS, Leonard et al. (2009) developed a comprehensive guideline including a series of frequently occurring morphological scenarios that should be adopted as a reference for accurate labeling of this sulcus. Besides, Garrison et al. (2015) suggested rigid criteria for the PCS measurement: i) T1-weighted volumetric images should be aligned to the bicommissural line (Anterior Commissure – Posterior Commissure; AC-PC); ii) the CS should be identified as the first major sulcus running in a rostro-caudal course, dorsally to the callosal sulcus, and recognizable for five continuous slices from the midline ($X = \pm 5$ mm); iii) the PCS is identified if running parallel, horizontal, and dorsally to the CS, and recognizable for three or more continuous slices; iv) the PCS is measured from the point in which the sulcus develops in a caudal direction to a vertical line perpendicular to the AC-PC line and passing through the AC; v) if the PCS continues after this line, it is measured until it ends; vi) fragments and interruptions are measured based on Ono's < 20mm criterium. While strict criteria exist, it seems evident that the classification and manual measurement of the PCS may be largely influenced by the rater's experience. For this reason, the PCS classification is typically performed by more than one expert rater and ambiguous cases are always expunged from the analyses. In recent years, deep learning algorithms have been successfully used to provide a more accurate and reliable classification of the PCS and will unquestionably become the gold standard in the near future (Borne et al., 2021; Yang et al., 2019).

PCS occurrence and cytological organization of the Cingulate Cortex

We have shown that the occurrence of a PCS on the brain's medial wall alters the local brain morphology. Remarkably, the impact of individual variability in cortical

folding is not limited to macroscopic changes. As a matter of fact, cortical fissurization is strongly intertwined with the microstructural organization of the cerebral cortex and is considered a reliable predictor of the brain's cytoarchitecture (Fischl et al., 2008). ACC double parallel and single patterns are associated with differences at the microstructural level. Evidence from post-mortem examinations has revealed that the occurrence of a PCS reshapes the spatial distribution of the 24' and 32' Brodmann areas in the cingulate cortex (Palomero-Gallagher et al., 2009; Vogt et al., 1995). When a PCS is absent (single pattern), the boundary between the two areas is buried between the dorsal and ventral banks of the CS. In contrast, when a PCS is present (double parallel pattern), this border is located more dorsally, on the PCG, while the area 24' covers both banks of the CS (Figure 2, 3)

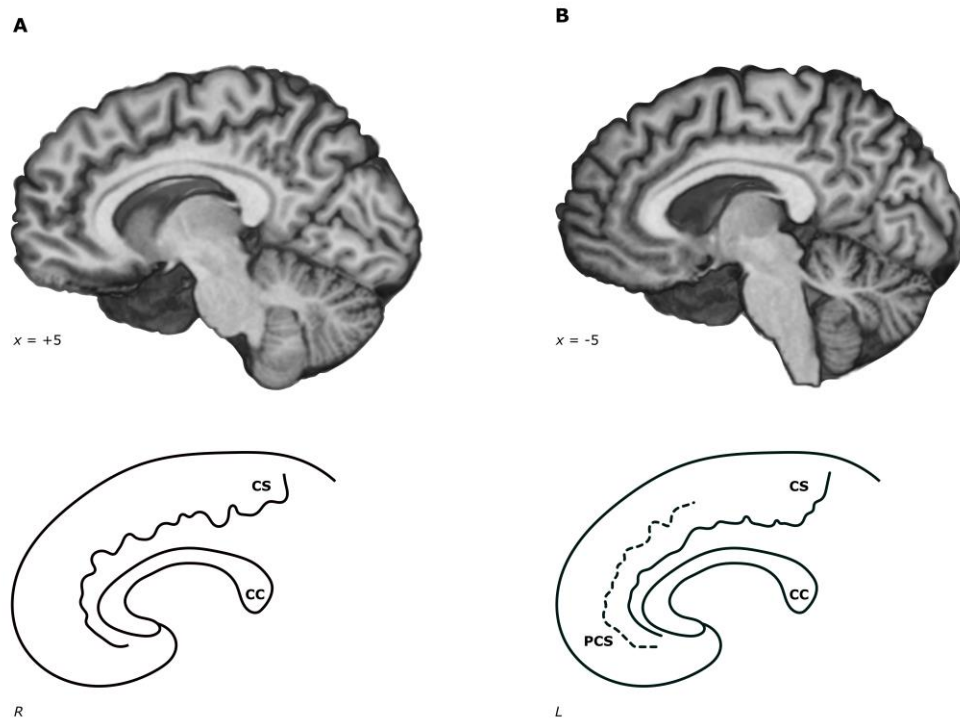


Figure 2. ParaCingulate Sulcus Occurrence. Skull-stripped brain of the same individual from the LEMON database (Babayán et al., 2016). Right hemisphere has been flipped on the X axis to better compare the two patterns. A) = Single (CS only) ACC sulcal pattern. B) = Double Parallel (CS and additional PCS) ACC sulcal pattern. CS = Cingulate Sulcus; PCS = Paracingulate Sulcus; CC = Corpus Callosum; R = Right; L = Left.

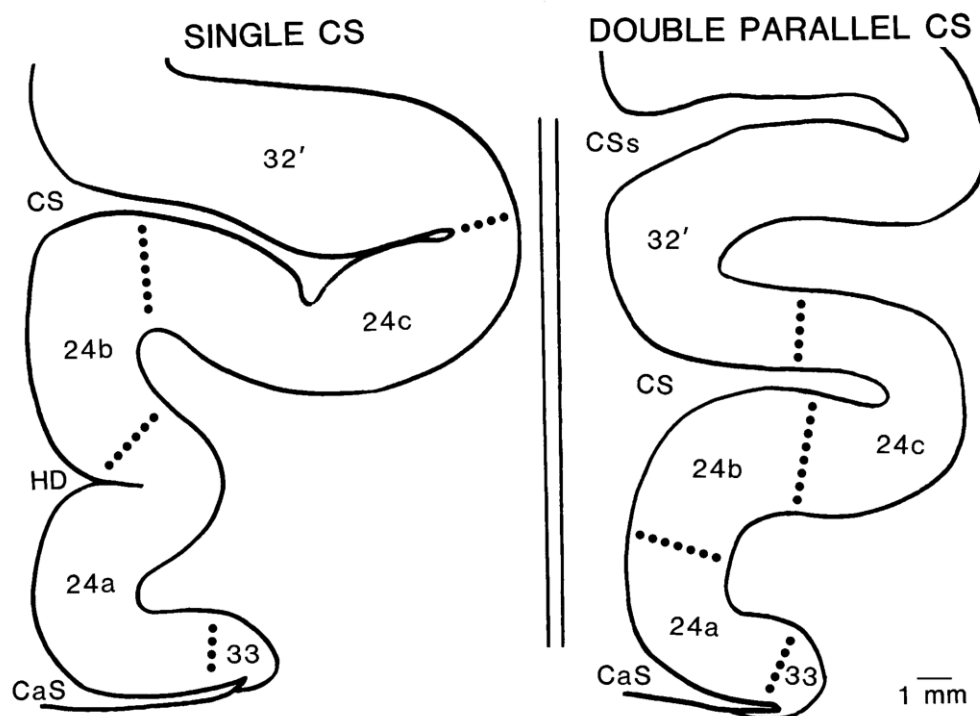


Figure 3. Anterior Cingulate Cortex coronal sections. Differences in ACC cytology and sulcal depth can be noticed between Single (left; CS only) and Double Parallel (right; CS and additional PCS) sulcal patterns. CS = Cingulate Sulcus; PCS = Paracingulate Sulcus. (The figure is adapted with permission from Vogt et al., 1995).

It should be noted that the presence of a PCS in double patterns doesn't correspond with a novel cytoarchitectonic area, but rather with an expansion of area 32'. These microstructural alterations are in fact associated with the cortical enlargement of the PCG (area 32'). Consequently, these changes may underlie the differences in GMV and surface area reported by Paus and colleagues (Amiez et al., 2019; Fornito et al., 2008; Paus et al., 1996a,b). Further in this chapter, we will discuss how differences in the microstructural organization of the ACC-MCC complex may also be related to the topological properties of local patterns of functional activity.

Hemispheric distribution of the PCS

The variable occurrence of a PCS leads to four anatomical patterns: (i) "single/single" or "double absence" ("SS" or "DA", when only the CS is present in

both hemispheres); (ii) “double parallel/double parallel” or “double presence” (“DD” or “DP”, when the CS and the PCS are present in both hemispheres); (iii) “leftward asymmetry” (when the PCS is present in the left hemisphere only); and (iv) “rightward asymmetry” (when the PCS is present in the right hemisphere only). The double absence and double presence patterns can be classified as “symmetric”, since both hemispheres show the same morphological features. In contrast, “leftward asymmetry” (LA) and “rightward asymmetry” (RA) patterns can be classified as “asymmetric”, since the two hemispheres show distinct morphological features. A PCS occurs in the left hemisphere in the double presence and leftward asymmetry patterns, while it occurs in the right hemisphere in the double presence and right asymmetry patterns.

It is largely established that the occurrence of a PCS is more probable in the left hemisphere, and leftward asymmetry is the most common pattern among the general population. This result has been confirmed by different research groups, considering thousands of brains overall (e.g., Amiez et al., 2019; Del Maschio et al., 2018a; Fornito et al., 2008; Leonard et al., 2009; Palomero-Gallagher et al., 2009; Paus et al., 1996a,b; Vogt et al., 1995; Wei et al., 2017; Yücel et al., 2001,2002). Recently, Amiez et al. (2019) reported that on a sample of 599 participants from the Human Connectome Project (HCP, www.humanconnectome.org/) a PCS occurred on the left hemisphere in the 58.3% of cases, while only in the 36.2% on the right hemisphere. Their results also showed that the frequency of leftward asymmetry was not modulated by handedness (but see Huster et al., 2007). Moreover, no significant effect of gender was found. With respect to gender, evidence is mixed, with other studies both in line with (Del Maschio et al., 2018a; Wei et al., 2017) and against this conclusion (Clark et al., 2010; Leonard et al., 2009; Yücel et al., 2001). Finally, ethnicity does not seem to be associated with differences in sulcal pattern distribution (Del Maschio et al., 2018a; Wei et al., 2017).

Compared with non-human primates, the greater occurrence of PCS leftward asymmetry seems to be a unique trait of our species (Amiez et al., 2019). It has been speculated that this morphological feature could be associated with functional hemispheric lateralization and specialization. Similar to what happens for other more known structural asymmetries, i.e., in the planum temporale and Broca’s area, this could be associated with advantages in language processing and other cognitive abilities. This interpretation is in line with known evidence of a modulation of the left cingulate

functional activity in language tasks (e.g., word generation) based on ACC sulcal profiles (see below; Crosson et al., 1999; Toga and Thompson, 2003).

Impact of the Paracingulate Sulcus occurrence on the functional activity of the Cingulate Cortex

In recent years, a growing wave of interest has surrounded the relationship between individual variability in cortical folding and its impact in modulating the topology of functional brain activity (Bijsterbosch et al., 2018; Bodin et al., 2018; Eichert et al., 2020; Miller et al., 2021a; Weiner et al., 2014). With respect to the cingulate cortex, solid evidence suggests that the spatial properties of task-related activity in the ACC are influenced by its sulcal anatomy. Crosson and colleagues (1999) showed for the first time that the spatial distribution of the brain's functional responses in a verbal fluency task was modulated by the variable occurrence of a PCS. The authors reported that when the PCS was absent, cingulate clusters of activation were centered on the CS. On the contrary, when the PCS was present, similar clusters of functional activity were centered on the PCS. The same difference in the topological organization was found for feedback-related functional responses in a trial-and-error learning task by Amiez and colleagues (2006, 2013). In this study, the percentage of BOLD (Blood-Oxygen-Level-Dependent) signal change measured from the clusters located in the CS (when PCS was absent) and in the PCS (when it was present) was very similar, showing that the two areas exhibited the same functional signature. The authors suggested that the functional activity originated from Brodmann area 32', which can be located on the dorsal banks of the CS in ACC single patterns or on the PCG in ACC double parallel patterns (Palomero-Gallagher et al., 2009; Vogt et al., 1995). Based on this interpretation, the two sulci should be considered as functionally homologous. Further studies have extended these findings to other functions, including saccadic and tongue movements (Amiez and Petrides, 2014) and pain processing and prediction errors (Jahn et al., 2016).

These results are in line with evidence that cortical sulci can represent morphological landmarks identifying cytoarchitectonic divisions and functional transitions (Fischl et al., 2008; Miller et al., 2021b; Passingham et al., 2002; Weiner et al., 2014). This macrostructural, microstructural, and functional relationship raises interesting

implications for the impact of sulcation pattern variability on cognitive abilities (Voorhies et al., 2021).

Impact of Sulcation Pattern variability on cognitive abilities

Different patterns of PCS hemispheric symmetry and asymmetry have been shown to significantly modulate the behavioral performance in a number of cognitive tasks. The impact of the hemispheric distribution of ACC sulcation patterns has been mainly investigated with respect to executive abilities such as inhibitory control and working memory (Borst et al. 2014; Cacia et al. 2014, 2017; Del Maschio et al., 2018a; Fornito et al., 2004; Huster et al. 2009; Tissier et al. 2018; Whittle et al. 2009). Other cognitive abilities showing an effect of ACC sulcation pattern distribution are verbal fluency (Fornito et al. 2004), and high order metacognitive abilities such as reality monitoring (i.e., ability of discerning memories coming from internal (imagined) or external (remembered) sources) (Buda et al., 2011). Collectively, these studies suggest that asymmetric patterns, with specific emphasis over leftward asymmetry, are typically associated with greater cognitive efficiency. This association can be traced back to the early stages of neural development. Cacia et al (2014) reported that 5-year-old children with asymmetric PCS patterns performed better in suppressing incongruent responses than age-matched participants with symmetric patterns in an animal Stroop task. On the other hand, working memory abilities were found to be similar among the two groups. This result indicates that sulcal asymmetry may be impactful on some executive abilities such as conflict monitoring and inhibitory control, but not with differences in others, such as the ability to maintain and manipulate information (however see Fornito et al., 2004 for a leftward-asymmetry advantage in adults in the spatial working memory CANTAB subtest; Owen et al., 1996). Similar evidence of an asymmetry-related advantage in inhibitory control was then confirmed in 9-year-old children using a color-word Stroop task (Borst et al., 2014; Tissier et al., 2018), and replicated in young adults with the Stroop and Flanker tasks (Cacia et al., 2017; Del Maschio et al., 2018a; Huster et al., 2014; Tissier et al., 2018).

This corpus of experimental evidence suggests that prenatally-determined and lifelong-stable individual differences in sulcation pattern variability constrain cognitive abilities

in the healthy population. It would be tempting to interpret this effect within a direct, deterministic, cause-effect framework. A 19th-century phrenologist could even support this claim providing remarkable anecdotal examples such as the pronounced PCS leftward asymmetry of Albert Einstein's brain (Men et al., 2014; here we must remind the readers that leftward asymmetry is also the most diffused pattern amongst the human population). There is, obviously, no such direct correspondence between cortical sulcation pattern variability and greater cognitive efficiency. Different neurobiological mechanisms have been suggested to possibly underlie the asymmetry-based advantage in the general population. Cachia and colleagues (2014) hypothesized that this effect is the reflection of a functional specialization caused by hemispheric lateralization and proposed an interpretation based on differences in intra- and inter-hemispheric connectivity between individuals with symmetric and asymmetric sulcation patterns. Experiment 1 digs into this idea, investigating the relationship between hemispheric symmetry and asymmetry of ACC sulcation patterns and the brain functional connectivity. Moreover, Experiment 2 examines in detail the relevance of ACC sulcation pattern distribution in modulating inhibitory control, providing for the first evidence of the neurofunctional correlates of the asymmetry-related advantage.

To further discourage a deterministic interpretation of this relationship, two considerations should be made regarding the size of the effect and the impact of environmental background. First, Cachia and colleagues reported that the PCS asymmetry was associated with 14% up to 27% of the behavioural interference scores variability in tasks involving inhibitory control (Cachia et al., 2014; Borst et al., 2014; Tissier et al., 2018). This finding indicates that, while significantly present, the extent of the impact of the ACC cortical folding on cognitive abilities is marginal to moderate.

Second, the work from Cachia et al. (2017), which we later confirmed and expanded (Del Maschio et al., 2018a), indicates that environmental factors can interact with and even revert this relationship. The authors tested whether the hemispheric distribution of ACC sulcation patterns predicted executive abilities differently when participants had distinct second-language experience. As we mentioned above, managing two languages and switching from one to another is an essential component of the bilingual experience. This effortful task requires the engagement of a dual language system that relies on a network of brain areas involved in cognitive control (Abutalebi and Green

2016; Calabria et al., 2018; Green and Abutalebi, 2013; Sulpizio et al., 2020a). fMRI studies have shown that, among these regions, the “dorsal Anterior Cingulate Cortex/pre-supplementary motor area” complex (dACC/pre-SMA) is particularly activated during language switching and provides a central contribution to the monitoring and regulation of both linguistic and cognitive conflicts (Abutalebi et al., 2012; Branzi et al., 2016; Calabria et al., 2018; Luk et al., 2012; Worringer et al., 2019). The dACC/pre-SMA complex corresponds to a portion of the MCC that entirely falls within the anatomical probability map of the PCG. Therefore, bilingualism seemed the ideal case-scenario to investigate the potential modulatory role of environmental experience on cortical folding – cognitive abilities relationship. Cuchia and colleagues (2017) compared the performance of bilingual and monolingual participants during a Flanker task, to measure individual differences in inhibitory control. The sample was stratified based on the cortical folding patterns. Results revealed that leftward asymmetry was associated with performance advantages (i.e., faster responses) in monolinguals, while symmetric patterns were associated with a detrimental effect. Bilinguals, however, showed an opposed pattern, with advantages correlated with symmetric, rather than asymmetric ACCs. We replicated the same “reverse” pattern by adopting a nine-times larger sample including different ethnicities, language groups, and age groups (Del Maschio et al., 2018a). Our results pointed towards a compensatory effect of bilingualism over invariant aspects of cortical anatomy, thus countering deterministic interpretations of the impact of sulcation pattern variability on cognitive abilities. Bilinguals tend to activate the bilateral ACC in tasks assessing executive functions (Abutalebi et al., 2012; De Baene et al., 2015), and bilingual experience is known to foster greater cingulo-frontal inter-hemispheric connectivity via the corpus callosum (Schlegel, Rudelson, and Tse, 2012). We hypothesized that, with respect to monolinguals, bilinguals would rely more on symmetric functional activity to sustain the cognitive efforts required by inhibitory control. This functional processing difference, anchored to structural connectivity organization and functional activity, would explain the positive association between symmetric patterns and executive efficiency in bilinguals.

Another relevant finding of Del Maschio et al (2018a) was that, irrespective of bilingualism, inhibitory control performance varied across age with larger interference

for older participants, and its increase was maximal for individuals with double absent sulcation patterns. Again, this result suggests that rather than being immutable, this relationship can change dynamically over time.

To summarize, a consistent, measurable, relationship exists between sulcal pattern asymmetry determined in utero and advantages in cognitive abilities throughout the life span. This relationship seems to depend on multiple factors, most probably brain functional and structural connectivity. Moreover, this relationship is affected by environmental factors such as second language experience and aging.

Relationship between patterns of Cingulate Cortex Sulcation and psychiatric disorders

We have discussed the wide impact of individual differences in ACC gyrosulcal variability in the healthy population. However, cortical folding has also been extensively investigated in relationship with neurodevelopmental disorders such as autism (Nordahl et al., 2007) and with psychiatric disorders. With respect to the latter, a vast literature focused on cortical folding abnormalities and psychotic disorders, the most known being schizophrenia. Symptoms of schizophrenia comprise hallucinations, delusions, disorganized speech, grossly disorganized or catatonic behavior, and negative symptoms (diminished emotional expression or avolition) (DSM 5th ed. American Psychiatric Association, 2013). Schizophrenia has been associated with both increased (Sasabayashi et al., 2019; Spalthoff et al., 2018; Falkai et al., 2007) and decreased (Kulynych et al., 1997; Nesvåg et al., 2014; Palaniyappan et al., 2011; Palaniyappan and Liddle, 2012) local gyrification with respect to healthy controls, pointing towards a multifaceted effect over the cerebral cortex morphology (Matsuda and Ohi, 2018). Most notably, increased gyrification (measured quantitatively, e.g., GI) has been reported in the ACC of schizophrenic patients (Sasabayashi et al., 2019; Matsuda and Ohi, 2018), and negatively correlated with patients' executive abilities. This result is in line with previous evidence of altered cognitive control in schizophrenia (Chambon et al., 2008) and suggests a neurofunctional impairment of the ACC in supporting executive functions. As for ACC sulcation patterns, reduced efficiency in executive functions in psychotic disorders has been associated with abnormal distribution, morphological features, and functional activity of the PCS. Schizophrenic individuals are less likely to exhibit the typical ACC leftward asymmetry than healthy controls and have diminished

cortical folding in the left hemisphere (Yucel et al., 2002a, b; Le Provost et al., 2003). Since leftward asymmetry is associated with advantages in executive functions such as inhibitory control and working memory, reduced frequency of this pattern has been suggested to explain cognitive disadvantages in psychotic disorders (Fornito et al., 2006). Moreover, ACC sulcation pattern abnormalities are accompanied by functional alterations. In a PET study, Yucel (2002a) observed that during a Stroop task healthy controls showed clusters of activations both over the CS and PCS. On the contrary, schizophrenic patients had hypoperfusion of the ACC, and increased activity only over the PCS (when present), but not of the CS. Moreover, the PCS was functionally engaged only in the right hemisphere in schizophrenic patients and never in the left. In case of PCS absence, Artiges et al. (2006) reported hypoperfusion of the bilateral ACC in a numerical task in contrast with healthy subjects that showed leftward lateralization. Taken together, these results show an interplay between brain activity and local morphology for schizophrenic patients that diverges from the neurofunctional binding observed in the healthy population, and concomitantly supports evidence of atypical leftward PCS asymmetry in schizophrenia.

Recent research has associated fragmented sulcal patterns in the ACC with hallucinations in schizophrenia (Cachia et al., 2015). Meredith and colleagues (2012) reported that interruptions of the CS are more frequent in individuals with (or high-risk of) schizophrenia in both hemispheres with respect to healthy controls. Moreover, Garrison and colleagues (2015, 2019) suggested that PCS morphology could be used as a biomarker to discriminate schizophrenic patients with or without hallucinations. A reduction in PCS sulcal length by 1 cm was associated with increased probability of hallucinations by 19.9%, independent of the sensory modality (e.g., auditory, visual) in which they were experienced (Garrison et al., 2015). Consistently, patients experiencing hallucinations exhibited significantly reduced gyrification in the medial prefrontal cortex and greater GMV near the PCS compared with matched patients without hallucinations. This finding is in line with those of Buda et al., (2011) suggesting that ACC sulcal patterns modulated reality monitoring in healthy individuals, a function that is compromised during hallucination episodes, and was negatively correlated with medial prefrontal GM (Buda et al., 2011). A tentative interpretation of this effect has been linked to altered connectivity within medial regions responsible for sensory

processing and decision-making induced by abnormal sulcal morphology (Garrison et al., 2015).

Overall, abnormalities of cortical sulcation patterns potentially represent an interesting, yet still largely unexploited, predictive biomarker of psychosis (Fornito et al., 2008), and could be possibly used for predated clinical preventive interventions.

1.4 NEURAL PLASTICITY: THE CASE OF BILINGUALISM

In the present dissertation, Experiment 1 and 2 focus on the impact of prenatally-determined individual differences in sulcal anatomy and the brain's functional activity and cognitive abilities. In the second half of the dissertation, Experiment 3 and 4 examine the dynamic interplay between the structural properties of the brain and the influence of experiential factors such as second language experience. In this section we define Neural Plasticity as an essential attribute of the brain. We then focus on bilingualism as a source of neural plasticity and provide a description of main neurobiological models of bilingualism. We conclude with a detailed description of the neurofunctional changes that happen as a consequence of second-language experience.

Neural Plasticity

Neural plasticity (or “Neuroplasticity”) is a core principle of brain organization. It represents the ability of the central nervous system to self-adjust and modify its functional and structural architecture as an adaptive response to protracted external and internal demands (Cramer et al., 2011; Dimou et al., 2013, see also Hebb, 1949). The term plasticity denotes that the brain can be metaphorically considered “ductile”, thus capable of enduring radical transformation without “breaking” its fundamental structure. Plasticity originates from a multitude of factors, including physiological demands, training and learning new skills throughout the lifespan, neural damage, and the emergence and neural development of brain functional and structural networks (Caroni et al. 2014; von Bernhardi et al., 2017). Neural plasticity occurs at different scales, ranging from the tens-of-nanometers size of neuronal synapses to the remapping of entire cortical functions (e.g., neurofunctional changes in the visual cortex of blind individuals, or the partial recovery of language functions in post-stroke aphasia).

Synaptic Plasticity

Two main processes have been identified as the base of synaptic neural plasticity: short-term plasticity and long-term potentiation. This subdivision is based

both on the timescale of changes that can occur in the brain and on the biological level that is affected by these changes.

Short-term plasticity happens at the synaptic level, in a temporal range that spans from tens of milliseconds to few minutes. It occurs because of previous activity in the synapse. Synaptic transmission is the biochemical mechanism that allows neuronal communication with other neurons and cells. During chemical synaptic transmission, presynaptic action potentials cause neurotransmitter molecules to be released from within the presynaptic terminal into the synaptic cleft. After the binding of the neurotransmitter molecules with specific receptors, a series of postsynaptic events are evoked. These reactions include the triggering of electrical responses in the postsynaptic neuron (von Bernhardt et al., 2017). Synaptic plasticity modulates the efficacy of this communication process, either by strengthening or weakening the synaptic transmission. Short-term facilitation increases the efficacy of synaptic transmission. It originates when a train of action potentials leads to an augmented probability of presynaptic terminals releasing neurotransmitters, or to an increase in the amount of release sites. Depending on their timescale, different types of facilitation have been defined, including sensitization (milliseconds), synaptic enhancement (tens to hundreds of milliseconds), and post-tetanic potentiation (30 seconds to minutes) (Barroso-Flores et al., 2017). Conversely, short-term depression corresponds to a decrease in the efficiency of synaptic transmission over time. It has been associated with habituation and sensory adaptation. Several mechanisms have been suggested to explain this phenomenon. Many authors agree that short-term synaptic depression occurs in response to very high stimulus frequency. Since action potentials induce the presynaptic release of neurotransmitter molecules, if the frequency is high enough vesicles are rapidly depleted. This leads to a systemic saturation that results in slowed transmission to allow vesicles replenishment and refilling (Barroso-Flores et al., 2017). Short-term biphasic plasticity happens when short-term facilitation is followed by short-term depression (Barroso-Flores et al., 2015, 2017).

It has been suggested that short-term synaptic plasticity may act as a source of temporal frequency filtering. Short-term depression would act as a low-pass filter (decreased responses as a consequence of excessively high frequent stimuli), short-term facilitation

as a high-pass filter (progressively increased responses for frequent stimuli), and short-term biphasic plasticity as a band-pass filter (Fortune and Rose, 2000).

With respect to short-term plasticity, long-term synaptic plasticity is much slower, occurring over minutes, hours, and even longer (Morris, 2003). Long-term plasticity is thought to be the primary biological mechanism that allows experience-dependent learning, memory formation, and behavioral adaptation, and has been associated with increase in volumetric increase of cortical and subcortical structures (Engert and Bonhoeffer, 1999; Yang and Calakos, 2013; Zatorre et al., .2012). It corresponds to the long-lasting enhancement of synaptic transmission efficiency, while long-term depression corresponds to a long-lasting reduction. Potentiation is achieved through protracted synchronous stimulation. The repeated synaptic transmission is associated with increased presynaptic release of neurotransmitter molecules and with changes in the quantity of postsynaptic receptors (Bekkers and Stevens, 1990; Yang and Calakos, 2013). The two processes combined over time generate a stronger link between neurons. Several studies have reported that long-term potentiation is associated with spinogenesis (i.e., the growth of new dendritic spines) and morphological changes in the postsynaptic dendrite spines. These structural modifications would promote a persistent improved electric signal transmission, increasing the amplitude of evoked postsynaptic potentials (Engert and Bonhoeffer, 1999; Yuste and Bonhoeffer, 2001). On the contrary, long-term depression would be associated with decreased presynaptic neurotransmitter release and with fewer postsynaptic receptors.

Long-term synaptic potentiation has been extensively studied in excitatory synapses of hippocampal neurons. Here, long-term potentiation is largely determined by the activation of the N-methyl-D-aspartate (NMDA) receptor complex and almost simultaneous postsynaptic depolarization (Paulsen and Sejnowski, 2000). This is achieved through the release and binding of glutamate immediately followed by a strong postsynaptic depolarization and the contribution of backpropagating action potentials. The temporal synchronization is essential to determine a long-term potentiation. The excitatory postsynaptic potential and the following action potential should occur within a 50 ms time window (Markram et al., 1997). This set of phenomena taking place in the hippocampal cortices is thought to determine the neuroplastic events that sustain the acquisition and storage of new memories and

associations (Takeuchi et al., 2014). Therefore, hippocampal long-term synaptic potentiation is a clear example of how neuroplastic changes, occurring at a microscopic scale, can affect brain functions and cognitive abilities on a much larger scale. It is noteworthy that neuroplastic effects induced by long-term potentiation, are not limited to the hippocampi, but may occur on other cortical and subcortical structures (Zatorre et al., 2012), inducing extensive changes in the brain structure and organization.

Neural Plasticity in brain structure and function

Brain plasticity is not limited to synaptic transmission. As a matter of fact, short-term and long-term synaptic plasticity represent two of the many biological mechanisms that contribute to the reshaping and self-adjustment of the main cerebral structures and neural networks. The diffusion of neuroimaging techniques has allowed revealing these macroscopic changes, providing structural and functional evidence of extensive neural plasticity (Lövdén et al., 2013; Sampaio-Baptista and Johansen-Berg, 2017; von Bernhardi et al., 2017; Zatorre et al., 2012).

Gray matter plasticity is thought to be caused by a combined influence of several factors including neurogenesis, axon sprouting, dendritic branching and synaptogenesis, gliogenesis, and changes in glial morphology, and angiogenesis (Zatorre et al., 2012). These changes are detectable and measurable since they impact tissue signal properties (e.g., relaxation time) and cortical morphology. Changes in cortical and subcortical GMV are typically observed with Voxel-Based Morphology (VBM) (Ashburner and Friston, 2000, 2005; Gaser and Dahnke, 2016). Surface-Based Morphometry (SBM) is also typically used to reconstruct a cerebral cortex surface mesh and investigate CT, surface area, and other features such as brain gyrification (Dale et al., 1999; Fischl and Dale, 2000; Gaser and Dahnke, 2016). The study on the hippocampus of London taxi drivers by Maguire et al. (2000; see also Maguire et al., 2006) is probably the most well-known example of GM experience-dependent neural plasticity. Through VBM analyses the authors reported that experienced taxi drivers had larger GMV in posterior hippocampi than controls. Moreover, the volume was correlated with the amount of driving experience, suggesting a neuroplastic effect developed over time. GM plasticity is not limited to navigation ability, as similar findings have been reported for a wide spectrum of experiences, including – but not limited to – juggling (Draganski et al.,

2004), musicianship (Bermudez et al., 2009), dancing (Hüfner et al., 2011), second language learning (Mårtensson et al., 2012), sports and physical activity (Erickson et al., 2014), meditation (Tang et al., 2020), and videogaming (Kühn et al., 2014). In the pioneering longitudinal study by Draganski et al. 2004, participants learned to perform the traditional three-ball cascade juggling routine. After three months of training, increased temporal and parietal GMV was detected by VBM. However, three months later, when participants had ceased to train, GM expansion was not visible anymore. The study, now considered a classic of neuroimaging literature, demonstrated that brain plasticity is a highly dynamic process. The increase in local cortical volume, as well as cortical thickening and surface expansion, is generally proportional to the training time and can appear/disappear even after relatively short periods. Besides, a relevant consequence of GM plasticity regards the aging population. Several studies have shown that prolonged performing of cognitive and physically demanding activity fosters both a neural and a cognitive reserve. These changes preserve individuals from pathological aging by slowing down the neurocognitive decline and age-related cortical atrophy (Benedict et al., 2013; Jochem et al., 2017; Müller et al., 2017).

Of note, despite its remarkable stability and resilience to environmental effects, recent research has suggested that also cortical gyrification may be impacted by neural plasticity to some extent. Bangert and Schlaug (2006) revealed that musicianship was associated with altered morphometric characteristics of the “omega-sign” anatomical feature of the precentral gyrus related with hand movement representation. Li et al. (2009) suggested that these changes are age-dependent, as a negative association has been reported between plastic effects in the hand area of the central sulcus and the age of onset of musical training. More recently, Luders and colleagues (2012) evaluated the degree of cortical folding in experienced meditation practitioners and controls. The authors revealed greater gyrification in the anterior insula, precentral gyri, precuneus, and bilateral fusiform gyrus, and a positive correlation between gyrification of the anterior insula and years of meditation. While still largely unexplored, these findings pave the way for future research on the relationship between neural plasticity and cortical folding.

Similar findings of have been observed when investigating learning effects in WM. Neural plasticity in WM occurs as the result of changes in fiber organization, such as

the number of axons, axon diameter, packing density, axon branching and sprouting, axon trajectories, and myelination (Zatorre et al., .2012). These changes are generally measured by fitting a model to diffusion-weighted imaging data. The most adopted model is the diffusion tensor (diffusion tensor imaging, DTI), an ellipsoid that indicates the direction and the rate of diffusion of water molecules in the brain (Jones et al., 2013; Soares et al., 2013). DTI allows to determine microstructural indexes such as fractional anisotropy (FA) and mean diffusivity (MD). MD indicates the overall amount of diffusion, while FA is a scalar measure representing the degree of anisotropy of water diffusion (i.e., how much water diffusion is constrained in one direction) and is associated with axonal diameter, fiber density, and myelination. Since water molecules diffusion is relatively limited in myelinated axons, the tensor assumes a characteristic shape and direction that can be used as a basis to perform fiber tracking and reconstruct the white-matter pathways. In Experiment 4 we will discuss diffusion-weighted imaging modeling and WM tractography, highlighting the intrinsic limitations of DTI. However, DTI is a relatively easy-to-implement technique that has allowed defining WM neuroplastic effects in a variety of contexts. Exactly like for gray-matter plasticity, also WM plasticity is associated with a variety of experiences such as musicianship (Bengtsson et al., 2005), juggling (Scholz et al., 2009), second language learning (Hosoda et al., 2013), etc. Such changes generally manifest as an increase in local WM FA and/or a decrease in MD. These microstructural effects are thought to reflect greater axonal myelination and enhanced axon packing density and can occur even after a relatively short time (e.g., hours) (Sampaio-Baptista and Johansen-Berg, 2017). Axonal myelination is one of the main mechanisms that increase the communication speed along neural fibers, permitting action potentials to travel long distances more rapidly. Therefore, WM plasticity would promote faster information transfer and stronger connectivity between brain regions. In older adults, WM tends to decline after 50 years of age, although stimulating activity can preserve its integrity and slow some negative effects of aging (Colmenares et al., 2021; McPhee et al., 2019; Sexton et al., 2014, 2016).

Another form of neural plasticity regards changes in brain functional activity and connectivity as measured by functional MRI during cognitive tasks and at rest. Functional plasticity is strongly linked with structural neuroplastic alterations in the

brain. However, measures of functional plasticity provide unique insights on changes in brain information processing and transfer. Some forms of functional neuroplasticity can occur naturally in the brain with healthy aging. Increasing age is associated with alterations of the brain activity and connectivity patterns that would typically sustain specific cognitive abilities in younger adults (Greenwood, 2007). Older adults show both hyper- and hypo-activations of cerebral networks, as well as occipital to frontal activity shifts, and reductions of functional hemispheric lateralization, when compared with younger controls. These changes are thought to reflect compensatory mechanisms when paired with relatively preserved cognitive performance (Grady, 2008; Cabeza 2002). Several neurocognitive models have been proposed to describe these neurofunctional alterations, although a complete understanding of aging-related functional plasticity is still far to be reached (Cabeza, 2002; Davis et al., 2007; Festini, Zahodne, and Reuter-Lorenz, 2018). In addition to this naturally occurring phenomenon, other forms of brain functional plasticity exist. A striking example of neuroplastic changes is represented by neurofunctional shifts in post-stroke aphasia. Recent methodological development (Fedeli and Abutalebi, 2019) has allowed studying post-stroke brain reorganization (Balaev et al., 2016; Nair et al., 2015; Sebastian et al., 2016; Sharp et al., 2010; Warren et al., 2009; Yang et al., 2017) and the efficacy of rehabilitative treatments (Gili et al., 2017; van Hees et al., 2014), demonstrating changes in inter- and intra-hemispheric functional connectivity. As an example, in a recent review on the role played by the two brain hemispheres during aphasia recovery, Anglade, Thiel, and Ansaldo (2014) presented a model of the functional activity changes through the recovery stages. Minor lesions would be associated with activation of the perilesional left hemisphere and with better recovery in the chronic stage. Moderate lesions would induce a right hemisphere activation during the sub-acute phase and a shift back towards the perilesional tissue in the left hemisphere during the chronic phase, resulting in partial recovery. Finally, when this could not be possible because of extensive damage over the left hemisphere encompassing primary language areas, the right hemisphere homologous regions would be recruited, though resulting in a less efficient recovery process. This model suggests dynamic processes of brain neuroplastic reorganization that can be altered by several factors such as lesion size and location. In most cases, however, neurofunctional plasticity is not uniquely a compensatory

consequence of extreme events such as vascular stroke, or cortical reorganization following the hearing, sight, or limb loss (Bedny et al., 2015; Bramati et al., 2019; Dormal and Collingnon, 2011; Singh et al., 2018a). Changes in the functional organization can frequently occur as an epiphenomenon of experience-based learning (Groussard et al., 2010; Guerra-Carrillo et al., 2014; Gurunandan et al., 2019; Hübner et al., 2011), that may manifest in many ways, including – but not limited to – activation of supplementary area, increased functional connectivity, and reduced activation as a sign of functional efficiency.

In the next section, we will present bilingualism as an ideal scenario for studying experience-related neuroplastic changes in the brain, including both structural and functional reorganization as the result of second language learning. The topic of brain plasticity and bilingualism will be further explored in Experiments 3 and 4.

Bilingualism

Bilingual individuals are able to acquire, store, access, and use two or more languages (Del Maschio and Abutalebi, 2019)². Bilingualism a widespread phenomenon, as many individuals know or are exposed to a second language.

Bilinguals generally use a main language (L1), which is commonly the speaker’s native language, and a second language (L2), which is commonly acquired later in life (i.e., “sequential bilinguals”, Butler and Hakuta, 2004). There are many exceptions to this general definition, as bilinguals can learn two languages at birth (i.e., “simultaneous bilinguals”), or even lose their native language because of reduced exposure and linguistic isolation (i.e., second language attrition, Köpke and Schmid, 2004; Schmid and Jarvis, 2014; Schmid and Köpke, 2017; see also Gallo et al., 2019, 2021). Therefore, it is evident that bilingual experience is not limited to knowing and using two languages, but it entails numerous factors that contribute to individual profiles of linguistic abilities throughout the lifespan. Earlier definitions of bilingualism tended to restrict this phenomenon to a dichotomic classification of bilingual and monolingual

² for the purposes of discussion herein, we use the terms 'bilingual' and 'multilingual' interchangeably, although the latter is generally referred to as the knowledge and usage of more than two languages.

individuals (Kremin and Byers-Heinlein, 2020). Empirical findings may result from a dichotomous classification of bilingual and monolingual participants and the adoption of inconsistent thresholds of language experience. Moreover, grouping different linguistic profiles based on a binary labeling could hide important aspects of the individual bilingual experience. Finally, focusing on a single trait of bilingualism may prevent discovering whether (and to what extent) other dimensions interact in shaping experience-dependent plasticity. Therefore, according to a growing literature bilingualism should be considered as a spectrum with multiple components, including (at least) the age of second language acquisition (L2 AoA), the quantity and context of second language input (L2 Exposure), and the second language expertise (L2 Proficiency) (see e.g., DeLuca et al., 2019; DeLuca, Rothman and Pliatsikas, 2019; Leivada et al., 2021; Surrain and Luk, 2019).

In the last two decades, neuroimaging has allowed to vastly increase the knowledge on the neural correlates of bilingualism. Previous studies, based on neuropsychological testing of bilingual individuals with brain lesions, suggested that multiple languages would be represented in distinct brain regions. However, it has been generally established that multiple languages share largely overlapping neural representations and that the neurobiology of bilingualism affects language and executive networks. In our recent Activation Likelihood Estimation (ALE) meta-analysis of 52 fMRI studies, we investigated brain activity involved in bilingual processing of lexico-semantic, syntactic, and phonological input (Sulpizio et al., 2020a). We observed that brain activity for the two languages shared common temporal, parietal, and frontal cortical regions in line with acknowledged models of dual-stream language processing (Hickok and Poeppel, 2004, 2007). However, the processing of lexico-semantic information in L1 seemed to be sustained by a wider network of cortical and subcortical areas, especially for late L2 AoA. Conversely, the processing of L2 input involved also regions associated with executive control, such as the globus pallidus as part of the basal ganglia. This finding is consistent with knowledge of bilinguals adopting top-down executive processes to monitor linguistic output and processing, detecting linguistic conflict, inhibiting linguistic intrusions, and switching from one language to another (Abutalebi and Green, 2007, 2016; Green and Abutalebi, 2013). In our meta-analysis, we also investigated brain activity during language switching, with results

further confirming the critical role of the executive network to face two-language interactional context demands. In line with the model of adaptive control model by Green and Abutalebi (2013, see Figure 4), we observed brain activity in prefrontal and parietal cortices, as well as the ACC and SMA complex, and caudate.

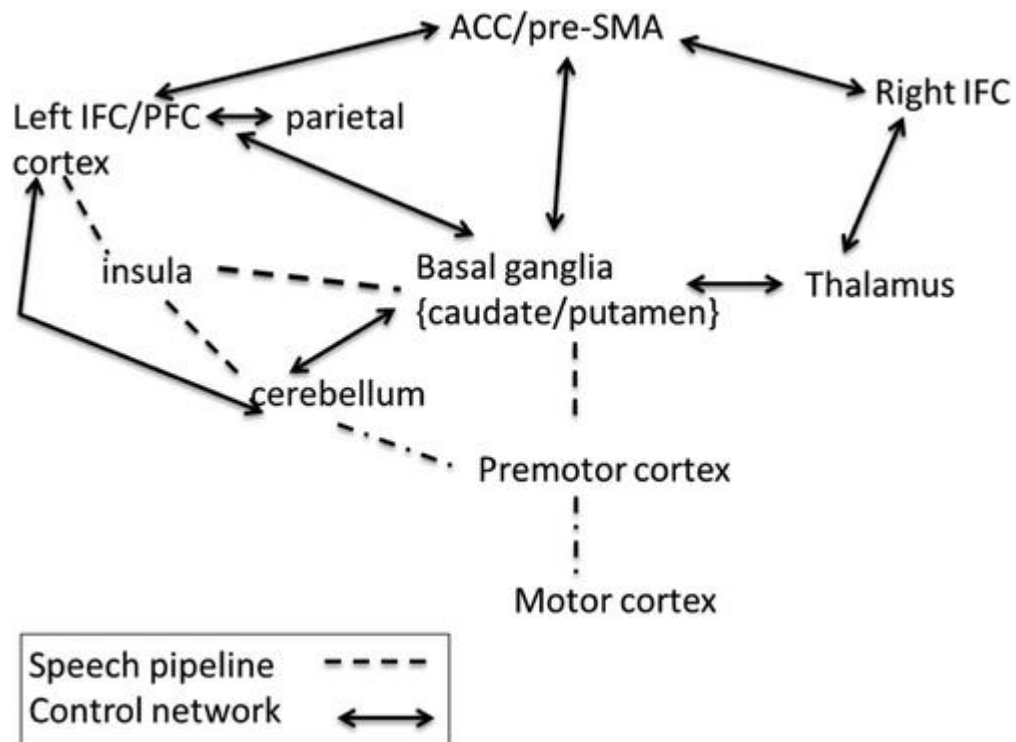


Figure 4. *Language control network and speech production regions according to the Adaptive Control model. IFC/PFC = Inferior Frontal Cortex/Prefrontal Cortex; ACC/pre-SMA = Anterior Cingulate Cortex/pre-Supplementary Motor Area. (The figure is adapted with permission from Green and Abutalebi, 2013).*

The extensive recruitment of the executive network represents a neural signature of bilingualism. This process, protracted over time, imprints structural and functional changes to the brain architecture that can be observed by means of neuroimaging techniques. It has also been speculated that, because of their enduring experience of managing two or more languages, bilinguals may have superior executive abilities with respect to monolinguals. The existence of such “bilingual advantage” is currently a highly debated topic in cognitive science, with evidence both in favor of and against it (Lehtonen et al., 2018; Van den Noort et al., 2019). Here we limit ourselves to discuss bilingualism as an ideal example of neural plasticity, without further exploring whether such advantage exists.

Structural and Functional neural plasticity in second language learning and bilingualism

Evidence of brain neurofunctional reorganization and plasticity has been widely confirmed in L2 learning (Osterhout et al., 2008) and bilingual experience (see Pliatsikas, 2019a for a review). VBM and SBM have been used to investigate both cross-sectionally and longitudinally changes in GMV and cortical features (i.e., thickness and surface area) in L2 learners and bilingual individuals. Results suggest local GM increases in cortical and subcortical regions that are involved in executive functions, such as the ACC-MCC complex, dorsolateral prefrontal cortices, inferior parietal lobules, and basal ganglia (i.e., putamen and caudate nuclei) (Abutalebi et al., 2012; Della Rosa et al., 2013; DeLuca et al., 2019; Legault et al., 2019a,b; Mechelli et al. 2004; Stein et al., 2012). In a pioneering study, Mechelli et al. (2004) observed that, with respect to monolinguals, bilingual individuals had greater GM density in the left inferior parietal lobule, a region important for language selection and monitoring. Moreover, GM density in that region was positively correlated with L2 proficiency and negatively with L2 AoA, pointing towards a structural reorganization dependent on the second language experience. More recently, by adopting a longitudinal paradigm, Legault et al., (2019) observed that changes in CT and GMV emerged throughout two semesters of L2 learning in young adults. After four months from the start of the course, participants showed increased CT in the left ACC and right middle temporal gyrus. Expanded middle temporal CT was positively correlated with the accuracy score in a language decision task. Moreover, CT changes in the ACC were also positively associated with functional connectivity between ACC and middle temporal gyrus. Together, these results indicate a dynamic relationship between L2 lexical acquisition, L2 proficiency and neuroplastic alterations in regions relevant to lexico-semantic processing and language control.

Moreover, comparative studies with monolinguals suggest that lifelong bilingualism is linked with preserved GM and CT in structures that are typically vulnerable to aging, such as the temporal pole (Abutalebi et al., 2014; Li et al., 2017; Olsen et al., 2015, see also Del Maschio, Fedeli, and Abutalebi, 2018, and Perani et al., 2017). In a recent experiment (Del Maschio et al., 2018c) we observed that in both younger and older

highly proficient bilingual adults GMV was consistently higher than monolinguals in regions of the executive network. Moreover, we found a behavioural advantage on the Flanker task, which requires efficient cognitive control, for bilingual older adults compared with monolingual controls. Therefore, we suggested that age-dependent decrease in cognitive abilities following GMV deterioration in the executive network appears hampered in bilingual individuals and that bilingualism acts as a source of both neural and cognitive reserve. Experiment 3 delves deeper into the neuroprotective effects of bilingualism while extending the knowledge of second language experience's impact on cortical gyrification.

Underneath the cortex, WM is also largely affected by bilingual experience (Table s1 in appendices reports a comprehensive list of studies that have used diffusion-based imaging to investigate WM neuroplasticity in bilinguals).

Overall, bilingualism seems to impact a variety of WM tracts, connecting fronto-temporo-parietal regions in the two hemispheres. Both longitudinal and cross-sectional studies on L2 learning report increased FA in the bilateral Inferior Frontal Occipital Fasciculus (IFOF), Superior Longitudinal Fasciculus (SLF), the and the CC (Hosoda et al., 2013; Kuhl et al., 2017; Luk et al., 2011). These findings support dual-stream models of language representation (Hickok and Poeppel, 2004; Saur et al., 2008), and models of executive networks required for efficient dual-language control (Abutalebi and Green, 2016; Calabria et al., 2018).

Hosoda and colleagues (2013), demonstrated in a longitudinal study that these changes can occur even after relatively short periods of L2 training (i.e., a 16-weeks L2 training), but can revert to pre-training levels if not maintained over time. These results suggested that bilingualism is a powerful source of WM plasticity. However, since brain plasticity is a highly dynamic phenomenon, protracted second-language experience is required to retain these changes. Lifelong bilingualism can arguably induce more long-lasting alterations of the neural architecture. Neuroprotective effects in bilingual individuals (e.g., preserved WM volume and microstructural integrity with respect to monolingual controls) have been observed in frontal regions, in the CC, and in the SLF and inferior longitudinal fasciculus (ILF) (Olsen et al., 2015; Luk et al., 2011). Moreover, these changes are associated with more distributed functional connectivity, implying a multimodal protective effect of the brain's neurofunctional organization

(Luk et al., 2011). These findings suggest that bilingualism may well act as a source of neural reserve, potentially decelerating cognitive consequences associated with brain aging (see also Perani et al., 2017). Neural reserve has been described as the resilience to the natural age-dependent decline and pathology of the human brain (Barulli & Stern, 2013).

Despite these accounts of bilingualism-induced WM plasticity, our knowledge of this phenomenon is still limited. In Experiment 4 I explored the influence of different second-language experiential factors (i.e., L2 AoA, Proficiency, and Exposure) on brain structural connectivity. This study largely expands our previous findings on WM microstructural properties of the bilingual brain (Del Maschio et al., 2019b), and simultaneously provides new methodological insights to better understand bilingualism-induced neuroplastic changes in brain organization.

Task-based fMRI has been extensively adopted to investigate dual-language processing. However, it is only very recently that researchers turned to resting-state connectivity as a tool to investigate bilingualism-induced functional plasticity. Most of these studies have focused on individual variability in bilingual experiential factors such as L2 AoA and proficiency (e.g., Berken et al., 2016; DeLuca et al., 2019; DeLuca, Rothman and Pliatsikas, 2019; Gullifer et al., 2018; Sun et al., 2019). We recently contributed to this topic by investigating the combined impact of L2 AoA, Proficiency, and language Entropy (i.e., a proxy measure of dual-language usage) on functional connectivity at rest in a sample of bilinguals (Sulpizio et al., 2020b). We observed that greater bilingual experience corresponded with stronger connectivity between regions of the language and executive network, including temporal, parietal cerebellar, and subcortical areas. These findings suggest that specific linguistic profiles correspond with a neuroplastic modulation of the dialogue between the areas that sustain language representation and those that are considered to be involved in language monitoring. Moreover, we observed significant interactions between factors, in particular for the effect of AoA, which was modulated by proficiency and entropy. Our findings highlight the dynamic plasticity that occurs in the brain's network organization and reveal the importance of considering bilingualism as a continuous and multi-componential phenomenon.

Overall, these findings suggest that bilingualism acts as a powerful source of change in the brain, impacting both its structural and functional architecture across the lifespan. Therefore, it represents an ideal scenario for investigating experience-related neural plasticity.

1.5 – EXPERIMENT 1 (INTRODUCTION): “SULCAL PATTERN VARIABILITY AND DORSAL ANTERIOR CINGULATE CORTEX FUNCTIONAL CONNECTIVITY ACROSS ADULT AGE”

This section refers to the study “*Sulcal pattern variability and dorsal Anterior Cingulate Cortex functional connectivity across adult age*”³ by Fedeli et al., 2020. The study was inspired by the pioneering exploration of ACC functional connectivity by Margulies et al., 2007. By adopting a similar methodological approach, we provided the first description of the influence of individual variability in cortical folding on the functional architecture of the dorsal portion of the ACC. Our results highlighted a relationship between brain structure and function that partly traces back to the early stages of brain development but is susceptible to changes throughout the lifespan.

As mentioned in section 1.3, the dorsal part of the ACC includes both portions of the anterior and middle cingulate cortices (Vogt & Palomero-Gallagher, 2012). This region mediates a set of regulatory functions essential for executive control and environmental adaptation (Botvinick et al., 2001; Bush et al., 2002; Sheth et al., 2012). Moreover, the ACC-MCC complex exhibits an extensive morphological variability in sulcal patterns, the set of gyri and sulci that gives the cortical ribbon its unique convoluted shape. While quantitative measures of the cortical surface can change, sulcal patterns in this region (i.e., the PCS) are determined prenatally and are invariably stable throughout the lifespan (Cachia et al., 2016; Tissier et al., 2018). The longitudinal stability of ACC sulcal patterns and its imperviousness to neuroplastic changes represent ideal features for investigating individual variability in structure-function mappings.

³ Fedeli, D., Del Maschio, N., Caprioglio, C., Sulpizio, S., & Abutalebi, J. (2020). *Sulcal Pattern Variability and Dorsal Anterior Cingulate Cortex Functional Connectivity Across Adult Age*. *Brain connectivity*, 10(6), 267-278. <https://doi.org/10.1089/brain.2020.0751>

Previous studies have reported that ACC gyrosulcal morphology influences the topological distribution of task-related clusters of functional activity (Amiez et al., 2013; Crosson et al., 1999; Jahn et al., 2016). Nonetheless, it is still utterly unknown whether variability in sulcal pattern might alter the functional organization of the ACC-MCC complex at rest. In this study, we combined structural MRI and seed-based rsFC to investigate the impact of ACC sulcal pattern variability on the local functional architecture. Furthermore, since rsFC varies considerably as aging (e.g., Chen et al., 2016; Damoiseaux, 2017), we inspected age-related changes in the relationship between ACC gyrosulcal variability and ACC functional connectivity. We considered a large sample consisting of 173 healthy adults (age range = 20-80), and we examined cross-sectionally the interaction between dACC sulcal pattern and age on rsFC.

Given previous accounts that variability of ACC sulcal morphology could be predictive of cognitive abilities (e.g., Borst et al., 2014; Cachia et al., 2014; Fornito et al., 2004; Tissier et al., 2018), we examined whether differences in connectivity profiles linked with sulcal pattern variability influenced participants' performance on a set of cognitive tasks.

Based on previous task-based reports (Jahn et al., 2016; Lopez-Persem et al., 2019), we hypothesized that different profiles of rsFC would be associated with distinct ACC sulcal patterns. We also suggested that this relationship could change as aging, because of specific structure-function interactions in young and older participants. Finally, the neural correlates underlying the known association between ACC morphological variability and executive functions are still poorly understood. We tested the correlation between ACC morphology and cognitive abilities as mediated by ACC functional connectivity to explore this mechanism.

1.6 – EXPERIMENT 2 (INTRODUCTION): “ACC FOLDING PATTERNS VARIABILITY MODULATES NEUROFUNCTIONAL ACTIVITY AND BEHAVIORAL PERFORMANCE DURING INHIBITORY CONTROL”

This section refers to the study "*ACC folding patterns variability modulates neurofunctional activity and behavioural performance during inhibitory control*" which, as of September 2021, has been submitted for publication in a peer-reviewed journal of the field (Fedeli et al., submitted). In experiment 1, we revealed a significant relationship between ACC morphological variability and functional connectivity at rest. Here, we turned to ACC neurofunctional activity during tasks involving inhibitory control. The main finding of this study is the first description of the neural signature of the behavioural advantage that has been often found in individuals with asymmetric ACC sulcation patterns when performing executive tasks. This result suggests that variability in brain morphological features determined prenatally can influence the brain's neurofunctional organization in a way that impacts cognitive abilities in adults.

Executive Functions are versatile control abilities necessary for environmental adaptation and the regulation of cognitive processes (Friedman et al., 2011; Miyake and Friedman, 2012). A fundamental executive function is inhibitory control, the ability to delay or suppress a thought or action intentionally. This function is often evaluated by examining participants' ability to refrain from producing a prepotent response (i.e., "response inhibition", RI). Successful inhibition requires participants to remain aware of the ongoing performance and consciously suppress inappropriate responses (MacLeod, 2007; Miyake and Friedman, 2012; Munakata et al., 2011). In everyday life, inhibitory control is necessary to promote flexible and effective adaptations to environmental demands that occasionally require one to interrupt spontaneous but inappropriate behavioural responses, e.g., not crossing the street if a car passes, even if the pedestrian traffic light is green. Functional neuroimaging research has repeatedly shown that RI engages a network of prefrontal areas, including the ACC (Botvinick et al., 2001, 2004, see also Hung et al., 2018 and Zhang et al., 2017 for large meta-analyses). As mentioned in the introduction, the ACC-MCC complex plays a central role in detecting, monitoring, and mediating conflicting information during a task. This area continuously updates cognitive strategies that promote behavioural adjustments and optimizations

crucial for inhibitory control (e.g., action withholding and cancellation) (Hung et al., 2018). A growing literature of behavioural studies has explored the relationship between ACC and RI by focusing on the role played by the extensive interindividual morphological variability of the ACC. In this study, we aimed to investigate for the first time the association between the interindividual variability in ACC sulcal patterns and brain functional activity during tasks assessing RI.

As detailed in section 1.3, the most distinguishable morphological feature of the ACC is the variable occurrence of the PCS, a tertiary sulcus that runs dorsal and parallel to the CS. Crucially, the interhemispheric distribution of the PCS is determined in utero and persists unchanged throughout the life span, being largely unaffected by post-natal brain development and environmental influences (Cachia et al., 2016; Li et al., 2013, 2014; Tissier et al., 2018). Remember that, based on the hemispheric occurrence of the PCS, one can classify ACC sulcal patterns into two discrete categories: PCS asymmetry (when the PCS is present in one hemisphere but not in the other) and PCS symmetry (when the PCS is concurrently present or absent in both hemispheres) (Cachia et al., 2014; Fornito et al., 2004; Huster et al., 2009; Whittle et al., 2009).

Behavioural studies have examined the relationship between ACC sulcal pattern variability and RI in healthy subjects employing the Stroop (Stroop, 1935) and the Flanker tasks (Eriksen, 1974; Fan et al., 2002, 2005). Cachia and colleagues (2013) reported that 5-year-old children with asymmetric ACC sulcal patterns had a better interference score (i.e., incongruent vs. congruent trials) during an animal Stroop task, both in terms of lower response times (RTs) and greater accuracy, when compared with age-matched children with symmetric ACC sulcal patterns. Similar results were found by adopting the classic color-word Stroop task in 9-year-old children (Borst et al., 2014; Tissier et al., 2018) and young adults (Huster et al., 2014; Tissier et al., 2018). In these studies, ACC sulcal patterns explained from 14% up to 27% of the behavioural interference scores variability (Cachia et al., 2013; Borst et al., 2014; Tissier et al., 2018), indicating a moderate but relevant association between individual morphological variability and RI efficiency. Similar reports of an advantage in RI associated with asymmetric PCS were also described for the Flanker task (Cachia et al., 2017; Del Maschio et al., 2018a). Taken together, these results suggest behavioural differences in inhibitory control between individuals with symmetric and asymmetric ACC sulcal

patterns and point towards asymmetry-related cognitive advantages that can be backtraced to the early stages of neural development.

What remains largely unknown is whether a clear neurofunctional signature backs up the asymmetry-related advantage reported in the literature and how ACC sulcal pattern variability impacts the local brain activity while performing tasks involving RI. In this study, we aimed at investigating this association, potentially providing the first account of a direct link between prenatally determined ACC variability, functional activity, and differences in behavioural performance. Individual differences in ACC morphology have been previously reported to modulate brain connectivity at rest (see experiment 1, Fedeli et al., 2020), as well as the topological distribution of local task-related clusters of functional activity during decision-making (Amiez et al., 2013), saccadic and tongue movements (Amiez and Petrides, 2014), word generation (Crosson et al., 1999), and pain processing (Jahn et al., 2016) (see section 1.3). While these findings are not specific for tasks involving executive functions, they represent an excellent argument to hypothesize an association between ACC sulcal pattern variability and brain activity modulation during RI. In line with the tasks adopted in the previous behavioural literature, in this study we utilized the Attention Network Task ("ANT"; Eriksen, 1974; Fan et al., 2002, 2005) to investigate the "Flanker" effect and the Numerical Stroop task (also referred to as "Counting Stroop task"; Stroop, 1935; Bush et al., 1998; Windes, 1968) to investigate the "Stroop" effect. The two tasks require distinct, although related, dimensions of inhibitory control, respectively "Attention Constraining" (i.e., suppressing interfering information) and "Attention Restraining" (i.e., suppressing automatic responses) (Unsworth et al., 2009, 2012, 2014; Unsworth and Spillers, 2010). During the ANT, participants must answer based on the direction of the central arrow in a string of stimuli, ignoring arrows flanked oppositely. This task requires Attention Constraining since participants must consciously constrain their focus to a target presented among distractors and suppress interfering information (i.e., suppressing the interference originating from arrows flanked in the opposite direction during incongruent trials). During the Numerical Stroop task, participants must indicate how many items compose a series of identical numbers or alphabetical characters while ignoring automatic responses based on the number values. This task implies Attention Restraining since participants must refrain from answering with prepotent but

inappropriate automatic responses in favor of new, goal-directed alternatives (i.e., suppressing the automatic answer "three" when presented "3 3 3 3" in an incongruent trial).

A sample of 42 participants performed the ANT and the Numerical Stroop task inside an MRI scanner. We used surface-based event-related fMRI (Brodoehl et al., 2020) to explore differences in brain activity between individuals with symmetric and asymmetric ACC sulcal patterns. We adopted Delta plot analyses (i.e., plotting the difference between task conditions as a function of RT; de Jong et al., 1994; Ridderinkhof, 2002, 2004) as an analytical tool to further explore temporal dynamics of RI in the two groups.

In line with previous findings, we expected greater efficiency in RI for participants with asymmetric profiles than symmetric profiles (i.e., faster RTs and better accuracy). Similarly, we expected participants with asymmetric profiles to show more pronounced evidence of efficient RI in delta plots. Concerning the functional activations, increased ACC dorsal activity has typically been associated with higher cognitive loads and increased task difficulty (Shenav et al., 2014; Botvinick et al., 2004; Paus et al., 1998). Therefore, we expected more significant functional activity in dorsal portions of the ACC associated with poorer inhibitory control in participants with symmetric sulcal patterns. We limited our analyses to the cingulate and prefrontal cortices to detect clusters of brain activity that would reveal cortical folding-dependent effects only in regions typically involved in RI (see Hung et al., 2018). Finally, we performed brain-behaviour correlations to test the relationship between ACC functional activity and task efficiency.

1.7 – EXPERIMENT 3 (INTRODUCTION): “THE RELATIONSHIP BETWEEN BILINGUAL EXPERIENCE AND GYRIFICATION IN ADULTHOOD: A CROSS-SECTIONAL SURFACE-BASED MORPHOMETRY STUDY”

This section refers to the study "*The relationship between bilingual experience and gyrification in adulthood: a cross-sectional surface-based morphometry study*"⁴ by Del Maschio et al., 2019a. The main finding of this experiment is the difference in the degree of cortical gyrification preservation as aging in bilingual individuals compared with monolingual controls. While in the first half of the dissertation experiments 1 and 2 focused on the impact of anatomical variability on brain function and cognitive abilities, we studied this relationship in the opposite direction, moving from lifelong invariant neural features to experience-related neural plasticity. The present study results highlight the role of bilingualism (intended as a measure of environmental experience in the context of the present dissertation) in modulating even very stable structural features of the brain, such as cortical folding.

Previous in this dissertation, we defined neural plasticity as the adaptive ability of the brain to modify its structure and functional activity as a response to protracted external and internal demands. The acquisition of a second language is a complex experience known to foster neuroplastic changes in GM and WM (Coggins et al., 2004; Osterhout et al., 2008). L2 learning involves acquiring additional linguistic information and mastering the abilities required to select and manage two concurrently activated languages based on the communicative context (see Calabria et al., 2018; Pliatsikas, 2019b; Sulpizio et al., 2020a,b). As mentioned in section 1.4, longitudinal studies have reported that L2 learning fosters neuroplastic effects in young adults in regions that sustain lexico-semantic processing and language control (Hosoda et al., 2013; Legault et al., 2019; Mårtensson et al., 2012). These findings are in line with cross-sectional comparisons between bilingual and monolingual older adults. Older bilingual adults show preserved brain integrity in the cingulate cortex and frontoparietal regions, which are associated with executive control and dual-language processing (e.g., Del Maschio

⁴ Del Maschio, N., Fedeli, D., Sulpizio, S., & Abutalebi, J. (2019). *The relationship between bilingual experience and gyrification in adulthood: A cross-sectional surface-based morphometry study*. *Brain and language*, 198, 104680. <https://doi.org/10.1016/j.bandl.2019.104680>

et al., 2018c; Del Maschio, Fedeli, and Abutalebi, 2018; Luk et al., 2011). These differences likely emerge from the lifelong protracted cognitive efforts required by the concurrent management of multiple languages (e.g., language inhibition, language shifting, and language monitoring, see Abutalebi and Green, 2016). Moreover, neuroprotective effects of bilingualism also occur in networks that are vulnerable to age-related atrophy, such as regions of the anterior temporal cortex supporting the formation, access, and retrieval of semantic memory (Abutalebi et al., 2014; Olsen et al., 2015). Preserved GMV within these regions allegedly results from higher cognitive and mnemonic demands that are necessary for the processing of a more extensive vocabulary in bilinguals (Abutalebi et al., 2014; Perani et al., 1998). Besides, several studies have suggested that the appearance of dementia symptoms are delayed in bilingual when compared with monolingual controls (e.g., Alladi et al., 2013; Bialystok et al., 2007; Perani et al., 2017). On these grounds, bilingualism might act as a source of neural reserve in older adults.

In this study, we investigated for the first time the impact of dual-language experience on cortical gyrification, a comprehensive measure of GMV that accounts for cortical curvature, from young adulthood to older age. Of note, previous studies on bilingualism-induced effects on the cortical GM have mostly used VBM (Ashburner and Friston, 2000), which is based on a volumetric modelization of the cerebral cortex. With respect to VBM, recently developed methods of cortical surface reconstruction offer additional and more detailed information on structural features of the cerebral cortex and its morphometric alterations as aging (Lemaitre et al., 2012). SBM entails a detailed representation of the cortical surface to measure additional parameters such as CT and gyrification. Thus, SBM may reveal itself as a valuable tool to investigate new neuroanatomical correlates of neural reserve associated with the dual-language experience. Besides, aggregate indices such as GMV may not necessarily mediate an age-related effect on cognitive abilities in bilinguals (Del Maschio et al., 2018c; Gold et al., 2013). Additional measures of cortical complexity, while still accounting for GMV expansion and shrinkage, may likely act as modulators of cognitive performance across the lifespan in bilingual individuals. As mentioned in section 1.2, brain gyrification is a quantitative measure that provides relevant information about variations on the cortical surface throughout the lifespan (e.g., Cao et al., 2017; White et al., 2010). Although

cortical folding emerges in fetal life and plateaus at birth (Armstrong et al., 1995; Chi et al., 1977), brain gyrification is a comprehensive measure of GMV that dynamically reflects the interplay between early neurodevelopmental mechanisms, experience-related reshaping, and neural decline during aging. Recent morphological studies on experienced musicians and meditators have reported that the impact of prolonged learning and training is not limited to GMV and WM changes but also affects cortical folding (Bangert and Schlaug, 2006; Li et al., 2009; Luders et al., 2012). These studies were primarily focused on environmentally-induced plasticity and did not investigate gyrification-cognition relationships. Still, growing literature shows that higher gyrification might positively affect cognitive abilities such as mental flexibility and working memory (Gautam et al., 2015; Green et al., 2019; Liu et al., 2012). At present, the precise neurobiological mechanism underlying this advantage is still largely unexplored. However, models of cortical folding presented in section 1.2 indicate that greater gyrification would be associated with a larger number of neurons, due to increased GMV, or faster neural communication thanks to the optimized axonal length between distant gyri (Chklovskii et al., 2002; Klyachko and Stevens, 2003). Considering these factors, we hypothesized that a cognitively stimulating experience such as bilingualism might modulate cortical gyrification in structures involved in dual-language processing and susceptible to age-dependent shrinkage. Therefore, we expected evidence of maintained gyrification in these structures and a potential association with preserved cognitive efficiency.

In this study, we focused on a network of cingular, frontal, and parietal regions that are known to be related with executive control, as well as temporal lobe structures supporting mnemonic functions. We investigated the whole-brain and local effects of L2 experience on cortical gyrification throughout the adult lifespan by comparing a large sample of bilingual and monolingual individuals. We used the ANT (Fan et al., 2005) to test executive abilities in our sample of participants and explore potential bilingualism-dependent effects on the relationship between cortical gyrification and cognitive abilities.

Finally, we tested the relationship between the local gyrification index and L2 AoA and proficiency to explore bilingualism-mediated cortical plasticity further. We hypothesized that older adult bilinguals would show maintained gyrification when

compared with monolingual controls in executive and temporal lobe structures and that these differences would be associated with the degree of second language experience.

1.8 – EXPERIMENT 4 (INTRODUCTION): THE BILINGUAL STRUCTURAL CONNECTOME: DUAL-LANGUAGE EXPERIENTIAL FACTORS MODULATE DISTINCT CEREBRAL NETWORKS

This section refers to the study “*The bilingual structural connectome: Dual-language experiential factors modulate distinct cerebral networks*” by Fedeli et al., 2021⁵. The main finding of the research is that individual differences in second language experience in bilingual individuals modulate the brain structural connectivity in specific networks. The experiment starts from the premises of experiment 3 and continues investigating the relationship between brain structure, function, and linguistic abilities. Our results expand the knowledge about environmental factors related with neuroplastic variations in brain structural properties and provide an exemplar depiction of the complex dynamics of neural plasticity.

Of note, we published a pilot version of this study (Del Maschio et al., 2019b) assessing a similar topic but with different sample and techniques. As a matter of fact, experiment 4 includes a larger sample of participants and expands the findings of this study by adopting a more advanced – and insightful – methodological framework. Hence, I opted to include only Fedeli et al., 2021 in the present dissertation.

WM comprises myelin-coated bundles of axons that allow efficient information transmission between adjacent and distant cerebral structures. WM circuits are remarkably predisposed to experience-dependent structural adjustments, even after "critical periods" of higher plasticity (Sampaio-Baptista and Johansen-Berg, 2017). Recently, increased interest has surrounded bilingualism-induced WM changes, with a growing number of studies measuring microstructural differences between bilingual and monolingual groups and longitudinal effects of L2 learning (Pliatsikas, 2019a; see also table s1 in appendices). In section 1.4, we described that L2 processing engages frontotemporal brain areas involved in language representation and requires top-down executive control to solve context-dependent linguistic competition arising from two concurrently activated languages (e.g., Abutalebi and Green, 2007; Hermans et al.,

⁵ Fedeli, D., Del Maschio, N., Sulpizio, S., Rothman, J., & Abutalebi, J. (2021). *The bilingual structural connectome: Dual-language experiential factors modulate distinct cerebral networks*. *Brain and Language*, 220, 104978. <https://doi.org/10.1016/j.bandl.2021.104978>

1998; Marian and Spivey, 2003). Besides, L2 proficiency and L2 onset are critical factors in modulating the cognitive efforts necessary for efficient bilingual communication (Del Maschio and Abutalebi, 2019; Sulpizio et al., 2020a). In line with these considerations, previous neuroimaging studies reported that bilinguals show microstructural enhancement of WM circuits proposed by dual-stream models of language representation and dual-language executive control (Abutalebi and Green, 2016; Calabria et al., 2018; Hickok and Poeppel, 2004; Saur et al., 2008). However, some cross-sectional and longitudinal studies reported inconsistent (Cummine and Boliek, 2013; Kuhl et al., 2016; Singh et al., 2018b) or opposite evidence (Elmer et al., 2011; Gold et al., 2013), suggesting reduced FA in bilinguals in IFOF, SLF, and CC. The majority of these studies utilized Tract-Based Spatial Statistics (TBSS) (Cummine and Boliek, 2013). TBSS is a popular method that allows whole-brain mapping of microstructural indices such as FA and MD. The partial incongruencies in these results may be related to intrinsic aspects of this method. TBSS is substantially limited in the anatomical precision of WM pathways reconstruction (Bach et al., 2014; Hämäläinen et al., 2017) and allows detecting only regional voxel-based effects. Therefore, TBSS results are uninformative of larger-scale interregional WM communication. Moreover, in almost the totality of the diffusion studies on bilingualism, WM microstructural indices have been computed from data modeled with DTI. This technique suffers from intrinsic flaws and is limited in reconstructing the crossing fibers present in > 90% of WM voxels (Farquharson et al., 2013; Jeurissen et al., 2013; Jones et al., 2013). These aspects suggest that scientific literature on bilingualism-induced WM plasticity suffers from methodological limitations that prevent a clear description of the phenomenon.

Network Neuroscience is an increasingly adopted methodological framework that conceives the brain as a "connectome", a complex system of nodes (regions) and edges (connections) (Bullmore and Sporns, 2009; Rubinov and Sporns, 2010). It adopts network science and graph theory tools and methods to describe the brain's structural and functional architecture. Consequently, Network Neuroscience can reveal neuroplastic effects influencing all possible pairwise connections between brain areas, allowing a comprehensive description of neural reorganization processes (see Fornito, Zalesky, and Bullmore, 2016). Thus, Network Neuroscience represents a valuable tool

to explore bilingualism-related neuroplastic changes that previous research on single structures/activations could not identify (Li and Grant, 2016).

In this study, we used Network Neuroscience to describe how distinct components of bilingual experience (i.e., L2 AoA, L2 Proficiency, and L2 Exposure) impact brain structural connectivity. In line with recent trends in the neuroscience of bilingualism (e.g., De Luca et al., 2019,2020; DeLuca, Rothman and Pliatsikas, 2019; Kousaie et al., 2017; Li et al., 2014; Leivada et al., 2021; Sulpizio et al., 2020b; Surrain and Luk, 2017), we defined bilingualism as a continuous and multi-componential construct (see section 1.4). We utilized whole-brain probabilistic tractography in a sample of seventy-seven Italian-English bilinguals.

We adopted state-of-the-art diffusion modeling and processing methods (e.g., Constrained Spherical Deconvolution, “CSD”, and Anatomically Constrained Tractography, “ACT”, Multi-Shell diffusion MRI acquisition) to overcome previous research's methodological limitations based on TBSS DTI.

We expected the Network Neuroscience framework to reveal distinct and overlapping language/executive regions that could mirror the specific contribution of L2 AoA, Proficiency, and Exposure in defining brain structural plasticity and organization. We used graph theory to define the topological properties of these networks, such as identifying the nodes with the most significant number of edges, those acting as central hubs of information transfer, and those organized in modular communities. Consequently, graph theory represents a fundamental tool to deconstruct the bilingual structural connectome in its primary experience-related components and describe how bilingual experience transforms the connections between the regions of these networks. For instance, node degree and betweenness of centrality allow describing whether a brain area plays a peripheral role in a network associated with L2 AoA despite its central importance in a network impacted by L2 Proficiency. Furthermore, modularity measures allow detecting clusters of connected regions within one network and reveal areas of local specialization that may contribute to L2 information processing. Finally, we used graph theory to define significant networks' local and global efficiency, thus revealing their degree of interconnectedness (see García-Pentón et al., 2014; Sulpizio et al., 2020a). With the description of these networks, we expected to provide original

information of neuroplastic effects driven by bilingual experience on the brain's structural organization.

Chapter 2 - AIM OF THE WORK

Converging evidence shows that individual differences in cognitive abilities are partly driven by “neuroanatomical constraints,” morphological features of the human brain determined during foetal life and largely unaffected by postnatal events. For instance, the large degree of intersubjective variability in cortical gyrification and sulcal anatomy of the Anterior Cingulate Cortex (ACC) has been associated with long-term differences in executive performance and functional activity. By contrast, “neural plasticity” is the capacity of the brain to continuously self-adjust and reorganize its structural and functional features as a response to experience-related variables such as prolonged learning and specific training. These two aspects, lifelong stable properties of the brain and everchanging neural adaptation processes, seem counterposed. However, both modulate the neural organization and cognitive functions of individuals.

This dissertation aims at describing a systematic investigation on the dynamic interplay between early neuroanatomical constraints, environmental background, brain functional activity, and cognitive performance across age. This work uses a combination of complementary multimodal neuroimaging techniques (i.e., structural and functional connectivity, and task-based fMRI), neuropsychological testing, and psycholinguistic assessment to better understand this complex relationship.

Experiments 1 (Fedeli et al., 2020) and 2 (Fedeli et al., submitted) inspect the impact of individual morphological variability of ACC sulcation patterns on brain functional activity at rest and during executive tasks. Experiment 3 (Del Maschio et al., 2019a) investigates the role of second language usage (here intended as a neuroplastic measure of prolonged cognitive experience) in modulating the developmental trajectories of relatively stable features of the brain cortex (i.e., cortical gyrification). Experiment 4 (Fedeli et al., 2021) investigates the impact of individual differences in second language experience on white matter plasticity, a more ductile brain structural property.

The four studies represent a continuum that starts by depicting the functional impact of elements of neural stability and ends by investigating the dynamics of brain plasticity. The consequences of our observations are far-reaching and provide new insights on the neural architecture of behavioral differences.

Chapter 3 – RESULTS

3.1 – EXPERIMENT 1 (RESULTS):

ACC sulcal pattern distribution. The distribution of ACC bi-hemispheric sulcation patterns across participants and split by gender are reported in Experiment 1; Table 1. The ‘leftward asymmetry’ pattern occurred more frequently than others in our sample (LA = 32.37%; SS = 27.75%; DD = 20.81%; RA = 19.7% ; $\chi^2(3) = 7.9249$, $p = .04759$) confirming a well-known leftward bias in the general population (e.g., Fornito et al., 2004; Huster et al., 2007; Paus et al., 1996a; Wei et al., 2017). No significant effect of gender was detected on ACC sulcal pattern distribution ($\beta = -0.280$, $SE = 0.301$, $p > .3$).

ACC sulcal pattern	Overall (N=173)	F (N=60)	M (N=113)
SS	48 (27.75)	23 (38.33)	25 (22.13)
DD	36 (20.81)	9 (15.00)	27 (23.89)
LA	56 (32.37)	15 (25.00)	41 (36.28)
RA	33 (19.07)	13 (21.67)	20 (17.70)

Experiment 1; Table 1. ACC Sulcal pattern distribution. ACC = Anterior Cingulate Cortex; F = Female; M = Male. DD = Double Presence (CS and additional PCS in both hemispheres); LA = leftward asymmetry (PCS present in the left hemisphere only); RA = rightward asymmetry (PCS present in the right hemisphere only); SS = Double Absence (CS only in both hemispheres).

Effects of ACC sulcal pattern variability on seed-based rsFC. Individual differences in sulcal pattern were associated with distinct profiles of functional organization of the ACC. Results for each sulcal pattern are described below, reported in Experiment 1; Table 2, and illustrated in Experiment 1; Figure 1.

- *Double Absence (SS) (CS only in both hemispheres).* The Double Absence > Double Presence contrast showed reduced rsFC of a ventral seed (V2 L) with the left insular cortex. Enhanced long-distance, intra-hemispheric rsFC was found between a left

middle (M3 L) seed and the cerebellum. The Double Absence > Leftward Asymmetry contrast was not associated with any significant difference. The Double Absence > Rightward Asymmetry contrast revealed extensive patterns of reduced long-distance rsFC between a right ventral seed (V1 R) and bilateral occipital cortices, as well as right temporo-occipital and cerebellar regions.

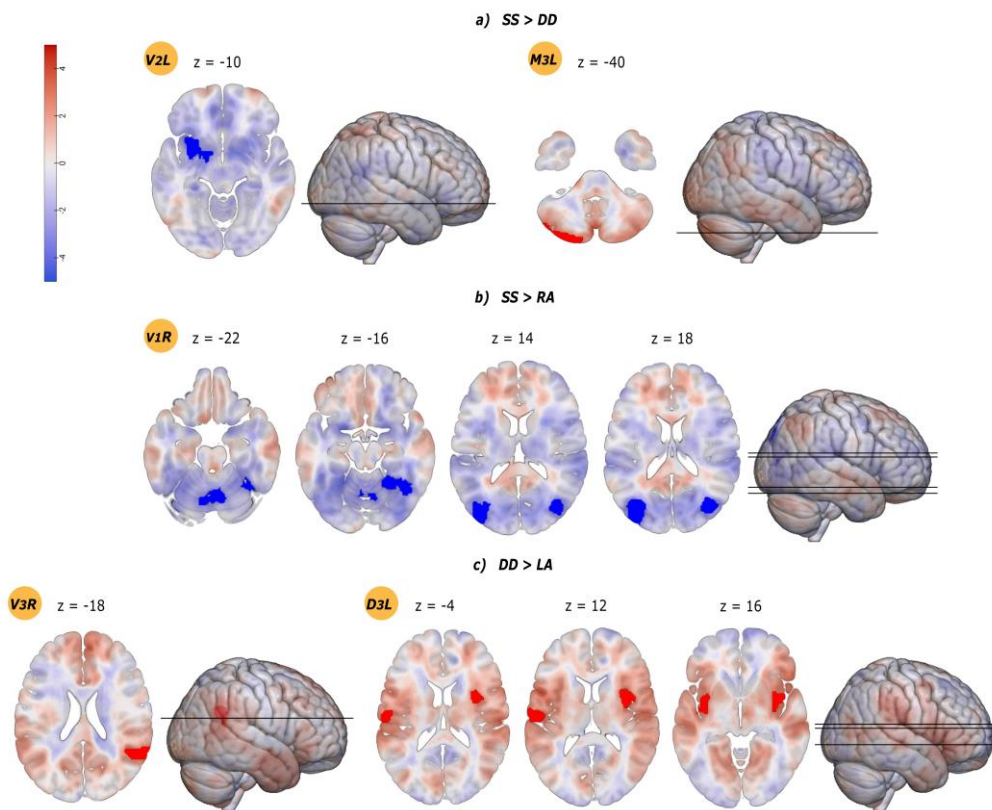
- *Double Presence (DD) (CS and PCS in both hemispheres)*. The Double Presence > Double Absence contrast showed enhanced rsFC of a ventral seed (V2 L) with the left insula. Reduced long-distance, intrahemispheric rsFC was found between a left middle (M3 L) seed and the cerebellum. The Double Presence > Leftward Asymmetry contrast showed enhanced intrahemispheric rsFC between a right ventral seed (V3 R) and the right angular gyrus, as well as between a left dorsal seed (D3 L) and bilateral insulo-opercular cortices. No difference in rsFC was found for the Double Presence > Rightward Asymmetry contrast.

- *Leftward Asymmetry (LA) (PCS in the left hemisphere only)*. The Leftward Asymmetry > Double Absence contrast showed no significant differences for any of the considered seeds. The Leftward Asymmetry > Double Presence contrast resulted in reduced intrahemispheric rsFC between a right ventral seed (V3 R) and the right angular gyrus, as well as between a left dorsal seed (D3 L) and bilateral insulo-opercular cortices. The Leftward Asymmetry > Rightward Asymmetry contrast showed no significant result.

- *Rightward Asymmetry (RA) (PCS in the right hemisphere only)*. The Rightward Asymmetry > Double Absence contrast revealed extensive patterns of enhanced long-distance rsFC between a right ventral (V1 R) seed and bilateral occipital cortices, as well as right temporo-occipital and cerebellar regions. No difference in rsFC was found for the Rightward Asymmetry > Double Presence contrast. The Rightward Asymmetry > Leftward Asymmetry contrast showed no significant difference as well.

<i>Contrast</i>	<i>Seed</i>	<i>MNI coordinates (X, Y, Z)</i>			<i>Harvard–Oxford Atlas region</i>	<i>Connectivity increase/ decrease</i>	<i>k</i>	<i>Z score</i>	<i>Cluster-level p-FWE</i>	<i>Voxel-level p-FWE</i>	
SS>DD	V2L	-30	10	-10	Insular cortex	-	372	5.2	0.000335	0.017112	
	M3L	-26	-84	-40	Cerebellum	+	660	4.47	0.000011	0.287691	
SS>LA	—	—	—	—	—	—	—	—	—	—	
SS>RA	V1 R	36	-74	18	Lateral occipital cortex, superior division	-	702	4.65	0.000003	0.163567	
		-36	-82	14	Lateral occipital cortex, superior division	-	621	4.76	0.000010	0.107210	
		24	-50	-16	Temporal occipital fusiform cortex	-	436	4.55	0.000202	0.235664	
		8	-64	-22	Cerebellum	-	396	4.73	0.000410	0.118297	
DD>LA	V3 R	62	-52	28	Angular gyrus	+	456	4.88	0.000069	0.071920	
		D3L	32	6	16	Insular cortex	+	552	4.25	0.000025	0.576600
		-56	-14	12	Central opercular cortex	+	548	4.27	0.000026	0.556079	
		-36	-4	-4	Insular cortex	+	405	4.48	0.000306	0.306549	
DD>RA	—	—	—	—	—	—	—	—	—		
LA>RA	—	—	—	—	—	—	—	—	—		

Experiment 1; Table 2. rsFC differences between ACC sulcal patterns. p -uncorrected <0.001 (voxel); p -FWE <0.00046 (cluster). V = ventral seeds; M = Middle seeds; D = Dorsal seeds. Voxel- p -FWE <0.05 is reported for additional information.



Experiment 1; Figure 1 . Effects of ACC morphological variability on seed-based rsFC. Results are reported as highlighted clusters overlaid onto unthresholded *T*-maps (Pernet and Madan, 2019). Axial slices are shown with Z MNI coordinates corresponding to the contrast local maxima with whole-brain height reference. (The figure is adapted with permission from Fedeli et al., 2020).

Effects of age-sulcal pattern interaction on seed-based rsFC. The relationship between ACC sulcal pattern and ACC connectivity changed with increasing age, albeit to varying degree depending on the specific sulcal pattern considered. Results for each sulcal pattern are described below, reported in Experiment 1; Table 3, and represented in Experiment 1; Figure 2.

- *Double Absence*Age*. The Double Absence*Age > Double Presence*Age contrast showed increased long-distance, intrahemispheric rsFC between a left middle (M3 L) seed and the cerebellum. The Double Absence*Age > Leftward Asymmetry*Age contrast showed increased rsFC between a right ventral (V3 R) seed with the temporal

cortex . The Double Absence *Age > Rightward Asymmetry*Age contrast showed no significant result.

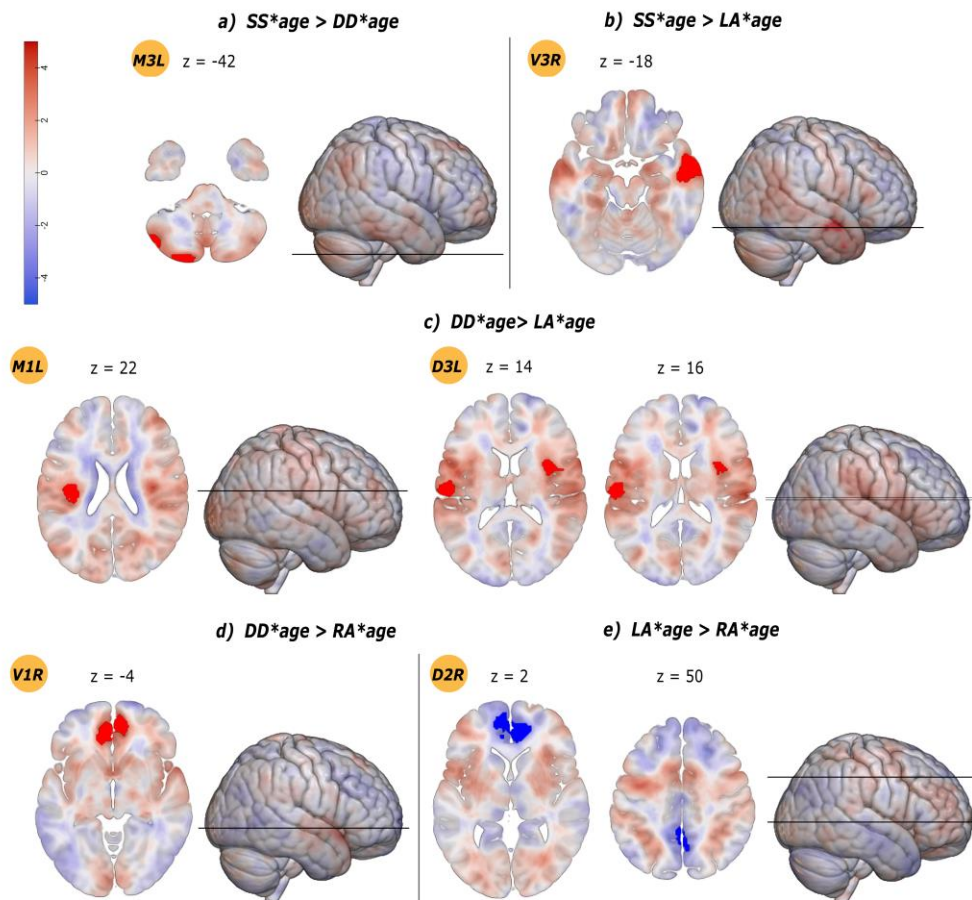
- *Double Presence*Age*. The Double Presence*Age > *Single/Single*Age* contrast showed decreased long-distance, intrahemispheric rsFC between a left middle seed (M3 L) and the cerebellum. The Double Presence*Age > Leftward Asymmetry*Age contrast revealed increased rsFC of middle (M1 L) and dorsal (D3 L) seeds with the bilateral Central Opercular Cortex. The Double Presence*Age > Rightward Asymmetry*Age contrast showed increased rsFC between a right ventral seed (V1 R) and the ipsilateral PCG.

- *Leftward Asymmetry*Age*. The Leftward Asymmetry*Age > Double Absence*Age contrast showed decreased rsFC with increasing age between a right ventral seed (V3 R) with the temporal cortex. The Leftward Asymmetry*Age > Double Presence*Age contrast revealed decreased rsFC of middle (M1 L) and dorsal (D3 L) seeds with the bilateral Central Opercular Cortex. The Leftward Asymmetry*Age > Rightward Asymmetry*Age contrast showed decreased rsFC between a dorsal seed (D2 R) and the ACC and Precuneus cortex.

- *Rightward Asymmetry*Age*. The Rightward Asymmetry*Age > Double Absence*Age contrast showed no significant result The Rightward Asymmetry*Age > Double Presence*Age contrast showed decreased rsFC between a right ventral seed (V1R) and the ipsilateral PCG. The Rightward Asymmetry*Age > Leftward Asymmetry*Age contrast showed increased rsFC between a dorsal (D2 R) seed and the ACC and Precuneus cortex.

Contrast	Seed	MNI coordinates (X, Y, Z)			Harvard–Oxford Atlas region	Connectivity increase/ decrease	k	Z score	Cluster-level p-FWE	Voxel-level p-FWE
SS*age>DD*age	M3 L	-18	-86	-42	Cerebellum	+	628	4.53	0.000018	0.234223
SS*age>LA*age	V3 R	56	-2	-18	Middle temporal gyrus, anterior division	+	554	4.89	0.000022	0.061480
SS*age>RA*age	—	—	—	—	—	—	—	—	—	—
DD*age>LA*age	M1 L	-36	-16	22	Central opercular cortex	+	394	5.07	0.000190	0.030792
	D3 L	-56	-18	14	Central opercular cortex	+	513	4.38	0.000048	0.411159
		38	6	16	Central opercular cortex	+	429	4.22	0.000204	0.620230
DD*age>RA*age	V1 R	8	50	-4	Paracingulate gyrus	+	587	4.39	0.000020	0.399625
LA*age>RA*age	D2 R	6	40	2	Cingulate gyrus, anterior division	-	1081	4.61	0.000000	0.192153
		0	-56	50	Precuneus cortex	-	404	3.84	0.000334	0.971300

Experiment 1; Table 3. Age * ACC sulcal patterns interaction on rsFC. *p*-uncorrected <0.001 (voxel); *p*-FWE <0.00046 (cluster). Voxel-*p*-FWE <0.05 is reported for additional information.



Experiment 1; Figure 2. Effects of Age * ACC morphological variability interaction on seed-based rsFC. Results are reported as highlighted clusters overlaid onto unthresholded T-maps. Axial slices are shown with Z MNI coordinates corresponding to the contrast local maxima with whole-brain height reference. (The figure is adapted with permission from Fedeli et al., 2020).

Correlations between ACC connectivity and cognitive performance

When testing for inter-group differences in correlations between connectivity values extracted from significant clusters and the scores from cognitive tests, no significant result emerged.

3.1.1 – Discussion

In experiment 1, we investigated the influence of cortical morphology variability on ACC functional connectivity across the lifespan. We found significant differences in

rsFC strength and topology associated with distinct ACC sulcal patterns. Moreover, we observed that aging reshapes ACC connectivity depending on the patterns of cortical folding.

Compared with the double absence pattern, the occurrence of a PCS on the right cingulate cortex (i.e., double presence and rightward asymmetry) promoted increased connectivity between ventral components of the ACC and the rest of the brain. Moreover, PCS double presence was linked with increased connectivity between ventral and dorsal seeds with the right angular gyrus and bilateral insular cortices with respect to the leftward asymmetry pattern. While PCS double presence was the most connected pattern amongst all, the double absence pattern was generally associated with diminished cortical rsFC (except for a cerebellar increase). Notably, no significant difference between asymmetric patterns (rightward and leftward asymmetry) was found. Taken together, these findings indicate a more extensive connectivity heterogeneity within symmetric patterns (i.e., double presence and absence) than asymmetric ones, and greater connectivity associated with a right hemispheric PCS occurrence. These differences occurred primarily in target regions within the SN and the DMN (e.g., insular, opercular, and posterior components). This finding is in line with the relevant role played by the ACC-MCC complex as a connectivity hub in both networks, as we highlighted in section 1.3 when describing patterns of cingulate connectivity. The relationship between cortical gyrification and functional architecture at rest is only marginally known. Folding of the cerebral cortex has been associated with structural connectivity alterations, as suggested by the axonal tension hypothesis of brain gyrification (see section 1.2) (Hilgetag and Barbas, 2005; Van Essen, 1997, 2020). Accordingly, it would be possible that structural differences in WM connectivity could modulate distinct profiles of ACC functional organization driven by PCS interhemispheric distribution. However, in the absence of conclusive evidence regarding the relationship between individual differences in ACC sulcal morphology and structural connectivity (see also Lim et al., 2019), we limit ourselves to reporting that ACC rsFC is associated with individual differences in local cortical morphology. These findings suggest a brain structure-function relationship that possibly originates from the early stages of cortical development when sulcal patterns are formed.

While we found greater ACC connectivity associated with PCS occurrence in the right hemisphere, ACC spontaneous activity at rest has been typically described as highly similar in both hemispheres. However, a more dominant incidence of anticorrelations from left hemispheric seeds have been reported by Margulies and colleagues (2007). Moreover, a greater functional connectivity strength with other cortical, subcortical and cerebellar regions has been found for the ACC in the right, and not in the left, hemisphere by Yan et al. (2009). Based on our results, we suggest that the incidence of a PCS could potentially enhance these naturally occurring ACC functional connectivity trajectories.

As for the seed distribution, differences in connectivity between closely placed seeds possibly reflect fine-graded changes in the cortical cytology of the cingulate cortex (e.g., Palomero-Gallagher et al., 2009,2018). Finally, to investigate functional homogeneity between PCS and CS (see Amiez et al., 2013) we performed a between-seed comparison between symmetric patterns. Our results revealed that differences in ACC connectivity associated with sulcal pattern variability seem to reflect more a change in terms of connectivity strength than in functional topology. The relationship between ACC sulcal patterns and ACC connectivity showed significant differences as a function of age. The leftward asymmetry was associated with remarkably decreased connectivity with increasing age than all other sulcal patterns. On the contrary, the rsFC of individuals with symmetric sulcal patterns was largely maintained compared to the other patterns.

A large corpus of evidence suggests that ACC rsFC encounters considerable changes as aging. Older adulthood is associated with diminished connectivity with other cortical and subcortical regions (Cao et al., 2014; Touroutoglou and Dickerson., 2019) and altered connectivity within/between intrinsic networks (e.g., DMN) (e.g., Betzel et al., 2014; Geerligs et al., 2015; Grady et al., 2016). These patterns have been linked with a gradual decrease in the specialization of functional systems with negative consequences to information processing in older age groups.

Our results indicate a significant interaction between ACC morphological variability and age-related effects shaping the brain's functional architecture. We reported the long-term contribution of lifelong stable neuroanatomical constraints on resting-state networks for the first time. Future studies could overcome the limitations

of a cross-sectional approach and thoroughly investigate whether symmetric PCS patterns might help individuals reach stable ACC connectivity patterns at an earlier age with a longitudinal approach.

In section 1.3, we reported extensive evidence showing that individual variability in ACC sulcal patterns modulates cognitive efficiency in executive functions (e.g., Borst et al., 2014; Cacia et al., 2014,2017; Del Maschio et al., 2018a; Fornito et al., 2004; Huster et al., 2009; Tissier et al., 2018). This modulation has been suggested to be mediated by differences in structural interhemispheric connectivity (Cacia et al., 2014; Tissier et al., 2018) or functional brain activity. Our correlational analyses did not find a significant association between morphology-driven brain connectivity changes and differences in cognitive abilities. However, since evidence for an association between sulcal variability and executive differences has been provided by other studies using different tests (e.g., versions of the Stroop and Flanker tests), a specific cognitive assessment may be required to obtain significant results.

In this study, we highlighted that prenatally-determined individual differences in ACC sulcal folding morphology are significantly impactful on the functional connectivity of the ACC with the rest of the brain across the lifespan. Additional research employing multimodal imaging and adequate behavioral assessment is necessitated to confirm these novel results and further investigate the cognitive effects of structure-function relationships. Moreover, a univocal model of the biological processes of the cerebral cortex gyrification is still necessary to collocate these findings within a robust theoretical framework (see section 1.2).

To resume, our results indicated that:

1. ACC connectivity at rest is linked with individual morphological variability. Different sulcal patterns are associated with specific profiles of connectivity strength and trajectories;
2. The relationship between ACC sulcal pattern and rsFC changes with increasing age, albeit to a varying, pattern-specific degree;
3. No significant cognitive effect linked with differences in structure-function relationships has been found by means of the cognitive assessment adopted in this study.

3.2 – EXPERIMENT 2 (RESULTS):

Results

ACC sulcal pattern classification.

Asymmetric ACC sulcal patterns were reported for 20 participants (47.62%), while symmetric patterns were reported for 22 participants (52.38%). A chi-square (χ^2) analysis revealed that sulcal patterns were equally distributed when considering asymmetry (i.e., asymmetry, symmetry; $\chi^2(1) = 0.09, p = .76$). No significant difference for age, education, gender, handedness, SES, fluid intelligence quotient, and visuo-spatial working memory was found between the two groups (all χ^2 s < 1; all p s > .3; all t s < 1)

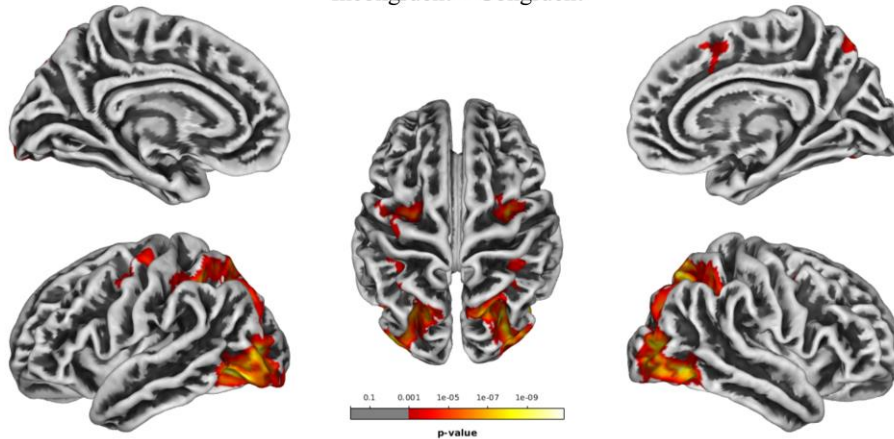
Neuroimaging analyses

ANT The incongruent > congruent contrast, irrespective of PCS asymmetry, resulted in the activation of fronto-occipital regions, including the right PCG and frontal orbital cortex. A similar fronto-occipital pattern was found for the incongruent > neutral contrast, with increased activity in the bilateral PCG, superior frontal gyrus, frontal orbital cortex and SMA (juxtapositional lobule cortex). The congruent > neutral contrast revealed the activation of posterior occipital regions and of the left superior parietal lobule. When inspecting differences in brain activity in individuals with symmetric and asymmetric PCS profiles, no significant effect was found. Results are reported in Experiment 2; Table 1 and Experiment 2; Figure 1.

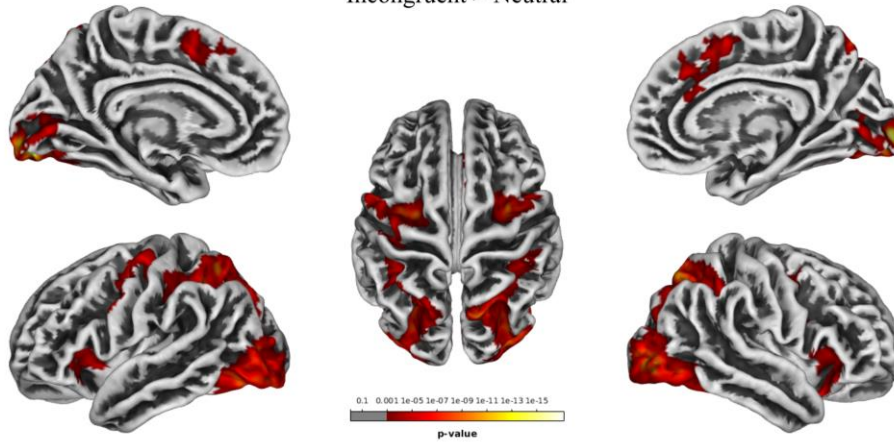
ANT										
Contrast	Hemisphere	Region (Harvard-Oxford)	cluster p(FWE-corr)	k (mm3)	T value	Z score	peak p(unc)	x	y	z
Congruent Neutral >	L	Occipital Fusiform Gyrus	< 0.001	439	12.26	Inf	< 0.001	-19	-83	-13
	R	Occipital Fusiform Gyrus	< 0.001	279	11.7	7.71	< 0.001	23	-79	-12
	R	Occipital Pole	< 0.001	94	11.62	7.68	< 0.001	11	-96	-7
	R	Occipital Pole	< 0.001	90	5.63	4.81	< 0.001	30	-93	8
	L	Superior Parietal Lobule	0.025	30	4.84	4.28	< 0.001	-27	-54	46
	R	Intracalcarine Cortex	0.15	21	4.57	4.09	< 0.001	15	-78	11
	L	Lateral Occipital Cortex	0.013	33	4.55	4.07	< 0.001	-26	-83	17
	L	Intracalcarine Cortex	< 0.001	50	4.16	3.78	< 0.001	-6	-87	3
Incongruent Neutral >	R	Occipital Pole	< 0.001	238	13.03	Inf	< 0.001	11	-96	-5
	L	Occipital Fusiform Gyrus	< 0.001	3019	12.41	Inf	< 0.001	-21	-82	-18
	R	Occipital Fusiform Gyrus	< 0.001	2762	9.74	6.97	< 0.001	24	-78	-14
	R	Middle Frontal Gyrus	< 0.001	400	8.76	6.54	< 0.001	33	-2	50
	L	Superior Frontal Gyrus	< 0.001	849	8.3	6.32	< 0.001	-22	-4	49
	L	Frontal Orbital Cortex	< 0.001	249	6.75	5.51	< 0.001	-31	26	-6
	R	Paracingulate Gyrus	< 0.001	359	6.47	5.34	< 0.001	5	17	43
	R	Frontal Orbital Cortex	< 0.001	534	6.24	5.2	< 0.001	26	14	-19
	L	Paracingulate Gyrus	0.048	27	6.07	5.1	< 0.001	-10	45	12
	L	Juxtapositional Lobule Cortex	< 0.001	163	5.7	4.86	< 0.001	-5	5	45
	R	Precentral Gyrus	< 0.001	107	5.44	4.69	< 0.001	47	9	29
	L	Juxtapositional Lobule Cortex	< 0.001	50	5.14	4.49	< 0.001	-6	-7	49
	R	Superior Frontal Gyrus	0.012	34	4.49	4.03	< 0.001	13	10	66
	R	Intracalcarine Cortex	0.01	35	4.32	3.9	< 0.001	15	-61	6
Incongruent Congruent >	R	Lateral Occipital Cortex, inferior division	< 0.001	2151	8.3	6.32	< 0.001	52	-68	-8
	L	Inferior Temporal Gyrus, temporooccipital part	< 0.001	2006	8.26	6.3	< 0.001	-42	-62	-3
	R	Precentral Gyrus	< 0.001	233	6.89	5.58	< 0.001	32	-4	46
	L	Precentral Gyrus	< 0.001	279	5.55	4.76	< 0.001	-24	-5	49
	L	Postcentral Gyrus	0.004	39	5.27	4.58	< 0.001	-46	-28	35
	L	Precentral Gyrus	0.019	31	4.67	4.16	< 0.001	-57	6	32
	R	Paracingulate Gyrus	< 0.001	82	4.27	3.86	< 0.001	6	23	47
	R	Frontal Orbital Cortex	0.008	35	4.24	3.84	< 0.001	31	25	-7
	R	Precentral Gyrus	0.002	43	4.03	3.67	< 0.001	46	8	35

Experiment 2; Table 1 -- t-contrast results for the effects detected in the ANT task. Significance threshold is set at vertex-p-uncorrected < 0.001 and cluster-p-FWE-corrected < 0.05. Only one local maximum per significant cluster is listed. R = Right hemisphere. L = Left hemisphere.

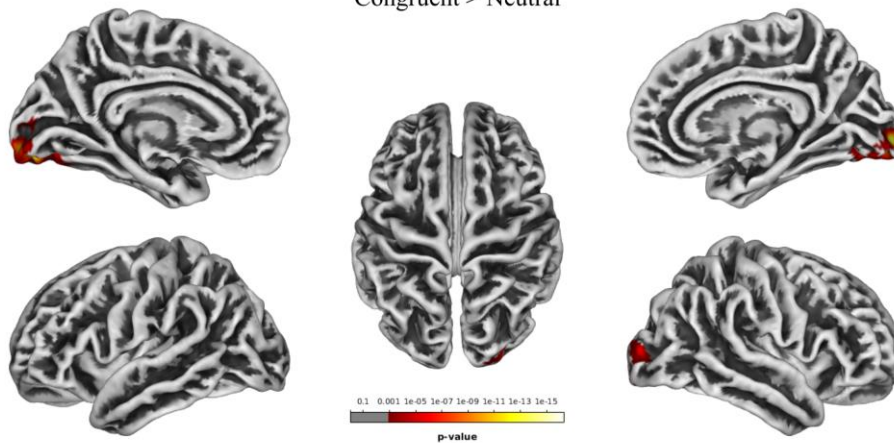
Incongruent > Congruent



Incongruent > Neutral



Congruent > Neutral



Experiment 2; Figure 1. Brain activity during the Attentional Network Task. Significant results are shown at cluster level FWE-corrected for multiple comparisons p -value < 0.05 , and vertex level uncorrected p -value < 0.001 .

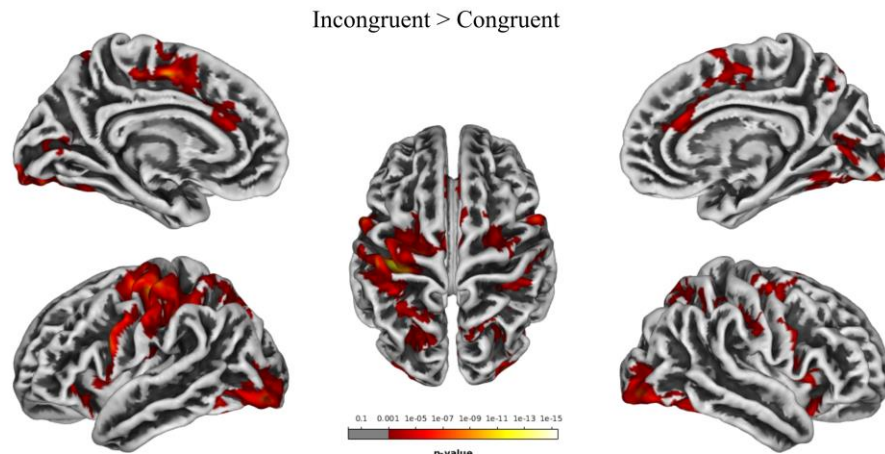
Numerical Stroop The incongruent > congruent (incongruency) contrast, irrespective of PCS asymmetry, resulted in the activation of frontal, insular, parietal, and occipital cortices, including the left PCG, the bilateral anterior cingulate and frontal orbital cortices, and the right superior frontal gyrus and SMA. The incongruent > neutral (interference) contrast resulted in the activation of frontal, parietal and occipital areas, including the left inferior frontal gyrus, but not medial aspects of the frontal cortex. The congruent > neutral (i.e., “facilitation” effect) contrast did not reveal any significant result. When investigating differences in brain activity between individuals with symmetric and asymmetric PCS profiles, a significant difference emerged for the incongruent > neutral contrast. Individuals with symmetric profiles showed greater activity in the right paracingulate cortex and in the left medial part of the superior frontal gyrus with respect to individuals with asymmetric profiles. Results are reported in Table 2 and Experiment 2; Figure 2.

Stroop										
Contrast	Hemisphere	Region (Harvard-Oxford)	cluster p(FWE-corr)	k (mm3)	T value	Z score	peak p(unc)	x	y	z
Congruent > Neutral	--	--	--	--	--	--	--	--	--	--
Incongruent > Neutral	L	Inferior Frontal Gyrus, pars opercularis	< 0.001	67	5.33	4.62	< 0.001	-45	16	9
	R	Postcentral Gyrus	< 0.001	91	5.31	4.6	< 0.001	46	-30	46
	L	Supramarginal Gyrus, anterior division	< 0.001	691	5.21	4.54	< 0.001	-52	-30	46
	R	Occipital Pole	0.043	28	5.18	4.52	< 0.001	28	-94	-12
	L	Angular Gyrus	< 0.001	72	5.06	4.43	< 0.001	-54	-57	33
	R	Superior Temporal Gyrus, posterior division	0.003	42	4.94	4.35	< 0.001	63	-24	-5
	L	Precentral Gyrus	< 0.001	155	4.92	4.33	< 0.001	-49	8	33
	R	Angular Gyrus	0.002	44	4.64	4.13	< 0.001	39	-55	43
	L	Inferior Frontal Gyrus, pars opercularis	0.004	40	3.96	3.63	< 0.001	-52	20	15
Incongruent > Congruent	L	Precentral Gyrus	< 0.001	2902	11.6	7.68	< 0.001	-34	-23	46
	L	Occipital Fusiform Gyrus	< 0.001	796	7.2	5.76	< 0.001	-28	-79	-14
	L	Precentral Gyrus	< 0.001	313	7.18	5.74	< 0.001	-56	9	23
	R	Lateral Occipital Cortex, inferior division	< 0.001	732	7.14	5.72	< 0.001	38	-86	-9
	R	Precentral Gyrus	< 0.001	122	6.67	5.46	< 0.001	55	11	32
	L	Central Opercular Cortex	< 0.001	78	6.46	5.33	< 0.001	-49	-21	21
	L	Lateral Occipital Cortex, superior division	< 0.001	729	6.27	5.22	< 0.001	-28	-67	31
	R	Cingulate Gyrus, anterior division	< 0.001	199	6.23	5.19	< 0.001	4	27	16
	R	Superior Frontal Gyrus	< 0.001	410	6.14	5.14	< 0.001	24	-8	58
	L	Frontal Orbital Cortex	< 0.001	104	6.08	5.1	< 0.001	-28	18	-16
	R	Insular Cortex	< 0.001	120	5.76	4.9	< 0.001	40	14	-7
	R	Frontal Orbital Cortex	< 0.001	79	5.62	4.81	< 0.001	26	15	-18
	R	Juxtapositional Lobule Cortex	< 0.001	247	5.57	4.78	< 0.001	8	3	46
	L	Insular Cortex	< 0.001	54	5.48	4.72	< 0.001	-37	9	-4
	R	Supramarginal Gyrus, posterior division	< 0.001	494	5.47	4.71	< 0.001	37	-37	42
	L	Paracingulate Gyrus	0.007	36	5.31	4.61	< 0.001	-12	46	2
	R	Lateral Occipital Cortex, superior division	< 0.001	134	5.28	4.58	< 0.001	30	-74	23
	R	Precuneous Cortex	0.004	39	5.07	4.44	< 0.001	4	-66	46
	L	Intracalcarine Cortex	< 0.001	163	4.92	4.34	< 0.001	-12	-77	10
	L	Cingulate Gyrus, anterior division	< 0.001	207	4.85	4.28	< 0.001	-2	31	19
	R	Intracalcarine Cortex	< 0.001	147	4.76	4.23	< 0.001	7	-73	10
	L	Cingulate Gyrus, posterior division	0.016	32	4.76	4.22	< 0.001	-2	-24	43
	L	Precuneous Cortex	0.011	34	4.72	4.19	< 0.001	-4	-57	32
	L	Cingulate Gyrus, posterior division	< 0.001	54	4.72	4.19	< 0.001	-2	-50	21
	R	Lateral Occipital Cortex, superior division	< 0.001	190	4.68	4.16	< 0.001	29	-62	53
	R	Angular Gyrus	0.036	28	4.67	4.16	< 0.001	41	-57	17
	L	Insular Cortex	0.001	44	4.26	3.85	< 0.001	-35	-4	16
	R	Superior Parietal Lobule	< 0.001	76	4.09	3.72	< 0.001	28	-48	50

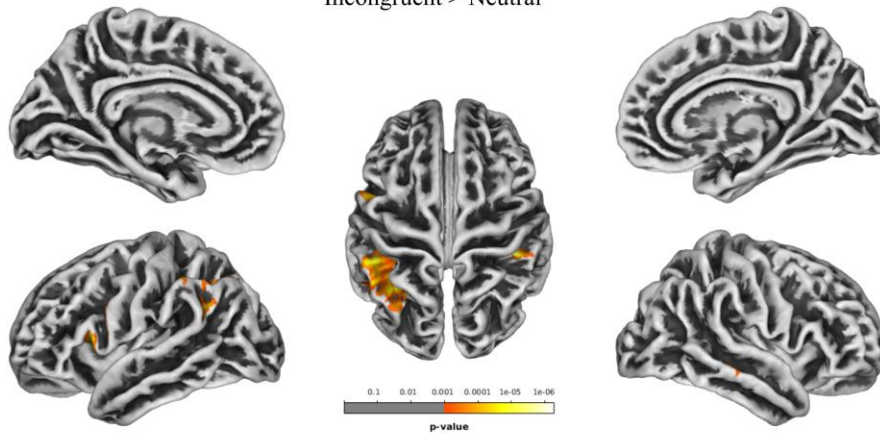
Stroop (Incongruent > Neutral)										
Contrast	Hemisphere	Region (Harvard-Oxford)	cluster p(FWE-corr)	k (mm3)	T value	Z score	peak p(unc)	x	y	z
Symmetric > Asymmetric	L	Superior Frontal Gyrus	0.013	33	5.01	4.36	< 0.001	-4	46	46
	R	Paracingulate Gyrus	0.002	43	4.84	4.24	< 0.001	5	35	30

Experiment 2; Table 2. t-contrast results for the effects detected in the Numerical Stroop task. Group differences between individuals with symmetric and asymmetric ACC sulcation patterns are also reported. Significance threshold is set at vertex-p-uncorrected < 0.001 and cluster-p-FWE-corrected < 0.05. Only one local maximum per significant cluster is listed. R = Right hemisphere. L = Left hemisphere.

a)

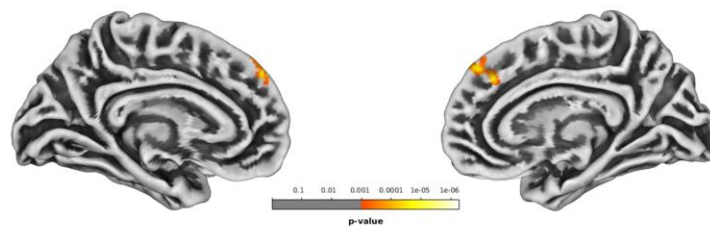


Incongruent > Neutral



b)

Symmetry > Asymmetry
(Incongruent > Neutral)



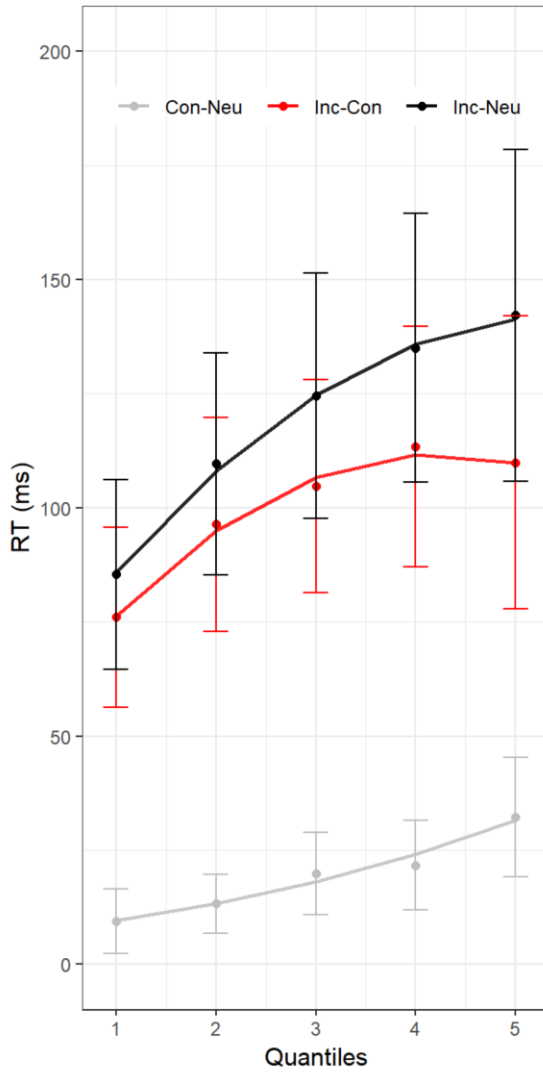
Experiment 2; Figure 2. a) Brain activity during the Numerical Stroop task. b) Difference in brain activity between individuals with Symmetric and Asymmetric ACC sulcation patterns for the Incongruent > Neutral contrast. Significant results are shown at cluster level FWE-corrected for multiple comparisons $p\text{-value} < 0.05$, and vertex level uncorrected $p\text{-value} < 0.001$.

Behavioral analyses

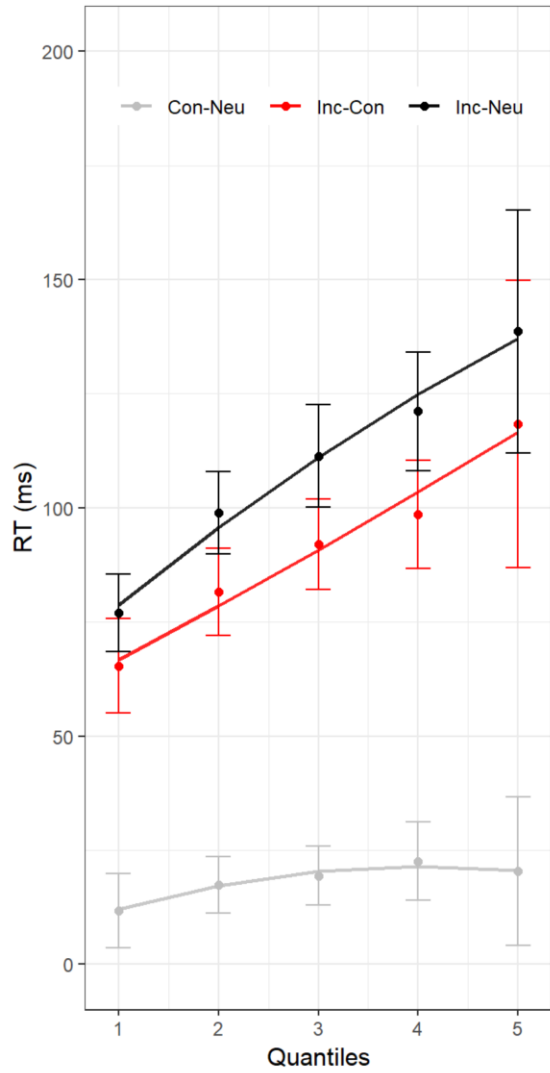
ANT. The model to test for the effect of ACC sulcal pattern asymmetry on mean RTs in the ANT showed a significant effect of Condition ($\chi^2 (2) = 1657.79$, $p < .001$), with faster responses for neutral trials compared to congruent trials ($b = -18.84$, $SE = 2.86$, $t = -6.59$) and faster responses for congruent trials than incongruent trials ($b = -95.75$, $SE = 2.86$, $t = -33.45$). No effect of ACC sulcal asymmetry was found ($\chi^2 (1) = 0.92$, $p = .34$), nor a 2-way interaction ($\chi^2 (1) = 3.2$, $p = .2$). The model including RTs quantiles as a fixed factor revealed a significant Condition x Quantile 2-way interaction ($\chi^2 (2) = 150.25$, $p < .001$); and a significant ACC sulcal asymmetry x Condition x Quantile 3-way interaction ($\chi^2 (4) = 41.81$, $p < .001$). Including the second-order polynomial in fitting RTs quantiles significantly increased the goodness of fit of the model ($\chi^2 (6) = 295.47$, $p < .001$). Delta plots are reported in Experiment 2; Figure 3.

Delta plots revealed that the incongruent > congruent (incongruency) effect increased linearly in individuals with asymmetric patterns. The incongruency effect increased nonlinearly in individuals with symmetric patterns, with a flatter slope that decreased in the fifth quantile associated with the slowest responses. The incongruent > neutral effect increased linearly in individuals with asymmetric patterns. Individuals with symmetric patterns also showed a positive effect growth, with a nonlinear slope that flattened in the latest quantile. The congruent > neutral effect was constant in individuals with asymmetric patterns with an almost flat slope across all quantiles. The same effect increased linearly across quantiles in individuals with symmetric patterns.

a) Symmetric PCS



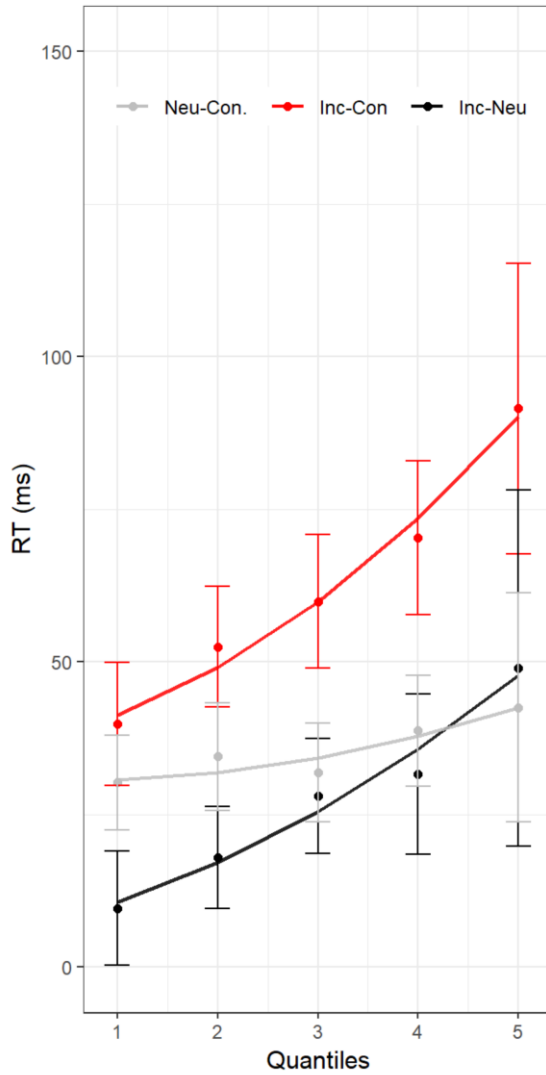
b) Asymmetric PCS



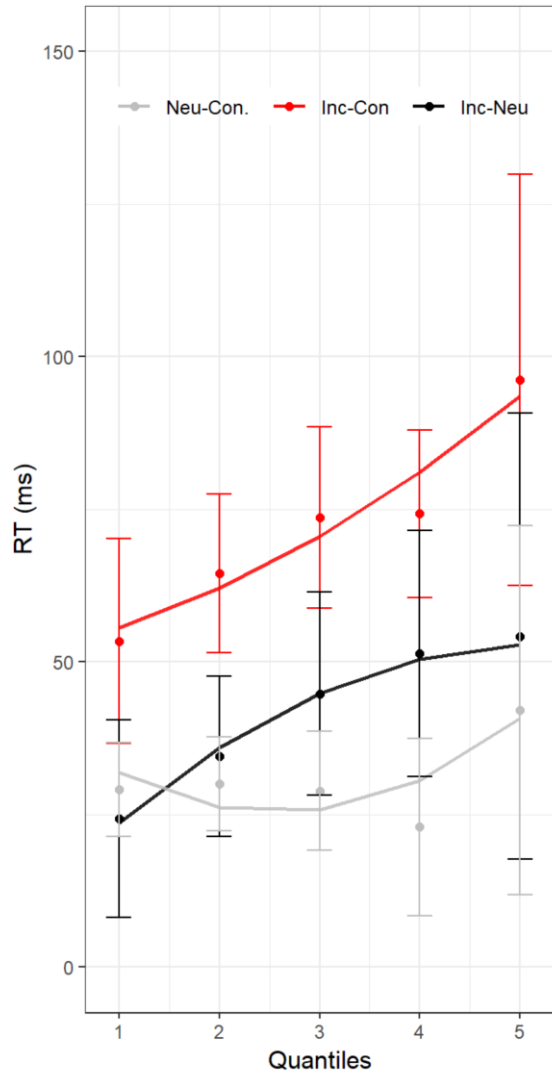
Experiment 2; Figure 3. Delta plots of the effects detected in the Attention Network Task, as a function of quantiles. Incong = Incongruent. Cong = Congruent. Neu = Neutral

Numerical Stroop. The model to test for the effect of ACC sulcal pattern asymmetry on RTs in the Numerical Stroop task showed a main effect of Condition (χ^2 (2) = 348.12, $p < .001$), with faster responses for congruent trials compared to neutral trials ($b = -33.59$, $SE = 3.54$, $t = -9.5$) and faster responses for congruent trials than incongruent trials ($b = -66.91$, $SE = 3.55$, $t = -18.84$), but no significant effect of ACC sulcal asymmetry (χ^2 (1) = 2, $p = .16$) nor a 2-way interaction (χ^2 (2) = 4.69, $p = .1$) were found. The model including RTs quantiles as a fixed factor revealed a significant Condition x Quantile 2-way interaction (χ^2 (2) = 63.81, $p < .001$), and a significant ACC sulcal asymmetry x Condition x Quantile 3-way interaction (χ^2 (4) = 28.48, $p < .001$). Including the second-order polynomial in fitting RTs quantiles significantly increased the goodness of fit of the model (χ^2 (6) = 691.33, $p < .001$). Delta plots are reported in Experiment 2; Figure 4. The incongruent > congruent effect (i.e., “incongruency” effect) increased across quantiles for both individuals with asymmetric and symmetric patterns with a similar linear slope. The incongruent > neutral effect (i.e., “interference” effect) increased nonlinearly in individuals with asymmetric patterns, flattening from the third quantile onwards. The effect increased linearly across quantiles in individuals with symmetric patterns. The neutral > congruent effect was stable for both individuals with asymmetric and symmetric patterns.

a) Symmetric PCS



b) Asymmetric PCS



Experiment 2; Figure 4. Delta plots of the effects detected in the Numerical Stroop task, as a function of quantiles. Incong = Incongruent. Cong = Congruent. Neu = Neutral

Brain-behavior interactions

Neuroimaging analyses showed a significant difference in brain activity between individuals with symmetric and asymmetric ACC sulcal patterns in the incongruent > neutral contrast of the Numerical Stroop task. A brain-behavior correlation analysis was performed to explore the relationship between brain activity and RTs associated with this effect. For each participant, the mean BOLD signal was extracted from the significant clusters resulting from the incongruent > neutral contrast in the Numerical Stroop task. Mean functional activity was then correlated with the differences in RTs between incongruent and neutral trials in the 4th and 5th quantiles (corresponding to the slowest responses) separately for individuals with symmetric and asymmetric PCS profiles (see Rousselet and Pernet, 2012). No significant correlation was found.

3.2.1 – Discussion

In this study, we aimed at investigating the neurofunctional impact of individual variability of ACC sulcal patterns during tasks assessing response inhibition (RI). Each participant performed the ANT and the Numerical Stroop tasks, and surface-based fMRI analyses were adopted to identify group differences in functional activity within the cingulate and prefrontal cortex. Behavioral measures were collected to explore group performance differences further.

ANT

Since we were interested in RI, in the analysis of the ANT task, we focused uniquely on the investigation of inhibitory control effects (i.e., Flanker effects) rather than on orienting and alerting components (see Del Maschio et al., 2018a and Cachia et al., 2017; contrasts investigating alerting and orienting components are reported in the appendices). Functional results associated with the incongruent > congruent and incongruent > neutral contrasts revealed significant brain activation in the frontal cortex's orbital, dorsolateral, and medial regions (including the PCG), and temporo-occipital areas. This pattern of brain activity is overall consistent with the first results reported by Fan and colleagues (2005) for the same task. The involvement of the dorsal aspects of the ACC (i.e., PCG and supplementary motor cortex) has been associated with RI within both the Flanker and Stroop tasks (Zhang et al., 2017), hinting at increased neural recruitment to deal with conflicting information when compared with congruent and neutral trials. The more extensive brain activity change found for the incongruent > neutral contrast compared to the incongruent > congruent contrast partly mirrors the differences in task difficulty as shown by the mean RTs (incongruent > congruent > neutral).

When investigating differences depending on ACC sulcation patterns, no significant result was found, neither in brain activity nor behavioral measures. Hence, we did not replicate the results of Cachia et al. (2017) and Del Maschio et al. (2018a), who described behavioral advantages related to asymmetric ACC sulcal patterns associated with the incongruency effect in the same task. A possible explanation might be linked with differences in the group classification between studies. Cachia et al.

(2017) divided their sample based on a two-level index (i.e., leftward – but not rightward – asymmetry, and symmetry), which was different from our classification, while Del Maschio et al. (2018a) adopted a more extensive four-level index (i.e., double present, double absent, leftward asymmetry, rightward asymmetry). In this study, our sample size would not allow us to adopt the four-level classification by Del Maschio et al., hence, we limited our analysis to asymmetry effects by dividing our participants into two equally sized subgroups. Nonetheless, the analysis of RTs divided into quantiles revealed a significant 3-way interaction between ACC sulcal pattern, Condition, and Quantile. Considering the delta plots, individuals with asymmetric patterns showed positive linear slopes for both incongruent > congruent and incongruent > neutral effects. On the other hand, these effects varied nonlinearly as a function of time for individuals with asymmetric patterns, and, following an initial increase, the slope became flatter (and even negative) for the slowest responses. In general, positive delta slopes have been found nearly ubiquitously in tasks assessing RI (except for the Simon task, e.g., see Ridderinkhof et al., 2004 and Burle et al., 2014). Besides, the leveling-off of the slope and negative-going components of delta plots have been typically associated with RI in the Flanker task when using manipulations of the arrow direction as experimental conditions (Pratte et al., 2021; Ridderinkhof et al., 2005; Tieges et al., 2009). Ridderinkhof and colleagues (2004, 2005) suggested that incongruent stimuli prompt rapid and automatic activation of inappropriate responses in tasks requiring inhibitory control, leading to large interference effects when responses are fast. Following an initial growth, this interference would be actively inhibited over time, and its influence on RTs reduced, leading to negative slopes (see the activation-suppression model of RI in Ridderinkhof et al., 2002, 2004). The top-down mechanism responsible for the selective suppression of incorrect responses would necessitate time to build up; hence, changes in the slope direction would mainly affect the slowest quantiles, proportional to inhibitory control efficiency (Van Den Wildenberg et al., 2010). We suggest that both individuals with symmetric and asymmetric ACC sulcal patterns experienced incongruency effects, leading to a positive slope in the first quantiles. However, participants with a symmetric sulcal pattern were more efficient in suppressing incongruent responses in the slowest quantiles, leading to a pronounced leveling-off and a negative slope change for this group. This finding suggests an

advantage in RI associated with symmetric ACC sulcal patterns. Without a significant difference in brain functional activity between groups, a tentative interpretation of this advantage should focus on the relationship between morphological symmetry and the brain's structural organization. Symmetric brains show greater transcallosal structural connectivity than asymmetric ones, causing a faster inter-hemispheric information transfer (Doron and Gazzaniga, 2008; Nowicka and Tacikowski, 2011; Toga and Thompson, 2003). Besides, the Flanker task is associated with bilateral information processing, as shown by evidence of symmetric task-related brain functional activity and connectivity in prefrontal clusters (Chen et al., 2018). We suggest that, for individuals with symmetric sulcal patterns, the greater transcallosal structural connectivity may have promoted better transfer and integration of bilateral information. As a result, a more symmetric neuroanatomical organization would be related to stronger inhibitory control efficiency during this task. This interpretation is partially in contrast with the findings of Del Maschio et al. (2018a) and Cachia et al. (2017), who suggested an opposite pattern of behavioral advantage for the Flanker task. However, there are fundamental differences in the sample classification implemented by the two studies and ours, as previously mentioned. Moreover, the adoption of delta plot analyses may also have glimpsed aspects of the temporal dynamics of inhibitory control associated with differences in information transfer that could have been passed unnoticed in the previous experiments. Our functional measures do not allow us to test adequately for these changes in inter-hemispheric connectivity. However, future studies may test this hypothesis by deepening the relationship between cortical folding variability and brain structural and functional connectivity measures in homologous prefrontal regions.

Numerical Stroop

Irrespective of ACC sulcal pattern, the incongruent > congruent contrast activated a large set of frontal, insular, parietal, and occipital regions, including the left PCG and the bilateral ACC. The activation of the ACC has been frequently associated with the Stroop effect, both using the original color-word task (Hung et al., 2018; Leung et al., 2000; Zhang et al., 2017) and in versions adopting numbers as experimental stimuli (Bush et al., 1998, 1999; Hart et al., 2010; Kaufmann et al., 2005, 2008). The

incongruent > neutral contrast was associated with the activation of frontal, parietal, and occipital areas, but no significant cluster was found in medial regions of the frontal cortex. The more extensive brain activity changes found for the incongruent > congruent contrast compared to the incongruent > neutral contrast may reflect differences in task difficulty, as revealed by the mean RTs incongruent > neutral > congruent.

A significant difference was found for the incongruent > neutral contrast when investigating differences in brain activity depending on the ACC sulcal pattern. With respect to individuals with a symmetric distribution of the PCS, individuals with asymmetric ACC sulcal patterns showed greater activation of the bilateral medial wall of the frontal lobe. In particular, we observed two main clusters: one located on the left medial frontal gyrus and a second located on the right PCG. This finding is highly interesting for its anatomical location and bilateral distribution, which reflect the symmetric sulcal pattern of the cingulate cortex. Compared with a neutral baseline, incongruency lead to greater activation of the dorsal aspects of the ACC, corresponding to the PCG. In a review of PET studies, Paus and colleagues (1998) reported greater activation of the dACC associated with task difficulty, explicitly referring to the involvement of the paralimbic portions located above the CS. Similarly, according to Kolling and colleagues (2016), the effect of task difficulty would be specifically associated with the functional involvement of these dorsal portions of the medial frontal wall (see also Shenav et al., 2014). On these grounds, we suggest that individuals with a symmetric distribution of the PCS may have experienced greater effort in inhibiting automatic incongruent responses associated with more significant activation of the PCG and medial frontal cortex. While in the opposite direction with respect to the Flanker task, this effect can also be attributed to brain asymmetries and hemispheric specialization. Cachia and colleagues (2013) proposed that increased efficiency in inhibitory control during an animal Stroop task found for individuals with asymmetric PCS could be the byproduct of hemispheric specialization (see also Fornito et al., 2004 for a preliminary formulation of this hypothesis). Inhibitory control during the Stroop Task involves partially lateralized processing (Brown et al., 2001; Chen et al., 2018; Vanderhasselt et al., 2009; Zhang et al., 2014). Moreover, information transfer is more efficient between spatially contiguous areas within the same hemisphere than between

contralateral regions through callosal fibers (Doron and Gazzaniga, 2008; Nowicka and Tacikowski, 2011; Toga and Thompson, 2003). According to Cacia and colleagues (2013), individuals with asymmetric ACC sulcal patterns would have more efficient inhibitory control because hemispheric specialization would prompt fast lateralized intra-hemispheric information transfer while individuals with morphological symmetries would rely on slower inter-hemispheric transfer to process information relevant to inhibit automatic responses. Based on our results, we suggest that the clusters of increased functional activity of bilateral dACC in individuals with symmetric ACC sulcal patterns reflect the difficulty of integrating information arising from the two conjointly activated hemispheres. The process of updating and combining information would arguably be costly in terms of RT. Such increased cost would represent a possible explanation behind the recurrently reported asymmetric advantage in incongruency effects during the Stroop task (Borst et al., 2014; Cacia et al., 2013; Huster et al., 2014; Tissier et al., 2018).

In this study, the analysis of RTs divided into quantiles revealed a significant 3-way interaction between ACC sulcal pattern, Condition, and Quantile. Considering the delta plots, both individuals with symmetric and asymmetric patterns of sulcation showed a non-linear positive increase of the incongruent > congruent effect as a function of the quantile. Even though individuals with asymmetric patterns show a slightly flatter slope, the trend is comparable between the two groups. When compared over the incongruent > neutral effect, however, the two patterns diverge. Participants with symmetric patterns show a positive slope, suggesting an increasing interference effect as a function of the quantile. Participants with asymmetric patterns showed an initial increase followed by a flattening of the slope. Remember that slower trials manifest the most the effect of selective response suppression, typically represented by a leveling-off of the delta-plot slope (Bub et al., 2006; Van Den Wildenberg et al., 2010). We suggest that for individuals with asymmetric ACC sulcal pattern after an initial increase of the interference effect, delta plot components in slow quantiles reflect efficient inhibition of incorrect automatic responses. In contrast, the almost linear increase of the incongruent > neutral effect for individuals with symmetric ACC sulcal patterns may represent the need to combine responses from bilaterally activated

cortices. Therefore, this increasingly pronounced interference effect as time passes would be generated by the difficulty associated with the integration process.

Concluding remarks

While both the ANT and the Numerical Stroop tasks were linked with increased ACC activity and longer RTs for incongruency trials, only the latter showed neurofunctional results supporting the notion of advantages related to asymmetric ACC sulcal patterns. Delta plots of behavioral effects revealed a partly incongruent pattern, with a symmetric-related advantage for the ANT and an asymmetric-related advantage for the Numerical Stroop task. Despite the two tasks being similar, they have been proposed to tackle distinct dimensions of RI (i.e., ANT: attention restraining, Numerical Stroop: attention constraining; Unsworth et al., 2009, 2012, 2014; Unsworth and Spillers, 2010). Hence, it is possible that, at the neural level, differences based on ACC morphology are more impactful on specific functions. However, a more straightforward explanation could rely on the neural activity underneath the two tasks. Chen et al. (2018) compared the functional activity and connectivity asymmetry indices between the Stroop and the Flanker tasks. While both were found to be associated with symmetric and asymmetric brain activity, the authors concluded that the first showed more significant functional asymmetries than the latter, which was more symmetric overall. Hence, we could speculate that ACC sulcal patterns interact with the degree of functional symmetry/asymmetry of one task, thus resulting in either beneficial or detrimental at the behavioral level. Based on our functional results, the significant group difference found only in the Numerical Stroop task implies that advantages would be more pronounced in the case of individuals with an asymmetric PCS while performing functionally asymmetric tasks, thanks to fast intra-hemispheric transfer. This study provides, for the first time, evidence of the neurofunctional signature behind the modulation of inhibitory control by individual morphological variability of the ACC. This phenomenon, previously investigated only at the behavioral level, defines a brain structural and functional relationship that is arguably determined during early development and still impacts cognitive abilities in young adults decades later. Such interaction expands the still marginal knowledge on the neurofunctional impact of cortical gyrification patterns and paves the way for future research investigating other

cognitive processes subserved by the ACC, such as decision making or language control (see Calabria et al., 2018; Del Maschio, Sulpizio, and Abutalebi, 2020). Moreover, our functional results imply that considering morphological variability is an essential requirement when investigating ACC neurofunctional activity at the group level and that this factor should be treated in the same way as gender and other relevant variables that are typically considered as covariates (see Fornito et al., 2008 for a similar opinion on this issue).

To conclude, our findings indicate that individual differences in ACC sulcation are related with differences in RTs during the ANT and the Numerical Stroop tasks. For the Numerical Stroop, the fMRI analysis suggests for the first time that the known advantage in executive functions associated with an asymmetric PCS is mirrored by a modulation of the neurofunctional activity in the cingulate cortex.

3.3 – EXPERIMENT 3 (RESULTS):

Neuroimaging Results

Whole-Brain. We observed age-dependent (irrespective of bilingualism) decreases in cortical gyrification in dorsolateral and mesial parts of a broad network of right frontal and parietal regions. A significant Age*Language Group interaction showed maintained right caudal ACC gyrification with increasing age in bilingual participants (see Experiment 3; Table 1).

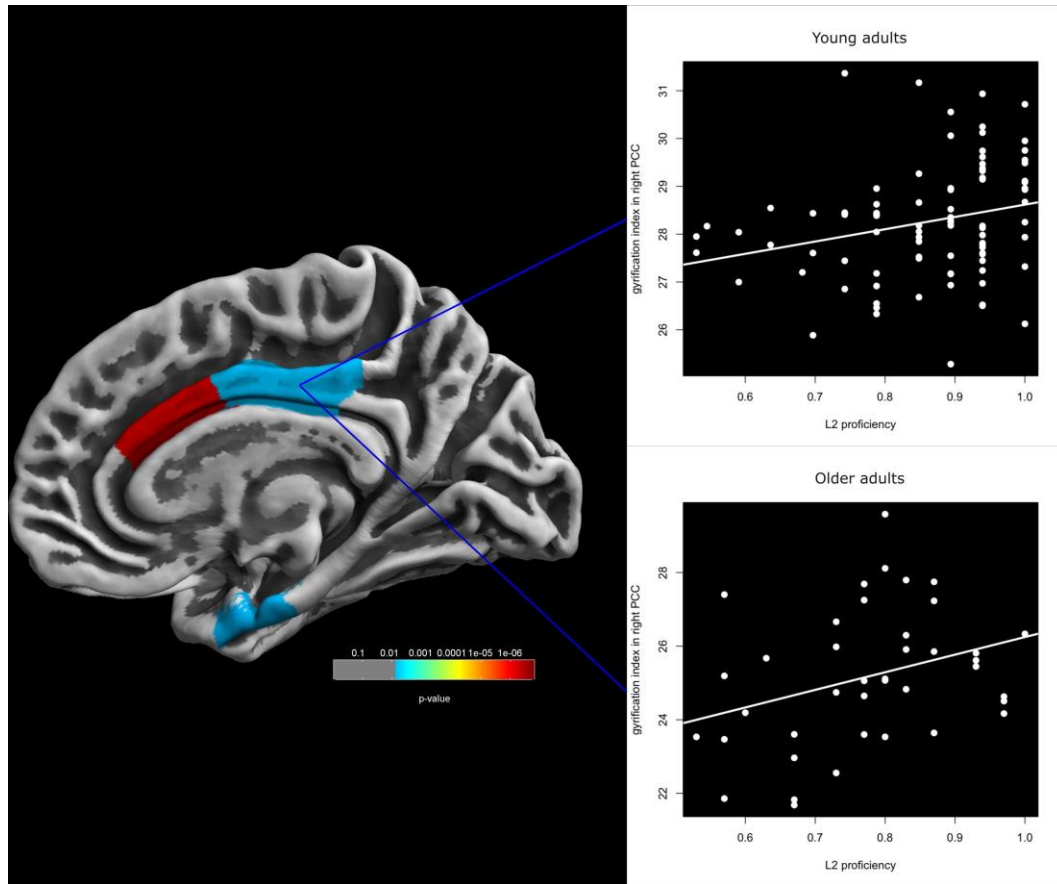
Atlas Region (DK40)	Hemisphere	K	p-value (FWE clust)	t	Equiv Z	MNI x	MNI y	MNI z
<i>Aging Effect (inverse)</i>								
Caudal Anterior Cingulate	R	7029	<0.001	15.24	Inf	4	15	24
Insula	R	1063	<0.001	8.45	7.81	36	-26	7
Precentral Gyrus	R	608	<0.001	5.93	5.69	26	-9	47
Superior Frontal Gyrus	R	196	0.001	5.11	4.95	5	4	67
Postcentral Gyrus	L	384	0.001	5.09	4.93	-18	-31	73
Superior Temporal Gyrus	L	102	0.002	4.97	4.82	-41	-25	1
Postcentral Gyrus	R	143	0.02	4.34	4.24	27	-36	58
Postcentral Gyrus	R	166	0.011	4.5	4.39	27	-36	58
<i>Age*Bilinguals > Age * Monolinguals</i>								
Caudal Anterior Cingulate	R	409	<0.001	5.92	5.68	4	19	29

Experiment 3; Table 1. Whole brain analyses; cluster threshold was set at $p < .05$ FWE corrected for multiple comparisons, with a $K > 50$ vert. spatial threshold.

Region of Interest (ROI). ROI analysis revealed diminished gyrification as aging in the majority of the ROIs, with a more pronounced impact on the right hemisphere. A significant Age*Language Group interaction was associated with maintained gyrification with increasing age in the right caudal ACC, PCC, and Entorhinal Cortex of bilingual participants. (see Experiment 3; Table 2 and Experiment 3; Figure 1).

Atlas Region (DK40)	Hemisphere	p-value (FWE)	t	Equiv Z
<i>Aging Effect (inverse)</i>				
Caudal Anterior Cingulate	R	<0.001	12.9	Inf
Isthmus Cingulate	R	<0.001	14.52	Inf
Lateral Orbitofrontal Cortex	R	<0.001	9.58	Inf
Posterior Cingulate	R	<0.001	11.28	Inf
Rostral Anterior Cingulate	R	<0.001	12.41	Inf
Fusiform Gyrus	R	<0.001	8.69	8.01
Medial Orbitofrontal Cortex	R	<0.001	8.67	7.99
Entorhinal cortex	R	<0.001	6.14	5.88
Transverse Temporal Gyrus	R	<0.001	5.28	5.11
Parahippocampal Gyrus	R	<0.001	5.17	5
Inferior Temporal Gyrus	R	<0.001	4.94	4.79
Transverse Temporal gyrus	L	0.001	4.15	4.06
<i>Age*Bilinguals > Age* Monolinguals</i>				
Caudal Anterior Cingulate	R	<0.001	5.73	5.52
Entorhinal Cortex	R	0.008	3.77	3.7
Posterior Cingulate	R	0.009	3.71	3.65

Experiment 3; Table 2. ROI Analyses. Statistical threshold was set at $p < 0.05$ FWE corrected for multiple comparisons.



Experiment 3; Figure 1. Language Group * Age interaction on cortical gyrification. Correlations with L2 proficiency (ROI level) are also reported. Left: maintained gyrification in the right ACC, PCC and Entorhinal Cortex. Right: scatterplots of the positive correlations between right PCC gyrification and young and older bilinguals' L2 naming scores (the figure is adapted with permission from Del Maschio et al., 2019a).

The Relationship between Gyrification and Executive Control Performance in Bilinguals and Monolinguals. Experiment 3; Table 3 reports RTs for correct responses in the ANT task. Behavioural analyses revealed that when right ACC gyrification was inserted as predictor, the model only showed main effects of Language group ($\beta = 107.83$, $SE = 53.24$, $t = 2.02$, $p = .04$) and Age ($\beta = -5.72$, $SE = 1.47$, $t = 3.88$, $p < .001$), and a Flanker condition * Age interaction ($\beta = 2.29$, $st. err. = 0.70$, $t = 3.27$, $p = .001$) showing that age-related performance decline was larger for the incongruent condition. When the right PCC gyrification was inserted as predictor, the model reported a main effect of Age ($\beta = 5.73$, $SE = 1.19$, $t = 4.80$, $p = < .001$), a main effect of PCC ($\beta = -116.80$, $SE = 39.96$, $t = -2.92$, $p = .004$), a Flanker condition * Age interaction ($\beta =$

1.65, SE = 0.55, $t = 2.99$, $p = .003$), a Language Group * PCC interaction ($\beta = 135.04$, SE = 54.58, $t = 2.47$, $p = .01$), and Age * PCC interaction ($\beta = 2.55$, SE = 0.95, $t = 2.66$, $p = .008$). Finally, when we split for Language Group a significant three-way Language Group * PCC gyrification * Age interaction was found ($\beta = -2.57$, SE = 1.18, $t = -2.17$, $p = .03$). The two-way Age * PCC was significant for monolinguals ($\beta = 2.21$, SE = 0.98, $t = 2.23$, $p = .02$) but non for bilinguals ($t < 1$, $p > .9$).

RT	Bilinguals	Monolinguals
Congruent Trials (M)	602.87	571.77
Congruent Trials (SD)	102.7	133.34
Incongruent Trials (M)	710	668.4
Incongruent Trials (SD)	126.05	148.53

Experiment 3; Table 3. Mean RTs for correct responses (Flanker Effect).

The Relationship between Gyrification and L2 Proficiency/AoA in Bilinguals. Correlational analyses showed a positive correlation between right PCC gyrification and L2 naming accuracy for both young ($p = .005$, $r = .29$) and older adult bilinguals ($t = 2.16$, $df = 38$, $p = .04$, $r = .32$). No significant correlation between L1 to L2 translation and right PCC GI was found. Moreover, results did not show a correlation between right ACC or entorhinal cortex GI and L2 proficiency measures. No significant correlation was found for bilingual younger and older adults between L2 AoA and GI in the right ACC, right PCC, or right entorhinal cortex.

3.3.1 – Discussion

In this study, we used SBM to determine whether bilingualism could act as a source of long-term environmental plasticity on the brain’s surface, affecting the degree of cortical folding. A maintained degree of cingular and medial temporal gyrification as aging was observed in bilinguals when compared with monolingual controls. Moreover, L2 proficiency was correlated with the gyrification of the right PCC for both young and older bilingual adults.

Whole-brain analysis performed irrespective of the language groups showed expected age-related bilateral decreases in brain gyrification in frontal, temporal, and parietal regions. These findings align with previous evidence of gyrification reductions

and cortical atrophy (i.e., diminished GMV) as aging. As mentioned in section 1.2, a large corpus of evidence suggests that aging causes flattening of cortical gyri and opening of cortical sulci, with regional vulnerabilities identified in the temporal lobes and frontal cortices (Cao et al., 2017; Dahnke and Gaser, 2018; Hogstrom et al., 2013; Jockwitz et al., 2017; Madan, 2021; Shen et al., 2018). The comparison between bilingual and monolingual whole-brain gyrification as aging showed that prolonged dual-language experience significantly reduces physiological surface atrophy in the right ACC-MCC complex. As described in section 1.4, bilinguals rely on an executive/language control network to monitor linguistic input and output, detecting dual-language conflict, inhibiting linguistic intrusions, and switching from one language to another (Abutalebi and Green, 2007, 2016; Calabria et al., 2018; Green and Abutalebi, 2013). The dorsal portion of the ACC (often referred to as dACC/pre-SMA complex in bilingualism research literature) plays a central role within this network, by monitoring and suppressing conflicting information (Abutalebi et al., 2012), and sustaining language switching (Abutalebi et al., 2007; Calabria et al., 2018; Price et al., 1999). The continuative usage of this network is associated with the neuroplastic changes observed in lifelong bilingualism, such as increased GMV in the cingulate cortex of younger and older bilingual adults when compared with monolingual controls (Abutalebi et al., 2012). Our findings expand these results and provide novel evidence of cortical surface plasticity associated with dual-language experience.

ROI analyses further confirmed bilingualism-related plasticity effects in the right ACC-MCC complex and revealed maintained cortical folding as aging in the PCC and EC. In section 1.3 we focused on the ACC and MCC components of the cingulate cortex, since these regions are highly impacted by individual morphological variability, a central topic of this dissertation. However, also the PCC represents an important hub in the DMN and functionally interacts with the dorsal attentional network, and the central executive network (Fan et al., 2019; Raichle et al., 2001, 2015). Converging evidence suggests that the PCC actively plays multiple neurofunctional roles. According to the “Arousal, Balance and Breadth of Attention” (ABBA) model (Leech and Sharp, 2013), the ventral part of the PCC, a fundamental component of the DMN, is associated memory retrieval and goal-directed planning. The dorsal portions of the PCC, which are strongly connected with the frontal lobes, would instead support the control of

attentional focus, i.e., the balance between internal and external attention. Especially the hypothesis of an active role for the dorsal PCC in the regulation of attention in response to environmental change detection fits well with our finding of preserved gyrification in this region exclusive to aging bilinguals, who capitalize on a lifelong experience of monitoring language choice, signaling errors and inhibiting unintended languages for communicative purposes. Although less frequent than the recruitment of its rostral counterparts, the activation of the right PCC has been reported during Simon and Numerical Stroop executive tasks in bilingual children (Mohades et al., 2014) and verbal language-switching tasks in young bilingual adults (de Bruin et al., 2014; Reverberi et al., 2015; Weissberger et al., 2015). Moreover, Green (2019) recently emphasised the role played by the PCC in tuning the focus of attention and controlling language input/output during a conversation in bilingual environments. Finally, our finding may also be coupled with Perani et al. (2017), who showed increased metabolic connectivity between the DMN's PCC and subcortical structures exclusive to bilingual versus monolingual patients with AD. Since AD is characterized by early disruption of the DMN, with prominent involvement of the PCC (Minoshima et al., 1997; Yu et al., 2017), the authors interpreted this finding as a bilingualism-induced compensatory mechanism against AD-related neurodegeneration. Taken together, these results point towards a bilingualism-related neuroprotective effect on PCC gyrification, possibly induced by the protracted recruitment of this area for the regulation of attentional states in dual-language contexts. Future research would further explore this interpretation. We observed a significant positive correlation between right PCC gyrification and L2 proficiency in young and older adult bilinguals. Krieger-Redwood et al. (2016) reported that the PCC increases its connectivity with cortical regions supporting cognitive control (e.g., prefrontal cortices) to perform difficult semantic decisions. Moreover, proficiency-dependent modulations of the PCC functional activity have been observed in picture-word matching (Nichols and Joanisse, 2016) and noun-verb generation tasks (Briellmann et al., 2004), allegedly associated with increased cognitive loads in low-proficient young bilingual adults.

Of note, we could not find significant correlations between cortical gyrification and L2 AoA. The age of second language onset is known to impact brain plasticity and individual variability in L2 experience (see Birdsong, 2018). However, it is also well

known that the brain can constantly reorganize its structural and functional architecture as a result of training and learning beyond critical periods of higher plasticity, as reflected in changes in GM and connectivity in late L2 learners (Li, Legault, and Litcofsky, 2014; Rossi et al., 2017; see also Sampaio-Baptista and Johansen-Berg, 2017). Our results indicate that the maintained degree of gyrification in the cingulate cortex is associated with proficiency rather than L2 AoA.

Aside from the PCC, our ROI findings included preserved cortical folding in the EC, a medial temporal structure closely interconnected with the hippocampus and parahippocampal cortex. This region, which participates in forming memories and sustains mnemonic abilities (Preston and Eichenbaum, 2013), is targeted by neural degeneration in the early stages of AD (Braak and Braak, 1991). Moreover, atrophy of the temporal lobe, including the EC, is associated with semantic memory loss in semantic dementia (Chan et al., 2001; Davies et al., 2004). Clinical evidence (Gabrieli et al., 1988; Kensinger et al., 2001) suggests that the entorhinal cortex might play a critical role in acquiring new semantic knowledge, essential for second-language learning. Our findings indicate that the extensive involvement of this region in lexico-semantic mappings may foster local neural reserve in aging bilinguals. In young participants, intensive L2 vocabulary training has been associated with increased hippocampal GMV and CT (Bellander et al., 2016; Mårtensson et al., 2012). Moreover, recent evidence has shown increased proficiency-related temporal pole GMV and preserved temporal pole CT in older bilinguals (Abutalebi et al., 2014; Olsen et al., 2015). Similar findings have also been observed in the left hippocampus for older bimodal bilinguals (Li et al., 2017; but see Gold et al., 2013 and Schweizer et al., 2012 for contradictory conclusions). To our knowledge, our results represent the first account of the neuroprotective effects of bilingualism on entorhinal cortex cortical folding in the aging population. These findings integrate and extend previous evidence based on voxel-based cortical measurements and highlight the necessity of investigating additional surface parameters to better account changes in gray matter (see our recent study on complementary methodological approaches on cortical quantitative analysis, Del Mauro et al., 2021).

This study should be regarded considering some relevant limitations. First, it was impossible to collect data accounting for all participants' socioeconomic status and

language usage. The neurocognitive impact of these factors is widely recognized. As partial compensation, we considered years of formal education and ethnicity as covariates in our models. While there is evidence of global and local ethnicity-driven differences in brain morphology (Kochunov et al., 2003; Uchiyama et al., 2013), the effects on cortical folding are largely unexplored. However, the available evidence indicates that ethnicity does not significantly affect regional sulcation patterns and cortical surface area (Del Maschio et al., 2018a; Jha et al., 2018; Wei et al., 2017). Concerning L1 and L2 exposure, we assume that bilingual participants in our sample used two languages almost daily. At the moment of data collection, all bilingual participants lived in extremely immersive bilingual environments with more than one officially recognized language, such as South Tyrol, Hong Kong, and Manado. An additional limitation is that Cantonese-English bilinguals spoke a tonal language as L1. Since lexical tone processing involves the temporal auditory system (see Liang and Du, 2018), there is a chance that the characteristic properties of Cantonese phonology partly drive structural differences in the medial temporal lobe.

Despite these limitations, our findings provide original information on the neuroplastic consequences of bilingual experience. Our results could be framed within neuroemergentist models defining bilingual experience as a non-linear construct originating from the interplay between distinct elements across time (e.g., Hernandez et al., 2005; Hernandez et al., 2019). Based on this theoretical framework, language experience can be defined in terms of the interaction of smaller non-linguistic factors (e.g., perception, working memory), and environmental factors. In line with these models, our neuroplastic results of cingular and temporal gyrification imply that bilingualism does more than just modifying the cortical regions strictly responsible for language representation and processing. Therefore, a significant level of interplay between language and other cognitive systems occurs in the bilingual brain. Moreover, the preserved degree of gyrification in older bilingual adults may indicate that bilingualism requires protracted time for dual-language experience and cognitive systems to interact and imprint cortical folding.

In conclusion, we reported the first description of bilingualism-related plasticity on adult gyrification trajectories in a large sample of participants. The present study

provides unique clues on the neuroanatomical correlates of bilingualism and novel insights on experience-related cortical reshaping.

3.4 – EXPERIMENT 4 (RESULTS):

Network-based Statistics (NBS) analyses.

- *L2 AoA*. No significant effect.

- *L2 Exposure*. Two Exposure-related subnetworks were revealed by NBS analyses (primary component-forming T-threshold = 3.6). The first component (FWE corrected p-value = .025) consisted of an extended temporal-parietal-occipital component encompassing brain structures in both hemispheres (see Experiment 4; Tables 1 and 2, Experiment 4; Figure 1). Three modules were identified:

1) A module centered around the left superior temporal sulcus, connected with left medial temporal regions (hippocampal, parahippocampal, and entorhinal cortices), the left amygdala, and the left supramarginal gyrus.

2) Temporal-parietal-occipital regions centered around the left fusiform gyrus and paracentral lobule, connected with the lateral occipital cortex, the inferior parietal lobule, and the right pallidum.

3) Temporal-parietal-occipital regions centered around the right paracentral lobule, connected with the isthmus of the right cingulate cortex, the right precentral gyrus, and the left lingual gyrus.

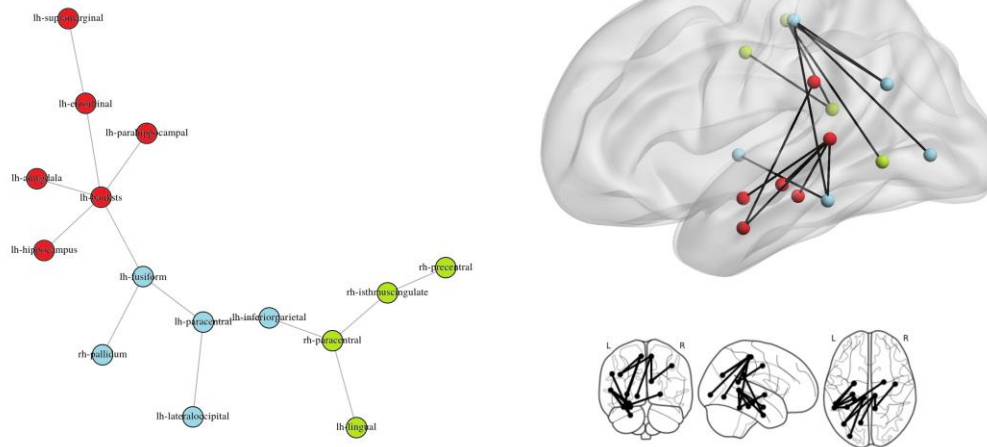
Network	Node (Desikian-Killany labels)	Node Degree	Betweenness of Centrality	Module (Louvain community)
Exposure I	lh-banksts	5	108	1
Exposure I	lh-fusifiform	3	110	2
Exposure I	lh-paracentral	3	106	2
Exposure I	rh-paracentral	3	70	3
Exposure I	lh-entorhinal	2	26	1
Exposure I	lh-inferiorparietal	2	80	2
Exposure I	rh-isthmuscingulate	2	26	3
Exposure I	lh-lateraloccipital	1	0	2
Exposure I	lh-lingual	1	0	3
Exposure I	lh-parahippocampal	1	0	1
Exposure I	lh-supramarginal	1	0	1
Exposure I	lh-hippocampus	1	0	1
Exposure I	lh-amygdala	1	0	1
Exposure I	rh-pallidum	1	0	2
Exposure I	rh-precentral	1	0	3
Exposure II	lh-medialorbitofrontal	3	28	2
Exposure II	lh-rostralanteriorcingulate	3	22	1
Exposure II	lh-lateralorbitofrontal	2	12	3
Exposure II	lh-parsopercularis	2	24	2
Exposure II	lh-caudalmiddlefrontal	1	0	1
Exposure II	lh-parstriangularis	1	0	2
Exposure II	lh-superiorfrontal	1	0	3
Exposure II	lh-insula	1	0	1
Proficiency	lh-rostralmiddlefrontal	4	48	1
Proficiency	lh-superiortemporal	4	48	2
Proficiency	rh-superiorparietal	4	87	4
Proficiency	lh-precuneus	3	58	3
Proficiency	lh-hippocampus	2	22	3
Proficiency	rh-precuneus	2	9	1
Proficiency	lh-isthmuscingulate	1	0	2
Proficiency	lh-temporalpole	1	0	3
Proficiency	lh-putamen	1	0	1
Proficiency	rh-hippocampus	1	0	3
Proficiency	rh-inferiorparietal	1	0	2
Proficiency	rh-paracentral	1	0	1
Proficiency	rh-precentral	1	0	4
Exposure* AoA	lh-caudalmiddlefrontal	6	94	1
Exposure* AoA	lh-middletemporal	1	0	2
Exposure* AoA	lh-parsopercularis	1	0	2
Exposure* AoA	lh-superiorfrontal	1	0	2

Exposure*AoA	rh-thalamus-proper	2	20	3
Exposure*AoA	rh-putamen	1	0	1
Exposure*AoA	rh-pallidum	1	0	1
Exposure*AoA	rh-hippocampus	1	0	1
Exposure*AoA	rh-caudalanteriorcingulate	1	0	3
Exposure*AoA	rh-caudalmiddlefrontal	4	54	2
Exposure*AoA	rh-precentral	2	20	4
Exposure*AoA	rh-supramarginal	1	0	4

Experiment 4; Table 1. Graph theory indices of significant networks. *rh = Right hemisphere; lh = Left Hemisphere.*

Node i (Desikan-Killiany labels)	Node j (Desikan-Killiany labels)	T-Value
<i>Exposure I</i>		
lh-banksts	lh-entorhinal	4.78
lh-banksts	lh-fusiform	3.83
lh-banksts	lh-parahippocampal	3.91
lh-fusiform	lh-paracentral	3.82
lh-inferiorparietal	lh-paracentral	3.88
lh-lateraloccipital	lh-paracentral	4.13
lh-entorhinal	lh-supramarginal	3.64
lh-banksts	lh-hippocampus	4.41
lh-banksts	lh-amygdala	4.63
lh-fusiform	rh-pallidum	3.86
lh-inferiorparietal	rh-paracentral	3.66
lh-lingual	rh-paracentral	4.44
rh-isthmuscingulate	rh-paracentral	3.78
rh-isthmuscingulate	rh-precentral	3.63
<i>Exposure II</i>		
lh-lateralorbitofrontal	lh-medialorbitofrontal	3.75
lh-medialorbitofrontal	lh-parsopercularis	4.07
lh-medialorbitofrontal	lh-parstriangularis	4.44
lh-caudalmiddlefrontal	lh-rostralanteriorcingulate	4.10
lh-parsopercularis	lh-rostralanteriorcingulate	3.92
lh-lateralorbitofrontal	lh-superiorfrontal	4.54
lh-rostralanteriorcingulate	lh-insula	3.72

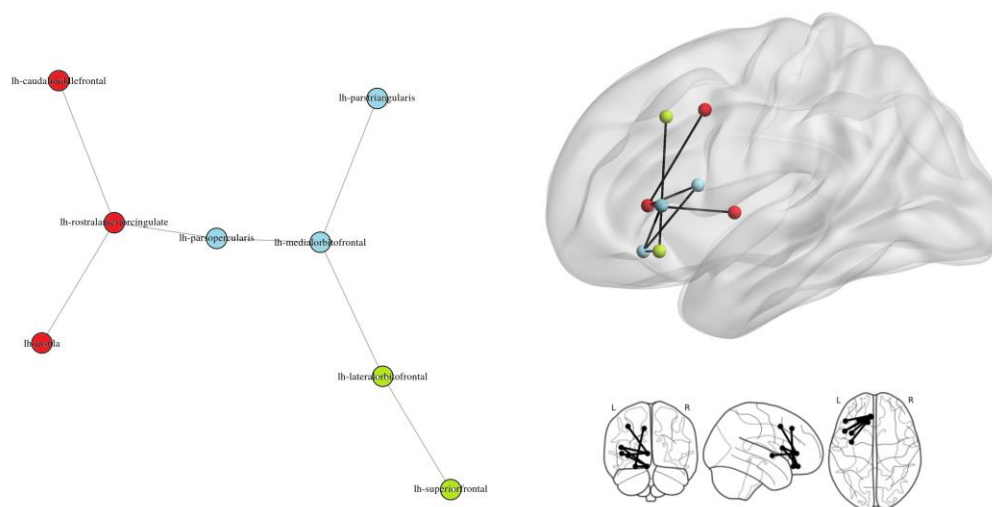
Experiment 4; Table 2. Exposure I and II networks NBS results



Experiment 4; Figure 1. Exposure I network (the figure is adapted with permission from Fedeli et al., 2021).

The second exposure-related network (FWE corrected p-value = .049) consisted of a left-hemispheric component including frontal-opercular and cingulate regions. Three modules were identified (see Experiment 4; Tables 1 and 2, Experiment 4; Figure 2):

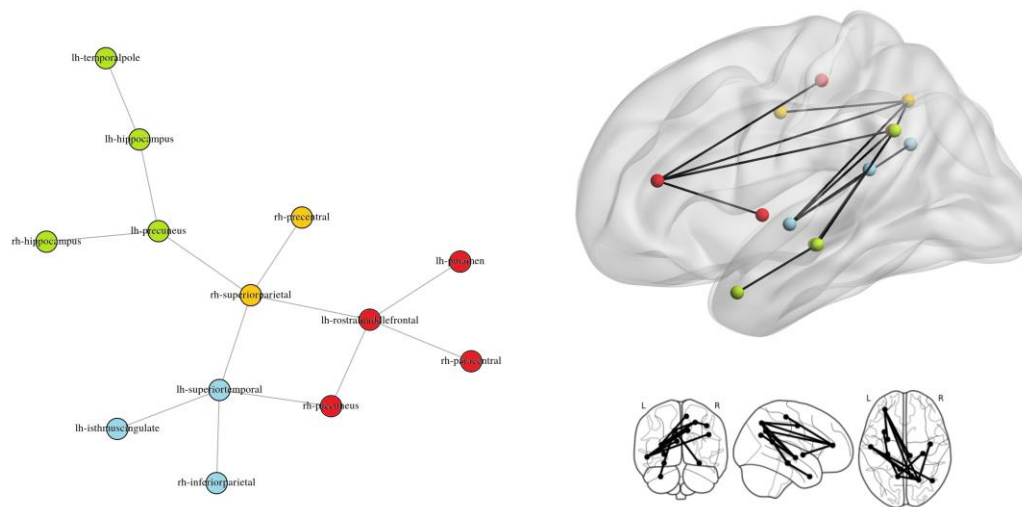
- 1) A module centered around the ACC connected with the insula and the caudal middle frontal gyrus.
- 2) A module centered around the medial orbitofrontal cortex, connected with the pars inferior frontal gyrus (pars triangularis and orbitalis).
- 3) A module including the lateral orbitofrontal cortex and the superior frontal gyrus



Experiment 4; Figure 2. Exposure II network (the figure is adapted with permission from Fedeli et al., 2021).

- *L2 Proficiency*. A large proficiency-related network resulted from NBS analyses (primary component-forming T-threshold = 2.85; FWE corrected p-value = .046). The connected component encompassed bi-hemispheric frontotemporal, parietal, and subcortical structures. Four modules were identified (see Experiment 4; Tables 1 and 3, Experiment 4; Figure 3):

- 1) A module centered around the rostral left middle frontal gyrus, including the right precuneus, paracentral lobule, and left putamen.
- 2) A second module centered around the left superior temporal gyrus, including the right inferior parietal lobule and the isthmus of the cingulate cortex;
- 3) A module centered around the left precuneus and including the hippocampi in both hemispheres and the left temporal pole;
- 4) A central model including the right superior parietal cortex (greatest betweenness of centrality) and the right precentral gyrus.



Experiment 4; Figure 3. L2 Proficiency network (the figure is adapted with permission from Fedeli et al., 2021).

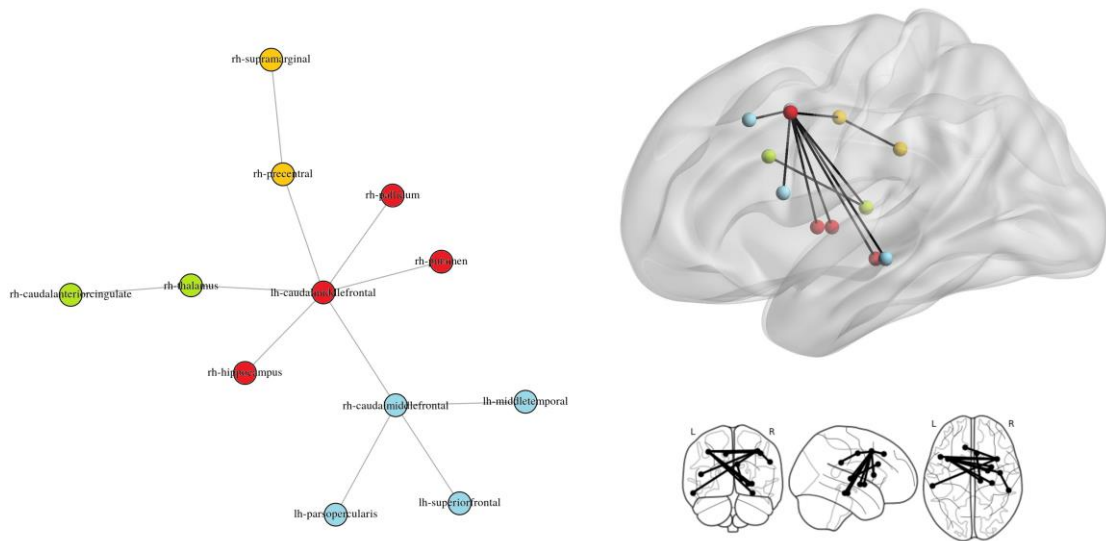
Node i (Desikan-Killiany labels)	Node j (Desikan-Killiany labels)	T-Value
lh-isthmuscingulate	lh-superiortemporal	2.93
lh-rostralmiddlefrontal	lh-putamen	2.87
lh-precuneus	lh-hippocampus	3.18
lh-temporalpole	lh-hippocampus	3.25
lh-precuneus	rh-hippocampus	3.15
lh-superiortemporal	rh-inferiorparietal	3.07
lh-rostralmiddlefrontal	rh-paracentral	3.39
lh-rostralmiddlefrontal	rh-precuneus	3.20
lh-superiortemporal	rh-precuneus	3.05
lh-precuneus	rh-superiorparietal	2.88
lh-rostralmiddlefrontal	rh-superiorparietal	3.23
lh-superiortemporal	rh-superiorparietal	3.53
rh-precentral	rh-superiorparietal	2.95

Experiment 4; Table 3. Proficiency network NBS results

- *L2 AoA * L2 Exposure*. A frontal-temporal network, including subcortical structures, resulted from NBS analyses investigating L2 AoA * Exposure interaction (primary component-forming T-threshold = 2.7; FWE corrected p-value = .018). The interconnected bilateral caudal middle frontal gyri, were the regions with the highest betweenness centrality. Graph theory revealed four modules (see Experiment 4; Table 1 and 4, Experiment 4; Figure 4):

- 1) A module centered around the caudal left middle frontal gyrus, including the right putamen, pallidum, and hippocampus.
- 2) A module centered around the caudal part of the right middle frontal gyrus, including the left temporal gyrus, superior frontal gyrus, and inferior frontal gyrus (pars opercularis).
- 3) A module centered around the right thalamus and including the ACC.
- 4) A module centered around the right precentral gyrus and including the supramarginal gyrus.

No other interaction lead to significant results.



Experiment 4; Figure 4. L2 AoA * Exposure network (the figure is adapted with permission from Fedeli et al., 2021).

Node i (Desikan-Killiany labels)	Node j (Desikan-Killiany labels)	T-Value
lh-caudalmiddlefrontal	rh-thalamus-proper	2.93
lh-caudalmiddlefrontal	rh-putamen	2.84
lh-caudalmiddlefrontal	rh-pallidum	3.23
lh-caudalmiddlefrontal	rh-hippocampus	3.04
rh-thalamus-proper	rh-caudalanteriorcingulate	2.70
lh-caudalmiddlefrontal	rh-caudalmiddlefrontal	3.68
lh-midtemporal	rh-caudalmiddlefrontal	2.98
lh-parsopercularis	rh-caudalmiddlefrontal	2.74
lh-superiorfrontal	rh-caudalmiddlefrontal	3.32
lh-caudalmiddlefrontal	rh-precentral	2.71
rh-precentral	rh-supramarginal	2.74

Experiment 4; Table 4 – L2 AoA * Exposure NBS results

Whole-Connectome Graph Analysis. Since no neighboring node triplets were found, Eloc computation was impossible for the connected components. Therefore, only Eglob was used for the subnetwork analyses. L2-proficiency network Eglob was significantly correlated with the Eglob ($r_s = .69$; $p < .001$) and Eloc ($r_s = .65$; $p < .001$) whole-connectome efficiency measures. Likewise, the L2 AoA * Exposure Eglob was

significantly associated with Eglob ($r_s = .38$; $p < .001$) and Eloc($r_s = .43$; $p < .001$) whole-connectome efficiency measures.

Correlation between efficiency measures and switching tendencies.

Finally, L2 AoA * Exposure Eglob was significantly correlated with the BSWQ US score ($r_s = -0.24$; $p < 0.05$).

3.4.1 – Discussion

In experiment 4, we described the distinct contribution of dual-language experience components in modulating the brain's structural connectome. We employed anatomically accurate whole-brain probabilistic tractography and NBS to define connected components of regions in which L2 Exposure, proficiency, and AoA modulated structural connectivity. Graph theoretical indices were computed to quantify if the properties of these networks altered whole-brain interconnectedness. In the following, we discuss our findings and their general implications.

Exposure – Subnetwork I (posterior). The first L2-exposure subnetwork included temporal-parietal-occipital regions. Nodal degree and betweenness of centrality indices revealed that the posterior part of the left superior temporal sulcus played a central role within the network. According to the dual-stream model by Hickok and Poeppel (2000, 2004, 2016), the superior temporal sulcus is connected with temporal regions underpinning phonological-to-conceptual mapping, mediating lexical access. In this network, the superior temporal sulcus was strongly coupled with the ventral and medial aspects of the temporal lobe (i.e., fusiform, lingual, entorhinal, and parahippocampal gyri, and hippocampus), which are extensively implicated in semantic processing (Hoeing and Scheef, 2005) and word learning (Bellander et al., 2016; Breitenstein et al., 2005; see also Davis and Gaskell, 2009 and Raslau et al., 2015)⁶.

⁶ See experiment 3 for a detailed description of the contribution of bilingual experience in preserving cortical gyrification in medial temporal lobe structures.

These regions are pivotal for the acquisition, maintenance, and retrieval of lexical and semantic knowledge.

These results indicate that dual-language Exposure impacts and strengthens a network of connected regions along the left ILF that are of primary importance for speech comprehension (i.e., accessing word conceptual-semantic meaning from a phonological input). This interpretation is coherent with the results of Kuhl and colleagues (2016). The authors reported significant correlations between microstructural indices of the ILF and the L2 listening and speaking Exposure, weighted by linguistic immersion (i.e., a proxy measure of continuous, intensive, naturalistic L2 experience).

The superior temporal sulcus was also indirectly communicating with parietal regions (i.e., left inferior parietal lobule and the supramarginal gyrus), probably by means of the Superior Longitudinal/Arcuate fasciculi in the dorsal stream. In accordance with this finding, in our recent functional connectivity study (Sulpizio et al., 2020b), we observed increased rsFC within parietal areas due to higher bilingual Exposure. Besides, the Adaptive Control hypothesis (Green and Abutalebi, 2013) collocates these areas in an interconnected set of regions sustaining context-dependent dual-language selection and controlling speech production. Parietal areas have also been proposed to play a substantial role in sensory-motor integration, enabling the monitoring and correction of speech errors (Buchsbaum et al., 2011; Hickok and Poeppel, 2016) and in the storing lexical and semantic information (see the "Dual Lexicon" model by Gow, 2012; Gold et al., 2007). However, the primary function of these regions in the bilingual brain remains dual-language selection and maintenance. On these grounds, we suggest that L2 Exposure modulates the connectivity within a set of regions in "Subnetwork I (posterior)", which supports elements of speech comprehension via the ventral stream and language selection via the dorsal stream.

Exposure – Subnetwork II (anterior). The second exposure-related subnetwork included left frontal-opercular and cingular areas, allegedly communicating through short-range intragyrus U-fibers and the left IFOF. The opercular and triangular parts of the left inferior frontal gyrus play a fundamental role in the verbal articulation and processing of syntactic information (Friederici 2009; Haagort, 2005; Hickok and Poeppel, 2004). As described in section 1.4 and highlighted by our recent meta-analysis

(Sulpizio et al., 2020a), a vast literature of fMRI studies has reported shared inferior frontal activations for L1 and L2 processing in bilinguals. In this network, the pars opercularis of the inferior frontal gyrus had one of the greatest centrality rates and communicated with a module comprising the left insular cortex, the ACC, and the middle frontal gyrus. The anterior insula participates in verbal production and vocal articulation (Ardila et al., 2014; Oh et al., 2014) and contributes to language switching by monitoring linguistic interferences during word retrieval (e.g., Parker Jones et al., 2012). As described in the introductory chapters, the ACC monitors cognitive and language conflicts (Botvinick et al., 2001; Luk et al., 2012) and participates in bilingual language control and switching (Branzi et al., 2016). Besides, extensive dual-language experience has been associated with neuroplastic modifications in the ACC and maintained GMV, CT, and cortical gyrification in this region as aging (see experiment 3; Abutalebi et al., 2015; Del Maschio et al., 2019a; see also Del Maschio et al., 2019b). Moreover, the middle and superior frontal gyri are prefrontal regions supporting language conflict resolution by monitoring interfering linguistic information (Abutalebi and Green, 2007; Branzi et al., 2016; Calabria et al., 2018).

Based on these considerations, we propose that dual-language Exposure strengthens a structural subnetwork connecting regions crucial for speech production and vocal articulation, actively controlled by executive areas. Greater L2 Exposure would promote reinforced frontal connectivity with executive areas due to the intensification of language-monitoring demands. This view is coherent with the "dynamic reconstruction model" proposed by Pliatsikas et al. (2019b), implying IFOF microstructural adaptations and enhanced control efficiency because of dual-language Exposure. Of note, in a structural connectivity study comparing monolinguals and early bilinguals, García-Pentón and colleagues (2014) described a remarkably similar connected component in the left hemisphere. Hence, our results expanded previous knowledge about this network by showing that L2 Exposure modulates WM connectivity within these regions.

Proficiency. Second language proficiency impacted a bilateral connected component, including parietal, frontal, and temporal areas. The rostralmost module comprised the left middle frontal gyrus communicating with the ipsilateral putamen. In line with Green

and Abutalebi (2013), frontal-putamen edges partake in the bilingual language control network. In this model, dorsolateral prefrontal regions such as the middle frontal gyrus would be required explicitly in conflict resolution (see above). As for the hippocampus, this structure is shared with the Exposure Subnetwork I. This structure, along with the left temporal cortex, is pivotal for collecting lexical and semantic information and supporting second language vocabulary learning in bilinguals (Li et al., 2017; Stein et al., 2012), while speech perception and comprehension are grounded on the left superior temporal gyrus (Hickok and Poeppel, 2004; 2007; 2016). In this module, L2 proficiency increased the connectivity of the left temporal pole with hippocampal and subcortical regions, possibly highlighting increased memory demands for an intensive word learning experience in bilinguals. Several studies suggest that the left temporal pole is of crucial importance for lexical representation and retrieval (Geranmayeh et al., 2015), and temporal pole lesions are associated with semantic errors (Pobric et al., 2007; Schwartz et al., 2009). However, the contribution of the temporal pole (and, in general, of the anterior temporal cortex) is not limited to the acquisition and retrieval of lexico-semantic information. Neurofunctional evidence suggests that this region is crucial for high-level integration of cognitive and linguistic information supporting combinational processes both in the syntactic and the semantic domain and is integral for sentence comprehension and syntactic elaboration (Brennan et al., 2009; Bornkessel-Schlesewsky and Friederici, 2007; Friederici and von Cramon, 2000; Friederici, et al., 2001,2003,2011,2012; Grodzinsky and Friederici 2006; see also Hitckock and Poeppel, 2016 for a perspective in which anterior temporal lobe contributes to syntactic processing and structure binding). Exemplarily, Friederici et al., (2000) investigated brain activity during auditory language processing of normal speech, sentences containing pseudo-words, and lists of words and pseudo-words. When compared with lists of single words, stimuli with a syntactic structure (i.e., speech and sentences) elicited greater activation of the anterior aspects of the temporal lobe. This finding, validated by subsequent studies (e.g., Humphries et al., 2005; Rogalsky and Hickok, 2009), points towards a general integrative function in sentence-level speech comprehension (e.g., conversation, discourses, stories) of the temporal pole (see also Bornkessel-Schlesewsky and Friederici, 2007). With respect to our results, it could be suggested that greater L2 proficiency increases the connectivity of several

language/executive regions with the left temporal pole, supporting improved integration of syntactic, lexico-semantic, and, possibly, phonological information from the two languages.

The caudalmost part of this component included several interconnected areas in the right parietal cortex. The inferior parietal lobule is associated with acquiring sensorimotor engrams when learning novel words (Lee et al., 2007; Mechelli et al., 2004) and maintaining language representations during dual-language production to deliver accurate speech output. (Abutalebi and Green, 2008). Neurological evidence suggests pathological second language selection and switching occur in bilinguals when this region is lesioned (Leischner, 1987; Pötzl, 1925).

By means of Graph theory indices, we observed that as Eglob increases within this network (i.e., nodes in the network become more interconnected), both Eloc and Eglob increase in the whole-brain connectome. This finding partially contradicts the conclusions of García-Pentón et al. (2014), who reported diminished whole-connectome efficiency as a function of enhanced subnetworks Eglob in bilingual participants. However, this difference can arguably be related to the fact that the authors adopted a dichotomic classification of bilingual/monolingual individuals while we relied on a multi-componential continuum. This theoretical choice may have lead to two non-perfectly-overlapping connectivity networks with specific topological characteristics. With respect to the findings of García-Pentón et al., our proficiency-driven connected component shows a greater number of nodes and inter-hemispheric edges. In a recent connectivity study on individuals with callosal agenesis, Owen and colleagues (2013) suggested that inter-hemispheric edges significantly modulate whole-brain efficiency, enabling long-range communication between distant connectivity hubs. Our findings indicate that bilingual proficiency is advantageous to the brain's small-world organization, i.e., the efficient information transfer over a range of local and global scales, notwithstanding a low wiring cost (Fornito, Zalesky and Bullmore, 2016; Latora and Marchiori, 2001).

In the central module, the superior parietal lobule had the most significant nodal degree and betweenness of centrality. This region is a fundamental component of the dorsal attention network (DAN). The DAN is formed by frontoparietal areas that sustain mechanisms of top-down attention orientation and selection of relevant stimuli

(Corbetta and Shulman, 2002). Several accounts of neurofunctional recruitment of parietal regions during bilingual naming tasks support the notion that efficient language switching is grounded on these functions (Consonni et al., 2013; Consonni et al., 2013; De Baene et al., 2015; Reverberi et al., 2015). Moreover, the right superior parietal lobule and the bilateral precuneus have been reported to participate in first and second language verb and noun production in bilingual participants (Consonni et al., 2013). On these grounds, we propose that bilingual proficiency strengthens WM structural connectivity between a set of brain nodes supporting L2 lexicon acquisition and learning. In this connected component, frontal and parietal regions act as a language selection system interacting with temporal nodes supporting lexical and semantic access and storing. As second language proficiency increases, stronger frontoparietal connections would orient the attention to the target language more efficiently and allow faster lexico-semantic information access. L2 learning and increased dual-language proficiency have been associated with alterations of microstructural indices (FA) in the right superior longitudinal and arcuate fasciculi (connecting frontal, temporal, and parietal regions) by both cross-sectional and longitudinal investigations (Hosoda et al., 2013; Mamiya et al., 2016; Nichols and Joanisse, 2016). Besides, in our recent functional connectivity study (Sulpizio et al., 2020b), we described similarly increased rsFC in temporal and parietal regions as a function of higher L2 proficiency. In line with the structural findings discussed above, we suggested that these connections would facilitate orienting attentional resources on the language's lexicon that needs to be accessed. Moreover, with increased L2 expertise, anterior temporal regions (i.e., temporal pole) would become more efficient in supporting dual-language speech comprehension by integrating syntactic, lexical, and phonological aspects of the discourse.

Interaction between AoA and Exposure. Despite several TBBS studies reported effects of AoA on WM microstructural organization, in this work no significant effect of L2 AoA was found. The lack of a direct effect of L2 AoA on WM network organization can be explained based on two considerations. First, the Italian school system introduces most children to English learning during primary school, hence in our sample mean L2 AoA was moderately low (7.65 ± 3.46) and skewed. If our sample had

included more participants with a much earlier L2 acquisition (e.g., simultaneous bilinguals), we would have possibly glimpsed direct AoA effects on WM network organization. Second, in line with DeLuca and colleagues (2019), we suggest that L2 onset per se can be treacherously uninformative of the real L2 usage history of one individual. Other measures such as L2 immersion periods (DeLuca et al., 2019) and L2 usage are possibly more meaningful for defining the individual bilingual experience after the acquisition of a second language. On this ground, the L2 AoA * Exposure interaction impacted the connectivity of a bi-hemispheric frontal connected component, encompassing subcortical and temporoparietal structures. The topological center of the network was represented by the directly connected bilateral middle frontal gyri, communicating with nodes in the opposite hemisphere. The right middle frontal gyrus was linked with the left middle temporal gyrus and the inferior, middle, and superior frontal gyri. This finding indicates strengthened connectivity between the right dorsolateral prefrontal cortex and contralateral regions responsible for language comprehension, production, and control. In the left hemisphere, the middle frontal gyrus communicated with the right middle frontal gyrus, parietal cortex, and subcortical structures (pallidum, thalamus, putamen, hippocampus). These regions are involved in L2 lexical and semantic processing, dual-language conflict monitoring and control, and language selection (Abutalebi and Green, 2016; Burgaleta et al., 2016; Mamiya et al., 2018). This network showed a strongly inter-hemispheric architecture. Hence, we suggest that L2 AoA and L2 Exposure jointly influence the frontal and callosal structural connectivity, in line with evidence of increased myelination in the CC as a result of bilingual experience (DeLuca et al., 2019; Luk et al., 2011; Pliatsikas et al., 2015; Rahmani et al., 2017). Plots of the Eglob measure showed that, on low levels of L2 Exposure, early (AoA \leq 6) and late (AoA $>$ 6) bilinguals displayed a comparable degree of efficiency. However, this network becomes more isolated (i.e., more locally and less globally efficient) in late L2 learners as a function of increasing Exposure. On the other hand, early bilingual participants showed a less steep slope indicating preserved Eglob with high L2 Exposure. These findings might indicate that late bilinguals rely on this network, and not on others, to face high levels of L2 Exposure. Recently, DeLuca et al. (2019) showed that the later an L2 is acquired, the more bilinguals show enhanced callosal connectivity. Besides, CC myelination correlates

with the duration of L2 immersion, thus implying that both L2 AoA and immersion would foster more efficient and spontaneous language control (DeLuca, Rothman, and Pliatsikas, 2019). The Eglob of the L2 AoA * Exposure component was negatively correlated with the BSWQ US, thus implying that increased segregation of this component could be beneficial to control between-language switching. This observation aligns with Bonfieni et al. (2019), who reported that greater L2 Exposure is associated with easier L1-to-L2 switching. Conversely, earlier L2 acquisition might promote the growth of broader WM interregional connectivity. Therefore, bilinguals that acquire their L2 early may rely on different pathways to sustain growing linguistic demands driven by greater L2 Exposure. Overall, the dynamic nature of bilingual dual-language control is exemplarily displayed by this connected component: second language representation and lifelong management are affected by multiple factors, including L2 AoA and the degree of Exposure. These findings also highlight the intrinsic limitations of using the L2 AoA metric by itself, as it tends to be meaningful in predicting bilingual abilities only in the early stages of neural and linguistic development (e.g., “critical periods”), while its relevance is progressively taken over by L2 Exposure and Proficiency (see Rossi et al., 2017). L2 Immersion, which accounts for periods of continuous, intensive, naturalistic L2 experience, seems to be a superior metric with respect to L2 AoA, and should be adopted in follow-up studies and future iterations of this experiment (DeLuca, Rothman, and Pliatsikas, 2019; DeLuca et al., 2019).

To resume, we capitalized on cutting-edge MRI diffusion processing techniques and NBS to study networks of regions in which distinct bilingual experiential factors modulated the brain's WM connectivity. L2 Exposure, L2 Proficiency, and L2 AoA (in interaction with Exposure) distinctively impacted the structural architecture of linguistic pathways and the connectivity between regions supporting language control. These findings are in accordance with well-recognized neurocognitive models of dual-language representation, processing, and monitoring. This study overcomes some methodological limitations of previous experiments and extends the knowledge about the neuroplastic effects of bilingual experience by providing original models of large-scale WM (re)organization in bilingual individuals.

Chapter 4 – DISCUSSION

This chapter resumes the overview of the background provided in chapter 1 and the empirical findings of experiments 1,2,3, and 4. Each study has been discussed separately in chapter 3. Here, we discuss the general implications of our results, as well as the limitations of our research. We conclude by suggesting possible directions for future research.

4.1 Resume of background and experimental findings

In the Section 1.2 of the Introduction, we defined brain gyrification as a measure of the degree of convolution of the cerebral cortex. We presented evidence from comparative neuroanatomy suggesting that the human brain has specific features that make it stand out among other mammals. These features include a highly gyrified cortex that allows constraining a massive number of cortical neuronal cells in a relatively small cerebral volume. We subsequently described the ontogeny of the cerebral cortex, showing how precursor cells build the cortical ribbon permitting it to grow and expand. Cortical folding follows precise developmental trajectories: Gyrification plateaus at birth and, unlike other structural properties of the cortex, remains relatively stable throughout the lifespan. We showed how the biological mechanisms underneath cortical folding are not wholly known, and we presented a series of candidate causal models. These models, each with its own merits and limitations, are insufficient by themselves to account for the complexity of cortical gyrification. However, we concluded by suggesting that an integrated view that takes important input from different biological and mechanical processes can accurately describe why the cortical mantle fissures and folds.

In the Section 1.3 of the Introduction, we focused on describing the individual morphological variability of cortical folding in the cingulate cortex. We first presented the cingulate cortex and the parcellation methods adopted to divide it into specific portions. These parcellations are based on structural, cytological, and functional properties. We then focused on the ACC-MCC complex, the part of the cingulate cortex that is primarily characterized by interindividual variability in sulcation patterns. The

ACC is a connectivity hub involved in the well-known DMN and a core region for emotional processing. The MCC sustains motor and high-order cognitive functions such as cognitive control, RI, and conflict monitoring. After having defined the ambiguities in naming the ACC-MCC complex, we turned to the description of the PCS. We defined the PCS as a sulcus that runs dorsally and parallel to the CS, and we provided demographic information regarding its occurrence in the general population. We described its variability in length, size, and morphology and its stability as a structural feature. We described the impact of the PCS on the cytology of Brodmann's areas 24' and 32' as well as on the local GMV. The impact of the PCS also extends to the functional profile of the ACC since it can alter the topology of the clusters of brain activity in a variety of tasks. After defining four different sulcation patterns based on the PCS hemispheric distribution, we provided a link between ACC morphology and cognitive abilities. We concluded by presenting data regarding the altered distribution of hemispheric ACC sulcation patterns and PCS morphology in the clinical population, focusing on schizophrenia and psychotic disorders.

In Section 1.4, we introduced neural plasticity as the force that drives change in the brain's structural and functional architecture. We presented the notion of short-term and long-term synaptic plasticity and showed how the brain learns and can self-adapt. We then introduced the concept of bilingualism as an ideal scenario to investigate neural plasticity. We described how bilingual individuals rely on executive functions to sustain the effort required to correctly switch from one language to another or suppress interferences from a second language. We concluded by providing evidence of the structural and functional reorganization because of second language experience.

In Experiment 1, we investigated for the first time the relationship between anatomical variability of the ACC and functional connectivity at rest in young and older adult individuals. We adopted a similar approach to Margulies et al. (2007) by using seed-to-voxel rsFC with spherical ROIs arranged over the ACC. We classified participants from the LEMON database based on their PCS hemispheric distribution. We then compared the functional connectivity profiles of individuals with double absent, double present, rightward asymmetry, and leftward asymmetry PCS sulcation patterns. Moreover, as functional connectivity tends to change over time, we investigated the interaction effect of aging in modulating pattern-specific connectivity.

Our analyses revealed that distinct ACC sulcal patterns are associated with specific profiles of connectivity strength and trajectories and that this relationship changes as age increases. Our findings provided novel insights into the relationship between early-determined morphological variants and the brain's functional architecture over adulthood.

In Experiment 2, we investigated the neural correlates of the behavioural advantage that has been frequently reported in executive tasks for individuals with asymmetric rather than symmetric ACC sulcation patterns. Participants were recruited and classified as either symmetric or asymmetric, based on the PCS hemispheric occurrence. All participants performed an ANT and a Numerical Stroop task in an MRI scanner. We investigated differences in brain activity and RT efficiency between individuals with symmetric and asymmetric ACC sulcal patterns. We observed greater activation of bilateral paracingulate gyri associated with a symmetric ACC sulcal pattern during the Stroop task, suggesting more effortful processing. Our results support previous evidence that ACC morphological variability modulates inhibitory control, and we provided novel insights into the functional correlates of this relationship. Moreover, we observed a behavioural advantage in the Stroop task for individuals with asymmetric PCS and an opposite pattern for the ANT task. Since the two tasks entail different levels of functional asymmetry, we concluded by suggesting that task-specific features may play a relevant role in determining behavioural advantages associated with sulcation pattern variability.

In Experiment 3, we investigated the neuroplastic effects of bilingualism in modulating a relatively stable structural feature of the brain, such as cortical gyrification. Previous neuroimaging studies suggested that bilingualism could act as a source of neural plasticity. Nevertheless, prior research had mainly focused on bilingualism-related changes in GMV and WM microstructure. In this study, we used SBM to investigate the impact of bilingual experience on cortical gyrification from early adulthood to old age in an international sample of bilingual and monolingual participants. Despite widespread gyrification reductions as a function of aging was found irrespective of the language group, maintained gyrification exclusive to bilinguals was detected in the right cingulate and entorhinal cortices, which are vulnerable to normal and pathological effects of aging. Our findings provided novel insights on

experience-related cortical reshaping and bilingualism-induced cortical plasticity throughout the life span.

In Experiment 4, we continued investigating the role of bilingualism as a source of neural plasticity to deepen the relationship between brain structure, function, and cognitive abilities. With respect to Experiment 3, in which we measured cortical gyrification, in this study we focused on a much more experience-responsive feature of the brain, i.e., WM connectivity. While previous research had investigated the impact of bilingualism on brain structural connectivity, there was mixed evidence on how distinct components of bilingual experience contributed to structural brain adaptations. This lack of consistency could be ascribed, at least in part, to methodological choices in data acquisition and processing. In Experiment 4, we adopted state-of-the-art WM tractography and the Network Neuroscience framework to investigate how individual differences in L2 Exposure, Proficiency, and AoA, relate to whole-brain structural organization. To overcome previous methodological limitations, we employed state-of-the-art diffusion modeling and analysis techniques. Moreover, in line with recent trends in the neuroscience of bilingualism, we conceptualized bilingual experience as a continuous and multi-componential construct rather than a monolithic variable. Our results showed that L2 Exposure strengthened the connectivity of two networks of brain areas supporting language comprehension (posterior) and production (anterior). Moreover, L2 Proficiency fostered increased structural connectivity in a parietal network of regions involved in language selection and word learning, and with the temporal lobe, crucial for combinational processing and integration of distinct linguistic information. Finally, the L2 AoA * Exposure interaction modulated inter-hemispheric information transfer between frontal regions and subcortical structures involved in executive/language control. Our results expanded and elucidated mechanistic knowledge about specific variations of the brain's macrostructural organization associated with the bilingual experience.

4.2 General Discussion

The present dissertation considers two dimensions of the relationship between brain structure, function, and cognitive abilities. The first element corresponds to

lifelong stable features of the brain, while the second is represented by neural plasticity due to environmental factors. The four studies we performed follow a continuum that covers both aspects. On one side, we observed how neuroanatomical constraints affect brain functional organization and activity, and cognitive abilities. On the other, we described how individual differences in second language experience (here intended as a proxy measure of environmental factors inducing brain plasticity) impact the brain's stable or malleable structural properties such as gyrification and WM connectivity.

Patterns of ACC sulcation, which develop in utero and remain stable throughout the lifespan, represented an ideal scenario for testing the impact of prenatally determined neuroanatomical constraints on functional properties of the brain and cognitive abilities. Previous evidence suggested that the variable PCS occurrence on the ACC-MCC complex was associated with altered topology of local functional activity in a range of cognitive tasks (Amiez et al., 2013; Crosson et al., 1999; Jahn et al., 2016). However, the association between ACC sulcation pattern and the brain functional organization at rest was barely known. In Experiment 1, we observed for the first time that individual differences in ACC sulcal patterns were also associated with distinct profiles of rsFC. Moreover, we revealed that this relationship changed with increasing age.

Nevertheless, in Experiment 1 we did not find a relevant association between the differences in structure-function relationships and cognitive abilities, despite previous accounts of asymmetry-related advantages reported in children and adults (Borst et al., 2014; Cachia et al., 2014, 2017; Del Maschio et al., 2018a; Tissier et al., 2018). We suggested that a more specific assessment, including the same executive task adopted in previous studies, would have been necessary to reveal these effects. In Experiment 2, we used the ANT and the Numerical Stroop tasks to test this hypothesis. In both tasks, we observed that behavioural measures associated with RI were significantly modulated by ACC sulcation pattern symmetry and asymmetry. Moreover, we described a difference in neural activity associated with the asymmetry-related advantage frequently reported in the literature.

Taken together, Experiment 1 and Experiment 2 have several implications and expand our understanding of how individual differences in cortical morphology are linked with

brain functional activity and cognitive abilities. The conclusions of the two studies can be synthesized as follows:

- Individual variability of the ACC sulcation pattern influences the brain's functional organization at rest.
- This structure-function relationship changes as aging.
- Patterns of PCS hemispheric symmetry and asymmetry modulate neurofunctional activity and behavioral performance during inhibitory control tasks.
- These differences are possibly grounded in the variability of underlying WM structural connectivity.

In experiment 1, the bilateral PCS occurrence was linked with increased connectivity than other profiles. Moreover, the presence of a PCS on the right hemisphere was always indicative of greater connectivity. Our results suggest that early-determined morphological patterns are impactful on the functional organization of the brain. These differences in rsFC were found for target regions included either in the DMN or in the SN. This result is relevant since the dorsal and ventral components of the ACC-MCC complex are considered fundamental connectivity hubs within these two networks. Therefore, variability of ACC sulcation patterns modulates pre-existent rather than new connections (either by augmenting or diminishing the strength of their relationship). We also revealed that sulcal pattern variability and aging jointly modulate the rsFC trajectories over adulthood (e.g., more stable connectivity with increasing age for symmetric patterns). This result has significant implications, indicating a long-term influence of lifelong stable morphological features on resting-state networks. Deficits of DMN regulation have been observed in older adults when compared to younger individuals (Spreng and Shacter, 2011) and associated with more significant local beta-amyloid neuronal toxicity (Ferreira and Busatto, 2013; Sheline et al., 2010) and poorer cognitive abilities (i.e., autobiographical memory) (Mével et al., 2013). Zhang and colleagues (2019) showed that the preserved or increased connectivity of the ACC as aging is associated with the conservation of youthful memory in "superager" older adults. Our data suggest the possibility that early determined configurations of cortical folding may act as a long-term neuroprotective factor as aging.

In experiment 2, we observed greater bilateral paracingulate functional activations associated with incongruency during a Numerical Stroop task in individuals with

symmetric ACC sulcation patterns. This finding, accompanied by differences in the temporal dynamics of RTs, corroborates previous evidence of asymmetry-related advantages in inhibitory control (Borst et al. 2014; Cachia et al. 2014, 2017; Tissier et al. 2018). As predicted during experiment 1, we revealed the neurofunctional correlations of this relationship by using a more specific assessment of executive abilities. The implications of this result are far-reaching. We showed that prenatally determined macroscopic properties of the cingulate cortex, driven by genetic factors and intrauterine environment (Amiez et al., 2019), can still be impactful to some extent on the brain functional activity and cognitive abilities much later in life. However, it should be noted that, for the ANT task, no difference in functional activity was found between individuals with symmetric and asymmetric ACC sulcation patterns. Moreover, behavioural data suggest an opposite pattern with respect to the Numerical Stroop task, with cognitive advantages for the symmetric – and not the asymmetric – group. Therefore, while we observed a significant brain structure-function-cognition relationship, the strength and direction of this association are probably dependent on features specific to the task adopted to test executive functions. The biological mechanisms underlying this association are still partially unknown. In both Experiment 1 and 2, we suggested that WM structural connectivity might play a relevant role, in line with the hypothesis formulated by Cachia et al. (2014; see also Del Maschio et al., 2018a). Symmetric brains tend to have a larger corpus callosum which sustains better inter-hemispheric information transfer⁷. In turn, individuals with asymmetric brains would rely more on intra-hemispheric transfer, which is considerably faster. The increased functional connectivity found for individuals with double presence patterns in Experiment 1 could be explained as a reflection of higher inter-hemispheric structural connectivity. Moreover, we observed bilateral activations of the paracingulate gyri in individuals with symmetric ACC folding patterns associated with incongruency in the Numerical Stroop task. This result might reflect the effortful integration of information from simultaneously activated hemispheres. With respect to direct brain-behavior

⁷ Note that while the size of the corpus callosum may change from symmetric to asymmetric brains, the overall volume of the two hemispheres is generally similar in individuals with asymmetric patterns. However, in section 1.3 we mentioned that when a PCS is present, the ACC volume is reduced by 39%, while the volume of the Paracingulate Gyrus is increased by 88% (Fornito et al., 2006). Therefore, significant hemispheric differences in brain tissue volume can be observed at the local (ACC), rather than global (whole brain) level, when comparing asymmetric hemispheres.

correlations, the lack of significant results is potentially explainable due to the ceiling-level performance in the two inhibition tasks (i.e., > 99% mean accuracy scores), that limited us to investigate RTs only. Therefore, future studies on the relationship between ACC individual morphology and local functional activity during RI would benefit from manipulating the degree of task difficulty by increasing stimulus frequency or complexity.

The association between qualitative macroscopic features of the cingulate cortex and structural connectivity has not been investigated yet. However, promising evidence comes from David et al. (2019), who combined state-of-the-art WM tractography, polarized light microscopy, and brain dissection to explore frontal connectivity. The authors described a previously undocumented fiber tract, the superoanterior fasciculus (SAF), which runs dorsal and parallel to the cingulum bundle and can occur in both hemispheres. Moreover, the SAF shows variability in its length and extension. The resemblance with the description of the PCS is striking. A similar finding has also been reported by Wang et al. (2016), who named "paracingulate" or "supracingulate" tract a variably occurring branch of the SLF/cingulum bundle. These results are synthesized within the new nomenclature of "mesial longitudinal system" (MesLS), as proposed by Mandonnet et al. (2018), which would comprise both the cingulum bundle and an outer branch, corresponding to David's SAF or Wang's supracingulate/paracingulate pathway. In Figure 5, we present a tractography reconstruction of the SAF from David et al. (2019) and Figure 6 shows structural data from our laboratory, suggesting evidence of a correspondence between ACC sulcal pattern and WM variability. Future research is required to confirm this association formally. However, we propose that differences in callosal and cingulo-frontal WM might represent the final piece of the puzzle necessary for understanding the impact of ACC folding patterns on cerebral organization and cognitive abilities.

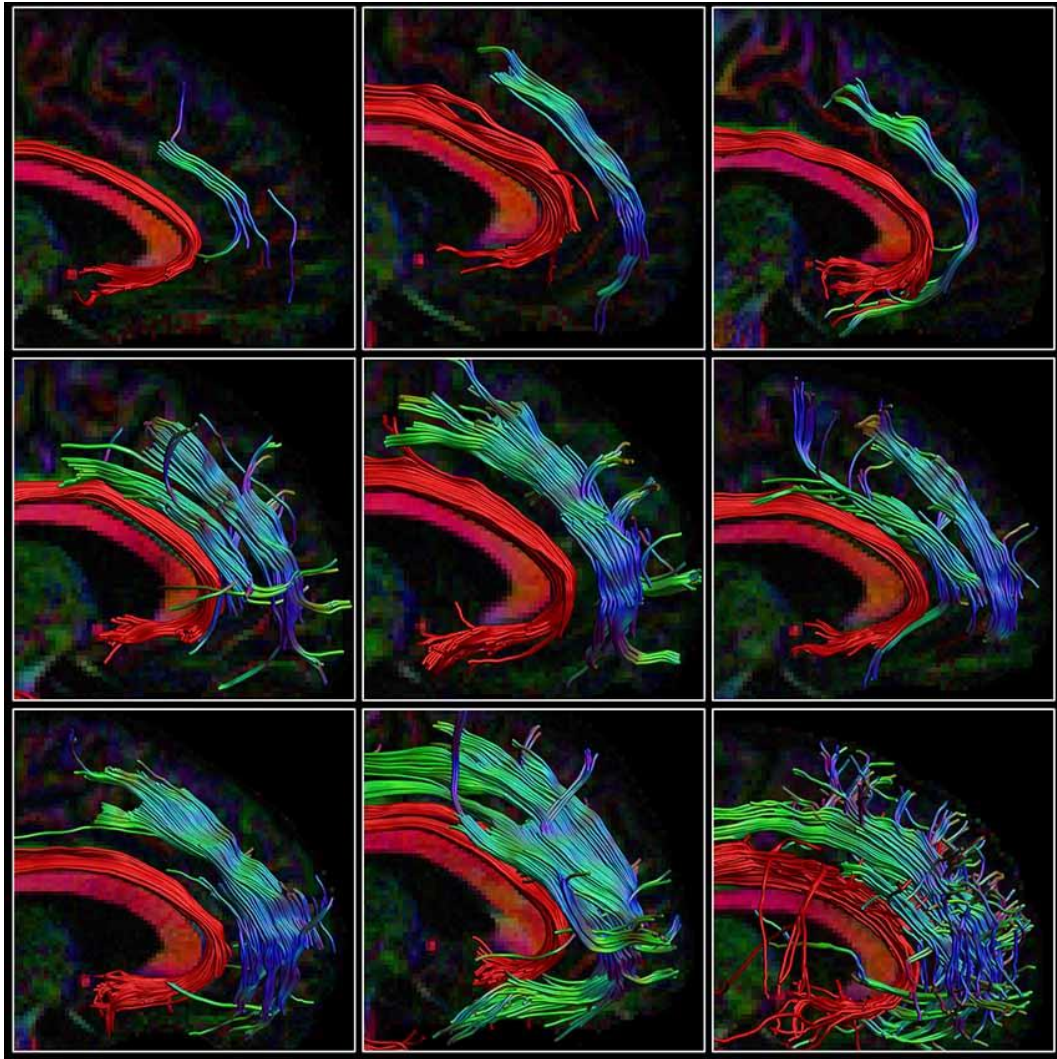


Figure 5. The right SAF and cingulum are depicted in sagittal view for nine subjects highlighting the large variability in extent of the SAF. The cingulum is shown in red to provide anatomical reference. (The figure is adapted with permission from David et al., 2019).

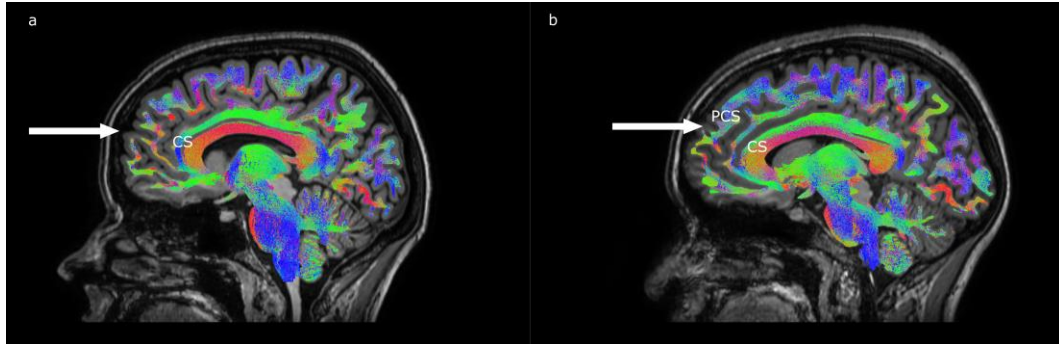


Figure 6 – ACC sulcal variability and diffusion MRI tractography. a) single ACC sulcal pattern profile (CS present, PCS absent); b) double parallel ACC sulcal pattern profile (both CS and PCS are present). An additional intra-gyral bundle of fibers, running dorsal and parallel to the cingulate bundle, can be seen in participant b. White arrow indicates the medial prefrontal cortex. Anatomically Constrained Tractography data from Fedeli et al., 2021.

Experiment 3 moves from the rather deterministic conclusions of Experiment 1 and 2 reported in the first half of the dissertation and focused on plastic effects on the brain's structural metrics. We highlighted how environmental factors could extensively impact stable properties of the brain, such as gyrification trajectories. We observed that cortical folding gradually decreases as a natural consequence of healthy aging, with gyral flattening and sulcal widening pointing towards a reduction of local GMV. Some brain regions, such as temporal lobes and frontal cortices, seemed more vulnerable to this process. We also observed that second-language experience acts as a source of neural plasticity and neural reserve, preserving the cortical complexity of the cingulate and entorhinal cortices throughout the lifespan. In chapter 1.4, we described how bilingual individuals rely on an executive network of brain regions to monitor their linguistic output, inhibit language intrusions, and switch from one language to another. These effortful and prolonged processes leave a trace in the cerebral cortex. The effect is so marked that it fosters resilience to age-related cortical shrinking and smoothing, especially in otherwise vulnerable regions. Bilingualism-induced neural plasticity and neural reserve were previously observed for GMV and WM microstructural integrity (Abutalebi et al., 2015; Del Maschio et al., 2018c; Luk et al., 2011; Olsen et al., 2015). However, the novelty of our study resides in having investigated gyrification, a comprehensive measure of GMV, that is thought to be substantially less ductile. We demonstrated that gyrification "is a dynamic process throughout life which likely

reflects the interplay between early neurodevelopmental mechanisms, experience-related reshaping, and neural decline during the course of aging" (from Del Maschio et al., 2019a). This finding has substantial implications for healthy aging and falls within the literature of the neuroprotective effects of bilingualism in older adults (see Del Maschio, Fedeli, Abutalebi, 2018).

Experiment 4 further expanded the knowledge of the neuroplastic effects of bilingualism. In the context of the present dissertation, this study represents the opposite extreme with respect to Experiment 1 and 2, as it revealed extensive experience-dependent reshaping of the brain connectivity. We observed that in young adults, individual differences in second language experience were associated with structural connectivity changes within distinct, although communicating, networks. In line with known models, these networks included both regions deputed to the processing of linguistic information (e.g., frontal and temporal cortices) and regions that sustain executive abilities (e.g., ACC, basal ganglia). In this study, we avoided the methodological and theoretical limitations of previous research. A methodological improvement was adopting anatomically constrained MSMT WM tractography (an alternative to classic TBSS) and modelling diffusion data with CSD instead of DTI. This practical choice increased the precision and the anatomical reliability of our data. At the same time, this technique allowed us to account for any individual difference in brain morphology, as all analyses were performed in subject space without the need of normalization.

Moreover, the usage of graph theory within the network neuroscience framework permitted us to report novel results on brain organization and network specialization as a consequence of second language experience. We hope that by providing clear benefits of adopting these techniques, our work will set a methodological standard for future diffusion-based research in bilingualism. From a theoretical point of view, we conceptualized bilingualism as a continuous and multi-componential construct instead of dividing our group into monolingual and bilingual participants. Avoiding the classic dichotomic "all-or-nothing" definition of this phenomenon is in line with the most recent models of the neurobiology of bilingualism and consented us to investigate the contribution of distinct experiential factors. As an example, the AoA of the second language was not associated with direct effects of neural plasticity (although a

significant interaction with second language exposure was found). This finding, accompanied by a similar lack of L2 AoA effects in Experiment 3, may indicate that extensive neuroplastic reshaping of the brain connectivity can occur even if a second language is learned beyond critical or sensitive periods of higher plasticity (see Rossi et al., 2017). Moreover, through graph theoretical measures, we observed how changes in these experience-dependent networks contribute to a general increase in the communication efficiency and inter-connectedness of the whole brain. Future studies on whether a “bilingual advantage” exists (see Leivada et al., 2021; Lehtonen et al., 2018; Van den Noort et al., 2019) might investigate if these whole-connectome modulations correlate with behavioural performance in executive tasks.

Together, experiments 3 and 4 presented in the second half of the dissertation demonstrate that neural plasticity is a powerful phenomenon that naturally and continuously occurs in the brain. Neural plasticity can both rewrite how brain regions communicate with each other and preserve to some extent the morphological integrity of the cerebral cortex from the consequences of aging.

4.3 Limitations

The experiments presented in this dissertation should be interpreted in light of a number of limitations. Most of these limitations have already been presented in the discussion paragraphs relative to each study in Chapter 3. However, here we would like to specifically address a limiting factor of Experiment 3.

In recent years a now established trend emerged in bilingualism research. Several authors highlighted the necessity to investigate the neural biology of second language learning by considering bilingual experience as a multi-faceted construct, and bilingualism as a continuous rather than a dichotomic variable (e.g., Deluca et al., 2019; DeLuca, Rothman and Pliatsikas, 2019; Kousaie et al., 2017; Leivada et al., 2021; Li et al., 2014; Sulpizio et al., 2020b; Surrain and Luk, 2017). We contributed to this new conceptualization. Our work on the functional correlates of bilingualism revealed that L2AoA, L2 Proficiency, and L2 Exposure and their interactions were associated with a modulation of the connectivity of the language and executive networks (Sulpizio et al., 2020). Moreover, our first diffusion-based study consented to observe the effects of

second language exposure in modulating WM organization (Del Maschio et al., 2019c). We expanded these findings employing cutting-edge methods in connectomics and graph theory in our recently published Experiment 4 (Fedeli et al., 2021). However, when considering Experiment 3, it should be noted that this study was performed on data collected before these new conceptual developments. Hence, we opted for a classic stratification of our participants by dividing them into "bilinguals" and "monolinguals". The comparative research with monolingual and bilingual speakers has provided invaluable information about both the bilingual cognitive architecture and the neural systems that mediate the specific demands of bilingual language processing. However, a dichotomous categorization of bilingualism may create ambiguities across studies that use different thresholds to indicate whether a participant is bilingual or monolingual (see e.g., Leivada et al., 2021). On the other hand, Experiment 3 presents original findings collected over many participants across two continents, with exciting implications for describing neural plasticity effects on brain gyrification. Therefore, despite these limitations, we think that Experiment 3 still provides a valuable contribution to our knowledge of the impact of bilingual experience on cortical folding trajectories. Future research might describe whether and to what extent bilingualism, defined as a gradient measure, impacts on brain gyrification, and the distinct contribution of specific experiential factors such as L2 Exposure, Proficiency, and AoA. Several structural MRI studies consistently suggest that GM response in young adult bilinguals is modulated by multiple factors, including the age of L2 onset exposure (e.g. Klein et al., 2014; Mechelli et al., 2004), L2 proficiency (e.g. Mechelli et al., 2004; Stein et al., 2012), and bilingual immersion (Pliatsikas et al., 2017). On this ground, we might hypothesize changes in cortical gyrification in regions supporting multiple language control such as the anterior cingulate and the prefrontal cortices to be associated with L2 proficiency and relative L2 use. With respect to L2 AoA, variations in early language experience have been shown to lead to plastic modulations detectable even in early adulthood (see Abutalebi et al., 2015b; Klein et al., 2014). However, these effects are dependent on the adopted metrics (Claussenius-Kalman et al., 2020) and may change as aging (Abutalebi et al., 2014, 2015b) when L2 protracted usage becomes more impactful than AoA (see Rossi et al., 2017), leading to difficult predictions on measuring potential neuroprotective effects on cortical gyrification. Moreover, in

Experiment 3 we examined only linear effects of age when performing the regression analyses. Growing evidence suggests non-linear relationships between aging and measures of cortical integrity with heterogeneous and asynchronous patterns (e.g., GMV of limbic and paralimbic cortices, see Terribili et al., 2011; see also Gennatas et al., 2017; Narvacan et al., 2017; Zimmerman et al., 2006). Ideally, future studies would combine the contemporary conceptualization of bilingualism as a gradient measure with a longitudinal, rather than cross-sectional, experimental framework. This approach would allow examining non-linear effects of age on cortical gyrification and describing to what extent different components of the bilingual experience (and their interactions) modulate the individual trajectories of age-related brain morphometric changes.

4.4 Future directions

Throughout this dissertation, we extensively conveyed the idea that the ACC-MCC complex participates in language control and language switching processes (see Sections 1.3 and 1.4 and Experiment 3 and 4 in the second half of the dissertation). We also reported evidence that ACC sulcation patterns impact both the brain's connectivity at rest in Experiment 1 and its functional activity during executive tasks, with repercussions over the behavioural performance in Experiment 2. Moreover, in Experiment 3 we measured cortical gyrification in bilingual participants, albeit we did not focus on individual variability in ACC-MCC sulcal patterns. At the time of the writing of this dissertation, we are performing a new experiment investigating the impact of individual morphological variability of ACC sulcal patterns on the functional activity during a language switching task in bilingual individuals. This study is largely in line with the topics of this thesis and constitutes an ideal bridge connecting the first half of the dissertation (Experiment 1 and 2) with the second one (Experiment 3 and 4). However, a large sample of participants is required to have an ideal stratification of both ACC sulcation patterns and second-language experience as a set of continuous variables. For this reason, this study has not been included in the present dissertation but represents the natural prosecution of our research. We expect this experiment to provide valuable information on the role of neuroanatomical constraints in language switching

and synthesize our recent research outcomes on both second language experience and ACC anatomical variability.

Finally, while in the first half of the dissertation we focused on the anatomical variability of the ACC, several other neuroanatomical constraints need to be investigated to better understand brain structure-function relationships and their impact on cognitive abilities. In fact, despite an increasingly vast literature on the topic, it is still largely unknown whether, and to what extent, brain asymmetries modulate the brain's organization and cognitive functions (e.g., Thiebaut de Schotten and Beckmann, 2021; Toga and Thompson, 2003). Future studies may investigate other patterns of sulcal asymmetry (e.g., variability of occipitotemporal sulcus; Borst et al., 2016), WM and GMV asymmetries (e.g., individual variability of the AF, CC, and other fasciculi see Thiebaut de Schotten et al., 2011; variable surface area of the planum temporale; see Tzourio-Mazoyer et al., 1998, 2010, 2015, 2017) and asymmetry of subcortical structures. To this regard, the bilateral hippocampi represent a particularly interesting scenario, given their fundamental importance in long-term memory. The relationship between structural hippocampal asymmetry and mnemonic abilities could be observed through novel techniques such as vertex analysis (Patenaude et al., 2011, which measures local variations in the shape of subcortical structures) and provide new evidence of potential cognitive advantages/disadvantages (see for a reference Richards et al., 2020; Shi et al., 2009; Wachinger et al., 2016; Woolard and Heckers, 2012).

4.5 Concluding remarks

“Nature or Nurture” has been, and continues to be, a debated issue in the field of cognitive neuroscience. This dissertation described the impact of prenatally-determined and experience-driven anatomical factors on the brain's functional activity and cognitive abilities. In line with contemporary models of an integrated/interacting view of multiple elements shaping brain development (e.g., Weaver, 2014), we revealed that the brain's neurofunctional organization is determined by a combination of these factors that contribute to its dynamic architecture. We showed that experience-based brain plasticity is a powerful force capable of contrasting age-related brain deterioration and

extensively reshaping whole-brain information transfer efficiency. Compared to these impressive effects, the contribution of individual cortical morphology differences determined prenatally in shaping brain organization and cognitive abilities was limited. However, we highlight the novelty of these findings, which point towards a modulation that, albeit modest, originates in the early development and seems to persist throughout the lifespan.

Our findings represent only a small contribution to the extensive neuroscientific literature on the relationship between brain structure, function, and cognition. However, we present original results that contribute to our understanding of this dynamic interplay and pave the way for future research.

Just like our hands, every brain is unique: A uniqueness driven both by individual characteristics and the experiences we live.

Chapter 5 – MATERIALS AND METHODS

5.1 – EXPERIMENT 1 (MATERIALS AND METHODS):

Participants

Participants' data were drawn from the publicly available Max Planck Institute "Leipzig Study for Mind-Body-Emotion Interactions" (LEMON) dataset, which includes neuroimaging and behavioral data from 227 subjects (mean age 38.95; 82 F) (http://fcon_1000.projects.nitrc.org/indi/retro/MPI_LEMON.html). The study was carried out in accordance with the Declaration of Helsinki; data were collected and analyzed under the local ethics committee approval. 42 subjects were excluded because of psychiatric disorders and/or positivity at drug or alcohol test at time of testing, resulting in a sample of 185 participants (see Experiment 1; Table 4 for participants' distribution across age ranges). Participants underwent a detailed imaging protocol consisting of: (i) Structural Magnetic Resonance Imaging scan, that is, a quantitative and weighted T1 Magnetization-Prepared 2 Rapid Acquisition Gradient Echoes (MP2RAGE) image, and T2-weighted image Fluid-attenuated inversion recovery (FLAIR); (ii) Resting state functional MRI; (iii) Diffusion-weighted imaging (DWI); (iv) Susceptibility-weighted imaging (SWI), and (v) gradient echo fieldmap scans. Participants also underwent an extensive set of test batteries for cognitive assessment. To investigate whether the relationship between ACC sulcation and cognitive performance is modulated by functional connectivity, we selected tests tapping verbal and non-verbal cognitive processes that engage the ACC: California Verbal Learning Task (CVLT), Test of Attentional Performance (TAP), Trail Making Test (TMT), Wortschatztest (WST), Leistungsprüfsystem 2 (LPS 2), and Regensburger Word Fluency Test (RWT). For a comprehensive description of the tests see Babayan et al., 2019.

Age range	F	M	Total
20–25	23	43	66
25–30	8	37	45
30–35	3	7	10
55–60	2	2	4
60–65	6	11	17
65–70	14	9	23
70–75	8	9	17
75–80	2	1	3
Total	66	119	185

Experiment 1; Table 4 – Participants’ age ranges

MRI acquisition

MP2RAGE sequences were acquired with a 3 Tesla scanner (MAGNETOM Verio, Siemens Healthcare GmbH, Erlangen, Germany) with the following parameters: Repetition time (TR) = 5000 ms, Echo Time (TE) = 2.92 ms; flip angle 1 = 4°, flip angle 2 = 5°, field of view (FOV) = 256 mm, number of slices = 176, voxel size = 1 mm³ isotropic, Generalized Autocalibrating Partial Parallel Acquisition (GRAPPA) acceleration factor = 3, slice order = interleaved. T2*-weighted gradient echo planar imaging (EPI) multiband BOLD scans were acquired with the following parameters: TR = 1400 ms, TE = 30 ms, flip angle = 69°, FOV = 202 mm, number of slices = 64, voxel size = 2.3 mm³ isotropic, imaging matrix = 88 × 88, slice thickness = 2.3 mm, echo spacing = 0.67 ms, bandwidth = 1776 Hz/pixel, partial Fourier 7/8, multiband acceleration factor = 4, volumes=657, slice order = interleaved. For further details on MRI acquisition parameters, see Babayan et al. (2019).

ACC sulcal pattern classification

Differences in ACC sulcation are largely based on the occurrence of the PCS, a variable secondary sulcus that runs dorsal and parallel to the CS (e.g., Ono et al., 1990; Paus et al., 1996a; Yücel et al., 2001). Here, following Ono and colleagues’ nomenclature (Ono et al., 1990), as in our previous studies (Cachia et al., 2017; Del Maschio et al., 2018a), two types of ACC sulcation were identified depending on the PCS occurrence in each hemisphere: A ‘single’ type (CS only) and a ‘double parallel’ type (CS and additional

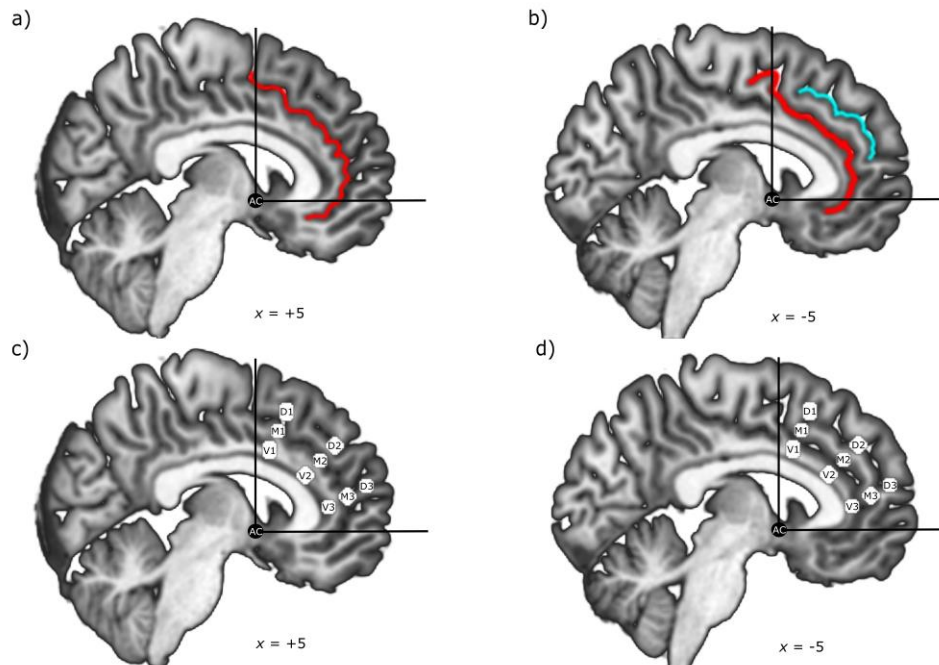
PCS) (see Experiment 1; Figure 3a,b). Based on this classification, we determined the bi-hemispheric occurrence of the PCS in each participant's brain, yielding four sulcal patterns: i) Double Absence ('Single/Single', SS) (CS only in both hemispheres); ii) Double Presence ('Double parallel/Double parallel', DD) (CS and additional PCS in both hemispheres); iii) 'Leftward Asymmetry' (LA) (PCS present in the left hemisphere only); iv) 'Rightward Asymmetry' (RA) (PCS present in the right hemisphere only).

All structural images were visually inspected for the presence of artifacts (e.g., excessive head movement, ghosting, field inhomogeneities or distortions) and 6 participants were excluded due to this reason. Moreover, 2 participants were excluded due to the presence of a calcified meningioma as assessed by an expert neurologist. Overall, T1-weighted MR images were obtained from 177 participants. The origin was set on all individual structural images to match the AC-PC line; subsequently, segmentation and skull-stripping were performed by means of Statistical Parametric Mapping (SPM) 12 (version 6906).

Following Garrison's PCS measurement protocol (Garrison, 2017, see also section 1.3), first reported in Garrison et al. (2015), all T1 images were imported into MANGO (Multi-image Analysis GUI, v 4.0, <http://ric.uthscsa.edu/mango/mango.html>, The University of Texas Health Science Center; see also Del Maschio et al., 2018a). The CS was identified at 4 mm laterally from the midline on either hemisphere, lying dorsal to the corpus callosum. The PCS was identified as the sulcus running dorsal and parallel to the CS. The anterior limit of the PCS was identified at $x = \pm 5$ mm, corresponding to the point at which the sulcus begins to move posteriorly from the anterior commissure and runs parallel to the CS for most of its length until it encounters an imaginary line perpendicular to the bicommissural line and passing through the anterior commissure. In each hemisphere, the PCS was classified as 'present' (≥ 20 mm) or 'absent' (≤ 19 mm). In case of PCS discontinuity, sulcus fragments were included in the analysis only if interruptions were ≤ 19 mm. At this stage, spatial normalization was not performed.

PCS measurement and ACC sulcal pattern classification, incorporating both visual inspection and automated components, were carried by 3 expert blind raters (inter-rater agreement = 97%). Disagreement among raters due to ambiguous ACC sulcation (see Leonard et al., 2009) was resolved by a fourth blind rater. Since ambiguity persisted after general inter-rater discussion for 4 participants (3% of the whole dataset), those

participants were excluded from subsequent analyses, yielding a final sample of 173 participants.



Experiment 1; Figure 3. *The two hemispheres of the skull-stripped brain of the same individual are shown. (a) ACC with a single pattern (CS only) in MNI space. The anterior branch of the CS is marked in red. (b) ACC with a double parallel pattern (CS and additional PCS) in MNI space. The anterior branch of the CS is marked in red, and PCS is marked in light blue. (c, d) Show V, M, and D seeds for rsFC analyses. (The figure is adapted with permission from Fedeli et al., 2020).*

Seed-to-voxel rsFC

Data preprocessing and rsFC analyses were run with CONN toolbox (version 18.b; Whitfield-Gabrieli and Nieto-Castanon, 2012) in SPM12 (Penny et al., 2011). Using the default preprocessing pipeline implemented in CONN, functional images were slice-timing corrected, realigned to the first image, unwarped, and centered to (0,0,0) coordinates. Outlier volumes with excessive head motion were detected and scrubbed using the Artifact Rejection Toolbox (ART, Power et al., 2012). Acquisitions with framewise displacement above 0.9 mm or global BOLD signal changes above 5 s.d. (over 95th percentile) were flagged as potential outliers. We allowed for scrubbing of up to 20% of functional volumes per subject. However, no subject in the final sample had to be discarded because of this reason. Structural images were segmented and

normalized with the unified segmentation-normalization approach with default parameters (Ashburner et al., 2001). Functional images were normalized to average template in MNI space and smoothed with a full-width at half maximum (FWHM) 8 mm Gaussian kernel. Since noise removal increases the reliability of rs-fMRI data, the anatomical component-based noise correction method (aCompCor) was applied to extract a representative noise signal from WM and Cerebrospinal Fluid (CSF) components on a voxel-by-voxel level (Behzadi et al. 2007; Chai et al., 2012). For each participant, realignment, scrubbing parameters, noise components from WM and CSF and “effect of rest” were entered as nuisance covariates in the first-level analysis (see Nieto-Castañón et al., 2020). Realignment parameters are defined as 12 components estimated from the subject motion parameters (3 translation, 3 rotation and their first-order temporal derivatives). Scrubbing parameters consist in subject-specific dummy variables indicating outlier volumes identified with ART. Physiological noise components from WM and CSF are defined as the significant principal components derived from non-GM “noise” regions in which the signal is supposed not to be modulated by the local neural activity (Behzadi et al. 2007). At first, WM and CSF masks are computed subjectwise by creating eroded-by-one-voxel binary masks of all the voxels with values greater than 50% within WM and CSF tissue probability maps. Afterwards, 5 noise components within each mask are estimated. The first consisting in the average BOLD signal and the other four as the result of a Principal Component Analysis (PCA) following the aCompCor method as implemented by Chai et al. (2012) (see also Nieto-Castañón et al., 2020). Additionally, a small trend at the very beginning of each participant’s functional session (defined as “effect of rest” or “session effect”) is automatically estimated by CONN. This regressor corresponds to a step function convolved with the hemodynamic response function (HRF) that allows to control for potential initial magnetization transient effects (or “ramping effects”) at the very beginning of the session, before the BOLD signal acquisition reaches steady-state behavior. Subsequently to the linear regression of potential confounding effects, functional images were band-pass-filtered (0.01-0.1 Hz) to remove low-frequency drifts and physiological high-frequencies noise.

A seed-to-voxel approach was implemented in CONN toolbox. Following Margulies et al. (2007), three parallel lines of spherical seeds (radius = 4 mm) were defined along the

dorsal-to-caudal gradient of the ACC: i) The Ventral seed line lies 5 mm above ACC callosal curve in the ACC; ii) The Middle seed line lies 15 mm above the callosal curve in the ACC, extending to the inferior part of the PCG, as defined by the anatomical mask of the probabilistic Harvard-Oxford atlas (distributed with the FMRIB Software Library FSL, Smith et al., 2004); (iii) The Dorsal seed line lies 25 mm above the callosal curve in the cingulo-frontal transition area, corresponding to the superior part of the PCG of the Harvard-Oxford atlas. One set of seeds, comprising the three parallel lines of spherical seeds, was created for each hemisphere at $x = \pm 5$ mm (see Experiment 1; Figure 3c,d)⁸. A seed to voxel analysis with spherical seeds was preferred to selecting seed ROIs based on anatomical parcellation. Indeed, anatomical variability (with specific reference to the cingulate cortex sulcation patterns) represents a source of large inter-package differences in brain parcellation schemes implemented in popular neuroimaging software, which may consequently jeopardize the result generalizability and compatibility (Mikhael et al., 2018).

A whole-brain bivariate correlation analysis was carried out between the BOLD time-series of each seed (i.e., signals average across all voxels within the seed) and the BOLD time-series of all other voxels of the brain. The Pearson's correlation coefficients obtained were then converted to normally distributed scores using Fisher's R to Z transform to allow for second level General Linear Model (GLM) analysis. Significance threshold was set at voxel-p-uncorrected < 0.001 and cluster-p-Family-Wise-Error(FWE)-corrected for multiple comparisons < 0.05 .

Statistical Analyses

Statistical analyses were conducted to (i) Explore the distribution of the ACC sulcal pattern in our sample; (ii) Investigate the effects of ACC sulcal pattern variability on seed-based rsFC; (iii) Assess whether the relationship between ACC sulcal pattern and seed-based rsFC changes with increasing age; (iv) Estimate correlations between connectivity profiles associated with distinct sulcal patterns and cognitive performance.

⁸ Ventral seeds MNI X, Y, Z coordinates: V1 (-5, 10, 33); V2 (-5, 27, 21); V3 (-5, 38, 6). Middle seeds MNI X, Y, Z coordinates: M1 (-5, 14, 42); M2 (-5, 34, 28); M3 (-5, 47, 11). Dorsal seeds MNI X, Y, Z coordinates: D1 (-5, 18, 51); D2 (-5, 41, 35); D3 (-5, 56, 16).

Analyses were performed with CONN toolbox and SPSS software (version 21; IBM Corp. Released 2012).

ACC sulcal pattern distribution. Incidence rates (%) of ACC sulcal pattern were calculated for all participants and compared with equal frequency distribution by means of chi-square goodness of fit. Since evidence of gender effects on sulcal pattern distribution is mixed (cf. Del Maschio et al., 2018a; Leonard et al., 2009; Yücel et al., 2001), an ordinal logistic regression model was run to explore the distribution of the ACC sulcal pattern with Gender as predictor (reference level: Male) and ACC Sulcal Pattern as dependent variable ('Double Absence', 'Double Presence', 'Leftward Asymmetry', 'Rightward Asymmetry').

Effects of ACC sulcal pattern variability on seed-based rsFC. To investigate the effects of individual differences in ACC sulcation on ACC connectivity, a GLM was run with ACC Sulcal Pattern as regressors ('Double Absence', 'Double Presence', 'Leftward Asymmetry', 'Rightward Asymmetry'), Age, Gender, and Education as nuisance covariates, and seed-based rsFC as dependent variable. For each ACC seed (9 per hemisphere), the following paired differences t-contrasts were computed: (i) Double Absence > Double Presence; (ii) Double Absence > Leftward Asymmetry; (iii) Double Absence > Rightward Asymmetry; (iv) Double Presence > Leftward Asymmetry; (v) Double Presence > Rightward Asymmetry; (vi) Leftward Asymmetry > Rightward Asymmetry. When each contrast was performed, other seeds were not covaried out. Connectivity differences between ACC sulcal patterns were tested each time for all the included seeds. Given the high number of performed univariate tests (i.e., 9 seeds * 2 hemispheres * 6 comparisons = 108 t-tests), the cluster level FWE corrected p-value threshold was additionally divided by the number of performed t-tests (i.e., $0.05/108 = 0.00046$).

Task-based fMRI studies have indicated topological modulations of clusters of brain activity based on the sulcal morphology of the ACC. When interpreting results from an fMRI decision-making task, Amiez and colleagues (2013) have suggested that the CS (when a PCS is absent) and the PCS (when present) are functionally homologous. In order to test this hypothesis on rsFC, we have performed an additional analysis by

comparing Dorsal (D) and Middle (M) seeds in individuals with and without a PCS. Unthresholded connectivity maps were generated to inspect spatial overlaps between M seeds and D seeds in the Double Presence and Double Absence groups. Connectivity differences were investigated by means of pairwise T-Tests selecting middle seeds for the Double Absence group (i.e., M1, M2, M3) and dorsal seeds for the Double Presence group (i.e., D1, D2, D3) (see Appendix).

Effects of age-sulcal pattern interaction on seed-based rsFC. To inspect for age-dependent changes in the relationship between ACC sulcal pattern and seed-based rsFC, a GLM was run with ACC Sulcal Pattern*age as regressors (Double Absence*age; Double Presence*age; Leftward Asymmetry*age; Rightward Asymmetry*age), Gender and Education as nuisance covariates, and seed-based rsFC as dependent variable. Contrasts were the same as those computed to investigate the effects of ACC sulcal pattern variability on seed-based rsFC.

Correlations between ACC connectivity and cognitive performance. To test for cognitive effects of sulcal-related differences in ACC connectivity, correlational analyses were performed between ACC connectivity values associated with distinct sulcal patterns and performance at the following test batteries: CVLT, TAP, TMT, WST, LPS 2, and RWT. For each significant cluster resulting from the seed-to-voxel rsFC analyses, individual connectivity values were extracted. Correlations between cognitive scores and individual connectivity values were performed groupwise (e.g., for a cluster resulting from SS>DD contrast, connectivity scores of individuals with SS pattern and DD pattern were separately correlated with each of the selected cognitive tests). In case of significant correlations resulting from the same cluster with the same cognitive test, correlations coefficients were compared between groups. Following guidelines for improving brain-behavior correlations (Rousselet and Pernet, 2012), all analyses were performed with the freely available Matlab toolbox “Robust Correlation Toolbox” (<http://sourceforge.net/projects/robustcorrtool/>) (Pernet et al., 2013) which allows assumption checking and outlier detection, and implements robust correlations (e.g., percentage-bend correlation and skipped correlation, see Wilcox, 1994, 2004). To

prevent the risk of false positive errors, all analyses were corrected for multiple comparisons.

5.2 – EXPERIMENT 2 (MATERIALS AND METHODS):

Participants

Forty-three Italian young adult participants were recruited. One subject was excluded from the analyses due to WM hyperintensities, thus resulting in a final sample of 42 participants (mean age: 25.19 ± 4.89 ; 30 F). All participants had no history of neurological or psychiatric disorders, had normal or corrected-to-normal vision, and were right-handed (Oldfield, 1971). For each participant the following measures were obtained: Socio-Economic Status (SES) (The MacArthur Scale of Subjective Social Status, <https://macses.ucsf.edu/research/psychosocial/subjective.php#measurement>) (mean years of formal education: 16.62 ± 1.45 ; mean personal income score: 1.52 ± 0.77 ; mean family income score: 3.62 ± 1.08); Fluid intelligence quotient (Raven's Standard Progressive Matrices for adults, Basso et al., 1987) (mean corrected score: 33.54 ± 2.52); visuo-spatial working memory (Corsi test, Monaco et al., 2013) (mean Corsi forward corrected score: 6.27 ± 1.16 ; mean Corsi backward corrected score: 5.27 ± 0.86). No participant was discarded because of low intelligence quotient or low working memory score.

The study was carried out in accordance with the Declaration of Helsinki and with the ethical approval from the Human Research Ethics Committee of the Vita-Salute San Raffaele University, Milan, Italy. All participants gave written informed consent.

Procedure

Participants performed two tasks inside of an MRI scanner. The order of the tasks was counterbalanced across participants, and the two tasks were separated from each other by a T1 structural sequence of the duration of ~7 minutes. Stimuli were presented with Presentation software (<https://www.neurobs.com>, version 20.3, build 02.25.2019).

The ANT (Fan et al., 2002, 2005) expands the classic Flanker task (Eriksen, 1974) and allows one to investigate the involvement of three different attentional networks/functions: alerting, orienting, and executive control. Attention alerting represents the ability of reaching and maintaining an alerted state; attention orienting

represents the ability of selecting specific information from an input; executive control represents the ability of solving conflict selecting only the appropriate responses. As we were mainly focused on investigating the interaction between the ACC sulcal pattern and the functional activity associated with inhibitory control (i.e., executive control), other effects associated with visual priming cues in the ANT (i.e., alerting, and orienting effects) were not presented in the final analyses and are reported in the appendices. The ANT was adapted from Abutalebi et al. (2012). Two ~8 minutes runs, each comprising 96 trials, were presented. The two runs were separated by a small (~30 seconds) break. The experiment was preceded by a short practice session of 16 trials. In each trial participants were shown a sequence of five arrows aligned horizontally and were instructed to answer as fast and accurate as possible based on the direction of the central arrow by pressing the left or right button of a response box. Stimuli were presented in congruent, incongruent, or neutral conditions (64 trials per each condition, pseudorandomized order). Congruent trials consisted in a sequence of arrows all flanked in the same direction ($\rightarrow\rightarrow\rightarrow\rightarrow\rightarrow$), incongruent trials consisted in a sequence of arrows with the central arrow flanked in opposite direction with respect to the central arrow ($\leftarrow\leftarrow\rightarrow\leftarrow\leftarrow$), and neutral trials consisted in a sequence of lines with only the central arrow flanked in one direction ($- - \rightarrow - -$). For each condition, target stimuli were presented in 50% of the cases above a central fixation cross (up) and in the other 50% below the central fixation cross (down). Stimuli were preceded by a fixation cross (+) (duration = 400 ms) at the center of the screen, and a visual cue (duration = 100 ms). Four visual cue conditions were adopted: no cue, center cue, double cue, and spatial cue. In the no cue condition, participants saw only the fixation cross for 100 ms after its original 400 ms presentation. In the center cue condition, an asterisk (*) was presented at the center of the screen, in place of the fixation cross for 100 ms. The double cue condition had identical timing, but participants saw two asterisks (*) above and below a central fixation cross, in the position corresponding to the two possible target stimuli locations. In the spatial-cue condition, an asterisk was presented above or below the central fixation cross for 100 ms, anticipating the target position. The spatial cues were always valid (i.e., correctly anticipated the target stimulus position). Target stimuli lasted for 1700 ms and remained displayed on the screen after the participant's response until the end of the presentation time. Inter stimulus interval (ISI) corresponded of a

black screen and was jittered with Dale's exponential function (Dale, 1999; mean ISI = 2797.66 ms; min ISI = 1873; max ISI = 4964 ms). RTs and accuracy scores were recorded for each trial.

The Numerical Stroop task (Stroop, 1935; Windes, 1968) was adapted from Hernández et al. (2010). Participants were presented two ~8 minutes runs. The two runs were separated by a small (~30 seconds) break. Each run consisted of 108 trials, and the experiment was preceded by a short practice session of 16 trials. In each trial, participants were asked to indicate the number of items composing a series of one, two, three, or four identical numbers (or alphabetical characters), by using the first, second, third, or fourth button of a response box. Stimuli were presented in congruent, incongruent, or neutral conditions (72 trials per condition, pseudorandomized order, stimulus duration = 2000 ms). During congruent trials, the number of items corresponded to the number values (i.e., 1; 22; 333; 4444); during incongruent trials, the number of digits was different from the number values (e.g., 11; 2222; 3; 444); during neutral trials, alphabetical characters were presented (e.g., Z; GG; MMM; ZZZZ). Stimuli were preceded by a central fixation cross (duration = 500 ms). Stimuli remained displayed on the screen after participant's response until the end of the presentation time. RTs and accuracy scores were recorded for each trial. Stimuli were followed by a jittered ISI (Dale, 1999; mean ISI = 1770.11 ms; min ISI = 1036 ms; max ISI = 4113 ms) consisting of a black screen.

MRI acquisition

MRI acquisition was performed at the Centro di Eccellenza Risonanza Magnetica ad Alto Campo (C.E.R.M.A.C., Unit of Neuroradiology) San Raffaele Hospital, Milan (Italy) with a 3 Tesla Philips Ingenia CX MR scanner (Philips Medical Systems, Best, Netherlands) with a 32 channels SENSitivity Encoding (SENSE) head coil.

For both the ANT and the Numerical Stroop tasks, functional scans were acquired with a fast speed EPI sequence (TE = 33 ms; TR = 2000 ms; Flip Angle = 85°; number of volumes per run = 236 (ANT); 256 (Numerical Stroop); FOV = 240 × 240; matrix size = 80 × 80; 35 axial slices per volume; slice thickness = 3; interslice gap = 0.75; voxel size = 3 × 3 × 3; Phase Encoding direction PE = (Anterior/Posterior) A/P; SENSE factor

= 2 (Check); whole brain coverage). Five dummy scans preceded each run to optimize EPI image signal.

A high-resolution Magnetization Prepared Rapid Gradient Echo (MPRAGE) T1-weighted anatomical image was acquired for each participant with the following parameters: TR = 9.9 ms, TE = 4.9 ms, flip angle = 8°, FOV = 269 mm, matrix size = 384 x 384, number of axial slices = 243, slice thickness = 1.4 mm, voxel size = 0.7 x 0.7 x 0.7 mm³, PE direction = A/P, SENSE factor = 2, with whole brain coverage.

ACC sulcal pattern classification

For all T1-weighted structural images the origin was set to match the AC-PC bicommissural line. Sulcal pattern classification was then performed following Garrison's protocol (Garrison et al., 2017). Images were imported into MANGO (v 4.0, <http://ric.uthscsa.edu/mango/mango.html>) and the PCS was identified as the sulcus running dorsal and parallel to the CS for most of its length. The anterior limit of the PCS was identified at $x = -5$ mm for the left hemisphere, and $x = +5$ mm for the right hemisphere, starting from the point at which the sulcus begins to move posteriorly from the anterior commissure. The posterior limit of the PCS was identified as a line passing through the anterior commissure and perpendicular to the bicommissural line. The PCS was then measured and classified as “present” ($PCS \geq 20$ mm) or “absent” ($PCS < 20$ mm). When the PCS was interrupted, sulcal sections were considered only if interruptions were ≤ 19 mm. Interruptions were not included in the computation of the total length of the PCS. Participants were classified as “asymmetric” when the PCS was present in only one hemisphere, but not in the other, and “symmetric” when the PCS was bilaterally present or bilaterally absent.

fMRI pre-processing

Functional data for both the ANT and Numerical Stroop tasks were processed by adopting the surface-based fMRI pipeline developed by Brodohel and colleagues (2020). With respect to standard volumetric processing, surface-based fMRI is supposed to greatly increase the anatomical precision of the functional findings. As a matter of fact, spatially smoothing volumetric data increases the risk of signal contamination (Yan et al., 2009) between anatomically distant regions. This is particularly true for

functional regions that may be adjacent in the folded cortex (i.e., volumetric space) but are separated in the unfolded cortex (i.e., surface space), such as the cingulate and paracingulate gyri when a PCS is present in the same hemisphere. Therefore, this approach better accounts for the individual variability in gyrosulcal morphology and allows to disentangle the specific contribution of neighboring functional regions on the ACC. Moreover, since the left and right ACC are very close to each other in the volumetric space, bilateral ACC activation patterns are often the consequence of the relatively large smoothing kernel (e.g., $8 \times 8 \times 8$ mm³ or $6 \times 6 \times 6$ mm³) that is adopted in classic volume-based analyses. While necessary for improving the signal-to-noise ratio (SNR), this methodological preprocessing step largely increases the chances of erroneously spreading functional activity located on one hemisphere onto the contralateral cortex. Surface-based fMRI combined with a small smoothing kernel ($3 \times 3 \times 3$ mm³) largely prevents this type of inter-hemispheric signal contamination. The following processing steps were performed: individual surface estimation; slice timing correction of functional data; spatial realignment and coregistration to skull-stripped bias corrected T1-weighted structural image; GLM estimation; mapping of the functional contrast-images in the native volumetric space to the individual surface; normalization and smoothing. T1-weighted structural images were segmented with the Computational Anatomy Toolbox (CAT12 v1429, <http://www.neuro.uni-jena.de/cat/>) based on SPM12 v7219 (www.fil.ion.ucl.ac.uk/spm/). Structural images were segmented into GM, WM, CSF, resulting in separate single-subject image volumes for each tissue class. CAT12 segmentation approach uses a spatial adaptive non-local mean (SANLM) denoising filter and a local adaptive segmentation (LAS) that applies a local intensity transformation of tissue classes to correct for regional inhomogeneities and intensity variations. Additionally, an Adaptive Maximum A Posterior (AMAP) technique (Rajapakse et al., 1997) and a Partial Volume Estimation (PVE) (Tohka, Zijdenbos and Evans, 2004) were carried out in order to obtain a more accurate segmentation. Central surface reconstruction was carried out for both hemispheres of each structural image using the CAT12 standard pipeline that employs a projection-based thickness (PBT) computation approach (Dahnke, Yotter, & Gaser, 2013). Functional images were slice-time corrected and realigned to the first volume and unwarped to correct for motion artifacts and geometric distortions. Realigned functional

volumes were coregistered to the bias-corrected structural brain image. Functional images were then entered in a separated GLM for each task. BOLD signal was convolved using the Canonical HRF, and a 128s high-pass filter was applied to the timeseries. Serial correlations were accounted for using the AR (1) model during parameter estimation. For each task, onsets for the Congruent, Incongruent, and Neutral conditions were entered into the model. Realignment parameters for the two sessions were entered as nuisance covariates. The following directional t-contrasts were estimated: incongruent > congruent; incongruent > neutral; congruent > neutral. Contrast-images estimated at the first level were then mapped to each participant's individual surfaces generated with CAT12, with absolute maximum option. Surface images were then resampled to the standard 32k HCP template provided by CAT12 and smoothed with a 3mm x 3mm x 3mm FWHM gaussian kernel, as recommended by Brodohel and colleagues (2020).

Despite the great advantages of performing surface-based rather than volume-based fMRI analyses, the latter approach is still the most adopted and is considered a gold standard. As a control analysis, a volumetric processing pipeline was also implemented with standard settings: slice-time correction; realignment and unwarping; segmentation of the structural image; coregistration to the reference bias-corrected skull-stripped structural image; normalization to the standard MNI volumetric template; and smoothing with a 8mm x 8mm x 8mm FWHM gaussian kernel. Results from this control pipeline are reported in the appendices.

Statistical analyses.

Neuroimaging analyses. At the second-level, smoothed and resampled individual con-images were entered into a GLM and a set of one-sample t-test were performed in order to test the effects of task conditions irrespective of ACC sulcal pattern. Subsequently, a full factorial design was used to investigate differences in brain activity between individuals with symmetric and asymmetric ACC sulcal pattern. The Incongruent > Congruent and Incongruent > Neutral contrasts were specifically adopted to describe the relationship between individual anatomical variability and executive abilities. Incongruency > Congruency contrast represents the “Incongruency effect”

while Incongruency > Neutral contrast is typically referred to as the “Interference effect”. Both account for the dimension of dealing with incongruent information, but while the incongruence effect compares the incongruency condition with one of facilitation, the interference effect compares the incongruency with a neutral baseline. Depending on the task, the two effects can be differently informative of the cognitive processes (and associated neural activity) adopted to deal with RI on distinct difficulty levels (see Botvinick et al., 2001). As we were interested in studying the impact of local morphological variability on the functional activity of the cingulate/prefrontal cortex, group analyses were performed within an inclusive mask created mapping to the surface the following bilateral regions from the Harvard-Oxford atlas (distributed with the FMRIB Software Library FSL, Smith et al., 2004): Cingulate Gyrus, anterior division; PCG; Superior Frontal Gyrus; Frontal Pole. Atlas-to-surface mapping was performed with CAT12, using the standard 32k HCP template as a reference. For the group analysis gender and years of formal education were entered as nuisance covariates. Gender was considered as a covariate because of evidence of gender-related differences in ACC sulcal pattern distribution (see Clark et al., 2010; Leonard et al., 2009; Yücel et al., 2001) and cortical complexity (Luders et al., 2004, 2006b; Del Mauro et al., 2021). Years of formal education were entered in the model as a covariate, since education has been reported to impact on Stroop RTs (Van der Elst et al., 2006). Age was not entered as a covariate to avoid multicollinearity since it was highly correlated with years of formal education ($R = 0.61$, $p < 0.001$). For all the analyses the statistical threshold was set at $p < 0.05$ FWE corrected for multiple comparisons at the cluster level, and at $p < 0.001$ uncorrected at the vertex level.

Behavioral analyses. For both the ANT and the Numerical Stroop task, statistical analyses were run to test the effects of ACC sulcal pattern on the executive performance. Since average accuracy was very high (i.e., reaching “ceiling effect”) in both tasks (ANT mean accuracy score = 99.65%; Numerical Stroop mean accuracy score = 99.10%), only RTs were considered for the analyses.

To reach this goal, we ran a set of general linear mixed-effects models separately for each task. The models were fitted using the `lmer` function implemented in the `lme4` package (version 1.1-27). All analyses were performed using R (R Core Team, 2015).

For each task, a linear mixed-effect model was run using participants' RTs to correct responses as a dependent variable, with task condition ("congruent" vs. "incongruent" vs. "neutral"; reference level = congruent), ACC sulcal pattern ("PCS asymmetry" vs. "PCS symmetry"; reference level = "PCS asymmetry"), and their two-way interaction as predictors. Likelihood ratio tests were performed to assess the significance of the fixed effects. For each fixed term we compared models in which that term was present versus absent. Fixed terms were retained only when their exclusion would significantly diminish the goodness of fit. In case of significant interactions, all lower-order terms were maintained in the final model. The model also included by-participants random intercepts. Coefficients were considered as significant when $t \geq |2|$. Additionally, we investigated differences in the distribution of RTs between conditions by means of delta plots (de Jong et al., 1994; Ridderinkhof, 2002, 2004). Delta plotting is an increasingly used analytical method that allows one to investigate the temporal dynamics of inhibitory control by plotting task effects as a function of response time (Ridderinkhof et al., 2004). The slopes of the incongruency effects can be highly informative in revealing inter-individual differences in the progressive growth of incongruency effects as time passes by. Besides, the reduction of the incongruency effect typically associated with the slowest RTs is thought to reflect suppression of incorrect behavioral responses (Ridderinkhof et al., 2004, 2005; Pratte et al., 2021). Therefore, the leveling-off of the slope in the latest quantiles represents a meaningful proxy measure of the variability of efficient inhibitory control across individuals. RTs of correct responses in each condition for each participant were sorted from the fastest to the slowest and grouped in five equal-sized bins (1st quantile = fastest 20% of the responses; 5th quantile = slowest 20% of the responses). Quantiles were then included in a second linear mixed-effects model as a fixed effect. Nonlinear relationships were tested by comparing this model with one in which nonlinearities were fitted by using orthogonal quadratic polynomials for the quantile fixed effect. Delta plots representing the difference between conditions as a function of RTs quantiles were generated for each task and separately for individuals with symmetric and asymmetric ACC sulcal patterns.

Brain-behavior interactions. A correlation analysis was performed to test whether the individual mean functional activity from clusters resulting from the group contrasts was correlated with the mean RTs associated with that effect in the two tasks. The same correlation analysis was also performed considering mean RTs from the slowest quantiles (4th and 5th), since the leveling-off of the slope for slow responses is typically associated with the efficiency of RI (Ridderinkhof et al., 2004, 2005; Van Den Wildenberg et al., 2010).

5.3 – EXPERIMENT 3 (MATERIALS AND METHODS):

Participants

212 right-handed participants with no previous history of neurological or psychiatric disorders took part to the study (90 M / 122 F; mean age = 35; SD = 19; range = 18-75). The sample included 129 bilingual individuals and 83 monolingual individuals. Monolinguals were native Italian speakers (L1 = Italian), while bilingual participants were either Italian-German (n = 27), Dutch-English (n = 17), Hindi-English (n = 32), and Cantonese-English (n = 53) speakers. All participants' years of formal education were collected (overall mean = 15.36; SD = 3.02). No significant difference between bi/monolinguals was found ($t < 1$, $p > .7$). The Mini-Mental State Examination (MMSE) (Cockrell and Folstein, 2002) was used to evaluate the cognitive state of participants > 50 years of age, and an inclusion threshold of ≥ 27 raw scores was set to avoid the inclusion of individuals showing cognitive impairment. No participant was excluded due to low MMSE scores (mean = 29, SD = 1.1). No significant differences in MMSE scores were found between bi/monolinguals ($t = -1.6$; $p > .1$). L2 proficiency was measured offline with a picture-naming task and an oral translation task from L1 to the L2 (only in bilinguals; see Abutalebi et al., 2014). Thirty colored pictures were taken from a revised version of the Snodgrass and Vanderwart picture set (1980) and used in the picture-naming task. The L1-to-L2 translation task included sixty-six words balanced for frequency (22 for low, medium, and high frequency). L2 AoA was collected for every bilingual participant. Demographic and linguistic data are reported in Experiment 3; Tables 4 and 5.

A subsample of 146 participants performed an ANT task (Fan et al., 2005) (82 bilinguals: mean age = 42.5; SD = 21.76; range = 19-75; 64 monolinguals: mean age = 36.96; SD = 18.85; range = 18-75). No significant difference in age ($t = .32$; $p = .75$), years of formal education ($t = .36$; $p = .72$) or MMSE raw scores ($t = 1.5$; $p = .13$) was found between bi- and monolinguals.

All data were collected under the approval of the Human Research Ethics Committees of the participating institutions: Vita-Salute San Raffaele University (Milan, Italy), University of Hong Kong (HKSAR), and the National Brain Research Centre (Manesar, India).

		Bilinguals (n = 129)	Monolinguals (n = 83)
Age	M	35	34.52
	SD	20.06	17.24
	Min	19	18
	Max	75	75
Education (in years)	M	15.4	15.42
	SD	2.97	2.79
	Min	6	5
	Max	26	25
MMSE	M	29.15	28.70
	SD	1.12	1.15
	Min	27	27
	Max	30	30
L2 naming accuracy %	M	85	–
	SD	10.7	–
	Min	53	–
	Max	100	–
L1 > L2 translation accuracy %	M	91.8	–
	SD	8.9	–
	Min	51	–
	Max	100	–
L2 AoA (in years)	M	5.4	–
	SD	3.2	–
	Min	1	–
	Max	18	–

Experiment 3; Table 4. Descriptive statistics of the participants sample, including linguistic assessment for bilingual participants.

		Italian- German (n = 27)	Dutch- English (n = 17)	Hindi- English (n = 32)	Cantonese- English (n = 53)
Age	M	65.3	21.4	22.97	32
	SD	6.07	2.03	2.32	18.04
	Min	52	20	20	19
	Max	75	26	28	75
Education (in years)	M	15.4	15.8	16.6	15.04
	SD	4.08	1.1	2.04	2.51
	Min	7	15	13	6
	Max	21	18	21	22
MMSE	M	29.5	–	–	28.4
	SD	0.8	–	–	1.3
	Min	28	–	–	27
	Max	30	–	–	30
L2 naming accuracy %	M	83	89	92	79
	SD	10	6	4	12
	Min	53	80	80	57
	Max	100	97	97	97
L1 > L2 translation accuracy %	M	91	97	93	90
	SD	13	4	4	10
	Min	51	83	84	51
	Max	100	100	98	100
L2 AoA (in years)	M	6	6.6	4.75	5.04
	SD	4.19	2	2.14	3.47
	Min	1	2	2	1
	Max	18	9	11	16

Experiment 3; Table 5. Descriptive statistics of the bilingual sample.

Structural MRI Acquisition and Image Pre-Processing

T1-weighted MPRAGE images were acquired using 3T Achieva Philips MR scanners (Philips Medical Systems, Best, Netherlands) at the Vita-Salute San Raffaele (Milan, Italy), the University of Hong Kong (HKSAR), and the National Brain Research Centre (Manesar, India). Identical exam cards were used with the following settings: TR = 8.03 ms, TE = 4.1 ms; flip angle = 8°, FOV = 250 x 250, matrix = 256, number of slices = 150, voxel size = 1.0 × 1.0 × 1.0 mm. Structural MRI images were first visually inspected to exclude the presence of imaging artifacts. Images' origin was manually set to match the AC-PC line with SPM12 v6685. Brain volume 3-tissues segmentation was performed using CAT12. Structural volumes were segmented into GM, WM, and CSF. The CAT12 segmentation approach uses a SANLM denoising filter (Manjon et al., 2010) and applies an intensity transformation to bias-correct for regional inhomogeneities and intensity variations. Additionally, CAT12 jointly uses an AMAP segmentation (Rajapakse et al., 1997) and a PVE for a more precise segmentation (Tohka, Zijdenbos, and Evans, 2004). Individual brain volumes were registered to CAT12 inbuilt brain template.

Cortical Surface Extraction and Gyrification Parameters Calculation

The automated CAT12 surface extraction pipeline was adopted to estimate a cortical mesh for each T1-weighted structural image. Compared with other surface reconstruction software tools (e.g., FreeSurfer), CAT12 produces equivalent results in the face of less computational power and with an overall faster pipeline, thus being particularly suitable for the processing of large (>100) neuroimaging databases when HCP is not an option (Righart et al., 2017; Seiger et al., 2018). CT and central surface reconstruction were simultaneously computed with PBT (Dahnke, Yotter, and Gaser, 2013) for each brain image's left and right hemispheres. Spherical harmonics-based topology correction was applied (Yotter et al., 2011a) to repair topological defects. Each participant's surface mesh was then reparameterized and registered to CAT12 spherical template map (Yotter et al., 2011b). The Gyrification Index (GI) was computed as the local absolute mean curvature (see Luders et al., 2006a; 2012). A surface-based 25mmx25mmx25mm FWHM Gaussian kernel was adopted to smooth GI maps.

Correlation analysis between linguistic measures

In order to avoid multicollinearity, we performed a set of correlation analyses between linguistic measures (i.e., L2 naming and L1>L2 translation; multicollinearity threshold: $r > .50$).

Neuroimaging Analyses.

Whole-Brain Analysis. A whole-brain exploratory analysis was performed. GI surface maps were entered into a full factorial model with Language Group ('monolingual' vs. 'bilingual') as factor and Age as a continuous regressor. Gender, Ethnicity, years of formal Education, Total Intracranial Volume (TIV), and Proficiency (i.e., L2 naming) were entered as nuisance covariates. The main effect of Age on GI across the whole cortex was computed for all participants, irrespective of Language Group. Directional contrasts in regression slopes were then assessed to investigate interactions effects between Age and Language Group on cortical GI (Age*bilinguals>Age*monolinguals; Age*monolinguals>Age*bilinguals).

ROI Analysis. An ROI analysis was performed to investigate GI differences in cortical regions involved in bilingual dual-language processing/control and vulnerable from early or greater-than-average degradation with aging. Cingular, frontal, and parietal regions associated with executive control (Abutalebi and Green, 2016) and temporal areas supporting mnemonic abilities (e.g., Squire and Zola-Morgan, 1991) were considered. The Desikan–Killiany atlas was adopted for ROI labeling. GI data were extracted from the following bi-hemispheric surface ROIs:

1.) Cingulo-fronto-parietal structures: Lateral orbital frontal cortex; Medial orbital frontal cortex; Rostral-ACC; Caudal-ACC; PCC; Isthmus – cingulate cortex; Middle frontal gyrus; Inferior frontal gyrus; Inferior parietal cortex.

2.) Temporal lobe structures: Superior temporal gyrus; Middle temporal gyrus; Transverse temporal gyrus; Inferior temporal gyrus; Parahippocampal gyrus; Entorhinal cortex; Fusiform gyrus; Temporal pole.

In a similar fashion as for the whole-brain analyses, GI data were entered into a full factorial model to investigate the main effect of aging and Age * Language Group interactions through directional contrasts (see above).

For both Whole-brain and ROI analyses, contrasts were computed with t-tests, and results were corrected using a $p < .05$ threshold with FWE correction for multiple comparisons.

The Relationship between Gyrfication and Executive Control Performance in Bilinguals and Monolinguals. Flanker effects were computed from the ANT task (Fan et al., 2005) in a subsample of 146 participants (see experiment 2 and Del Maschio et al., 2018a). Flanker effect measures the ability to resolve conflicts between competing stimuli and responses. How quickly and accurately participants respond to response-compatible versus -incompatible trials is generally interpreted as an index of conflict resolution and RI ability. A linear mixed-effects model was run (using R software) with Flanker's RTs as dependent variable and Flanker condition ('congruent' vs. 'incongruent'), GI (as a continuous variable), Language Group ('monolingual' vs. 'bilingual') and Age (as a continuous variable) as predictors. Gender, Ethnicity, and years of formal Education were included in the model as covariates. By-participants random intercepts were also included.

The Relationship between Gyrfication and L2 Proficiency/L2 AoA in Bilinguals. We performed correlation analyses to explore the bilingualism-mediated cortical plasticity further. The association between significant GI values and bilinguals' L2 proficiency and AoA was computed. Pearson correlations were used for normally distributed measures, while in the other cases, we adopted Spearman correlations. Bilinguals were split into two groups of younger and older adults of similar size (age threshold ≥ 53 years old) to explore the relationship between GI and bilingual experience at different ages.

5.4 – EXPERIMENT 4 (MATERIALS AND METHODS):

Participants

77 bilingual young adults participated to the study (46 F; mean age = 25.27, SD = 4; mean years of formal education = 17.1, SD = 1.86). All participants were right-handed (Oldfield, 1971), had a normal or corrected-to-normal vision, and reported no history of psychiatric or neurological disorders. Participants' SES was assessed with the MacArthur Scale of Subjective Social Status. All participants were native Italian (L1) speakers who spoke English as an L2. The following measures of L2 AoA, L2 Proficiency, L2 daily Exposure, and Language Switching habits were collected for each participant:

- 1) L2 AoA: self-report questionnaire.
- 2) L2 Proficiency: 1) the online Cambridge Test for adult learners, consisting of 25 items that assess grammatical and conversational knowledge (see Sulpizio et al., 2019); 2) an L1->L2 Translation Test, consisting of 30 high, 30 medium, and 30 low-frequency words (Van Heuven et al., 2014).
- 3) L2 Exposure: self-report questionnaire (L2 hours per day usage in different contexts including family, friends/classmates, partner, study/job, reading and writing, media, other) (see Del Maschio et al., 2019b). Participants were asked to consider both the workweek and the weekend when estimating L2 Exposure. The maximum L2 hours per day score was set at 18 hours, however no participant reported values exceeding this threshold.
- 4) Language switching habits: the Bilingual Switching Questionnaire (BSWQ; Rodriguez-Fornells et al., 2012). Participants evaluated their language switching tendencies using a 5-point scale (1 = never; 5 = always). The questionnaire can be decomposed into four indices (3 items per index) corresponding to different aspects of switching behavior (L1 switching tendencies, L1s = the tendency to switch to L1; L2 switching tendencies, L2s = the tendency to switch to L2; contextual switch, CS = the frequency of switches in particular situations or environments, i.e., triggered externally; unintended switch, US = the lack of awareness of language switches, i.e., triggered internally). Each factor's score ranges from a minimum of 3 to a maximum of 15. The questionnaire is

remarkably accurate in providing a comprehensive assessment of self-perceived individual differences in language switching, as switching tendencies tend to correlate negatively with L2 proficiency and usage, and positively with AoA (Rodriguez-Fornells et al., 2012). The BSWQ overall score (i.e., the sum of all item scores) was not adopted in this study, being under-informative with respect to the distinct factors of language switching tendencies.

In addition to the linguistic assessment, fluid and verbal intelligence were measured with the Raven’s Standard Progressive Matrices for adults (Basso et al., 1987) and the Test di Intelligenza Breve (TIB; Colombo et al., 2002; see NART Nelson, 1982). Sample data are reported in Experiment 4; Table 5.

The present study was performed in compliance with the Human Research Ethics Committee of the Vita-Salute San Raffaele University (Milan, Italy). All participants gave their written consent.

	Mean (SD)	Range
Age (years)	25.27 (4)	18-38
Education (years)	17.16 (1.86)	13-21
Annual family income (score)	3.59 (1.11)	1-5
L2 Age of Acquisition (AoA)	7.65 (3.46)	3-19
L2 Exposure (hours per day)	4.65 (3.55)	0-14
Translation task (L1>L2) (% correct responses)	57.29 (3.94)	19-89
Cambridge Test (score)	18.26 (3.35)	9-25
BSWQ L1s (score)	6.92 (1.74)	3-10
BSWQ L2s (score)	9.19 (1.58)	4-13
BSWQ CS (score)	6.84 (2.62)	3-15
BSWQ US (score)	7.95 (1.30)	5 -11
Raven’s Matrices (corrected score)	31-37 (2.79)	26-36
Test Intelligenza Breve (score)	47.24 (2.15)	38.5-50

Experiment 4; Table 5. Descriptive statistics of Demographic, Cognitive, and Linguistic measures.

MRI acquisition

M.R.I. acquisition was performed at the C.E.R.M.A.C., Vita-Salute San Raffaele University/San Raffaele Hospital, Milan (Italy) employing a 3-T Philips Ingenia CX MR scanner (Philips Medical Systems, Best, Netherlands) with a 32 channels SENSE head coil. A high-resolution MPRAGE T1-weighted anatomical image was acquired for

each participant with the following parameters: TR = 9.9 ms, TE = 4.9 ms, flip angle = 8°, FOV = 260 mm, matrix size = 256 x 256, number of axial slices = 243, slice thickness = 1.4 mm, voxel size = 0.7 x 0.7 x 0.7 mm³, PE direction PE = A/P, SENSE factor = 2, with whole-brain coverage.

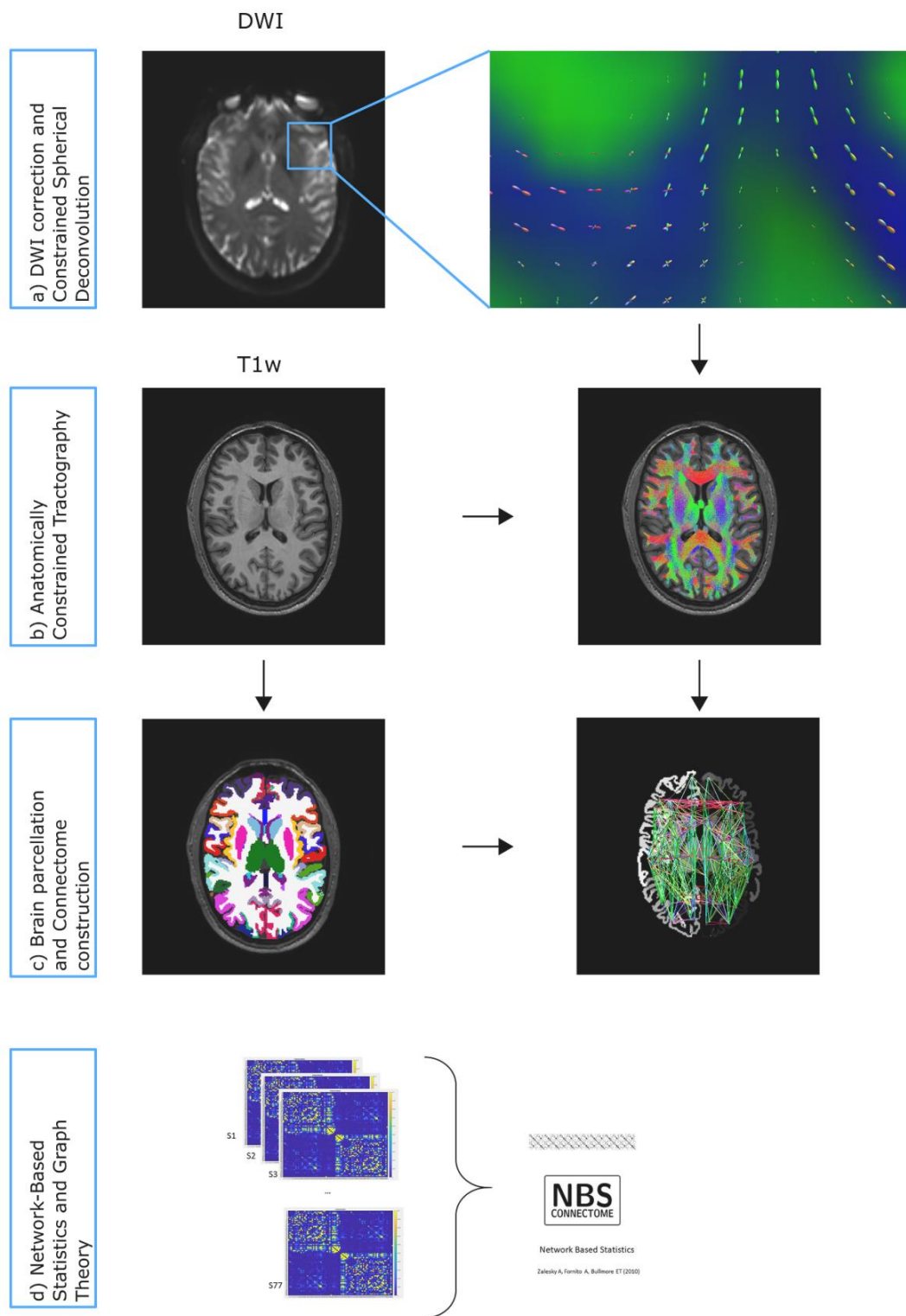
DWI were acquired with a multi-shell sequence (applied b values = 700, 1000, 2855 s/mm², in 6, 30, and 60 gradient directions respectively, with 10 b₀ images distributed within the sequence) with the following parameters: 106 diffusion-encoding gradient directions, TR = 5900 ms, TE = 78 ms, flip angle = 90°, FOV = 240 mm, matrix size = 128 x 128, number of axial slices = 56, slice thickness = 2.3, voxel size = 1.875 x 1.875 x 2.3 mm, PE = A/P, SENSE factor = 2, with whole brain coverage. Additionally, four b = 0 images were collected with reversed phase-encode blips (i.e., volumes with distortions going in opposite direction) for distortion correction purposes.

Diffusion MRI Preprocessing

Diffusion MRI preprocessing was performed using the open-source software MRtrix3 (Tournier et al., 2019), which implements several different options of voxel-level modelling, including Multi-Shell Multi-Tissue CSD (MSMT, Jeurissen et al., 2013,2014). For every participant, the following pipeline was adopted for data cleansing and voxel-level modelling:

- 1) Visual inspection for major artifacts.
- 2) Data denoising to enhance SNR (Veraart et al., 2016);
- 3) Gibbs ringing artefacts removal (unringing) (Kellner et al., 2016; Andersson et al. 2016).
- 4) Motion and distortion correction (Andersson and Sotiropoulos 2016), with Topup and Eddy tools implemented from FSL (Smith et al. 2004).
- 5) Estimation of Fiber Orientation Distribution (FOD) (Tournier et al., 2019) with the “Dhollander” algorithm, which adopts MSMT CSD to take advantage of the multiple b-values to overcome potential biases occurring in voxels with partial volumes (e.g., voxels containing both GM and WM), and permits an accurate estimation of the orientation of all fibers crossing each voxel of the brain (Dhollander et al., 2016, 2019).

6) Intensity normalization to correct for effects of residual intensity inhomogeneities. Diffusion MRI preprocessing, along with subsequent analyses steps, are illustrated in Experiment 4; Figure 5.



Experiment 4; Figure 5. Diffusion MRI preprocessing and analyses: a) Diffusion MRI denoising; motion/distortion correction; MSMT CSD modelling; b) T1w – Diffusion MRI registration; 1million streamlines ACT; c) T1w segmentation and parcellation; connectome construction; d) NBS and Graph Theory

Anatomically Constrained Tractography (ACT).

After data preprocessing, ACT was computed (Smith et al., 2012). ACT makes use of anatomical priors from high-resolution T1-weighted structural images as a reference to precisely reconstruct only biologically plausible WM fibers trajectories, thus improving the overall accuracy of streamline generation (e.g., ACT allows to reject unrealistic streamlines that end in CSF). This method is beneficial for connectome construction and network analyses where nodes are generated from GM parcellations since streamlines terminate only in valid areas of the brain (Smith et al., 2012). T1 images were segmented into 5 tissues and registered to the preprocessed DWI utilizing FSL. 1,000,000 (one million) streamlines were generated for each participant by seeding from the GM/WM boundary and employing the iFOD2 probabilistic tractography algorithm (Tournier, et al., 2010). The backtracking option was selected to truncate streamlines terminating in anatomically implausible regions (e.g., CSF) and re-tracking them to more anatomically meaningful ending points (Smith et al., 2012). Finally, spherical-deconvolution informing filtering of tractograms (SIFT2) (Smith et al., 2015) was performed to correct for potential biases in overestimation of longer streamlines in CSD tractography while concurrently retaining the entire generated tractogram (i.e., a weight parameter is associated to each streamline, thus avoiding the need to remove some of them).

Connectome Construction.

The usage of connectivity matrices allowed the reduction of the brain's complexity to a more manageable and understandable structure that represents the strength of the structural connectivity between all the possible pairwise connections of regions that are part of a brain parcellation. For each participant, T1-weighted images were segmented with Freesurfer (v6.0.0, Fischl, 2012). Cortical, cerebellar, and subcortical areas were parcellated into 84 distinct regions based on the Desikan/Killiany atlas (Desikan et al., 2006). Brain parcellation was then registered to each participant's tractogram in diffusion space, and 84x84 symmetric, weighted, undirected connectivity matrices were generated based on streamline count scaled by regional volume (Hagmann et al., 2008).

Statistical analyses

Correlation analyses between linguistic, demographic and cognitive measures.

To check for multicollinearity, we performed a set of correlational analyses between Age, years of formal Education, L2 AoA, L2 Exposure, L1->L2 Translation Test, Cambridge Test, and TIB. Pearson's correlation coefficient was adopted to compute the correlation between each pair of measures when variables were normally distributed. In all other cases, as revealed by the Kolmogorov-Smirnov test, we computed Spearman's correlations (multicollinearity threshold: $r > .50$, see, e.g., Taylor, 1990). Age and Education were significantly correlated ($r_s = .57$; $p < 0.001$), therefore only Education was entered into the model as a covariate. L1->L2 Translation Test and Cambridge Test scores were highly correlated ($r_s = .75$; $p < .001$). Since the Cambridge Test was also more significantly correlated with L2 Exposure than the Translation Test ($r_s = .46$; $p < .001$), the latter was preferred as a measure representative of participants' L2 Proficiency (see appendices). No other measure was excluded from the following analyses. All analyses were performed with SciPy (Virtanen et al., 2020).

Network-based Statistic analyses. We made use of the NBS Connectome toolbox (v 1.2; Zalesky et al., 2010) running on Matlab (v. 2019a) to test the effects of distinct bilingual experiential factors on WM structural connectivity. NBS is a robust nonparametric analytical method that allows the description of the structural networks affected by distinct effects of interest (e.g., psychiatric pathologies, brain lesions, experience-induced brain plasticity, etc.). NBS assumes that such effects are rarely restricted to a single connection and typically include multiple nodes generating interconnected subnetworks in the topological space (Fornito, Zalesky, and Bullmore, 2016). Each participant's 84 x 84 connectivity matrix was entered into a GLM as the dependent variable. The following regressors were also entered into the model: Gender, years of formal Education, L2 AoA, L2 Exposure, L2 Proficiency (Translation Test score), TIB, and model intercept. A multiple regression analysis was computed to test for effects of L2 Exposure, Proficiency, and AoA. NBS tests the same hypothesis for every possible network edge (connectome-wide analysis) so that each network's edge has a given test statistic value associated with it. A user-defined test statistic threshold is then applied to each edge, and only the supra-threshold connections are maintained (see

Fornito, Zalesky, and Bullmore, 2016). Following NBS recommendations, network-forming threshold values were selected to balance network extension (avoiding excessive connections) and effect strength (see Zalesky et al., 2010). Subsequently, NBS performs a form of clustering on the surviving edges by finding connected graph components in the topological space (equivalent to clusters of pixels or voxels in physical space in fMRI mass univariate analyses). A *connected component* can be described as a network structure in which a path always exists between any two nodes. A network Intensity measure was computed for each component as the sum of each connection's test values. Compared with other less complex indices such as network Extent (i.e., the total number of connections of a connected component), Intensity accounts for variations in effect sizes associated with each edge (similarly to Cluster Mass measure, see Bullmore, 1999). Additionally, Intensity is recommended to detect solid and focal effects associated with connectivity strength accurately. FWE multiple comparison correction was applied to each generated connected component using permutation testing with 5,000 permutations (FWE corrected p-value < .05). NBS analyses provide two outputs: significant effect-related connected components (i.e., effect-related subnetworks) and FWE corrected p-values associated with each component.

Graph theory Metrics of NBS Connected Components. The usage of Graph theory metrics and indices allows estimating the topological properties of complex systems. Brain networks can be considered complex systems of interacting elements formed by nodes and edges (Fornito, Zalesky, and Bullmore, 2016). We performed two graph theoretical analyses:

- 1) a set of indices was estimated to better describe the architecture of connected components associated with specific bilingual experiential factors (i.e., L2 Exposure, Proficiency, and AoA) from the NBS analyses. We generated a weighted undirected adjacency matrix for each significant effect-related network, with edges' weight corresponding to the t-values associated with the investigated effects. The following measures were then computed:
 - *Node Degree.* Node degree corresponds to the most basic graph theoretical index and represents the number of edges of each node

(Fornito, Zalesky, and Bullmore, 2016). The higher the node degree, the higher the number of connections linked with that node. Node degree computation ignores edge weights.

- *Betweenness of Centrality.* The betweenness of centrality index measures the proportion of all possible shortest paths (i.e., the minimum number of edges required to link any couple of nodes of a network) containing a given node (Brandes, 2001). The higher the betweenness of centrality of a node, the more the node takes part in several shortest paths influencing other nodes (Freeman, 1978). Edge weights are considered in the Betweenness of Centrality computation (Brandes, 2001).
- *Modularity.* A well-known property of most brain networks is their modular structure (Bullmore and Sporns, 2012). The Louvain method for community detection classifies a given network into non-overlapping "communities" of nodes by simultaneously maximizing the number of within-community edges and minimizing the number of between-communities edges (Blondel et al., 2008). This method allows one to investigate areas of segregation and specialization of information processing within a brain network. Edge weights are considered in Modularity computation (Blondel et al., 2008).

All graph theory measures were computed employing the Brain Connectivity Toolbox (BCT) (Rubinov and Sporns, 2010).

Whole-Connectome Graph Analysis.

- 2) We performed a second analysis was performed by comparing Graph Theory indices of the NBS significant effect-related connected components with the same measures computed at the whole-brain level. This analysis aimed to understand how the properties of effect-related subnetworks associated with dual language experiential factors could alter the whole-brain connectivity matrix. The previously estimated effect-related adjacency matrices were binarized, and edge values were replaced with each participant's connectivity value for that edge to obtain a participant-specific effect-related

connected component. The following measures were then computed for the whole brain connectomes and the effect-related networks:

- Global Efficiency (Eglob). Global Efficiency is the average of the inverse shortest path length between each node and all other nodes in the network (Latora and Marchiori, 2001), and represents a measure of connectome integration and inter-connectedness. The larger the Eglob value, the easier brain regions communicate, and specialized information is combined from all parts of the connectome (Rubinov and Sporns, 2010). Edge weights are considered in Eglob computation (Rubinov and Sporns, 2010).
- Local Efficiency (Eloc). Local Efficiency (Latora and Marchiori, 2001) is related to clustering measures and reflects the global Efficiency computed on the neighborhood of a given node. In other words, local Efficiency is the extent of the integration of a sub-graph consisting of only the nodes surrounding a particular node. Edge weights are considered in Eloc computation (Rubinov and Sporns, 2010).

Eglob and Eloc were computed with BCT. Correlation analyses between the Efficiency of connected components and that of the whole-brain network were performed employing the Robust Correlation Toolbox (Pernet et al., 2013).

Correlation analyses between efficiency measures and switching tendencies. Finally, to investigate the relationship between the efficiency of effect-related subnetworks and each participant's self-reported switching measures, Eglob and Eloc measures from significant connected components were correlated with the BSWQ sub-scores.

Chapter 6 - REFERENCES

A

Abutalebi, J., Brambati, S. M., Annoni, J.-M., Moro, A., Cappa, S. F., & Perani, D. (2007). The neural cost of the auditory perception of language switches: an event-related functional magnetic resonance imaging study in bilinguals. *Journal of Neuroscience*, *27*(50), 13762–13769.

Abutalebi, J., & Green, D. (2007). Bilingual language production: The neurocognition of language representation and control. *Journal of neurolinguistics*, *20*(3), 242-275.

Abutalebi, J., & Green, D. W. (2008). Control mechanisms in bilingual language production: Neural evidence from language switching studies. *Language and cognitive processes*, *23*(4), 557-582.

Abutalebi, J., Della Rosa, P. A., Green, D. W., Hernandez, M., Scifo, P., Keim, R., ... & Costa, A. (2012). Bilingualism tunes the anterior cingulate cortex for conflict monitoring. *Cerebral cortex*, *22*(9), 2076-2086.

Abutalebi, J., Canini, M., Della Rosa, P. A., Sheung, L. P., Green, D. W., & Weekes, B. S. (2014). Bilingualism protects anterior temporal lobe integrity in aging. *Neurobiology of aging*, *35*(9), 2126-2133.

Abutalebi, J., Guidi, L., Borsa, V., Canini, M., Della Rosa, P. A., Parris, B. A., & Weekes, B. S. (2015a). Bilingualism provides a neural reserve for aging populations. *Neuropsychologia*, *69*, 201-210.

Abutalebi, J., Canini, M., Della Rosa, P. A., Green, D. W., & Weekes, B. S. (2015b). The neuroprotective effects of bilingualism upon the inferior parietal lobule: a structural neuroimaging study in aging Chinese bilinguals. *Journal of Neurolinguistics*, *33*, 3-13.

Abutalebi, J., & Green, D. W. (2016). Neuroimaging of language control in bilinguals: neural adaptation and reserve. *Bilingualism: Language and cognition*, 19(4), 689-698.

Alladi, S., Bak, T.H., Duggirala, V., Surampudi, B., Shailaja, M., Shukla, A.K., Chaudhuri, J.R., Kaul, S., (2013). Bilingualism delays age at onset of dementia, independent of education and immigration status. *Neurology* 10–1212.

American Psychiatric Association. (2013). *Diagnostic and statistical manual of mental disorders* (5th ed.). Washington, DC.

Amiez, C., Joseph, J. P., & Procyk, E. (2006). Reward encoding in the monkey anterior cingulate cortex. *Cerebral cortex*, 16(7), 1040-1055.

Amiez, C., Neveu, R., Warrot, D., Petrides, M., Knoblach, K., & Procyk, E. (2013). The location of feedback-related activity in the midcingulate cortex is predicted by local morphology. *Journal of Neuroscience*, 33(5), 2217-2228.

Amiez, C., & Petrides, M. (2014). Neuroimaging evidence of the anatomo-functional organization of the human cingulate motor areas. *Cerebral cortex*, 24(3), 563-578.

Amiez, C., Sallet, J., Hopkins, W. D., Meguerditchian, A., Hadj-Bouziane, F., Hamed, S. B., ... & Petrides, M. (2019). Sulcal organization in the medial frontal cortex provides insights into primate brain evolution. *Nature communications*, 10(1), 1-14.

Andersson, J. L., & Sotiropoulos, S. N. (2016). An integrated approach to correction for off-resonance effects and subject movement in diffusion MR imaging. *Neuroimage*, 125, 1063-1078.

Andersson, J. L., Graham, M. S., Zsoldos, E., & Sotiropoulos, S. N. (2016). Incorporating outlier detection and replacement into a non-parametric framework for movement and distortion correction of diffusion MR images. *Neuroimage*, 141, 556-572.

Anglade, C., Thiel, A., & Ansaldo, A. I. (2014). The complementary role of the cerebral hemispheres in recovery from aphasia after stroke: a critical review of literature. *Brain Injury*, 28(2), 138-145.

Arias-Carrión, O., Stamelou, M., Murillo-Rodríguez, E., Menéndez-González, M., & Pöppel, E. (2010). Dopaminergic reward system: a short integrative review. *International archives of medicine*, 3(1), 1-6.

Ardila, A., Bernal, B., & Rosselli, M. (2014). Participation of the insula in language revisited: a meta-analytic connectivity study. *Journal of Neurolinguistics*, 29, 31-41.

Armstrong, E., Schleicher, A., Omran, H., Curtis, M., & Zilles, K. (1995). The ontogeny of human gyrification. *Cerebral cortex*, 5(1), 56-63.

Artiges, E., Martelli, C., Naccache, L., Bartrés-Faz, D., LeProvost, J. B., Viard, A., ... & Martinot, J. L. (2006). Paracingulate sulcus morphology and fMRI activation detection in schizophrenia patients. *Schizophrenia research*, 82(2-3), 143-151.

Ashburner, J., & Friston, K. J. (2000). Voxel-based morphometry—the methods. *Neuroimage*, 11(6), 805-821.

Ashburner, J., & Friston, K. J. (2005). Unified segmentation. *Neuroimage*, 26(3), 839-851.

B

Babayan, A., Erbey, M., Kumral, D., Reinelt, J. D., Reiter, A. M., Röbbing, J., ... & Villringer, A. (2019). A mind-brain-body dataset of MRI, EEG, cognition, emotion, and peripheral physiology in young and old adults. *Scientific data*, 6(1), 1-21.

Bach, M., Laun, F. B., Leemans, A., Tax, C. M., Biessels, G. J., Stieltjes, B., & Maier-Hein, K. H. (2014). Methodological considerations on tract-based spatial statistics (TBSS). *Neuroimage*, 100, 358-369.

Balaev, V., Petrushevsky, A., & Martynova, O. (2016). Changes in functional connectivity of default mode network with auditory and right frontoparietal networks in poststroke aphasia. *Brain connectivity*, 6(9), 714-723.

Bangert, M., & Schlaug, G. (2006). Specialization of the specialized in features of external human brain morphology. *European Journal of Neuroscience*, 24(6), 1832-1834.

Barron, D. H. (1950). An experimental analysis of some factors involved in the development of the fissure pattern of the cerebral cortex. *Journal of Experimental Zoology*, 113(3), 553-581.

Barroso-Flores, J., Herrera-Valdez, M. A., Galarraga, E., & Bargas, J. (2017). Models of short-term synaptic plasticity. *The Plastic Brain*, 41-57.

Barroso-Flores, J., Herrera-Valdez, M. A., Lopez-Huerta, V. G., Galarraga, E., & Bargas, J. (2015). Diverse short-term dynamics of inhibitory synapses converging on striatal projection neurons: differential changes in a rodent model of parkinson's disease. *Neural plasticity*.

Barulli, D., & Stern, Y. (2013). Efficiency, capacity, compensation, maintenance, plasticity: emerging concepts in cognitive reserve. *Trends in cognitive sciences*, 17(10), 502-509.

Basso, A., Capitani, E., & Laiacona, M. (1987). Raven's coloured progressive matrices: normative values on 305 adult normal controls. *Functional neurology*, 2(2), 189-194.

Beckmann, M., Johansen-Berg, H., & Rushworth, M. F. (2009). Connectivity-based parcellation of human cingulate cortex and its relation to functional specialization. *Journal of Neuroscience*, 29(4), 1175-1190.

Bedny, M., Richardson, H., & Saxe, R. (2015). “Visual” cortex responds to spoken language in blind children. *Journal of Neuroscience*, 35(33), 11674-11681.

Behzadi, Y., Restom, K., Liau, J., & Liu, T. T. (2007). A component based noise correction method (CompCor) for BOLD and perfusion based fMRI. *Human Brain Mapping Journal*, 37(1), 90–101.

Bellander, M., Berggren, R., Mårtensson, J., Brehmer, Y., Wenger, E., Li, T. Q., ... & Lövdén, M. (2016). Behavioral correlates of changes in hippocampal gray matter structure during acquisition of foreign vocabulary. *NeuroImage*, 131, 205-213.

Bekkers, J. M., & Stevens, C. F. (1990). Presynaptic mechanism for long-term potentiation in the hippocampus. *Nature*, 346(6286), 724-729.

Bengtsson, S. L., Nagy, Z., Skare, S., Forsman, L., Forssberg, H., & Ullén, F. (2005). Extensive piano practicing has regionally specific effects on white matter development. *Nature neuroscience*, 8(9), 1148-1150.

Benedict, C., Brooks, S. J., Kullberg, J., Nordenskjöld, R., Burgos, J., Le Grevès, M., ... & Schiöth, H. B. (2013). Association between physical activity and brain health in older adults. *Neurobiology of aging*, 34(1), 83-90.

Berken, J. A., Chai, X., Chen, J. K., Gracco, V. L., & Klein, D. (2016). Effects of early and late bilingualism on resting-state functional connectivity. *Journal of Neuroscience*, 36(4), 1165-1172.

- Bermudez, P., Lerch, J. P., Evans, A. C., & Zatorre, R. J. (2009). Neuroanatomical correlates of musicianship as revealed by cortical thickness and voxel-based morphometry. *Cerebral cortex*, 19(7), 1583-1596.
- Betzel, R. F., Byrge, L., He, Y., Goñi, J., Zuo, X. N., & Sporns, O. (2014). Changes in structural and functional connectivity among resting-state networks across the human lifespan. *Neuroimage*, 102, 345-357.
- Bialystok, E., Craik, F. I. M., Freedman, M., (2007). Bilingualism as a protection against the onset of symptoms of dementia. *Neuropsychologia* 45, 459–464.
- Bijsterbosch, J. D., Woolrich, M. W., Glasser, M. F., Robinson, E. C., Beckmann, C. F., Van Essen, D. C., ... & Smith, S. M. (2018). The relationship between spatial configuration and functional connectivity of brain regions. *Elife*, 7, e32992.
- Birdsong, D. (2018). Plasticity, variability and age in second language acquisition and bilingualism. *Frontiers in psychology*, 9, 81.
- Blondel, V. D., Guillaume, J. L., Lambiotte, R., & Lefebvre, E. (2008). Fast unfolding of communities in large networks. *Journal of statistical mechanics: theory and experiment*, 2008(10), P10008.
- Bludau, S., Eickhoff, S. B., Mohlberg, H., Caspers, S., Laird, A. R., Fox, P. T., ... & Amunts, K. (2014). Cytoarchitecture, probability maps and functions of the human frontal pole. *Neuroimage*, 93, 260-275.
- Bodin, C., Takerkart, S., Belin, P., & Coulon, O. (2018). Anatomic-functional correspondence in the superior temporal sulcus. *Brain Structure and Function*, 223(1), 221-232.

- Borne, L., Rivi re, D., Cachia, A., Roca, P., Mellerio, C., Oppenheim, C., & Mangin, J. F. (2021). Automatic recognition of specific local cortical folding patterns. *NeuroImage*, 118208.
- Bornkessel-Schlesewsky, I., & Friederici, A. D. (2007). Neuroimaging studies of sentence and discourse comprehension. *The Oxford handbook of psycholinguistics*, 407-424.
- Borrell, V. (2018). How cells fold the cerebral cortex. *Journal of Neuroscience*, 38(4), 776-783.
- Borst, G., Cachia, A., Vidal, J., Simon, G., Fischer, C., Pineau, A., ... & Houd , O. (2014). Folding of the anterior cingulate cortex partially explains inhibitory control during childhood: a longitudinal study. *Developmental cognitive neuroscience*, 9, 126-135.
- Botvinick, M. M., Braver, T. S., Barch, D. M., Carter, C. S., & Cohen, J. D. (2001). Conflict monitoring and cognitive control. *Psychological review*, 108(3), 624.
- Botvinick, M. M., Cohen, J. D., & Carter, C. S. (2004). Conflict monitoring and anterior cingulate cortex: an update. *Trends in cognitive sciences*, 8(12), 539-546.
- Braak, H., & Braak, E. (1991). Neuropathological staging of Alzheimer-related changes. *Acta neuropathologica*, 82(4), 239-259.
- Bramati, I. E., Rodrigues, E. C., Sim es, E. L., Melo, B., H fle, S., Moll, J., ... & Tovar-Moll, F. (2019). Lower limb amputees undergo long-distance plasticity in sensorimotor functional connectivity. *Scientific reports*, 9(1), 1-10.
- Brandes, U. (2001). A faster algorithm for betweenness centrality. *Journal of mathematical sociology*, 25(2), 163-177.

- Branzi, F. M., Della Rosa, P. A., Canini, M., Costa, A., & Abutalebi, J. (2016). Language control in bilinguals: monitoring and response selection. *Cerebral Cortex*, 26(6), 2367-2380.
- Breitenstein, C., Jansen, A., Deppe, M., Foerster, A. F., Sommer, J., Wolbers, T., & Knecht, S. (2005). Hippocampus activity differentiates good from poor learners of a novel lexicon. *NeuroImage*, 25(3), 958–968
- Brennan, J., Nir, Y., Hasson, U., Malach, R., Heeger, D. J., & Pylkkänen, L. (2012). Syntactic structure building in the anterior temporal lobe during natural story listening. *Brain and language*, 120(2), 163-173.
- Briellmann, R. S., Saling, M. M., Connell, A. B., Waites, A. B., Abbott, D. F., & Jackson, G. D. (2004). A high-field functional MRI study of quadri-lingual subjects. *Brain and Language*, 89(3), 531-542.
- Brodmann, K. (1909). *Vergleichende Lokalisationslehre der Grosshirnrinde in ihren Prinzipien dargestellt auf Grund des Zellenbaues*. Barth.
- Brodoehl, S., Gaser, C., Dahnke, R., Witte, O. W., & Klingner, C. M. (2020). Surface-based analysis increases the specificity of cortical activation patterns and connectivity results. *Scientific reports*, 10(1), 1-13.
- Brown, W. S., Thrasher, E. D., & Paul, L. K. (2001). Interhemispheric Stroop effects in partial and complete agenesis of the corpus callosum. *Journal of the International Neuropsychological Society*, 7(3), 302-311.
- Bub, D. N., Masson, M. E., & Lalonde, C. E. (2006). Cognitive control in children: Stroop interference and suppression of word reading. *Psychological Science*, 17(4), 351-357.

Bubb, E. J., Metzler-Baddeley, C., & Aggleton, J. P. (2018). The cingulum bundle: anatomy, function, and dysfunction. *Neuroscience & Biobehavioral Reviews*, 92, 104-127.

Buchsbaum, B. R., Baldo, J., Okada, K., Berman, K. F., Dronkers, N., D'Esposito, M., & Hickok, G. (2011). Conduction aphasia, sensory-motor integration, and phonological short-term memory—an aggregate analysis of lesion and fMRI data. *Brain and language*, 119(3), 119-128.

Buda, M., Fornito, A., Bergström, Z. M., & Simons, J. S. (2011). A specific brain structural basis for individual differences in reality monitoring. *Journal of Neuroscience*, 31(40), 14308-14313.

Bullmore, E. T., Suckling, J., Overmeyer, S., Rabe-Hesketh, S., Taylor, E., & Brammer, M. J. (1999). Global, voxel, and cluster tests, by theory and permutation, for a difference between two groups of structural MR images of the brain. *IEEE transactions on medical imaging*, 18(1), 32-42.

Bullmore, E., & Sporns, O. (2009). Complex brain networks: graph theoretical analysis of structural and functional systems. *Nature reviews neuroscience*, 10(3), 186-198.

Bullmore, E., & Sporns, O. (2012). The economy of brain network organization. *Nature Reviews Neuroscience*, 13(5), 336-349.

Burgalata, M., Sanjuán, A., Ventura-Campos, N., Sebastian-Galles, N., & Ávila, C. (2016). Bilingualism at the core of the brain. Structural differences between bilinguals and monolinguals revealed by subcortical shape analysis. *NeuroImage*, 125, 437-445.

Burle, B., Spieser, L., Servant, M., & Hasbroucq, T. (2014). Distributional reaction time properties in the Eriksen task: marked differences or hidden similarities with the Simon task? *Psychonomic bulletin & review*, 21(4), 1003-1010.

Bush, G., Whalen, P. J., Rosen, B. R., Jenike, M. A., McInerney, S. C., & Rauch, S. L. (1998). The counting Stroop: an interference task specialized for functional neuroimaging—validation study with functional MRI. *Human brain mapping*, 6(4), 270-282.

Bush, G., Frazier, J. A., Rauch, S. L., Seidman, L. J., Whalen, P. J., Jenike, M. A., ... & Biederman, J. (1999). Anterior cingulate cortex dysfunction in attention-deficit/hyperactivity disorder revealed by fMRI and the Counting Stroop. *Biological psychiatry*, 45(12), 1542-1552.

Bush, G., Vogt, B. A., Holmes, J., Dale, A. M., Greve, D., Jenike, M. A., & Rosen, B. R. (2002). Dorsal anterior cingulate cortex: a role in reward-based decision making. *Proceedings of the National Academy of Sciences*, 99(1), 523-528.

Butler, Y. G., & Hakuta, K. (2004). Bilingualism and second language acquisition. *The handbook of bilingualism*, 114-144.

C

Cabeza, R., Anderson, N. D., Locantore, J. K., & McIntosh, A. R. (2002). Aging gracefully: compensatory brain activity in high-performing older adults. *Neuroimage*, 17(3), 1394-1402.

Cachia, A., Borst, G., Vidal, J., Fischer, C., Pineau, A., Mangin, J. F., & Houdé, O. (2014). The shape of the ACC contributes to cognitive control efficiency in preschoolers. *Journal of cognitive neuroscience*, 26(1), 96-106.

Cachia, A., Amad, A., Brunelin, J., Krebs, M. O., Plaze, M., Thomas, P., & Jardri, R. (2015). Deviations in cortex sulcation associated with visual hallucinations in schizophrenia. *Molecular psychiatry*, 20(9), 1101-1107.

Cachia, A., Borst, G., Tissier, C., Fisher, C., Plaze, M., Gay, O., ... & Raznahan, A. (2016). Longitudinal stability of the folding pattern of the anterior cingulate cortex during development. *Developmental cognitive neuroscience*, 19, 122-127.

- Cachia, A., Del Maschio, N., Borst, G., Della Rosa, P. A., Pallier, C., Costa, A., ... & Abutalebi, J. (2017). Anterior cingulate cortex sulcation and its differential effects on conflict monitoring in bilinguals and monolinguals. *Brain and language*, 175, 57-63.
- Calabria, M., Costa, A., Green, D. W., & Abutalebi, J. (2018). Neural basis of bilingual language control. *Annals of the New York Academy of Sciences*, 1426(1), 221-235.
- Cao, W., Luo, C., Zhu, B., Zhang, D., Dong, L., Gong, J., ... & Li, J. (2014). Resting-state functional connectivity in anterior cingulate cortex in normal aging. *Frontiers in Aging Neuroscience*, 6, 280.
- Cao, B., Mwangi, B., Passos, I. C., Wu, M. J., Keser, Z., Zunta-Soares, G. B., ... & Soares, J. C. (2017). Lifespan gyrification trajectories of human brain in healthy individuals and patients with major psychiatric disorders. *Scientific Reports*, 7(1), 1-8.
- Caroni, P., Chowdhury, A., & Lahr, M. (2014). Synapse rearrangements upon learning: from divergent–sparse connectivity to dedicated sub-circuits. *Trends in neurosciences*, 37(10), 604-614.
- Chai, X. J., Castañón, A. N., Öngür, D., & Whitfield-Gabrieli, S. (2012). Anticorrelations in resting state networks without global signal regression. *Neuroimage*, 59(2), 1420-1428.
- Chambon, V., Franck, N., Koechlin, E., Fakra, E., Ciuperca, G., Azorin, J. M., & Farrer, C. (2008). The architecture of cognitive control in schizophrenia. *Brain*, 131(4), 962-970.
- Chan, D., Fox, N. C., Scahill, R. I., Crum, W. R., Whitwell, J. L., Leschziner, G., Rossor, M. N. (2001). Patterns of temporal lobe atrophy in semantic dementia and Alzheimer's disease. *Annals of Neurology*, 49(4), 433–442.

Chen, P. Y., Chiou, J. M., Yang, Y. F., Chen, Y. T., Hsieh, H. L., Chang, Y. L., & Tseng, W. Y. I. (2016). Heterogeneous aging effects on functional connectivity in different cortical regions: A resting-state functional mri study using functional data analysis. *PloS one*, 11(9).

Chen, Z., Zhao, X., Fan, J., & Chen, A. (2018). Functional cerebral asymmetry analyses reveal how the control system implements its flexibility. *Human brain mapping*, 39(12), 4678-4688.

Chi, J. G., Dooling, E. C., & Gilles, F. H. (1977). Gyral development of the human brain. *Annals of neurology*, 1(1), 86-93.

Chklovskii, D. B., Schikorski, T., & Stevens, C. F. (2002). Wiring optimization in cortical circuits. *Neuron*, 34(3), 341-347.

Clark, G. M., Mackay, C. E., Davidson, M. E., Iversen, S. D., Collinson, S. L., James, A. C., ... & Crow, T. J. (2010). Paracingulate sulcus asymmetry; sex difference, correlation with semantic fluency and change over time in adolescent onset psychosis. *Psychiatry Research: Neuroimaging*, 184(1), 10-15.

Claussenius-Kalman, H., Vaughn, K. A., Archila-Suerte, P., & Hernandez, A. E. (2020). Age of acquisition impacts the brain differently depending on neuroanatomical metric. *Human brain mapping*, 41(2), 484-502.

Cockrell, J. R., & Folstein, M. F. (2002). Mini-mental state examination. *Principles and practice of geriatric psychiatry*, 140-141.

Coggins, P. E., Kennedy, T. J., & Armstrong, T. a. (2004). Bilingual corpus callosum variability. *Brain and Language*, 89(1), 69–75.

Colmenares, A. M., Voss, M. W., Fanning, J., Salerno, E. A., Gothe, N. P., Thomas, M. L., ... & Burzynska, A. Z. (2021). White matter plasticity in healthy older adults: the effects of aerobic exercise. *Neuroimage*, 239, 118305.

Colombo, L., Sartori, G., & Brivio, C. (2002). Stima del quoziente intellettivo tramite l'applicazione del TIB (test breve di Intelligenza). *Giornale Italiano di Psicologia*, 29(3), 613-638.

Consonni, M., Cafiero, R., Marin, D., Tettamanti, M., Iadanza, A., Fabbro, F., & Perani, D. (2013). Neural convergence for language comprehension and grammatical class production in highly proficient bilinguals is independent of age of acquisition. *Cortex*, 49(5), 1252-1258.

Cooper, J. A. (2013). Mechanisms of cell migration in the nervous system. *Journal of Cell Biology*, 202(5), 725-734.

Corbetta, M., & Shulman, G. L. (2002). Control of goal-directed and stimulus-driven attention in the brain. *Nature reviews neuroscience*, 3(3), 201-215.

Cramer, S. C., Sur, M., Dobkin, B. H., O'brien, C., Sanger, T. D., Trojanowski, J. Q., ... & Vinogradov, S. (2011). Harnessing neuroplasticity for clinical applications. *Brain*, 134(6), 1591-1609.

Crosson, B., Sadek, J. R., Bobholz, J. A., Gökçay, D., Mohr, C. M., Leonard, C. M., ... & Briggs, R. W. (1999). Activity in the paracingulate and cingulate sulci during word generation: an fMRI study of functional anatomy. *Cerebral cortex*, 9(4), 307-316.

Cummine, J., & Boliek, C. A. (2013). Understanding white matter integrity stability for bilinguals on language status and reading performance. *Brain Structure and Function*, 218(2), 595-601.

D

Dahnke, R., Yotter, R. A., & Gaser, C. (2013). Cortical thickness and central surface estimation. *Neuroimage*, 65, 336-348.

Dahnke, R., & Gaser, C. (2018). *Brain Morphometry*.

Dale, A. M., Fischl, B., & Sereno, M. I. (1999). Cortical surface-based analysis: I. Segmentation and surface reconstruction. *Neuroimage*, 9(2), 179-194.

Dale, A. M. (1999). Optimal experimental design for event-related fMRI. *Human brain mapping*, 8(2-3), 109-114.

Damoiseaux, J. S. (2017). Effects of aging on functional and structural brain connectivity. *Neuroimage*, 160, 32-40.

David, S., Heemskerk, A. M., Corrivetti, F., Thiebaut de Schotten, M., Sarubbo, S., Corsini, F., ... & Leemans, A. (2019). The superoanterior fasciculus (SAF): a novel white matter pathway in the human brain?. *Frontiers in neuroanatomy*, 13, 24.

Davies, R. R., Graham, K. S., Xuereb, J. H., Williams, G. B., & Hodges, J. R. (2004). The human perirhinal cortex and semantic memory. *European Journal of Neuroscience*, 20(9), 2441-2446.

Davis, S. W., Dennis, N. A., Daselaar, S. M., Fleck, M. S., & Cabeza, R. (2008). Que PASA? The posterior–anterior shift in aging. *Cerebral cortex*, 18(5), 1201-1209.

Davis, M. H., & Gaskell, M. G. (2009). A complementary systems account of word learning: neural and behavioural evidence. *Philosophical Transactions of the Royal Society B: Biological Sciences*, 364(1536), 3773-3800.

De Baene, W., Duyck, W., Brass, M., & Carreiras, M. (2015). Brain circuit for cognitive control is shared by task and language switching. *Journal of cognitive neuroscience*, 27(9), 1752-1765.

de Bruin, A., Roelofs, A., Dijkstra, T., & FitzPatrick, I. (2014). Domain-general inhibition areas of the brain are involved in language switching: FMRI evidence from trilingual speakers. *NeuroImage*, 90, 348-359.

De Jong, R., Liang, C. C., & Lauber, E. (1994). Conditional and unconditional automaticity: a dual-process model of effects of spatial stimulus-response correspondence. *Journal of Experimental Psychology: Human Perception and Performance*, 20(4), 731.

Della Rosa, P. A., Videsott, G., Borsa, V. M., Canini, M., Weekes, B. S., Franceschini, R., & Abutalebi, J. (2013). A neural interactive location for multilingual talent. *Cortex*, 49(2), 605-608.

Del Maschio, N., Sulpizio, S., Fedeli, D., Ramanujan, K., Ding, G., Weekes, B. S., ... & Abutalebi, J. (2018a). ACC sulcal patterns and their modulation on cognitive control efficiency across lifespan: A neuroanatomical study on bilinguals and monolinguals. *Cerebral Cortex*, 29(7), 3091-3101.

Del Maschio, N., Fedeli, D., & Abutalebi, J. (2018b). Bilingualism and aging: Why research should continue. *Linguistic Approaches to Bilingualism*, 11(4), 505-519.

Del Maschio, N., Sulpizio, S., Gallo, F., Fedeli, D., Weekes, B. S., & Abutalebi, J. (2018c). Neuroplasticity across the lifespan and aging effects in bilinguals and monolinguals. *Brain and cognition*, 125, 118-126.

Del Maschio, N., Fedeli, D., Sulpizio, S., & Abutalebi, J. (2019a). The relationship between bilingual experience and gyrification in adulthood: A cross-sectional surface-based morphometry study. *Brain and language*, 198, 104680.

Del Maschio, N., Sulpizio, S., Toti, M., Caprioglio, C., Del Mauro, G., Fedeli, D., & Abutalebi, J. (2019b). Second language use rather than second language knowledge

relates to changes in white matter microstructure. *Journal of Cultural Cognitive Science*, 4(2), 165-175.

Del Maschio, N., & Abutalebi, J. (2019). Language organization in the bilingual and multilingual brain. *The handbook of the neuroscience of multilingualism*, 197-213.

Del Maschio, N., Sulpizio, S., & Abutalebi, J. (2020). Thinking outside the box: The brain-bilingualism relationship in the light of early neurobiological variability. *Brain and language*, 211, 104879.

Del Mauro, G., Del Maschio, N., Sulpizio, S., Fedeli, D., Perani, D., & Abutalebi, J. (2021). Investigating sexual dimorphism in human brain structure by combining multiple indexes of brain morphology and source-based morphometry. *Brain Structure and Function*, 1-11.

DeLuca, V., Rothman, J., Bialystok, E., & Pliatsikas, C. (2019). Redefining bilingualism as a spectrum of experiences that differentially affects brain structure and function. *Proceedings of the National Academy of Sciences*, 116(15), 7565-7574.

DeLuca, V., Rothman, J., & Pliatsikas, C. (2019). Linguistic immersion and structural effects on the bilingual brain: a longitudinal study. *Bilingualism: Language and Cognition*, 22(5), 1160-1175.

DeLuca, V., Rothman, J., Bialystok, E., & Pliatsikas, C. (2020). Duration and extent of bilingual experience modulate neurocognitive outcomes. *NeuroImage*, 204, 116222.

Desikan, R. S., Ségonne, F., Fischl, B., Quinn, B. T., Dickerson, B. C., Blacker, D., ... & Killiany, R. J. (2006). An automated labeling system for subdividing the human cerebral cortex on MRI scans into gyral based regions of interest. *Neuroimage*, 31(3), 968-980.

Dhollander, T. Mito, R. Raffelt, D. & Connelly, A. (2019). Improved white matter response function estimation for 3-tissue constrained spherical deconvolution. *Proc Intl Soc Mag Reson Med*, 555.

Dhollander, T.; Raffelt, D. & Connelly, A. Unsupervised 3-tissue response function estimation from single-shell or multi-shell diffusion MR data without a co-registered T1 image. *ISMRM Workshop on Breaking the Barriers of Diffusion MRI*, 2016, 5

Dimou, S., Biggs, M., Tonkin, M., Hickie, I. B., & Lagopoulos, J. (2013). Motor cortex neuroplasticity following brachial plexus transfer. *Frontiers in human neuroscience*, 7, 500.

Dormal, G., & Collignon, O. (2011). Functional selectivity in sensory-deprived cortices. *Journal of neurophysiology*, 105(6), 2627-2630.

Doron, K. W., & Gazzaniga, M. S. (2008). Neuroimaging techniques offer new perspectives on callosal transfer and interhemispheric communication. *Cortex*, 44(8), 1023-1029.

Draganski, B., Gaser, C., Busch, V., Schuierer, G., Bogdahn, U., & May, A. (2004). Changes in grey matter induced by training. *Nature*, 427(6972), 311-312.

Dubois, J., Benders, M., Cachia, A., Lazeyras, F., Ha-Vinh Leuchter, R., Sizonenko, S. V., ... & Hüppi, P. S. (2008). Mapping the early cortical folding process in the preterm newborn brain. *Cerebral Cortex*, 18(6), 1444-1454.

Dum, R. P., & Strick, P. L. (1993). Cingulate motor areas. In *Neurobiology of cingulate cortex and limbic thalamus* (pp. 415-441). Birkhäuser, Boston, MA.

E

Eichert, N., Watkins, K. E., Mars, R. B., & Petrides, M. (2020). Morphological and functional variability in central and subcentral motor cortex of the human brain. *Brain Structure and Function*, 226(1), 263-279.

Elmer, S., Hänggi, J., Meyer, M., & Jäncke, L. (2011). Differential language expertise related to white matter architecture in regions subserving sensory-motor coupling, articulation, and interhemispheric transfer. *Human brain mapping*, 32(12), 2064-2074.

Engert, F., & Bonhoeffer, T. (1999). Dendritic spine changes associated with hippocampal long-term synaptic plasticity. *Nature*, 399(6731), 66-70.

Eriksen, B. A., & Eriksen, C. W. (1974). Effects of noise letters upon the identification of a target letter in a nonsearch task. *Perception & psychophysics*, 16(1), 143-149.

Erickson, K. I., Leckie, R. L., & Weinstein, A. M. (2014). Physical activity, fitness, and gray matter volume. *Neurobiology of aging*, 35, S20-S28.

F

Farquharson, S., Tournier, J. D., Calamante, F., Fabinyi, G., Schneider-Kolsky, M., Jackson, G. D., & Connelly, A. (2013). White matter fiber tractography: why we need to move beyond DTI. *Journal of neurosurgery*, 118(6), 1367-1377.

Falkai, P., Honer, W. G., Kasper, T., Dustert, S., Vogele, K., Schneider-Axmann, T., ... & Tepest, R. (2007). Disturbed frontal gyrification within families affected with schizophrenia. *Journal of Psychiatric Research*, 41(10), 805-813.

Fan, J., McCandliss, B. D., Sommer, T., Raz, A., & Posner, M. I. (2002). Testing the efficiency and independence of attentional networks. *Journal of cognitive neuroscience*, 14(3), 340-347.

Fan, J., McCandliss, B. D., Fossella, J., Flombaum, J. I., & Posner, M. I. (2005). The activation of attentional networks. *Neuroimage*, 26(2), 471-479.

Fan, Y., Borchardt, V., von Düring, F., Leutritz, A. L., Dietz, M., Herrera-Meléndez, A. L., ... & Walter, M. (2019). Dorsal and ventral posterior cingulate cortex switch network assignment via changes in relative functional connectivity strength to noncanonical networks. *Brain connectivity*, 9(1), 77-94.

Fedeli, D., & Abutalebi, J., (2019) Neuroimaging e afasia. in Gilardone, M., & Monti, A. (Eds.). *Afasiologia: Clinica, valutazione, trattamento*. FrancoAngeli.

Fedeli, D., Del Maschio, N., Caprioglio, C., Sulpizio, S., & Abutalebi, J. (2020). Sulcal Pattern Variability and Dorsal Anterior Cingulate Cortex Functional Connectivity Across Adult Age. *Brain connectivity*, 10(6), 267-278.

Fedeli, D., Del Maschio, N., Sulpizio, S., Rothman, J., & Abutalebi, J. (2021). The bilingual structural connectome: Dual-language experiential factors modulate distinct cerebral networks. *Brain and Language*, 220, 104978.

Fedeli, D., Del Maschio, N., Del Mauro, G., Defendenti, F., Sulpizio, S., & Abutalebi, J. (Submitted). ACC morphology modulates Inhibitory Control: Evidence from neurofunctional activity and behavioral performance. Submitted to *Cortex*.

Ferreira, L. K., & Busatto, G. F. (2013). Resting-state functional connectivity in normal brain aging. *Neuroscience & Biobehavioral Reviews*, 37(3), 384-400.

Festini, S. B., Zahodne, L., & Reuter-Lorenz, P. A. (2018). Theoretical Perspectives on Age Differences in Brain Activation: HAROLD, PASA, CRUNCH—How Do They STAC Up?. In *Oxford Research Encyclopedia of Psychology*.

Fischl, B., & Dale, A. M. (2000). Measuring the thickness of the human cerebral cortex from magnetic resonance images. *Proceedings of the National Academy of Sciences*, 97(20), 11050-11055.

Fischl, B., Rajendran, N., Busa, E., Augustinack, J., Hinds, O., Yeo, B. T., ... & Zilles, K. (2008). Cortical folding patterns and predicting cytoarchitecture. *Cerebral cortex*, 18(8), 1973-1980.

Fischl, B. (2012). FreeSurfer. *Neuroimage*, 62(2), 774-781.

Fornito, A., Yücel, M., Wood, S., Stuart, G. W., Buchanan, J. A., Proffitt, T., ... & Pantelis, C. (2004). Individual differences in anterior cingulate/paracingulate morphology are related to executive functions in healthy males. *Cerebral cortex*, 14(4), 424-431.

Fornito, A., Whittle, S., Wood, S. J., Velakoulis, D., Pantelis, C., & Yücel, M. (2006). The influence of sulcal variability on morphometry of the human anterior cingulate and paracingulate cortex. *Neuroimage*, 33(3), 843-854.

Fornito, A., Wood, S. J., Whittle, S., Fuller, J., Adamson, C., Saling, M. M., ... & Yücel, M. (2008). Variability of the paracingulate sulcus and morphometry of the medial frontal cortex: associations with cortical thickness, surface area, volume, and sulcal depth. *Human brain mapping*, 29(2), 222-236.

Fornito, A., Zalesky, A., & Bullmore, E. (2016). *Fundamentals of brain network analysis*. Academic Press.

Fortune, E. S., & Rose, G. J. (2000). Short-term synaptic plasticity contributes to the temporal filtering of electrosensory information. *Journal of Neuroscience*, 20(18), 7122-7130.

Freeman, L. C. (1978). Centrality in social networks conceptual clarification. *Social networks*, 1(3), 215-239.

Friederici, A. D., Meyer, M., & Von Cramon, D. Y. (2000). Auditory language comprehension: an event-related fMRI study on the processing of syntactic and lexical information. *Brain and language*, 74(2), 289-300.

Friederici, A. D., & von Cramon, D. Y. (2000). Syntax in the brain: Linguistic versus neuroanatomical specificity. *Behavioral and Brain Sciences*, 23(1), 32-33.

Friederici, A. D., & Kotz, S. A. (2003). The brain basis of syntactic processes: functional imaging and lesion studies. *Neuroimage*, 20, S8-S17.

Friederici, A. D. (2009). Pathways to language: fiber tracts in the human brain. *Trends in cognitive sciences*, 13(4), 175-181.

Friederici, A. D. (2011). The brain basis of language processing: from structure to function. *Physiological reviews*, 91(4), 1357-1392.

Friederici, A. D. (2012). The cortical language circuit: from auditory perception to sentence comprehension. *Trends in cognitive sciences*, 16(5), 262-268.

Friedman, N. P., Miyake, A., Robinson, J. L., & Hewitt, J. K. (2011). Developmental trajectories in toddlers' self-restraint predict individual differences in executive functions 14 years later: a behavioral genetic analysis. *Developmental psychology*, 47(5), 1410.

G

Gabrieli, J. D., Cohen, N. J., & Corkin, S. (1988). The impaired learning of semantic knowledge following bilateral medial temporal-lobe resection. *Brain and cognition*, 7(2), 157-177.

Gallo, F., Bermudez-Margaretto, B., Shtyrov, Y., Abutalebi, J., Kreiner, H., Chitaya, T., ... & Myachykov, A. (2019). First language attrition: what it is, what it isn't, and what it can be. *Frontiers in Human Neuroscience*, 513.

Gallo, F., Ramanujan, K., Shtyrov, Y., & Myachykov, A. (2021). Attriters and Bilinguals: What's in a Name?. *Frontiers in Psychology*, 12.

García-Pentón, L., Fernández, A. P., Iturria-Medina, Y., Gillon-Dowens, M., & Carreiras, M. (2014). Anatomical connectivity changes in the bilingual brain. *Neuroimage*, 84, 495-504.

Garrison, J. R., Fernyhough, C., McCarthy-Jones, S., Haggard, M., & Simons, J. S. (2015). Paracingulate sulcus morphology is associated with hallucinations in the human brain. *Nature communications*, 6(1), 1-6.

Garrison, J. R., Fernyhough, C., McCarthy-Jones, S., Simons, J. S., & Sommer, I. E. (2019). Paracingulate sulcus morphology and hallucinations in clinical and nonclinical groups. *Schizophrenia bulletin*, 45(4), 733-741.

Gaser, C., & Dahnke, R. (2016). CAT-a computational anatomy toolbox for the analysis of structural MRI data. *Hbm*, 2016, 336-348.

Gautam, P., Anstey, K. J., Wen, W., Sachdev, P. S., & Cherbuin, N. (2015). Cortical gyrification and its relationships with cortical volume, cortical thickness, and cognitive performance in healthy mid-life adults. *Behavioural Brain Research*, 287, 331–339.

Gay, O., Plaze, M., Oppenheim, C., Gaillard, R., Olié, J. P., Krebs, M. O., & Cachia, A. (2017). Cognitive control deficit in patients with first-episode schizophrenia is associated with complex deviations of early brain development. *Journal of psychiatry & neuroscience: JPN*, 42(2), 87.

Geerligs, L., Renken, R. J., Saliassi, E., Maurits, N. M., & Lorist, M. M. (2015). A brain-wide study of age-related changes in functional connectivity. *Cerebral cortex*, 25(7), 1987-1999.

Gennatas, E. D., Avants, B. B., Wolf, D. H., Satterthwaite, T. D., Ruparel, K., Ciric, R., ... & Gur, R. C. (2017). Age-related effects and sex differences in gray matter density, volume, mass, and cortical thickness from childhood to young adulthood. *Journal of Neuroscience*, 37(20), 5065-5073.

Geranmayeh, F., Leech, R., & Wise, R. J. (2015). Semantic retrieval during overt picture description: left anterior temporal or the parietal lobe? *Neuropsychologia*, 76, 125-135.

Gholipour, A., Rollins, C. K., Velasco-Annis, C., Ouaalam, A., Akhondi-Asl, A., Afacan, O., ... & Warfield, S. K. (2017). A normative spatiotemporal MRI atlas of the fetal brain for automatic segmentation and analysis of early brain growth. *Scientific reports*, 7(1), 1-13.

Gili, T., Fiori, V., De Pasquale, G., Sabatini, U., Caltagirone, C., & Marangolo, P. (2017). Right sensory-motor functional networks subserve action observation therapy in aphasia. *Brain imaging and behavior*, 11(5), 1397-1411.

Glasser, M. F., Coalson, T. S., Robinson, E. C., Hacker, C. D., Harwell, J., Yacoub, E., ... & Van Essen, D. C. (2016). A multi-modal parcellation of human cerebral cortex. *Nature*, 536(7615), 171-178.

Gold, B. T., Powell, D. K., Xuan, L., Jiang, Y., & Hardy, P. A. (2007). Speed of lexical decision correlates with diffusion anisotropy in left parietal and frontal white matter: evidence from diffusion tensor imaging. *Neuropsychologia*, 45(11), 2439-2446.

Gold, B. T., Johnson, N. F., Powell, D. K., (2013). Lifelong bilingualism contributes to cognitive reserve against white matter integrity declines in aging. *Neuropsychologia* 51, 2841–2846.

Gow Jr, D. W. (2012). The cortical organization of lexical knowledge: a dual lexicon model of spoken language processing. *Brain and language*, 121(3), 273-288.

Grady, C. L. (2008). Cognitive neuroscience of aging. *Annals of the new york Academy of Sciences*, 1124(1), 127-144.

Grady, C., Sarraf, S., Saverino, C., & Campbell, K. (2016). Age differences in the functional interactions among the default, frontoparietal control, and dorsal attention networks. *Neurobiology of aging*, 41, 159-172.

Green, D. W., & Abutalebi, J. (2013). Language control in bilinguals: The adaptive control hypothesis. *Journal of Cognitive Psychology*, 25(5), 515-530.

Green, D. W. (2019). Language Control and Attention during Conversation: An Exploration. *The Handbook of the Neuroscience of Multilingualism*, 427-446.

Greenwood, P. M. (2007). Functional plasticity in cognitive aging: review and hypothesis. *Neuropsychology*, 21(6), 657.

Greicius, M. D., Srivastava, G., Reiss, A. L., & Menon, V. (2004). Default-mode network activity distinguishes Alzheimer's disease from healthy aging: evidence from functional MRI. *Proceedings of the National Academy of Sciences*, 101(13), 4637-4642.

Grodzinsky, Y., & Friederici, A. D. (2006). Neuroimaging of syntax and syntactic processing. *Current opinion in neurobiology*, 16(2), 240-246.

Groussard, M., La Joie, R., Rauchs, G., Landeau, B., Chetelat, G., Viader, F., ... & Platel, H. (2010). When music and long-term memory interact: effects of musical expertise on functional and structural plasticity in the hippocampus. *PLoS One*, 5(10), e13225.

Guerra-Carrillo, B., Mackey, A. P., & Bunge, S. A. (2014). Resting-state fMRI: a window into human brain plasticity. *The Neuroscientist*, 20(5), 522-533.

Gullifer, J. W., Chai, X. J., Whitford, V., Pivneva, I., Baum, S., Klein, D., & Titone, D. (2018). Bilingual experience and resting-state brain connectivity: Impacts of L2 age of acquisition and social diversity of language use on control networks. *Neuropsychologia*, 117, 123-134.

Gurunandan, K., Carreiras, M., & Paz-Alonso, P. M. (2019). Functional plasticity associated with language learning in adults. *NeuroImage*, 201, 116040.

H

Hagmann, P., Cammoun, L., Gigandet, X., Meuli, R., Honey, C. J., Wedeen, V. J., & Sporns, O. (2008). Mapping the structural core of human cerebral cortex. *PLoS Biol*, 6(7), e159.

Hagoort, P. (2005). On Broca, brain, and binding: a new framework. *Trends in cognitive sciences*, 9(9), 416-423.

Hämäläinen, S., Sairanen, V., Leminen, A., & Lehtonen, M. (2017). Bilingualism modulates the white matter structure of language-related pathways. *Neuroimage*, 152, 249-257.

Hart, S. J., Green, S. R., Casp, M., & Belger, A. (2010). Emotional priming effects during Stroop task performance. *Neuroimage*, 49(3), 2662-2670.

Hebb, D. O. (1949). *The organisation of behaviour: a neuropsychological theory*. New York: Science Editions.

Heilbronner, S. R., & Hayden, B. Y. (2016). Dorsal anterior cingulate cortex: a bottom-up view. *Annual review of neuroscience*, 39, 149-170.

Herculano-Houzel, S., 2012a. The remarkable, yet not extraordinary, human brain as a scaled-up primate brain and its associated cost. *Proceedings of the National Academy of Sciences*, 109(Supplement 1), 10661-10668.

Herculano-Houzel, 2012b in the human nervous system, Paxinos, G., & Mai, J. K. (2012). *The human nervous system*. Elsevier.

Hermans, D., Bongaerts, T., de Bot, K., & Schreuder, R. (1998). Producing words in a foreign language: Can speakers prevent interference from their first language? *Bilingualism: Language and Cognition*, 1(3), 213-229.

Hernandez, A., Li, P., & MacWhinney, B. (2005). The emergence of competing modules in bilingualism. *Trends in cognitive sciences*, 9(5), 220-225.

Hernandez, A. E., Claussenius-Kalman, H. L., Ronderos, J., Castilla-Earls, A. P., Sun, L., Weiss, S. D., & Young, D. R. (2019). Neuroemergentism: A framework for studying cognition and the brain. *Journal of neurolinguistics*, 49, 214-223.

Hickok, G., & Poeppel, D. (2000). Towards a functional neuroanatomy of speech perception. *Trends in cognitive sciences*, 4(4), 131-138.

Hickok, G., & Poeppel, D. (2004). Dorsal and ventral streams: a framework for understanding aspects of the functional anatomy of language. *Cognition*, 92(1-2), 67-99.

Hickok, G., & Poeppel, D. (2007). The cortical organization of speech processing. *Nature reviews neuroscience*, 8(5), 393-402.

Hickok, G., & Poeppel, D. (2016). Neural basis of speech perception. *Neurobiology of language*, 299-310.

Hilgetag, C. C., & Barbas, H. (2005). Developmental mechanics of the primate cerebral cortex. *Anatomy and embryology*, 210(5-6), 411.

Hoenig, K., & Scheef, L. (2005). Mediotemporal contributions to semantic processing: fMRI evidence from ambiguity processing during semantic context verification. *Hippocampus*, 15(5), 597-609.

Hoffstaedter, F., Grefkes, C., Caspers, S., Roski, C., Palomero-Gallagher, N., Laird, A. R., ... & Eickhoff, S. B. (2014). The role of anterior midcingulate cortex in cognitive motor control: evidence from functional connectivity analyses. *Human brain mapping*, 35(6), 2741-2753.

Hogstrom, L. J., Westlye, L. T., Walhovd, K. B., & Fjell, A. M. (2013). The structure of the cerebral cortex across adult life: age-related patterns of surface area, thickness, and gyrfication. *Cerebral cortex*, 23(11), 2521-2530.

Hosoda, C., Tanaka, K., Nariai, T., Honda, M., & Hanakawa, T. (2013). Dynamic neural network reorganization associated with second language vocabulary acquisition: A multimodal imaging study. *Journal of Neuroscience*, 33(34), 13663-13672.

Hüfner, K., Binetti, C., Hamilton, D. A., Stephan, T., Flanagin, V. L., Linn, J., ... & Brandt, T. (2011). Structural and functional plasticity of the hippocampal formation in professional dancers and slackliners. *Hippocampus*, 21(8), 855-865.

Humphries, C., Love, T., Swinney, D., & Hickok, G. (2005). Response of anterior temporal cortex to syntactic and prosodic manipulations during sentence processing. *Human brain mapping*, 26(2), 128-138.

Hung, Y., Gaillard, S. L., Yarmak, P., & Arsalidou, M. (2018). Dissociations of cognitive inhibition, response inhibition, and emotional interference: Voxelwise ALE meta-analyses of fMRI studies. *Human brain mapping*, 39(10), 4065-4082.

Huster, R. J., Westerhausen, R., Kreuder, F., Schweiger, E., & Wittling, W. (2007). Morphologic asymmetry of the human anterior cingulate cortex. *Neuroimage*, 34(3), 888-895.

Huster, R. J., Wolters, C., Wollbrink, A., Schweiger, E., Wittling, W., Pantev, C., & Junghofer, M. (2009). Effects of anterior cingulate fissurization on cognitive control during stroop interference. *Human brain mapping*, 30(4), 1279-1289.

Huster, R. J., Enriquez-Geppert, S., Pantev, C., & Bruchmann, M. (2014). Variations in midcingulate morphology are related to ERP indices of cognitive control. *Brain Structure and Function*, 219(1), 49-60.

Hutchins, K. D., Martino, A. M., & Strick, P. L. (1988). Corticospinal projections from the medial wall of the hemisphere. *Experimental Brain Research*, 71(3), 667-672.

I

J

Jahn, A., Nee, D. E., Alexander, W. H., & Brown, J. W. (2016). Distinct regions within medial prefrontal cortex process pain and cognition. *Journal of Neuroscience*, 36(49), 12385-12392.

Jeurissen, B., Leemans, A., Tournier, J. D., Jones, D. K., & Sijbers, J. (2013). Investigating the prevalence of complex fiber configurations in white matter tissue with diffusion magnetic resonance imaging. *Human brain mapping*, 34(11), 2747-2766.

Jeurissen, B., Tournier, J. D., Dhollander, T., Connelly, A., & Sijbers, J. (2014). Multi-tissue constrained spherical deconvolution for improved analysis of multi-shell diffusion MRI data. *NeuroImage*, 103, 411-426.

Jha, S. C., Xia, K., Ahn, M., Girault, J. B., Li, G., Wang, L., ... & Gilmore, J. H. (2018). Environmental influences on infant cortical thickness and surface area. *Cerebral Cortex*, 29(3), 1139-1149.

Jochem, C., Baumeister, S. E., Wittfeld, K., Leitzmann, M. F., Bahls, M., Schminke, U., ... & Grabe, H. J. (2017). Domains of physical activity and brain volumes: a population-based study. *Neuroimage*, 156, 101-108.

Jockwitz, C., Caspers, S., Lux, S., Jütten, K., Schleicher, A., Eickhoff, S. B., ... & Zilles, K. (2017). Age-and function-related regional changes in cortical folding of the default mode network in older adults. *Brain Structure and Function*, 222(1), 83-99.

Jones, D. T., Machulda, M. M., Vemuri, P., McDade, E. M., Zeng, G., Senjem, M. L., ... & Jack, C. R. (2011). Age-related changes in the default mode network are more advanced in Alzheimer disease. *Neurology*, 77(16), 1524-1531.

Jones, D. K., Knösche, T. R., & Turner, R. (2013). White matter integrity, fiber count, and other fallacies: the do's and don'ts of diffusion MRI. *Neuroimage*, 73, 239-254.

K

Kaufmann, L., Koppelstaetter, F., Delazer, M., Siedentopf, C., Rhomberg, P., Golaszewski, S., ... & Ischebeck, A. (2005). Neural correlates of distance and congruity effects in a numerical Stroop task: an event-related fMRI study. *Neuroimage*, 25(3), 888-898.

Kaufmann, L., Ischebeck, A., Weiss, E., Koppelstaetter, F., Siedentopf, C., Vogel, S. E., ... & Wood, G. (2008). An fMRI study of the numerical Stroop task in individuals with and without minimal cognitive impairment. *cortex*, 44(9), 1248-1255.

Kellner, E., Dhital, B., Kiselev, V. G., & Reisert, M. (2016). Gibbs-ringing artifact removal based on local subvoxel-shifts. *Magnetic resonance in medicine*, 76(5), 1574-1581.

Kensinger, E. A., Ullman, M. T., & Corkin, S. (2001). Bilateral medial temporal lobe damage does not affect lexical or grammatical processing: Evidence from amnesic patient HM. *Hippocampus*, 11(4), 347-360.

Klein, D., Mok, K., Chen, J. K., & Watkins, K. E. (2014). Age of language learning shapes brain structure: a cortical thickness study of bilingual and monolingual individuals. *Brain and Language*, 131, 20-24.

Kochunov, P., Mangin, J. F., Coyle, T., Lancaster, J., Thompson, P., Rivière, D., ... & Zilles, K. (2005). Age-related morphology trends of cortical sulci. *Human brain mapping*, 26(3), 210-220.

Kolling, N., Behrens, T. E., Wittmann, M. K., & Rushworth, M. F. (2016). Multiple signals in anterior cingulate cortex. *Current opinion in neurobiology*, 37, 36-43.

Köpke, B., & Schmid, M. S. (2004). Language attrition. *First language attrition: Interdisciplinary perspectives on methodological issues*, 28(1).

Kousaie, S., Chai, X. J., Sander, K. M., & Klein, D. (2017). Simultaneous learning of two languages from birth positively impacts intrinsic functional connectivity and cognitive control. *Brain and cognition*, 117, 49-56.

Kremin, L. V., & Byers-Heinlein, K. (2020). Why not both? Rethinking categorical and continuous approaches to bilingualism.

Kroll, J., Bobb, S., Misra, M., & Guo, T. (2008). Language selection in bilingual speech: Evidence for inhibitory processes. *Acta Psychologica*, 128, 416-430.

Krieger-Redwood, K., Jefferies, E., Karapanagiotidis, T., Seymour, R., Nunes, A., Ang, J. W. A., ... & Smallwood, J. (2016). Down but not out in posterior cingulate cortex: Deactivation yet functional coupling with prefrontal cortex during demanding semantic cognition. *NeuroImage*, 141, 366-377.

Kriegstein, A., Noctor, S., & Martínez-Cerdeño, V. (2006). Patterns of neural stem and progenitor cell division may underlie evolutionary cortical expansion. *Nature Reviews Neuroscience*, 7(11), 883-890.

Kuhl, P. K., Stevenson, J., Corrigan, N. M., van den Bosch, J. J., Can, D. D., & Richards, T. (2016). Neuroimaging of the bilingual brain: Structural brain correlates of listening and speaking in a second language. *Brain and Language*, 162, 1-9.

Kühn, S., Gleich, T., Lorenz, R. C., Lindenberger, U., & Gallinat, J. (2014). Playing Super Mario induces structural brain plasticity: gray matter changes resulting from training with a commercial video game. *Molecular psychiatry*, 19(2), 265-271.

Kulynych, J. J., Luevano, L. F., Jones, D. W., & Weinberger, D. R. (1997). Cortical abnormality in schizophrenia: an in vivo application of the gyrification index. *Biological Psychiatry*, 41(10), 995-999.

L

Latora, V., & Marchiori, M. (2001). Efficient behavior of small-world networks. *Physical review letters*, 87(19), 198701.

Lee, H., Devlin, J. T., Shakeshaft, C., Stewart, L. H., Brennan, A., Glensman, J., ... & Price, C. J. (2007). Anatomical traces of vocabulary acquisition in the adolescent brain. *Journal of Neuroscience*, 27(5), 1184-1189.

Leech, R., & Sharp, D. J. (2013). The role of the posterior cingulate cortex in cognition and disease. *Brain*, 137(1), 12-32.

Legault, J., Grant, A., Fang, S. Y., & Li, P. (2019). A longitudinal investigation of structural brain changes during second language learning. *Brain and Language*, 197, 104661.

Le Gros Clark WE. 1945. Deformation patterns on the cerebral cortex. In *Essays on Growth and Form*, ed. WE Le Gros Clark, PB Medawar, pp. 1–22. London: Clarendon

Lehtonen, M., Soveri, A., Laine, A., Järvenpää, J., De Bruin, A., & Antfolk, J. (2018). Is bilingualism associated with enhanced executive functioning in adults? A meta-analytic review. *Psychological bulletin*, 144(4), 394.

Leischner, A. (1987). *Aphasien und Sprachentwicklungsstörungen*. Stuttgart, Germany: Thieme Verlag.

Leivada, E., Westergaard, M., Duñabeitia, J. A., & Rothman, J. (2021). On the phantom-like appearance of bilingualism effects on neurocognition:(How) should we proceed?. *Bilingualism: Language and Cognition*, 24(1), 197-210.

Lemaitre, H., Goldman, A. L., Sambataro, F., Verchinski, B. A., Meyer-Lindenberg, A., Weinberger, D. R., & Mattay, V. S. (2012). Normal age-related brain morphometric changes: nonuniformity across cortical thickness, surface area and gray matter volume?. *Neurobiology of aging*, 33(3), 617-e1.

Lent, R., Azevedo, F. A., Andrade-Moraes, C. H., & Pinto, A. V. (2012). How many neurons do you have? Some dogmas of quantitative neuroscience under revision. *European Journal of Neuroscience*, 35(1), 1-9.

- Leonard, C. M., Towler, S., Welcome, S., & Chiarello, C. (2009). Paracingulate asymmetry in anterior and midcingulate cortex: sex differences and the effect of measurement technique. *Brain Structure and Function*, 213(6), 553-569.
- Leung, H. C., Skudlarski, P., Gatenby, J. C., Peterson, B. S., & Gore, J. C. (2000). An event-related functional MRI study of the Stroop color word interference task. *Cerebral cortex*, 10(6), 552-560.
- Le Provost, J. B., Bartrés-Faz, D., Paillère-Martinot, M. L., Artiges, E., Pappata, S., Recasens, C., ... & Martinot, J. L. (2003). Paracingulate sulcus morphology in men with early-onset schizophrenia. *The British Journal of Psychiatry*, 182(3), 228-232.
- Liang, B., & Du, Y. (2018). The Functional Neuroanatomy of Lexical Tone Perception: An Activation Likelihood Estimation Meta-Analysis. *Frontiers in neuroscience*, 12.
- Li, S., Han, Y., Wang, D., Yang, H., Fan, Y., Lv, Y., ... & He, Y. (2009). Mapping surface variability of the central sulcus in musicians. *Cerebral Cortex*, 20(1), 25-33.
- Li, G., Nie, J., Wang, L., Shi, F., Lin, W., Gilmore, J. H., & Shen, D. (2013). Mapping region-specific longitudinal cortical surface expansion from birth to 2 years of age. *Cerebral Cortex*, 23(11), 2724–2733.
- Li, P., Legault, J., & Litcofsky, K. A. (2014). Neuroplasticity as a function of second language learning: anatomical changes in the human brain. *Cortex*, 58, 301-324.
- Li, G., Wang, L., Shi, F., Lyall, A. E., Lin, W., Gilmore, J. H., & Shen, D. (2014). Mapping longitudinal development of local cortical gyrification in infants from birth to 2 years of age. *Journal of Neuroscience*, 34(12), 4228–4238.
- Li, P., & Grant, A. (2016). Second language learning success revealed by brain networks. *Bilingualism: Language and cognition*, 19(4), 657-664.

Li, L., Abutalebi, J., Emmorey, K., Gong, G., Yan, X., Feng, X., ... & Ding, G. (2017). How bilingualism protects the brain from aging: Insights from bimodal bilinguals. *Human brain mapping*, 38(8), 4109-4124.

Lim, S., Radicchi, F., van den Heuvel, M. P., & Sporns, O. (2019). Discordant attributes of structural and functional brain connectivity in a two-layer multiplex network. *Scientific reports*, 9(1), 1-13.

Liu, T., Lipnicki, D. M., Zhu, W., Tao, D., Zhang, C., Cui, Y., Jin, J. S., Sachdev, P. S., Wen, W., (2012). Cortical gyrification and sulcal spans in early stage Alzheimer's disease. *PLoS One* 7, e31083.

Lopez-Persem, A., Verhagen, L., Amiez, C., Petrides, M., & Sallet, J. (2019). The human ventromedial prefrontal cortex: sulcal morphology and its influence on functional organization. *Journal of Neuroscience*, 39(19), 3627-3639.

Lövdén, M., Wenger, E., Mårtensson, J., Lindenberger, U., & Bäckman, L. (2013). Structural brain plasticity in adult learning and development. *Neuroscience & Biobehavioral Reviews*, 37(9), 2296-2310.

Luders, E., Narr, K. L., Thompson, P. M., Rex, D. E., Jancke, L., Steinmetz, H., & Toga, A. W. (2004). Gender differences in cortical complexity. *Nature neuroscience*, 7(8), 799-800.

Luders, E., Thompson, P. M., Narr, K. L., Toga, A. W., Jancke, L., & Gaser, C. (2006). A curvature-based approach to estimate local gyrification on the cortical surface. *Neuroimage*, 29(4), 1224-1230.

Luders, E., Narr, K. L., Thompson, P. M., Rex, D. E., Woods, R. P., DeLuca, H., Jancke, L., & Toga, A. W. (2006b). Gender effects on cortical thickness and the influence of scaling. *Human Brain Mapping*, 27(4), 314-324.

Luders, E., Kurth, F., Mayer, E. A., Toga, A. W., Narr, K. L., & Gaser, C. (2012). The unique brain anatomy of meditation practitioners: alterations in cortical gyrfication. *Frontiers in human neuroscience*, 6, 34.

Luk, G., Bialystok, E., Craik, F. I., & Grady, C. L. (2011). Lifelong bilingualism maintains white matter integrity in older adults. *Journal of Neuroscience*, 31(46), 16808-16813.

Luk, G., Green, D. W., Abutalebi, J., & Grady, C. (2012). Cognitive control for language switching in bilinguals: A quantitative meta-analysis of functional neuroimaging studies. *Language and cognitive processes*, 27(10), 1479-1488.

Luo, C., Guo, Z. W., Lai, Y. X., Liao, W., Liu, Q., Kendrick, K. M., ... & Li, H. (2012). Musical training induces functional plasticity in perceptual and motor networks: insights from resting-state FMRI. *PLoS one*, 7(5), e36568.

Luppino, G., Matelli, M., Camarda, R. M., Gallese, V., & Rizzolatti, G. (1991). Multiple representations of body movements in mesial area 6 and the adjacent cingulate cortex: an intracortical microstimulation study in the macaque monkey. *Journal of Comparative Neurology*, 311(4), 463-482.

M

MacLeod, C. M. (2007). The concept of inhibition in cognition. In D. S. Gorfein & C. M. (3–23)

Madan, C. R. (2021). Age-related decrements in cortical gyrfication: Evidence from an accelerated longitudinal dataset. *European Journal of Neuroscience*, 53(5), 1661-1671.

Magnotta, V. A., Andreasen, N. C., Schultz, S. K., Harris, G., Cizadlo, T., Heckel, D., ... & Flaum, M. (1999). Quantitative in vivo measurement of gyrfication in the human brain: changes associated with aging. *Cerebral Cortex*, 9(2), 151-160.

- Maguire, E. A., Gadian, D. G., Johnsrude, I. S., Good, C. D., Ashburner, J., Frackowiak, R. S., & Frith, C. D. (2000). Navigation-related structural change in the hippocampi of taxi drivers. *Proceedings of the National Academy of Sciences*, 97(8), 4398-4403.
- Maguire, E. A., Woollett, K., & Spiers, H. J. (2006). London taxi drivers and bus drivers: a structural MRI and neuropsychological analysis. *Hippocampus*, 16(12), 1091-1101.
- Mak, L. E., Minuzzi, L., MacQueen, G., Hall, G., Kennedy, S. H., & Milev, R. (2017). The default mode network in healthy individuals: a systematic review and meta-analysis. *Brain connectivity*, 7(1), 25-33.
- Mamiya, P. C., Richards, T. L., Coe, B. P., Eichler, E. E., & Kuhl, P. K. (2016). Brain white matter structure and COMT gene are linked to second-language learning in adults. *Proceedings of the National Academy of Sciences*, 113(26), 7249-7254.
- Mamiya, P. C., Richards, T. L., & Kuhl, P. K. (2018). Right forceps minor and anterior thalamic radiation predict executive function skills in young bilingual adults. *Frontiers in psychology*, 9, 118.
- Mandonnet, E., Sarubbo, S., & Petit, L. (2018). The nomenclature of human white matter association pathways: proposal for a systematic taxonomic anatomical classification. *Frontiers in neuroanatomy*, 12, 94.
- Manjón, J. V., Coupé, P., Martí-Bonmatí, L., Collins, D. L., & Robles, M. (2010). Adaptive non-local means denoising of MR images with spatially varying noise levels. *Journal of Magnetic Resonance Imaging*, 31(1), 192-203.
- Margulies, D. S., Kelly, A. C., Uddin, L. Q., Biswal, B. B., Castellanos, F. X., & Milham, M. P. (2007). Mapping the functional connectivity of anterior cingulate cortex. *Neuroimage*, 37(2), 579-588.

Marian, V., & Spivey, M. (2003). Competing activation in bilingual language processing: Within-and between-language competition. *Bilingualism: Language and Cognition*, 6(2), 97.

Marín, O., Valiente, M., Ge, X., & Tsai, L. H. (2010). Guiding neuronal cell migrations. *Cold Spring Harbor perspectives in biology*, 2(2), a001834.

Markram, H., Lübke, J., Frotscher, M., & Sakmann, B. (1997). Regulation of synaptic efficacy by coincidence of postsynaptic APs and EPSPs. *Science*, 275(5297), 213-215.

Mårtensson, J., Eriksson, J., Bodammer, N. C., Lindgren, M., Johansson, M., Nyberg, L., & Lövdén, M. (2012). Growth of language-related brain areas after foreign language learning. *NeuroImage*, 63(1), 240-244.

Matelli, M., & Umiltà, C. (2007). *Il cervello: anatomia e funzione del sistema nervoso centrale. Il mulino.*

Matsuda, Y., & Ohi, K. (2018). Cortical gyrfication in schizophrenia: current perspectives. *Neuropsychiatric Disease and Treatment*, 14, 1861.

McCutcheon, R. A., Nour, M. M., Dahoun, T., Jauhar, S., Pepper, F., Expert, P., ... & Howes, O. D. (2019). Mesolimbic dopamine function is related to salience network connectivity: an integrative positron emission tomography and magnetic resonance study. *Biological psychiatry*, 85(5), 368-378.

McPhee, G. M., Downey, L. A., & Stough, C. (2019). Effects of sustained cognitive activity on white matter microstructure and cognitive outcomes in healthy middle-aged adults: A systematic review. *Ageing research reviews*, 51, 35-47.

Mechelli, A., Crinion, J. T., Noppeney, U., O'Doherty, J., Ashburner, J., Frackowiak, R. S., & Price, C. J. (2004). Structural plasticity in the bilingual brain. *Nature*, 431(7010), 757-757.

Men, W., Falk, D., Sun, T., Chen, W., Li, J., Yin, D., ... & Fan, M. (2014). The corpus callosum of Albert Einstein's brain: another clue to his high intelligence?. *Brain*, 137(4), e268-e268.

Menon, V. (2015). Salience network. *Brain Mapping: An Encyclopedic Reference*, 2, 597-611.

Meredith, S. M., Whyler, N. C. A., Stanfield, A. C., Chakirova, G., Moorhead, T. W. J., Job, D. E., ... & Lawrie, S. M. (2012). Anterior cingulate morphology in people at genetic high-risk of schizophrenia. *European psychiatry*, 27(5), 377-385.

Mevel, K., Landeau, B., Fouquet, M., La Joie, R., Villain, N., Mézenge, F., ... & Chételat, G. (2013). Age effect on the default mode network, inner thoughts, and cognitive abilities. *Neurobiology of aging*, 34(4), 1292-1301.

Mikhael, S., Hoogendoorn, C., Valdes-Hernandez, M., & Pernet, C. (2018). A critical analysis of neuroanatomical software protocols reveals clinically relevant differences in parcellation schemes. *Neuroimage*, 170, 348-364.

Miller, J. A., Voorhies, W. I., Lurie, D. J., D'Esposito, M., & Weiner, K. S. (2021a). Overlooked tertiary sulci serve as a meso-scale link between microstructural and functional properties of human lateral prefrontal cortex. *Journal of Neuroscience*, 41(10), 2229-2244.

Miller, J. A., D'Esposito, M., & Weiner, K. S. (2021b). Using tertiary sulci to map the "cognitive globe" of prefrontal cortex. *Journal of Cognitive Neuroscience*, 1-18.

Minoshima, S., Giordani, B., Berent, S., Frey, K. A., Foster, N. L., & Kuhl, D. E. (1997). Metabolic reduction in the posterior cingulate cortex in very early Alzheimer's disease. *Annals of Neurology: Official Journal of the American Neurological Association and the Child Neurology Society*, 42(1), 85-94.

Miyake, A., & Friedman, N. P. (2012). The nature and organization of individual differences in executive functions: Four general conclusions. *Current directions in psychological science*, 21(1), 8-14.

Mohades, S. G., Struys, E., Van Schuerbeek, P., Baeken, C., Van De Craen, P., & Luypaert, R. (2014). Age of second language acquisition affects nonverbal conflict processing in children: an fMRI study. *Brain and behavior*, 4(5), 626-642.

Monaco, M., Costa, A., Caltagirone, C., & Carlesimo, G. A. (2013). Forward and backward span for verbal and visuo-spatial data: standardization and normative data from an Italian adult population. *Neurological Sciences*, 34(5), 749-754.

Morecraft, R. J., & van Hoesen, G. W. (1992). Cingulate input to the primary and supplementary motor cortices in the rhesus monkey: evidence for somatotopy in areas 24c and 23c. *Journal of Comparative Neurology*, 322(4), 471-489.

Morris, R. G. (2003). Long-term potentiation and memory. *Philosophical Transactions of the Royal Society of London. Series B: Biological Sciences*, 358(1432), 643-647.

Mountcastle, V. B. (1997). The columnar organization of the neocortex. *Brain: a journal of neurology*, 120(4), 701-722.

Munakata, Y., Herd, S. A., Chatham, C. H., Depue, B. E., Banich, M. T., & O'Reilly, R. C. (2011). A unified framework for inhibitory control. *Trends in cognitive sciences*, 15(10), 453-459.

Müller, P., Rehfeld, K., Schmicker, M., Hökelmann, A., Dordevic, M., Lessmann, V., ... & Müller, N. G. (2017). Evolution of neuroplasticity in response to physical activity in old age: the case for dancing. *Frontiers in aging neuroscience*, 9, 56.

N

Nair, V. A., Young, B. M., La, C., Reiter, P., Nadkarni, T. N., Song, J., ... & Jensen, M. B. (2015). Functional connectivity changes in the language network during stroke recovery. *Annals of clinical and translational neurology*, 2(2), 185-195.

Narvacan, K., Treit, S., Camicioli, R., Martin, W., & Beaulieu, C. (2017). Evolution of deep gray matter volume across the human lifespan. *Human Brain Mapping*, 38(8), 3771-3790.

Nelson, H. E. (1982). *National Adult Reading Test (NART): For the assessment of premorbid intelligence in patients with dementia: Test manual*. Windsor: Nfer-Nelson.

Nesvåg, R., Schaer, M., Haukvik, U. K., Westlye, L. T., Rimol, L. M., Lange, E. H., ... & Eliez, S. (2014). Reduced brain cortical folding in schizophrenia revealed in two independent samples. *Schizophrenia research*, 152(2-3), 333-338.

Nichols, E. S., & Joanisse, M. F. (2016). Functional activity and white matter microstructure reveal the independent effects of age of acquisition and proficiency on second-language learning. *NeuroImage*, 143, 15-25.

Nieto-Castañón, A. (2020). *Handbook of functional connectivity Magnetic Resonance Imaging methods in CONN*. Hilbert Press.

Norbury, A., Manohar, S., Rogers, R. D., & Husain, M. (2013). Dopamine modulates risk-taking as a function of baseline sensation-seeking trait. *Journal of Neuroscience*, 33(32), 12982-12986.

Nordahl, C. W., Dierker, D., Mostafavi, I., Schumann, C. M., Rivera, S. M., Amaral, D. G., & Van Essen, D. C. (2007). Cortical folding abnormalities in autism revealed by surface-based morphometry. *Journal of Neuroscience*, 27(43), 11725-11735.

Nowicka, A., & Tacikowski, P. (2011). Transcallosal transfer of information and functional asymmetry of the human brain. *Laterality*, 16(1), 35-74.

O

Oh, A., Duerden, E. G., & Pang, E. W. (2014). The role of the insula in speech and language processing. *Brain and language*, 135, 96-103.

Oldfield, R. C. (1971). The assessment and analysis of handedness: the Edinburgh inventory. *Neuropsychologia*, 9(1), 97-113.

Olsen, R. K., Pangelinan, M. M., Bogulski, C., Chakravarty, M. M., Luk, G., Grady, C. L., & Bialystok, E. (2015). The effect of lifelong bilingualism on regional grey and white matter volume. *Brain research*, 1612, 128-139.

Ono, M., Kubik, S., & Abarnathey, C. (1990). *Atlas of the cerebral sulci*. New York: Georg Thieme, Verlag.

Osterhout, L., Poliakov, A., Inoue, K., McLaughlin, J., Valentine, G., Pitkanen, I., ... & Hirschensohn, J. (2008). Second-language learning and changes in the brain. *Journal of neurolinguistics*, 21(6), 509-521.

Owen, A. M., Morris, R. G., Sahakian, B. J., Polkey, C. E., & Robbins, T. W. (1996). Double dissociations of memory and executive functions in working memory tasks following frontal lobe excisions, temporal lobe excisions or amygdalo-hippocampectomy in man. *Brain*, 119(5), 1597-1615.

Owen, J. P., Li, Y. O., Ziv, E., Strominger, Z., Gold, J., Bukhpun, P., ... & Mukherjee, P. (2013). The structural connectome of the human brain in agenesis of the corpus callosum. *Neuroimage*, 70, 340-355.

P

Padmanabhan, A., Lynch, C. J., Schaer, M., & Menon, V. (2017). The default mode network in autism. *Biological Psychiatry: Cognitive Neuroscience and Neuroimaging*, 2(6), 476-486.

Palaniyappan, L., Mallikarjun, P., Joseph, V., White, T. P., & Liddle, P. F. (2011). Folding of the prefrontal cortex in schizophrenia: regional differences in gyrification. *Biological psychiatry*, 69(10), 974-979.

Palaniyappan, L., & Liddle, P. F. (2012). Aberrant cortical gyrification in schizophrenia: a surface-based morphometry study. *Journal of psychiatry & neuroscience: JPN*, 37(6), 399.

Palomero-Gallagher, N., Vogt, B. A., Schleicher, A., Mayberg, H. S., & Zilles, K. (2009). Receptor architecture of human cingulate cortex: Evaluation of the four-region neurobiological model. *Human brain mapping*, 30(8), 2336-2355.

Palomero-Gallagher, N., Hoffstaedter, F., Mohlberg, H., Eickhoff, S. B., Amunts, K., & Zilles, K. (2019). Human pregenual anterior cingulate cortex: structural, functional, and connectional heterogeneity. *Cerebral Cortex*, 29(6), 2552-2574.

Parker Jones, Ö., Green, D. W., Grogan, A., Pliatsikas, C., Filippopolitis, K., Ali, N., ... & Seghier, M. L. (2012). Where, when and why brain activation differs for bilinguals and monolinguals during picture naming and reading aloud. *Cerebral Cortex*, 22(4), 892-902.

- Passingham, R. E., Stephan, K. E., & Kötter, R. (2002). The anatomical basis of functional localization in the cortex. *Nature Reviews Neuroscience*, 3(8), 606-616.
- Patenaude B, Smith SM, Kennedy DN, Jenkinson M (2011) A Bayesian model of shape and appearance for subcortical brain segmentation. *Neuroimage* 56:907–92
- Paulsen, O., & Sejnowski, T. J. (2000). Natural patterns of activity and long-term synaptic plasticity. *Current opinion in neurobiology*, 10(2), 172-180.
- Paus, T., Tomaiuolo, F., Otaky, N., MacDonald, D., Petrides, M., Atlas, J., ... & Evans, A. C. (1996a). Human cingulate and paracingulate sulci: pattern, variability, asymmetry, and probabilistic map. *Cerebral cortex*, 6(2), 207-214.
- Paus, T., Otaky, N., Caramanos, Z., Macdonald, D., Zijdenbos, A., d'Avirro, D., ... & Evans, A. C. (1996b). In vivo morphometry of the intrasulcal gray matter in the human cingulate, paracingulate, and superior-rostral sulci: Hemispheric asymmetries, gender differences and probability maps. *Journal of Comparative Neurology*, 376(4), 664-673.
- Penfield, W., & Rasmussen, T. (1950). *The cerebral cortex of man; a clinical study of localization of function*.
- Penny, W. D., Friston, K. J., Ashburner, J. T., Kiebel, S. J., & Nichols, T. E. (Eds.). (2011). *Statistical parametric mapping: the analysis of functional brain images*. Elsevier.
- Perani, D., Paulesu, E., Galles, N. S., Dupoux, E., Dehaene, S., Bettinardi, V., & Mehler, J. (1998). The bilingual brain. Proficiency and age of acquisition of the second language. *Brain: a Journal of Neurology*, 121(10), 1841–1852.
- Perani, D., Farsad, M., Ballarini, T., Lubian, F., Malpetti, M., Fracchetti, A., ... & Abutalebi, J. (2017). The impact of bilingualism on brain reserve and metabolic connectivity in Alzheimer's dementia. *Proceedings of the National Academy of Sciences*, 114(7), 1690-1695.

Pernet, C. R., Wilcox, R. R., & Rousselet, G. A. (2013). Robust correlation analyses: false positive and power validation using a new open source matlab toolbox. *Frontiers in psychology*, 3, 606.

Pernet CR, Madan CR. 2020, Data visualization for inference in tomographic brain imaging. *Eur J Neurosci* 51:695–705.

Picard, N., & Strick, P. L. (2001). Imaging the premotor areas. *Current opinion in neurobiology*, 11(6), 663-672.

Pizzagalli, F., Auzias, G., Yang, Q., Mathias, S. R., Faskowitz, J., Boyd, J. D., ... & Jahanshad, N. (2020). The reliability and heritability of cortical folds and their genetic correlations across hemispheres. *Communications biology*, 3(1), 1-12.

Pliatsikas, C., Moschopoulou, E., & Saddy, J. D. (2015). The effects of bilingualism on the white matter structure of the brain. *Proceedings of the National Academy of Sciences*, 112(5), 1334-1337.

Pliatsikas, C., DeLuca, V., Moschopoulou, E., & Saddy, J. D. (2017). Immersive bilingualism reshapes the core of the brain. *Brain Structure and Function*, 222(4), 1785-1795.

Pliatsikas, C. (2019a). Multilingualism and brain plasticity (pp. 170-196). In: Schwieter, J. W. (ed.) *The handbook of the neuroscience of multilingualism*. Wiley-Blackwell. ISBN 9781119387695

Pliatsikas, C. (2019b). Understanding structural plasticity in the bilingual brain: The Dynamic Restructuring Model. *Bilingualism: Language and Cognition*, 1-13.

Pobric, G., Jefferies, E., & Ralph, M. A. L. (2007). Anterior temporal lobes mediate semantic representation: mimicking semantic dementia by using rTMS in normal participants. *Proceedings of the National Academy of Sciences*, 104(50), 20137-20141.

Pötzl, O. (1925). Ueber die parietal bedingte Aphasie und ihren Einfluss auf das Sprechen mehrerer Sprachen. *Zeitschrift für die gesamte Neurologie und Psychiatrie*, 96(1), 100-124.

Power, J. D., Barnes, K. A., Snyder, A. Z., Schlaggar, B. L., & Petersen, S. E. (2012). Spurious but systematic correlations in functional connectivity MRI networks arise from subject motion. *Neuroimage*, 59(3), 2142-2154.

Pratte, M. S. (2021). Eriksen flanker delta plot shapes depend on the stimulus. *Attention, Perception, & Psychophysics*, 83(2), 685-699.

Preston, A. R., & Eichenbaum, H. (2013). Interplay of hippocampus and prefrontal cortex in memory. *Current Biology*, 23(17), R764–R773.

Price, C. J., Green, D. W., & Von Studnitz, R. (1999). A functional imaging study of translation and language switching. *Brain*, 122(12), 2221–2235.

Price, C. J., Green, D. W., & Von Studnitz, R. (1999). A functional imaging study of translation and language switching. *Brain*, 122(12), 2221–2235.

Q

R

Raghavan, R., Lawton, W., Ranjan, S. R., & Viswanathan, R. R. (1997). A continuum mechanics-based model for cortical growth. *Journal of Theoretical Biology*, 187(2), 285-296.

Rahimi-Balaei, M., Bergen, H., Kong, J., & Marzban, H. (2018). Neuronal migration during development of the cerebellum. *Frontiers in cellular neuroscience*, 12, 484.

Rahmani, F., Sobhani, S., & Aarabi, M. H. (2017). Sequential language learning and language immersion in bilingualism: diffusion MRI connectometry reveals microstructural evidence. *Experimental Brain Research*, 235(10), 2935-2945.

Raichle, M. E., MacLeod, A. M., Snyder, A. Z., Powers, W. J., Gusnard, D. A., & Shulman, G. L. (2001). A default mode of brain function. *Proceedings of the National Academy of Sciences*, 98(2), 676-682.

Raichle, M. E. (2015). The brain's default mode network. *Annual review of neuroscience*, 38, 433-447.

Rajagopalan, V., Scott, J., Habas, P. A., Kim, K., Corbett-Detig, J., Rousseau, F., ... & Studholme, C. (2011). Local tissue growth patterns underlying normal fetal human brain gyrification quantified in utero. *Journal of neuroscience*, 31(8), 2878-2887.

Rajapakse, J. C., Giedd, J. N., & Rapoport, J. L. (1997). Statistical approach to segmentation of single-channel cerebral MR images. *IEEE transactions on medical imaging*, 16(2), 176-186.

Rakic, P. Specification of cerebral cortical areas. *Science* 241, 170–176 (1988).

Raslau, F. D., Mark, I. T., Klein, A. P., Ulmer, J. L., Mathews, V., & Mark, L. P. (2015). Memory part 2: the role of the medial temporal lobe. *American Journal of Neuroradiology*, 36(5), 846-849.

Reillo, I., de Juan Romero, C., García-Cabezas, M. Á., & Borrell, V. (2011). A role for intermediate radial glia in the tangential expansion of the mammalian cerebral cortex. *Cerebral cortex*, 21(7), 1674-1694.

Reverberi, C., Kuhlen, A., Abutalebi, J., Greulich, R. S., Costa, A., Seyed-Allaei, S., & Haynes, J. D. (2015). Language control in bilinguals: Intention to speak vs. execution of speech. *Brain and language*, 144, 1-9.

Richards, R., Greimel, E., Kliemann, D., Koerte, I. K., Schulte-Körne, G., Reuter, M., & Wachinger, C. (2020). Increased hippocampal shape asymmetry and volumetric ventricular asymmetry in autism spectrum disorder. *NeuroImage: Clinical*, 26, 102207.

Richman, D. P., Stewart, R. M., Hutchinson, J. W., & Caviness, V. S. (1975). Mechanical model of brain convolitional development. *Science*, 189(4196), 18-21.

Ridderinkhof, R. K. (2002). Micro-and macro-adjustments of task set: activation and suppression in conflict tasks. *Psychological research*, 66(4), 312-323.

Ridderinkhof, K. R., van den Wildenberg, W. P., Wijnen, J., & Burle, B. (2004). Response inhibition in conflict tasks is revealed in delta plots. *Cognitive neuroscience of attention*, 369, 377.

Ridderinkhof, K. R., Scheres, A., Oosterlaan, J., & Sergeant, J. A. (2005). Delta plots in the study of individual differences: new tools reveal response inhibition deficits in AD/Hd that are eliminated by methylphenidate treatment. *Journal of abnormal psychology*, 114(2), 197.

Righart, R., Schmidt, P., Dahnke, R., Biberacher, V., Beer, A., Buck, D., ... & Mühlau, M. (2017). Volume versus surface-based cortical thickness measurements: A comparative study with healthy controls and multiple sclerosis patients. *PloS one*, 12(7), e0179590.

Rodriguez-Fornells, A., Kramer, U., Lorenzo-Seva, U., Festman, J., & Münte, T. F. (2012). Self-assessment of individual differences in language switching. *Frontiers in Psychology*, 2, 388.

Rogalsky C, Hickok G. Selective attention to semantic and syntactic features modulates sentence processing networks in anterior temporal cortex. *Cereb Cortex* 19: 786–796, 2009.

Ronan, L., Voets, N., Rua, C., Alexander-Bloch, A., Hough, M., Mackay, C., ... & Fletcher, P. C. (2014). Differential tangential expansion as a mechanism for cortical gyrification. *Cerebral Cortex*, 24(8), 2219-2228.

Ronan, L., & Fletcher, P. C. (2015). From genes to folds: a review of cortical gyrification theory. *Brain Structure and Function*, 220(5), 2475-2483.

Rossi, E., Cheng, H., Kroll, J. F., Diaz, M. T., & Newman, S. D. (2017). Changes in White-Matter Connectivity in Late Second Language Learners: Evidence from Diffusion Tensor Imaging. *Frontiers in psychology*, 8, 2040.

Rousselet, G. A., & Pernet, C. R. (2012). Improving standards in brain-behavior correlation analyses. *Frontiers in human neuroscience*, 6, 119.

Ruan, J., Bludau, S., Palomero-Gallagher, N., Caspers, S., Mohlberg, H., Eickhoff, S. B., ... & Amunts, K. (2018). Cytoarchitecture, probability maps, and functions of the human supplementary and pre-supplementary motor areas. *Brain Structure and Function*, 223(9), 4169-4186.

Rubinov, M., & Sporns, O. (2010). Complex network measures of brain connectivity: uses and interpretations. *Neuroimage*, 52(3), 1059-1069.

S

Sampaio-Baptista, C., & Johansen-Berg, H. (2017). White matter plasticity in the adult brain. *Neuron*, 96(6), 1239-1251.

- Sasabayashi, D., Takayanagi, Y., Takahashi, T., et al. (2019). Increased brain gyrification in the schizophrenia spectrum. *Psychiatry and clinical neurosciences*, 74, 70:76.
- Saur, D., Kreher, B. W., Schnell, S., Kümmerer, D., Kellmeyer, P., Vry, M. S., ... & Weiller, C. (2008). Ventral and dorsal pathways for language. *Proceedings of the national academy of Sciences*, 105(46), 18035-18040.
- Schlegel, A. A., Rudelson, J. J., & Tse, P. U. (2012). White matter structure changes as adults learn a second language. *Journal of cognitive neuroscience*, 24(8), 1664-1670.
- Schmid, M. S., & Jarvis, S. (2014). Lexical access and lexical diversity in first language attrition. *Bilingualism: Language and Cognition*, 17(4), 729-748.
- Schmid, M. S., & Köpke, B. (2017). The relevance of first language attrition to theories of bilingual development. *Linguistic Approaches to Bilingualism*, 7(6), 637-667.
- Scholz, J., Klein, M. C., Behrens, T. E., & Johansen-Berg, H. (2009). Training induces changes in white-matter architecture. *Nature neuroscience*, 12(11), 1370-1371.
- Schwartz, M. F., Kimberg, D. Y., Walker, G. M., Faseyitan, O., Brecher, A., Dell, G. S., & Coslett, H. B. (2009). Anterior temporal involvement in semantic word retrieval: voxel-based lesion-symptom mapping evidence from aphasia. *Brain*, 132(12), 3411-3427.
- Schweizer, T. A., Ware, J., Fischer, C. E., Craik, F. I., & Bialystok, E. (2012). Bilingualism as a contributor to cognitive reserve: Evidence from brain atrophy in Alzheimer's disease. *Cortex*, 48(8), 991-996.
- Sebastian, R., Long, C., Purcell, J. J., Faria, A. V., Lindquist, M., Jarso, S., ... & Hillis, A. E. (2016). Imaging network level language recovery after left PCA stroke.

Restorative neurology and neuroscience, 34(4), 473-489.

Seeley, W. W., Menon, V., Schatzberg, A. F., Keller, J., Glover, G. H., Kenna, H., ... & Greicius, M. D. (2007). Dissociable intrinsic connectivity networks for salience processing and executive control. *Journal of Neuroscience*, 27(9), 2349-2356.

Seiger, R., Ganger, S., Kranz, G. S., Hahn, A., & Lanzenberger, R. (2018). Cortical Thickness Estimations of FreeSurfer and the CAT12 Toolbox in Patients with Alzheimer's Disease and Healthy Controls. *Journal of Neuroimaging*.

Sexton, C. E., Walhovd, K. B., Storsve, A. B., Tamnes, C. K., Westlye, L. T., Johansen-Berg, H., & Fjell, A. M. (2014). Accelerated changes in white matter microstructure during aging: a longitudinal diffusion tensor imaging study. *Journal of Neuroscience*, 34(46), 15425-15436.

Sexton, C. E., Betts, J. F., Demnitz, N., Dawes, H., Ebmeier, K. P., & Johansen-Berg, H. (2016). A systematic review of MRI studies examining the relationship between physical fitness and activity and the white matter of the ageing brain. *Neuroimage*, 131, 81-90.

Sharp, D. J., Turkheimer, F. E., Bose, S. K., Scott, S. K., & Wise, R. J. (2010). Increased frontoparietal integration after stroke and cognitive recovery. *Annals of Neurology*, 68, 753–756.

Sheline, Y. I., Barch, D. M., Price, J. L., Rundle, M. M., Vaishnavi, S. N., Snyder, A. Z., ... & Raichle, M. E. (2009). The default mode network and self-referential processes in depression. *Proceedings of the National Academy of Sciences*, 106(6), 1942-1947.

Sheline, Y. I., Raichle, M. E., Snyder, A. Z., Morris, J. C., Head, D., Wang, S., & Mintun, M. A. (2010). Amyloid plaques disrupt resting state default mode network connectivity in cognitively normal elderly. *Biological psychiatry*, 67(6), 584-587.

Shen, X., Liu, T., Tao, D., Fan, Y., Zhang, J., Li, S., ... & Wen, W. (2018). Variation in longitudinal trajectories of cortical sulci in normal elderly. *Neuroimage*, 166, 1-9.

Shenhav, A., Straccia, M. A., Cohen, J. D., & Botvinick, M. M. (2014). Anterior cingulate engagement in a foraging context reflects choice difficulty, not foraging value. *Nature neuroscience*, 17(9), 1249-1254.

Sheth, S. A., Mian, M. K., Patel, S. R., Asaad, W. F., Williams, Z. M., Dougherty, D. D., ... & Eskandar, E. N. (2012). Human dorsal anterior cingulate cortex neurons mediate ongoing behavioural adaptation. *Nature*, 488(7410), 218-221.

Shi, F., Liu, B., Zhou, Y., Yu, C., & Jiang, T. (2009). Hippocampal volume and asymmetry in mild cognitive impairment and Alzheimer's disease: Meta-analyses of MRI studies.

Singh, A. K., Phillips, F., Merabet, L. B., & Sinha, P. (2018). Why does the cortex reorganize after sensory loss?. *Trends in cognitive sciences*, 22(7), 569-582.

Singh, N. C., Rajan, A., Malagi, A., Ramanujan, K., Canini, M., Della Rosa, P. A., ... & Abutalebi, J. (2018). Microstructural anatomical differences between bilinguals and monolinguals. *Bilingualism: Language and Cognition*, 21(5), 995-1008.

Smith, G. E. (1907). A new topographical survey of the human cerebral cortex, being an account of the distribution of the anatomically distinct cortical areas and their relationship to the cerebral sulci. *Journal of anatomy and physiology*, 41(Pt 4), 237.

Smith SM, Jenkinson M, Woolrich MW, Beckmann CF, Behrens TE, Johansen-Berg H, et al. 2004. Advances in functional and structural MR image analysis and implementation as FSL. *Neuroimage* 23:S208–S219.

Smith, R. E., Tournier, J. D., Calamante, F., & Connelly, A. (2012). Anatomically-constrained tractography: improved diffusion MRI streamlines tractography through effective use of anatomical information. *Neuroimage*, 62(3), 1924-1938.

Smith, R. E., Tournier, J. D., Calamante, F., & Connelly, A. (2015). SIFT2: Enabling dense quantitative assessment of brain white matter connectivity using streamlines tractography. *Neuroimage*, 119, 338-351.

Snodgrass, J. G., & Vanderwart, M. (1980). A standardized set of 260 pictures: norms for name agreement, image agreement, familiarity, and visual complexity. *Journal of experimental psychology: Human learning and memory*, 6(2), 174.

Soares, J., Marques, P., Alves, V., & Sousa, N. (2013). A hitchhiker's guide to diffusion tensor imaging. *Frontiers in neuroscience*, 7, 31.

Spalthoff, R., Gaser, C., & Nenadić, I. (2018). Altered gyrification in schizophrenia and its relation to other morphometric markers. *Schizophrenia research*, 202, 195-202.

Spreng, R. N., & Schacter, D. L. (2012). Default network modulation and large-scale network interactivity in healthy young and old adults. *Cerebral Cortex*, 22(11), 2610-2621.

Squire, L. R., & Zola-Morgan, S. (1991). The medial temporal lobe memory system. *Science*, 253(5026), 1380-1386.

Stein, M., Federspiel, A., Koenig, T., Wirth, M., Strik, W., Wiest, R., ... & Dierks, T. (2012). Structural plasticity in the language system related to increased second language proficiency. *Cortex*, 48(4), 458-465.

Stevens, F. L., Hurley, R. A., & Taber, K. H. (2011). Anterior cingulate cortex: unique role in cognition and emotion. *The Journal of neuropsychiatry and clinical neurosciences*, 23(2), 121-125.

Striedter, G. F., Srinivasan, S., & Monuki, E. S. (2015). Cortical folding: when, where, how, and why?. *Annual review of neuroscience*, 38, 291-307.

Stroop, J. R. (1935). Studies of interference in serial verbal reactions. *Journal of experimental psychology*, 18(6), 643.

Sulpizio, S., Toti, M., Del Maschio, N., Costa, A., Fedeli, D., Job, R., & Abutalebi, J. (2019). Are you really cursing? Neural processing of taboo words in native and foreign language. *Brain and language*, 194, 84-92.

Sulpizio, S., Del Maschio, N., Fedeli, D., & Abutalebi, J. (2020a). Bilingual language processing: A meta-analysis of functional neuroimaging studies. *Neuroscience & Biobehavioral Reviews*, 108, 834-853.

Sulpizio, S., Del Maschio, N., Del Mauro, G., Fedeli, D., & Abutalebi, J. (2020b). Bilingualism as a gradient measure modulates functional connectivity of language and control networks. *NeuroImage*, 205, 116306.

Sun, X., Li, L., Ding, G., Wang, R., & Li, P. (2019). Effects of language proficiency on cognitive control: Evidence from resting-state functional connectivity. *Neuropsychologia*, 129, 263-275.

Surrain, S., & Luk, G. (2019). Describing bilinguals: A systematic review of labels and descriptions used in the literature between 2005–2015. *Bilingualism: Language and Cognition*, 22(2), 401-415.

Symonds, L. L., Archibald, S. L., Grant, I., Zisook, S., & Jernigan, T. L. (1999). Does an increase in sulcal or ventricular fluid predict where brain tissue is lost?. *Journal of Neuroimaging*, 9(4), 201-209.

T

Tallinen, T., Chung, J. Y., Biggins, J. S., & Mahadevan, L. (2014). Gyrification from constrained cortical expansion. *Proceedings of the National Academy of Sciences*, 111(35), 12667-12672.

Tallinen, T., Chung, J. Y., Rousseau, F., Girard, N., Lefèvre, J., & Mahadevan, L. (2016). On the growth and form of cortical convolutions. *Nature Physics*, 12(6), 588-593.

Takeuchi, T., Duzskiewicz, A. J., & Morris, R. G. (2014). The synaptic plasticity and memory hypothesis: encoding, storage and persistence. *Philosophical Transactions of the Royal Society B: Biological Sciences*, 369(1633), 20130288.

Tang, R., Friston, K. J., & Tang, Y. Y. (2020). Brief mindfulness meditation induces gray matter changes in the brain hub. *Neural Plasticity*, 2020.

Taylor, R. (1990). Interpretation of the correlation coefficient: a basic review. *Journal of diagnostic medical sonography*, 6(1), 35-39.

Terribilli, D., Schaufelberger, M. S., Duran, F. L., Zanetti, M. V., Curiati, P. K., Menezes, P. R., ... & Busatto, G. F. (2011). Age-related gray matter volume changes in the brain during non-elderly adulthood. *Neurobiology of aging*, 32(2), 354-368.

Thiebaut de Schotten, M. , Bizzi, A., Dell'Acqua, F., Allin, M., Walshe, M., Murray, R., ... & Catani, M. (2011). Atlasing location, asymmetry and inter-subject variability of white matter tracts in the human brain with MR diffusion tractography. *Neuroimage*, 54(1), 49-59.

Thiebaut de Schotten, M., & Beckmann, C. F. (2021). Asymmetry of brain structure and function: 40 years after Sperry's Nobel Prize.

Tieges, Z., Snel, J., Kok, A., & Ridderinkhof, K. R. (2009). Caffeine does not modulate inhibitory control. *Brain and cognition*, 69(2), 316-327.

Tissier, C., Linzarini, A., Allaire-Duquette, G., Mevel, K., Poirel, N., Dollfus, S., ... & Cachia, A. (2018). Sulcal polymorphisms of the ifc and acc contribute to inhibitory control variability in children and adults. *Eneuro*, 5(1).

Toga, A. W. & Thompson, P. M. Mapping brain asymmetry. *Nat. Rev. Neurosci.* 4, 37–48 (2003).

Tohka, J., Zijdenbos, A., & Evans, A. (2004). Fast and robust parameter estimation for statistical partial volume models in brain MRI. *Neuroimage*, 23(1), 84-97.

Toro, R. & Burnod, Y. A morphogenetic model for the development of cortical convolutions. *Cereb. Cortex* 15, 1900–1913 (2005).

Touroutoglou, A., & Dickerson, B. C. (2019). Cingulate-centered large-scale networks: normal functions, aging, and neurodegenerative disease. *Handbook of clinical neurology*, 166, 113-127.

Tournier, J. D., Calamante, F., & Connelly, A. (2010). Improved probabilistic streamlines tractography by 2nd order integration over fibre orientation distributions. In *Proceedings of the international society for magnetic resonance in medicine (Vol. 1670)*. *Ismrm*.

Tournier, J. D., Smith, R., Raffelt, D., Tabbara, R., Dhollander, T., Pietsch, M., ... & Connelly, A. (2019). MRtrix3: A fast, flexible and open software framework for medical image processing and visualisation. *NeuroImage*, 202, 116137.

Tzourio, N., Nkanga-Ngila, B., & Mazoyer, B. (1998). Left planum temporale surface correlates with functional dominance during story listening. *Neuroreport*, 9(5), 829-833.

Tzourio-Mazoyer, N., Simon, G., Crivello, F., Jobard, G., Zago, L., Perchey, G., ... & Mazoyer, B. (2010). Effect of familial sinistrality on planum temporale surface and brain tissue asymmetries. *Cerebral Cortex*, 20(6), 1476-1485.

Tzourio-Mazoyer, N., Marie, D., Zago, L., Jobard, G., Perchey, G., Leroux, G., ... & Mazoyer, B. (2015). Heschl's gyrification pattern is related to speech-listening hemispheric lateralization: FMRI investigation in 281 healthy volunteers. *Brain Structure and Function*, 220(3), 1585-1599.

Tzourio-Mazoyer, N., Perrone-Bertolotti, M., Jobard, G., Mazoyer, B., & Baciú, M. (2017). Multi-factorial modulation of hemispheric specialization and plasticity for language in healthy and pathological conditions: A review. *Cortex*, 86, 314-339.

U

Uchiyama, H. T., Seki, A., Tanaka, D., & Koeda, T. (2013). A study of the standard brain in Japanese children: Morphological comparison with the MNI template. *Brain and Development*, 35(3), 228-235.

Unsworth, N., Spillers, G. J., & Brewer, G. A. (2009). Examining the relations among working memory capacity, attention control, and fluid intelligence from a dual-component framework. *Psychological Test and Assessment Modeling*, 51(4), 388.

Unsworth, N., & Spillers, G. J. (2010). Working memory capacity: Attention control, secondary memory, or both? A direct test of the dual-component model. *Journal of Memory and Language*, 62(4), 392-406.

Unsworth, N., McMillan, B. D., Brewer, G. A., & Spillers, G. J. (2012). Everyday attention failures: An individual differences investigation. *Journal of experimental psychology: learning, memory, and cognition*, 38(6), 1765.

Unsworth, N., Fukuda, K., Awh, E., & Vogel, E. K. (2014). Working memory and fluid intelligence: Capacity, attention control, and secondary memory retrieval. *Cognitive psychology*, 71, 1-26.

V

Van den Noort, M., Struys, E., Bosch, P., Jaswetz, L., Perriard, B., Yeo, S., ... & Lim, S. (2019). Does the bilingual advantage in cognitive control exist and if so, what are its modulating factors? A systematic review. *Behavioral Sciences*, 9(3), 27.

Van Den Wildenberg, W. P., Wylie, S. A., Forstmann, B. U., Burle, B., Hasbroucq, T., & Ridderinkhof, K. R. (2010). To head or to heed? Beyond the surface of selective action inhibition: a review. *Frontiers in human neuroscience*, 4, 222.

Van der Elst, W., Van Boxtel, M. P., Van Breukelen, G. J., & Jolles, J. (2006). The Stroop color-word test: influence of age, sex, and education; and normative data for a large sample across the adult age range. *Assessment*, 13(1), 62-79.

Vanderhasselt, M. A., De Raedt, R., & Baeken, C. (2009). Dorsolateral prefrontal cortex and Stroop performance: tackling the lateralization. *Psychonomic bulletin & review*, 16(3), 609-612.

Van Essen, D. C. (1997). A tension-based theory of morphogenesis and compact wiring in the central nervous system. *Nature*, 385(6614), 313-318.

Van Essen, D. C. (2020). A 2020 view of tension-based cortical morphogenesis. *Proceedings of the National Academy of Sciences*, 117(52), 32868-32879.

Van Hees, S., McMahon, K., Angwin, A., de Zubicaray, G., Read, S., & Copland, D. A. (2014). A functional MRI study of the relationship between naming treatment outcomes

and resting state functional connectivity in post-stroke aphasia. *Human brain mapping*, 35(8), 3919-3931.

Van Heuven, W. J., Mandera, P., Keuleers, E., & Brysbaert, M. (2014). SUBTLEX-UK: A new and improved word frequency database for British English. *Quarterly journal of experimental psychology*, 67(6), 1176-1190.

Veraart, J., Novikov, D. S., Christiaens, D., Ades-Aron, B., Sijbers, J., & Fieremans, E. (2016). Denoising of diffusion MRI using random matrix theory. *Neuroimage*, 142, 394-406.

Virtanen, P., Gommers, R., Oliphant, T. E., Haberland, M., Reddy, T., Cournapeau, D., ... & van der Walt, S. J. (2020). SciPy 1.0: fundamental algorithms for scientific computing in Python. *Nature methods*, 17(3), 261-272.

Vogt, C., & Vogt, O. (1926). Die vergleichend-architektonische und die vergleichend-reizphysiologische Felderung der Großhirnrinde unter besonderer Berücksichtigung der menschlichen. *Naturwissenschaften*, 14(50), 1190-1194.

Vogt, B. A. (1993). Structural organization of cingulate cortex: areas, neurons, and somatodendritic transmitter receptors. In *Neurobiology of cingulate cortex and limbic thalamus* (pp. 19-70). Birkhäuser, Boston, MA.

Vogt, B. A., Nimchinsky, E. A., Vogt, L. J., & Hof, P. R. (1995). Human cingulate cortex: surface features, flat maps, and cytoarchitecture. *Journal of Comparative Neurology*, 359(3), 490-506.

Vogt BA, Hof PR, Vogt LJ (2004): Cingulate gyrus. In: Paxinos G, Mai JK, editors. *The Human Nervous System*. Amsterdam. Elsevier. pp 915–949

Vogt & Palomero-Gallagher, 2012 in the human nervous system, Paxinos, G., & Mai, J. K. (2012). *The human nervous system*. Elsevier.

Volkow, N. D., Fowler, J. S., Wang, G. J., & Swanson, J. M. (2004). Dopamine in drug abuse and addiction: results from imaging studies and treatment implications. *Molecular psychiatry*, 9(6), 557-569.

von Bartheld, C. S., Bahney, J., & Herculano-Houzel, S. (2016). The search for true numbers of neurons and glial cells in the human brain: a review of 150 years of cell counting. *Journal of Comparative Neurology*, 524(18), 3865-3895.

von Bernhardi, R., Eugénin-von Bernhardi, L., & Eugénin, J. (2017). What is neural plasticity?. *The plastic brain*, 1-15.

von Bonin, G., & Bailey, P. (1961). *Pattern of the Cerebral Isocortex*. Karger Publishers.

Voorhies, W. I., Miller, J. A., Yao, J. K., Bunge, S. A., & Weiner, K. S. (2021). Cognitive insights from tertiary sulci in prefrontal cortex. *Nature Communications*, 12(1), 1-14.

W

Wang, X., Pathak, S., Stefanescu, L., Yeh, F. C., Li, S., & Fernandez-Miranda, J. C. (2016). Subcomponents and connectivity of the superior longitudinal fasciculus in the human brain. *Brain Structure and Function*, 221(4), 2075-2092.

Wachinger, C., Salat, D. H., Weiner, M., Reuter, M., & Alzheimer's Disease Neuroimaging Initiative. (2016). Whole-brain analysis reveals increased neuroanatomical asymmetries in dementia for hippocampus and amygdala. *Brain*, 139(12), 3253-3266.

Warren, J. E., Crinion, J. T., Lambon Ralph, M. A., & Wise, R. J. (2009). Anterior temporal lobe connectivity correlates with functional outcome after aphasic stroke. *Brain*, 132, 3428–3442.

Washington, S. D., Gordon, E. M., Brar, J., Warburton, S., Sawyer, A. T., Wolfe, A., ... & VanMeter, J. W. (2014). Dysmaturation of the default mode network in autism. *Human brain mapping*, 35(4), 1284-1296.

Weaver, I. C. (2014). Integrating early life experience, gene expression, brain development, and emergent phenotypes: unraveling the thread of nature via nurture. *Advances in genetics*, 86, 277-307.

Wei, X., Yin, Y., Rong, M., Zhang, J., Wang, L., Wu, Y., ... & Jiang, T. (2017). Paracingulate sulcus asymmetry in the human brain: effects of sex, handedness, and race. *Scientific reports*, 7(1), 1-8.

Weiner, K. S., Golarai, G., Caspers, J., Chuapoco, M. R., Mohlberg, H., Zilles, K., ... & Grill-Spector, K. (2014). The mid-fusiform sulcus: a landmark identifying both cytoarchitectonic and functional divisions of human ventral temporal cortex. *Neuroimage*, 84, 453-465.

Weiner, K. S., Barnett, M. A., Lorenz, S., Caspers, J., Stigliani, A., Amunts, K., ... & Grill-Spector, K. (2017). The cytoarchitecture of domain-specific regions in human high-level visual cortex. *Cerebral cortex*, 27(1), 146-161.

Weissberger, G. H., Gollan, T. H., Bondi, M. W., Clark, L. R., & Wierenga, C. E. (2015). Language and task switching in the bilingual brain: Bilinguals are staying, not switching, experts. *Neuropsychologia*, 66, 193-203.

Welker, W. (1990). Why does cerebral cortex fissure and fold?. In *Cerebral cortex* (pp. 3-136). Springer, Boston, MA.

Whitfield-Gabrieli, S., & Nieto-Castanon, A. (2012). Conn: a functional connectivity toolbox for correlated and anticorrelated brain networks. *Brain connectivity*, 2(3), 125-141.

White, T., Su, S., Schmidt, M., Kao, C.-Y., Sapiro, G., (2010). The development of gyrification in childhood and adolescence. *Brain & Cognition* 72, 36–45.

Whittle, S., Allen, N. B., Fornito, A., Lubman, D. I., Simmons, J. G., Pantelis, C., & Yücel, M. (2009). Variations in cortical folding patterns are related to individual differences in temperament. *Psychiatry Research: Neuroimaging*, 172(1), 68-74.

Wilcox, R. R. (1994). The percentage bend correlation coefficient. *Psychometrika*, 59(4), 601-616.

Wilcox, R. (2004). Inferences based on a skipped correlation coefficient. *Journal of Applied Statistics*, 31(2), 131-143.

Windes, J. D. (1968). Reaction time for numerical coding and naming of numerals. *Journal of Experimental Psychology*, 78(2p1), 318.

Wise, R. A., & Robble, M. A. (2020). Dopamine and addiction. *Annual review of psychology*, 71, 79-106.

Woolard, A. A., & Heckers, S. (2012). Anatomical and functional correlates of human hippocampal volume asymmetry. *Psychiatry Research: Neuroimaging*, 201(1), 48-53.

Worringer, B., Langner, R., Koch, I., Eickhoff, S. B., Eickhoff, C. R., & Binkofski, F. C. (2019). Common and distinct neural correlates of dual-tasking and task-switching: a meta-analytic review and a neurocognitive processing model of human multitasking. *Brain Structure and Function*, 224(5), 1845-1869.

X

Xu, G., Bayly, P. V., & Taber, L. A. (2009). Residual stress in the adult mouse brain. *Biomechanics and modeling in mechanobiology*, 8(4), 253-262.

Xu, G., Knutsen, A. K., Dikranian, K., Kroenke, C. D., Bayly, P. V., & Taber, L. A. (2010). Axons pull on the brain, but tension does not drive cortical folding.

Y

Yan, H., Zuo, X. N., Wang, D., Wang, J., Zhu, C., Milham, M. P., ... & Zang, Y. (2009). Hemispheric asymmetry in cognitive division of anterior cingulate cortex: a resting-state functional connectivity study. *Neuroimage*, 47(4), 1579-1589.

Yang, Y., & Calakos, N. (2013). Presynaptic long-term plasticity. *Frontiers in synaptic neuroscience*, 5, 8.

Yang, M., Li, J., Li, Z., Yao, D., Liao, W., & Chen, H. (2017). Whole-brain functional connectome-based multivariate classification of post-stroke aphasia. *Neurocomputing*, 269, 199-205.

Yang, J., Wang, D., Rollins, C., Leming, M., Liò, P., Suckling, J., ... & Cachia, A. (2019). Volumetric segmentation and characterisation of the paracingulate sulcus on MRI scans. *bioRxiv*, 859496.

Yeo, B. T., Sabuncu, M. R., Vercauteren, T., Holt, D. J., Amunts, K., Zilles, K., ... & Fischl, B. (2010). Learning task-optimal registration cost functions for localizing cytoarchitecture and function in the cerebral cortex. *IEEE transactions on medical imaging*, 29(7), 1424-1441.

Yotter, R. A., Dahnke, R., Thompson, P. M., & Gaser, C. (2011a). Topological correction of brain surface meshes using spherical harmonics. *Human brain mapping*, 32(7), 1109-1124.

Yotter, R. A., Nenadic, I., Ziegler, G., Thompson, P. M., & Gaser, C. (2011b). Local cortical surface complexity maps from spherical harmonic reconstructions. *NeuroImage*, 56(3), 961-973.

Yu, E., Liao, Z., Mao, D., Zhang, Q., Ji, G., Li, Y., & Ding, Z. (2017). Directed functional connectivity of posterior cingulate cortex and whole brain in Alzheimer's disease and mild cognitive impairment. *Current Alzheimer Research*, 14(6), 628-635.

Yücel, M., Stuart, G. W., Maruff, P., Velakoulis, D., Crowe, S. F., Savage, G., & Pantelis, C. (2001). Hemispheric and gender-related differences in the gross morphology of the anterior cingulate/paracingulate cortex in normal volunteers: an MRI morphometric study. *Cerebral cortex*, 11(1), 17-25.

Yücel, M., Stuart, G. W., Maruff, P., Wood, S. J., Savage, G. R., Smith, D. J., ... & Pantelis, C. (2002). Paracingulate morphologic differences in males with established schizophrenia: a magnetic resonance imaging morphometric study. *Biological psychiatry*, 52(1), 15-23.

Yuste, R., & Bonhoeffer, T. (2001). Morphological changes in dendritic spines associated with long-term synaptic plasticity. *Annual review of neuroscience*, 24(1), 1071-1089.

Z

Zalesky, A., Fornito, A., & Bullmore, E. T. (2010). Network-based statistic: identifying differences in brain networks. *Neuroimage*, 53(4), 1197-1207.

Zatorre, R. J., Fields, R. D., & Johansen-Berg, H. (2012). Plasticity in gray and white: neuroimaging changes in brain structure during learning. *Nature neuroscience*, 15(4), 528-536.

Zhang, L., Sun, J., Sun, B., Luo, Q., & Gong, H. (2014). Studying hemispheric lateralization during a Stroop task through near-infrared spectroscopy-based connectivity. *Journal of biomedical optics*, 19(5), 057012.

Zhang, R., Geng, X., & Lee, T. M. (2017). Large-scale functional neural network correlates of response inhibition: an fMRI meta-analysis. *Brain Structure and Function*, 222(9), 3973-3990.

Zhang, J., Andreano, J. M., Dickerson, B. C., Touroutoglou, A., & Barrett, L. F. (2019). Stronger Functional Connectivity in the Default Mode and Salience Networks Is Associated with Youthful Memory in Superaging. *Cerebral Cortex*.

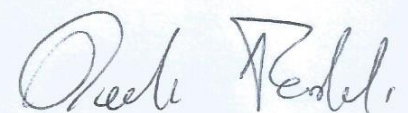
Zhao, X. H., Wang, P. J., Li, C. B., Hu, Z. H., Xi, Q., Wu, W. Y., & Tang, X. W. (2007). Altered default mode network activity in patient with anxiety disorders: an fMRI study. *European journal of radiology*, 63(3), 373-378.

Zilles, K., Schleicher, A., Langemann, C., Amunts, K., Morosan, P., Palomero-Gallagher, N., ... & Roland, P. E. (1997). Quantitative analysis of sulci in the human cerebral cortex: development, regional heterogeneity, gender difference, asymmetry, intersubject variability and cortical architecture. *Human brain mapping*, 5(4), 218-221.

Zilles, K., & Amunts, K. (2012) Architecture of the Cerebral Cortex. In: *The human nervous system*, Paxinos, G., & Mai, J. K. (2012). The human nervous system. Elsevier.

Zilles, K., Palomero-Gallagher, N., & Amunts, K. (2013). Development of cortical folding during evolution and ontogeny. *Trends in neurosciences*, 36(5), 275-284.

Zimmerman, M. E., Brickman, A. M., Paul, R. H., Grieve, S. M., Tate, D. F., Gunstad, J., ... & Gordon, E. (2006). The relationship between frontal gray matter volume and cognition varies across the healthy adult lifespan. *The American journal of geriatric psychiatry*, 14(10), 823-833.



Chapter 7 – APPENDICES

Appendix; Table S1. List of diffusion-based MRI studies investigating white matter changes as a consequence of bilingual experience and second language learning

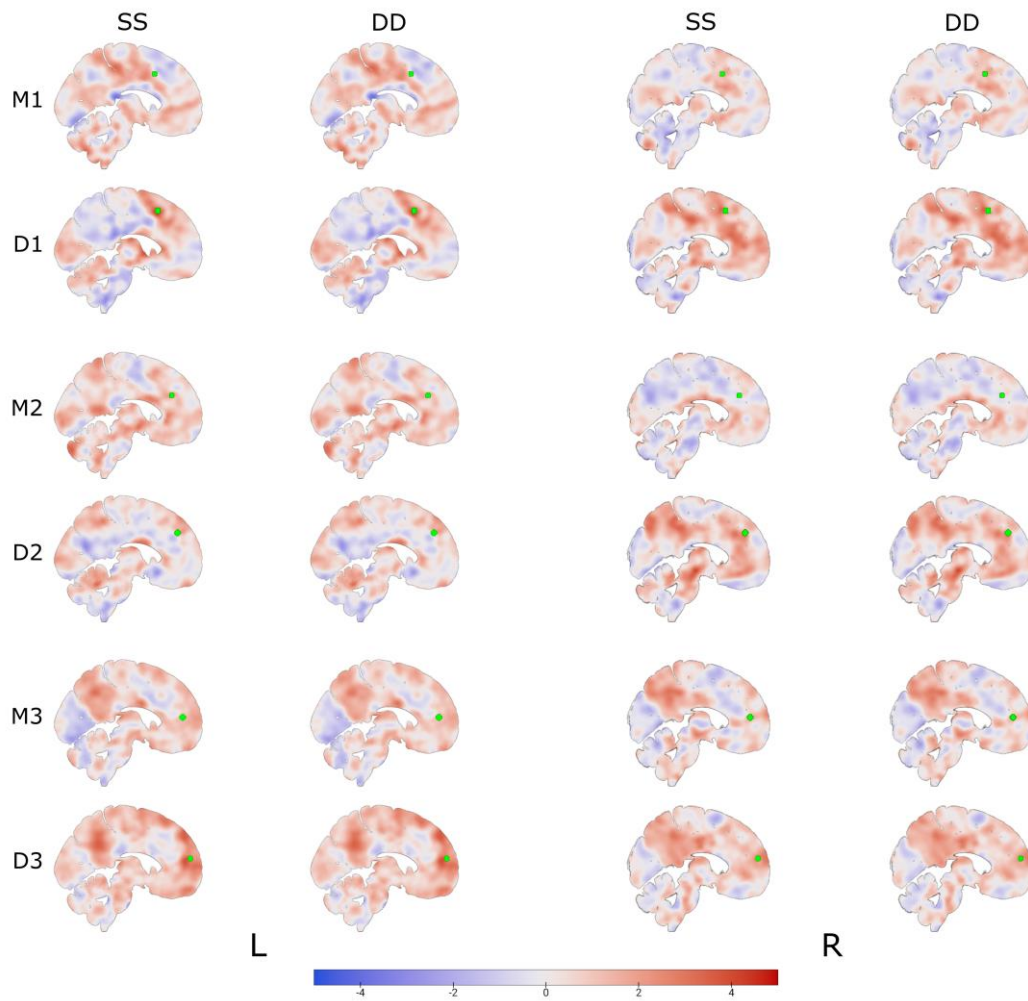
AD = axial diffusivity
MD = mean diffusivity
SLF = superior longitudinal fasciculus
IFOF = Inferior Frontal Occipital fasciculus
CR = corona radiata
EC = external capsule
CC = corpus callosum
AF = arcuate fasciculus
RTs = reaction times
TR = thalamic radiations
CB = cingulum bundle
ILF = inferior longitudinal fasciculus
Fm = forceps minor
RD = radial diffusivity
Bi = bilinguals
Mono = monolinguals
Sim = simultaneous bilinguals
Seq = sequential bilinguals
FM = forceps major
UF = uncinata fasciculus
CST = cortico-spinal tract
IC = internal capsule

1st Author	DOI	Year	Participants	Men age	L1	L2	L2_AoA	Modelling	Directions	b vals/(mm^2)	Method	Results
Anderson	https://doi.org/10.1016/j.neuroimage.2017.11.038	2018	31; 23	74; 74.09	English; English	not reported	3.03; 2.41	DTI	64	not reported	TBSS	Bi > Mono: higher AD in left SLF, IFOF, bilateral CR, right EC, and CC Bi > Mono: stronger correlation between RTs in a reading task and MD in right AF and bilateral SLF
Bakhtiari	https://doi.org/10.3389/fnhum.2014.00507	2014	1; 12	28.5; 24.25	English; Chinese	English	> 5	DTI	12	1000	Tractography	Mono > Bi: higher FA in right IFOF and bilateral TR; higher MD in left IFOF and Fm. Bi > Mono: higher MD in bilateral CB, right TR, and ILF L2 exposure is associated with higher FA in CC, left CB, bilateral CR and SLF
Cummine	https://doi.org/10.1007/s41809-019-00039-z	2019	50	25.78	Italian ; Italian	English	8.4	DTI	30	1000	TBSS	L2 AoA is associated with higher FA in CC
Del Maschio	https://doi.org/10.1073/pnas.1811513116	2019	65	31.7	English; Various	English	8.51	DTI	64	1000	TBSS	Linguistic immersion is associated with increase MD in left Fm
DeLuca	https://doi.org/10.1017/S1366728918000883	2019	26	35.33	English; Various	English	10.5	DTI	not reported	not reported	TBSS	Mono > Bi: higher FA in CC, bilateral Fm, left CB, CST, and insula, right fronto-parietal and subcortical regions. Lower FA values in Bi are associated with lower Ad and higher RD
Eitner	https://doi.org/10.1092/hbm.21169	2011	12;12	37.928.4	not reported	not reported	not reported	DTI	15	1000	TBSS	Bi > Mono: stronger structural connectivity in two subnetworks, greater graph-efficiency
García-Pentón	https://doi.org/10.1016/j.neuroimage.2013.08.064	2014	13; 13	29.7; 24.08	Spanish; Spanish	Basque	0.46	DTI	64	1500	NBS	Bi > Mono: higher FA in right SLF
Gao	https://doi.org/10.1002/hbm.24936	2020	30; 28	25.33; 26.32	Mandarin; Mandarin	Bai	0	DTI	32	1000	TBSS	Mono > Bi: higher FA in bilateral IFOF and ILF, Fornix and CC, and lower RD in overlapping regions
Gold	https://doi.org/10.1016/j.cortex.2013.09.037	2013	60; 23	64.4; 63.9	English; English	Various	not reported	DTI	36	1000	TBSS; VBM	Sim > Seq: higher FA in left AF; Seq > Sim: lower MD in bilateral IFOF
Hämäläinen	https://doi.org/10.1016/j.neuroimage.2017.02.081	2017	15; 15	26.86; 29.21	Finnish; Finnish	Swedish; English	2.72; 8.92	DTI	64	1000	TBSS; Tractography	L2 vocabulary size is associated with higher FA in right SLF, AF and ILF. L2 Learners > Controls: higher FA in right SLF, correlated with proficiency; greater right dorsal pathway and fronto-caudate connectivity
Hosoda	https://doi.org/10.1523/JNEUROSCI.0410-13.2013	2013	137; 24; 20	21.820; 120.5	Japanese	English	11.0	DTI	not reported	700	TBSS; Tractography	Bi > Mono: higher FA and lower MD and RD in bilateral TR, Fm, FM, CB, CST, IFOF, SLF, UF, CC and cerebellum; proportional to L2 immersion
Kuhl	https://doi.org/10.1016/j.bandl.2016.07.004	2017	16; 15	29.625.5	Spanish; English	English	not reported	DTI	32	1000	TBSS	L2 AoA is negatively associated with FA in CC
Luk	https://doi.org/10.1523/JNEUROSCI.4563-11.2011	2011	14; 14	70.6; 70.3	English; English	not reported	< 11	DTI	30	900	TBSS	Bi > Mono: higher MD in the fornix; higher FA, lower MD, AD and RD in CB and lower RD in right UF
Luk	https://doi.org/10.1016/j.jneuroling.2020.100937	2020	31	25.16	English; Various	Various; English	7.55	DTI	67	1000	TBSS	L2 learners > Controls: higher FA and lower RD in right SLF; FA is correlated with days of immersion program; FA predicts class grade; FA declined after immersion program
Marin-Marin	https://doi.org/10.1111/ene.14135	2020	53; 35	72.83; 73.51	Spanish; Catalan	Spanish	not reported	DTI	20	1000	TBSS	Sim > Seq: higher FA in left IFOF; Mono > Sim: higher FA in CC. Intermediate values for Seq
Mamiya	https://doi.org/10.1073/pnas.1606602113	2016	44; 35	20.02	Chinese	English	> 6	DTI	64	1500	TBSS	Sim > Seq: higher FA in left IFOF; Mono > Sim: higher FA in CC. Intermediate values for Seq
Mohades	https://doi.org/10.1016/j.brainres.2011.12.005	2012	15; 15; 10	9.33; 9.68; 9.58	French or Dutch	Germanic or Romance	> 3; 0	DTI	15	700	Tractography	L2 AoA is associated with higher FA in CC, left AF and bilateral ILF; L2 Proficiency is associated with higher FA in right ILF, AF and Fm
Mohades	https://doi.org/10.1371/journal.pone.0117968	2015	14; 16; 10	11.42; 11.33; 11.08	French or Dutch	Germanic or Romance	> 3; 0	DTI	15	700	Tractography	Bi > Mono: higher FA in CC and bilateral IFOF; UF, and SLF. No effect of L2 linguistic immersion
Nichols	https://doi.org/10.1016/j.neuroimage.2016.08.053	2016	22	22.18	Mandarin	English	13.82	DTI	64	1000	TBSS; Tractography	Bi > Mono: increased connectivity CC, bilateral CB, AF, and left IFOF. Nonsignificant trend in correlation between FA and L2 immersion
Pfaukas	https://doi.org/10.1073/pnas.1414183112	2015	20; 25	31.85; 28.16	Various; English	English	10.15	DTI	30	1000	TBSS	Bi > Mono: higher FA in CC, left hemispheric language areas, right temporal lobe; lower RD in bilateral frontal regions; FA increases over training time and correlates with grade
Rahmani	https://doi.org/10.1007/s00221-017-5029-x	2017	20; 25	31.85; 28.16	Various; English	English	10.15	QSDR	30	1000	Tractography	Mono > Bi: higher FA in right TR, IFOF and ILF. Bi > Mono: higher MD in Fm, right IFOF, left ILF, bilateral SLF; higher RD in Fm; right SLF, TR and ILF; greater AD in Fm, CT, right TR and SLF.
Rossi	https://doi.org/10.3389/fpsyg.2017.02040	2017	24; 25	not reported	English; English	Spanish	12	DTI	20	1000	TBSS	L2 learners > Controls: higher FA in CC, left hemispheric language areas, right temporal lobe; lower RD in bilateral frontal regions; FA increases over training time and correlates with grade
Schegel	https://doi.org/10.1162/jocn_a_00240	2012	15; 12	20.05; 20.05	English; English	Mandarin	20.5	DTI	32	1000	Tractography	Bi > Mono: higher FA in right TR, IFOF and ILF. Bi > Mono: higher MD in Fm, right IFOF, left ILF, bilateral SLF; higher RD in Fm; right SLF, TR and ILF; greater AD in Fm, CT, right TR and SLF.
Singh	https://doi.org/10.1017/S1366728917000438	2017	18; 18	23.94; 23.72	Hindi; Italian	English	5	DTI	35	1000	TBSS	

Experiment 1

Cross-seed analyses

Appendix; Experiment 1; Figure S1 shows unthresholded rsFC maps of middle and dorsal seeds of the DD and SS groups. Directional contrasts were performed by selection M seeds for participants with double PCS absence and D seeds for participants with double PCS presence (threshold: $p < 0.001$ unc. vox. level; $p < 0.0042$ FWE clust. level) (see Appendix-Experiment 1; Table S1). rsFC results showed large similarities and overlap between groups, while cross-seed showed largely significant differences.



Appendix; Experiment 1; Figure S 1. Middle and dorsal seed connectivity in double absence and double presence patterns. Unthresholded T-maps are displayed, and color map indicates raw t-values. Seeds are shown in green at $z = \pm 5$. Middle seeds are labeled as M1, M2, M3; dorsal seeds are labeled as D1, D2, D3.

Contrast	MINI coordinates (x,y,z)			Harvard-Oxford Atlas region	k	Z score	Cluster-level p- FWE	Voxel-level p- FWE
SS (M1L) > DD (D1L)	-6	14	42	Paracingulate Gyrus	28100	Inf	<0.001	<0.001
	54	4	12	Precentral Gyrus	6842	5.9	<0.001	<0.001
	36	46	38	Frontal Pole	717	5.55	<0.001	0.001
	-54	-68	6	Lateral Occipital Cortex, inferior division	633	4.92	<0.001	0.006
DD (D1L) > SS (M1L)	-6	18	52	Superior Frontal Gyrus	15585	Inf	<0.001	<0.001
	-52	-58	38	Angular Gyrus	3306	6.97	<0.001	<0.001
	-62	-34	-12	Middle Temporal Gyrus	3204	6.74	<0.001	<0.001
	56	-58	38	Angular Gyrus,	1890	6.18	<0.001	<0.001
	42	-66	-46	Cerebellum	3458	5.98	<0.001	<0.001
	-14	-40	34	Cingulate Gyrus, posterior division	1517	5.62	<0.001	0.001
	50	36	-14	Frontal Pole	1403	5.49	<0.001	0.002
	60	-38	-18	Inferior Temporal Gyrus, posterior division	2432	5.4	<0.001	0.003
SS (M1R) > DD (D1R)	6	14	40	Paracingulate Gyrus	11825	Inf	<0.001	<0.001
	-14	-56	-10	Lingual Gyrus	12656	5.76	<0.001	<0.001
	-32	0	-22	Parahippocampal Gyrus, anterior division	3704	5.41	<0.001	0.003
	-26	-52	-52	Cerebellum	456	4.89	<0.001	0.029
	-34	-20	38	Postcentral Gyrus	513	4.65	<0.001	0.08
DD (D1R) > SS (M1R)	6	18	52	Superior Frontal Gyrus	9855	Inf	<0.001	<0.001
	50	-44	50	Supramarginal Gyrus, posterior division	2899	7.21	<0.001	<0.001
	-12	-74	-30	Cerebellum	4655	6.27	<0.001	<0.001
	60	-38	-20	Inferior Temporal Gyrus, posterior division	1559	5.98	<0.001	<0.001
	-48	10	50	Middle Frontal Gyrus	3387	5.09	<0.001	0.012
	-44	-48	50	Supramarginal Gyrus, posterior division	812	4.92	<0.001	0.025
	-56	-38	-24	Inferior Temporal Gyrus, posterior division	611	4.3	<0.001	0.28
SS (M2L) > DD (D2L)	-4	34	28	Paracingulate Gyrus	10896	Inf	<0.001	<0.001
	44	-54	-34	Cerebellum	346	5.74	0.003	0.001
	-36	-52	-32	Cerebellum	1328	5.55	<0.001	0.001
	-14	6	64	Superior Frontal Gyrus	343	5.24	0.004	0.006
	8	-28	26	Cingulate Gyrus, posterior division	527	5.11	<0.001	0.012
	6	-36	-48	Brain-Stem	405	4.96	0.001	0.023
	-12	-66	50	Lateral Occipital Cortex, superior division	373	4.74	0.002	0.059
	16	-66	42	Precuneous Cortex	687	4.68	<0.001	0.074
	0	-18	-16	Brain-Stem	1151	4.6	<0.001	0.102
	DD (D2L) > SS (M2L)	-6	42	36	Superior Frontal Gyrus	2666	Inf	<0.001
-60		-32	-8	Middle Temporal Gyrus, posterior division	10232	Inf	<0.001	<0.001
64		-32	-2	iddle Temporal Gyrus, posterior division	4487	6.27	<0.001	<0.001
6		50	-22	Frontal Medial Cortex	2138	6.21	<0.001	<0.001
-38		14	50	Middle Frontal Gyrus	912	6.09	<0.001	<0.001
-8		-48	30	Cingulate Gyrus, posterior division	503	4.92	<0.001	0.027
62		-58	28	Angular Gyrus	894	4.78	<0.001	0.05

	20	-76	-30	Cerebellum		420	4.76	0.001	0.053
SS (M2R) > DD (D2R)									
	6	34	28	Paracingulate Gyrus		3261	Inf	<0.001	<0.001
	38	14	-8	Insular Cortex		477	5.45	<0.001	0.004
	-40	46	28	Frontal Pole		975	5.03	<0.001	0.02
	-32	-54	-36	Cerebellum		1004	4.7	<0.001	0.064
	-2	-22	28	Cingulate Gyrus, posterior division		433	4.34	0.001	0.152
	0	-84	-22	Cerebellum		541	4.13	<0.001	0.186
DD (D2R) > SS (M2R)									
	6	42	36	Superior Frontal Gyrus		1926	Inf	<0.001	<0.001
	-2	58	-22	Frontal Pole		1473	5.88	<0.001	0.001
	56	16	-20	Temporal Pole		4215	5.73	<0.001	0.002
	-54	-28	-4	Middle Temporal Gyrus		7082	5.69	<0.001	0.002
	8	-36	68	Postcentral Gyrus		1353	4.35	<0.001	0.085
	44	-60	18	Middle Temporal temporooccipital part	Gyrus,	708	4.31	<0.001	0.085
	66	-12	36	Postcentral Gyrus		353	3.9	0.003	0.256
SS (M3L) > DD (D3L)									
	-6	46	10	Paracingulate Gyrus		2422	Inf	<0.001	<0.001
	-48	-68	-44	Cerebellum		764	5.98	<0.001	<0.001
	-10	-58	40	Precuneous Cortex		1475	4.12	<0.001	0.478
DD (D3L) > SS (M3L)									
	-6	56	16			267	Inf	<0.001	<0.001
	-64	-20	28	Postcentral Gyrus		1209	5.32	<0.001	0.004
	34	-8	-14	Putamen		2021	5.24	<0.001	0.006
	64	-18	28	Postcentral Gyrus		1257	4.83	<0.001	0.039
	44	34	4	Inferior Frontal Gyrus		338	4.54	0.004	0.126
	-18	-48	66	Superior Parietal Lobule		507	4.44	<0.001	0.183
	-52	6	4	Precentral Gyrus		759	4.29	<0.001	0.296
	-4	0	58	Juxtapositional Lobule Cortex		670	4.25	<0.001	0.342
SS (M3R) > DD (D3R)									
	6	46	12	Paracingulate Gyrus		700	Inf	<0.001	<0.001
	-44	-64	-44	ateral Occipital Cortex, inferior division		806	5.36	<0.001	0.003
	36	56	0	Frontal Pole		481	4.45	0.001	0.17
	-2	-42	46	Precuneous Cortex		495	4.17	<0.001	0.415
	28	32	54	Superior Frontal Gyrus		471	3.94	0.001	0.691
	64	-34	-28	Inferior Temporal temporooccipital part	Gyrus,	353	3.94	0.004	0.696
DD (D3R) > SS (M3R)									
	6	56	16	Superior Frontal Gyrus		207	Inf	0.004	<0.001
	-28	2	-26	Temporal Pole		209	4.51	0.004	0.137

Appendix; Experiment 1; Table S 1. DD > SS and SS > DD cross-seed contrasts. DD = double Presence; SS = Double Absence.

Experiment 2

ANT										
Contrast	Hemisphere	Region (Harvard-Oxford)	cluster p(FWE-corr)	k (mm ³)	T value	Z score	peak p(unc)	x	y	z
Congruent > Neutral	R	Occipital Fusiform Gyrus	<0.001	5077	14.11	65535.00	<0.001	20	-82	-12
	L	Temporal Pole	<0.001	375	5.30	4.60	<0.001	-42	16	-18
	R	Superior Frontal Gyrus	<0.001	409	4.82	4.26	<0.001	22	0	56
	L	Superior Frontal Gyrus	0.05	200	4.14	3.76	<0.001	-24	-6	48
Incongruent > Neutral (Peak FWE p<0.05 corrected)	L	Occipital Pole	<0.001	2164	15.03	65535.00	<0.001	-16	-92	-10
	R	Occipital Pole	<0.001	3779	13.41	65535.00	<0.001	20	-90	-6
	L	Lateral Occipital Cortex	<0.001	948	7.95	6.15	<0.001	-30	-58	62
	L	Precentral Gyrus	<0.001	550	7.44	5.88	<0.001	-24	-10	46
	R	Middle Frontal Gyrus	<0.001	478	7.41	5.87	<0.001	32	-2	50
	R	Frontal Orbital Cortex	<0.001	248	7.03	5.66	<0.001	36	22	-20
	R	Cerebellum	<0.001	135	6.69	5.47	<0.001	4	-70	-34
	R	Paracingulate Gyrus	<0.001	175	6.43	5.32	<0.001	4	8	50
	L	Cerebellum	<0.001	17	6.19	5.17	<0.001	0	-58	-30
	L	Precentral Gyrus	<0.001	68	6.15	5.15	<0.001	-48	4	34
	L	Frontal Orbital Cortex	0.001	38	5.78	4.92	<0.001	-36	24	-2
	R	Lingual Gyrus	0.009	11	5.74	4.89	<0.001	2	-82	-4
	R	Cerebellum	0.011	9	5.64	4.82	<0.001	6	-72	-22
	R	Paracingulate Gyrus	0.035	1	5.43	4.69	<0.001	8	30	32
	R	Precentral Gyrus	0.029	2	5.42	4.68	<0.001	48	6	32
Incongruent > Congruent	R	Inferior Temporal Gyrus	<0.001	4882	9.75	6.98	<0.001	44	-60	-10
	L	Lateral Occipital Cortex	<0.001	4178	8.08	6.21	<0.001	-38	-86	8
	L	Precentral Gyrus	<0.001	675	5.75	4.90	<0.001	-34	-4	52
	R	Middle Frontal Gyrus	<0.001	967	4.99	4.38	<0.001	30	-4	60

Alerting Effect	--	--	--	--	--	--	--	--	--	--
Orienting Effect	--	--	--	--	--	--	--	--	--	--

Appendix; Experiment 2; Table S 1. t-contrast results for the effects detected in the ANT task (volume-based analysis). Significance threshold is set at voxel p -uncorrected < 0.001 and cluster- p -FWE-corrected < 0.05 . Only one local maximum per significant cluster is listed. R = Right hemisphere. L = Left hemisphere. The Incongruent $>$ Neutral contrast is reported at voxel p -FWE corrected < 0.05 threshold, since the voxel p -uncorrected < 0.001 threshold lead to large but uninterpretable clusters of functional activity.

Stroop										
Contrast	Hemisphere	Region (Harvard-Oxford)	cluster p(FWE-corr)	k (mm ³)	T value	Z score	peak p(un-c)	x	y	z
Congruent > Neutral	L	Caudate	0.03	223	5.26	4.57	<0.001	-4	4	20
Incongruent > Neutral	L	Supramarginal Gyrus	<0.001	1940	5.81	4.94	<0.001	-58	-52	28
	L	Middle Frontal Gyrus	<0.001	1515	5.37	4.65	<0.001	-42	10	34
	L	Paracingulate Gyrus	<0.001	721	4.86	4.29	<0.001	-6	44	24
	R	Frontal Operculum Cortex	0.002	434	4.85	4.29	<0.001	46	20	-2
	R	Angular Gyrus	0.010	282	4.83	4.27	<0.001	60	-50	32
	L	Superior Frontal Gyrus	0.017	235	4.10	3.73	<0.001	-4	22	54
Incongruent > Congruent (Peak FWE corrected) p<0.05	L	Postcentral Gyrus	<0.001	3389	10.34	7.21	<0.001	-42	-26	56
	R	Occipital Pole	<0.001	366	8.78	6.55	<0.001	24	-94	-10
	L	Supplementary Motor Cortex	<0.001	520	7.63	5.98	<0.001	-6	-4	50
	R	Cerebellum	<0.001	490	7.56	5.95	<0.001	26	-50	-28
	R	Precentral Gyrus	<0.001	342	7.35	5.84	<0.001	26	-12	56
	L	Lateral Occipital Cortex	<0.001	539	7.10	5.70	<0.001	-34	-84	-12
	R	Cingulate Gyrus	<0.001	145	6.86	5.57	<0.001	8	30	20
	L	Frontal Orbital Cortex	<0.001	55	6.69	5.47	<0.001	-30	22	-16
	L	Caudate	<0.001	170	6.64	5.44	<0.001	-12	8	6
	R	Thalamus	<0.001	106	6.50	5.36	<0.001	12	-20	8
	R	Lateral Occipital Cortex	<0.001	48	6.23	5.20	<0.001	26	-66	32
	R	Insular Cortex	<0.001	73	6.16	5.15	<0.001	36	18	-2
	R	Precentral Gyrus	0.005	15	6.12	5.13	<0.001	56	6	32
	R	Temporal Occipital Fusiform Cortex	0.003	23	5.96	5.03	<0.001	26	-58	-12
	L	Temporal Occipital Fusiform Cortex	0.007	13	5.91	5.00	<0.001	-32	-44	-24
	R	Cingulate Gyrus	0.023	3	5.83	4.95	<0.001	6	-24	36
	L	Brainstem	0.004	19	5.78	4.91	<0.001	-8	-24	-6
	L	Insular Cortex	0.002	28	5.70	4.86	<0.001	-34	6	-4
	R	Frontal Orbital Cortex	0.013	7	5.69	4.86	<0.001	30	20	-16
	R	Supramarginal Gyrus	<0.001	65	5.68	4.85	<0.001	46	-28	40
	R	Lateral Occipital Cortex	0.013	7	5.62	4.81	<0.001	36	-84	8
	R	Cingulate Gyrus	0.017	5	5.54	4.76	<0.001	10	16	30

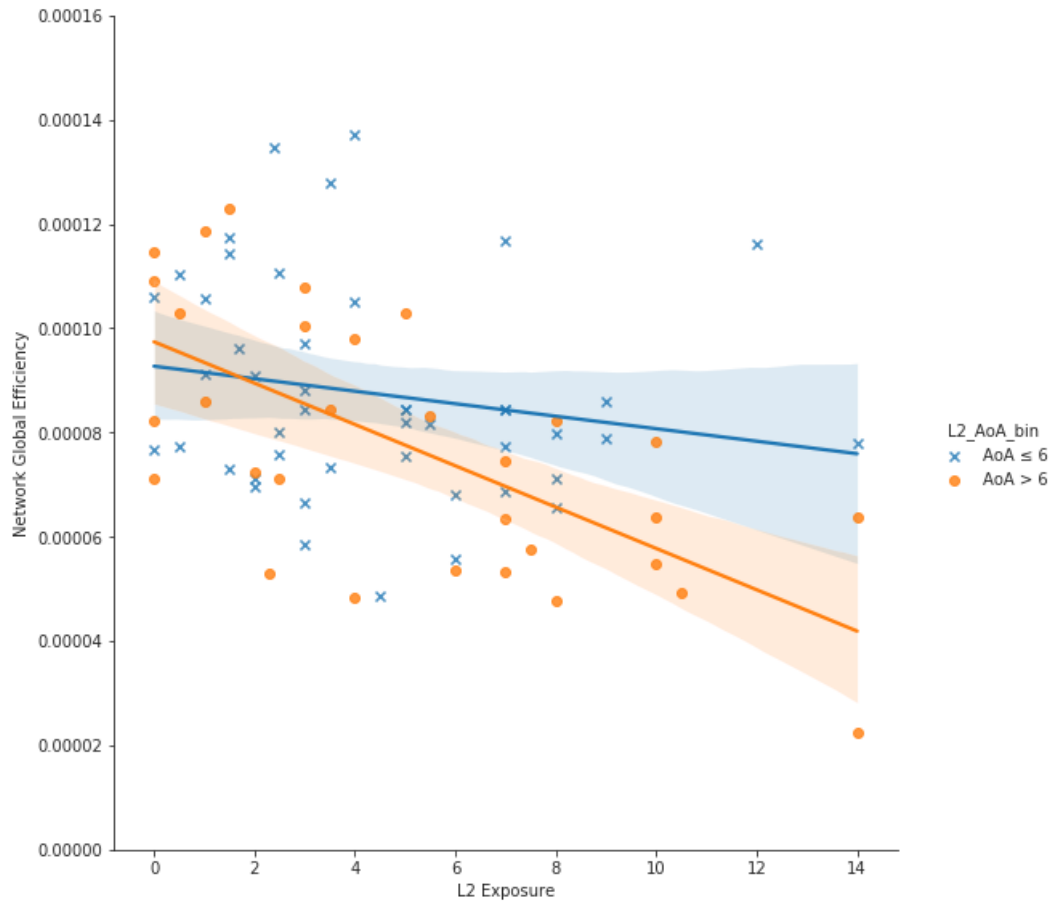
	R	Thalamus	0.020	4	5.52	4.75	<0.001	8	-10	-6
	L	Temporal Occipital Fusiform Cortex	0.028	2	5.51	4.74	<0.001	-36	-58	-16
	R	Paracingulate Gyrus	0.028	2	5.50	4.73	<0.001	4	22	36
	L	Cerebellum	0.035	1	5.44	4.69	<0.001	-10	-56	-24
	R	Superior Frontal Gyrus	0.028	2	5.44	4.69	<0.001	22	6	62
	L	Cerebellum	0.035	1	5.42	4.68	<0.001	-12	-54	-26
	L	Paracingulate Gyrus	0.035	1	5.39	4.66	<0.001	-8	48	10
	R	Occipital Fusiform Gyrus	0.020	4	5.39	4.66	<0.001	38	-66	-12
	L	Intracalcarine Cortex	0.035	1	5.39	4.66	<0.001	-12	-68	12
	R	Inferior Frontal Gyrus	0.035	1	5.37	4.65	<0.001	56	12	16
	L	Central Opercular Cortex	0.035	1	5.37	4.65	<0.001	-52	-20	18

Appendix; Experiment 2; Table S 2. t-contrast results for the effects detected in the Numerical Stroop task (volume-based analysis). Significance threshold is set at voxel p -uncorrected < 0.001 and cluster- p -FWE-corrected < 0.05 . Only one local maximum per significant cluster is listed. R = Right hemisphere. L = Left hemisphere. The Incongruent $>$ Congruent contrast is reported at voxel p -FWE corrected < 0.05 threshold, since the voxel p -uncorrected < 0.001 threshold lead to large but uninterpretable clusters of functional activity.

Experiment 4

Spearman ρ	Age	Education	AoA	Exposure	Translation	Cambridge	TIB
Age	1.0***						
Education	0.57***	1.0***					
L2_AoA	0.31**	0.19	1.0***				
Exposure	0.03	0.06	0.05	1.0***			
Translation	0.18	0.31**	-0.1	0.4***	1.0***		
Cambridge	0.1	0.25*	-0.07	0.46***	0.75***	1.0***	
TIB	0.22	0.25*	0.01	0.1	0.4***	0.3**	1.0***

*Appendix; Experiment 4, Table S 1. Spearman correlation matrices. Age = participants' age. Education = years of formal education; AoA = age of second language acquisition; Exposure = mean daily second language exposure time; Translation = first to second language translation score; Cambridge = Cambridge test score; TIB = Test di Intelligenza Breve test score. * $p < .05$; ** $p < .01$; *** $p < .001$*



*Appendix; Experiment 4, Figure S 1. Global efficiency (E_{glob}) plots from L2 Age of Acquisition * Exposure connected component. L2_AoA_bin = binarized L2 Age of Acquisition.*

Full list of publications

Full list of peer-reviewed scientific publications in chronological order:

- **Fedeli, D.**, Del Maschio, N., Del Mauro, G., Defendenti, F., Sulpizio, S., Abutalebi., J, (submitted). ACC morphology modulates Inhibitory Control: Evidence from neurofunctional activity and behavioral performance. *Cortex*.

The present work was performed by Davide Fedeli in partial fulfilment of the requirements for obtaining the PhD degree at Vita-Salute San Raffaele University, Milano, Italy.

- Del Mauro, G., Del Maschio, N., Sulpizio, S., **Fedeli, D.**, Perani, D., Abutalebi., J, (2021). Investigating sex differences in human brain structure using source, voxel, and surface-based morphometry. *Brain Structure and Function*, 1-11.

Work performed by Gianpaolo Del Mauro and colleagues was in partial fulfilment of the requirements for obtaining the PhD degree at Vita-Salute San Raffaele University, Milano, Italy.

- **Fedeli, D.**, Del Maschio, N., Sulpizio, S., Rothman J., Abutalebi., J, (2021). The Bilingual Structural Connectome: Dual-language experiential factors modulate distinct cerebral networks. *Brain and Language*, 220, 104978.

The present work was performed by Davide Fedeli in partial fulfilment of the requirements for obtaining the PhD degree at Vita-Salute San Raffaele University, Milano, Italy.

- **Fedeli, D.**, Del Maschio, N., Caprioglio, C., Sulpizio, S., Abutalebi., J, (2020). Sulcal Pattern Variability and Dorsal Anterior Cingulate Cortex Functional Connectivity Across Adult Age. *Brain Connectivity*, 10 (6), 267-278

The present work was performed by Davide Fedeli in partial fulfilment of the requirements for obtaining the PhD degree at Vita-Salute San Raffaele University, Milano, Italy.

- Sulpizio, S., Del Maschio, N., Del Mauro, G., **Fedeli, D.**, Abutalebi., J, (2019). Bilingualism as a gradient measure modulates functional connectivity of language and control networks. *NeuroImage*, 205, 116306

Work performed by dr. Simone Sulpizio and colleagues was in partial fulfilment of the requirements for obtaining the PhD degree at Vita-Salute San Raffaele University, Milano, Italy.

- Sulpizio, S., Del Maschio, N., **Fedeli, D.**, Abutalebi., J, (2019). Bilingual language processing: A meta-analysis of functional neuroimaging studies. *Neuroscience and Biobehavioral Reviews*, 108, 834-853.

Work performed by dr. Simone Sulpizio and colleagues was in partial fulfilment of the requirements for obtaining the PhD degree at Vita-Salute San Raffaele University, Milano, Italy.

- Del Maschio, N., **Fedeli, D.**, Sulpizio, S., Abutalebi., J, (2019). The relationship between bilingual experience and gyrification in adulthood: A cross-sectional surface-based morphometry study. *Brain and language*, 198, 104680.

Work performed by dr. Nicola Del Maschio and colleagues was in partial fulfilment of the requirements for obtaining the PhD degree at Vita-Salute San Raffaele University, Milano, Italy.

- Del Maschio, N., Sulpizio, S., Toti, M., Caprioglio, C., Del Mauro, G., **Fedeli, D.**, Abutalebi., J, (2019). Second language use rather than second language knowledge relates to changes in white matter microstructure. *Journal of Cultural Cognitive Science*, 1-11.

Work performed by dr. Nicola Del Maschio and colleagues was in partial fulfilment of the requirements for obtaining the PhD degree at Vita-Salute San Raffaele University, Milano, Italy.

- Sulpizio, S., Toti, M., Del Maschio, N., Costa, A., **Fedeli, D.**, Job, R., Abutalebi., J, (2019). Are you really cursing? Neural processing of taboo words in native and foreign language. *Brain and Language*, 194, 84-92.

Work performed by dr. Simone Sulpizio and colleagues was in partial fulfilment of the requirements for obtaining the PhD degree at Vita-Salute San Raffaele University, Milano, Italy.

(Before PhD start)

- Del Maschio, N., Sulpizio, S., **Fedeli, D.**, Ramanujan, K., Ding, G., Weekes., B., Cachia, A., Abutalebi., J, (2018). ACC Sulcal Patterns and their Modulation on Cognitive Control Efficiency across Lifespan. *Cerebral Cortex*, 1, 11.
- Del Maschio, N., **Fedeli, D.**, Abutalebi., J, (2018). Bilingualism and aging: why research should continue. *Linguistic approaches to bilingualism*. 11(4), 505-519.
- Del Maschio, N., Sulpizio, S., Gallo, F., **Fedeli, D.**, Weekes., B., Abutalebi., J, (2018). Neuroplasticity across the lifespan and aging effects in bilinguals and monolinguals. *Brain and cognition*, 125, 118-126.

- Lo Gerfo, E., Pisoni, A., Ottone, S., Ponzano, F., Zarri, L., Vergallito, A., Varioli, E., **Fedeli, D.**, Romero Lauro, L. J., (2018). Goal achievement failure drives corticospinal modulation in promotion and prevention contexts. *Frontiers in behavioral neuroscience*, 12.

(Book Chapters)

- **Fedeli, D.**, Abutalebi, J, (2019) Neuroimaging e Afasia in Gilardone, M., Monti, A. (Eds.). (2019) Afasiologia: Clinica, valutazione, trattamento. FrancoAngeli.

The present work was performed by Davide Fedeli in partial fulfillment of the requirements for obtaining the PhD degree at Vita-Salute San Raffaele University, Milano, Italy.